

# Lawrence Berkeley National Laboratory

## Lawrence Berkeley National Laboratory

### **Title**

CONTAMINATION OF GROUNDWATER BY ORGANIC POLLUTANTS LEACHED FROM IN-SITU SPENT SHALE

### **Permalink**

<https://escholarship.org/uc/item/08z153cp>

### **Author**

Amy, Gary L.

### **Publication Date**

1978-06-01



# Lawrence Berkeley Laboratory

UNIVERSITY OF CALIFORNIA

## ENERGY & ENVIRONMENT DIVISION

### CONTAMINATION OF GROUNDWATER BY ORGANIC POLLUTANTS LEACHED FROM IN-SITU SPENT SHALE

Gary L. Amy  
(Ph.D. thesis)

June 1978

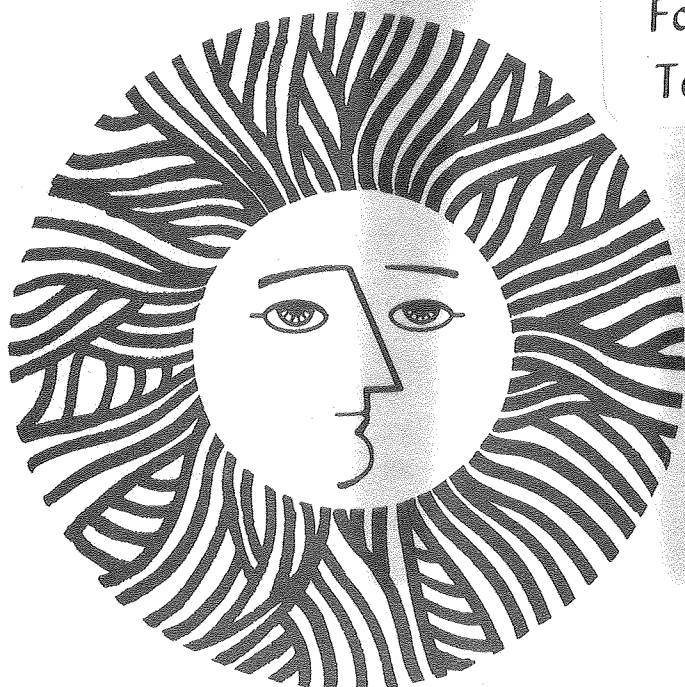
RECEIVED  
LIBRARY  
BERKELEY LABORATORY

MAY 28 1981

LIBRARY  
DOCUMENTS

**TWO-WEEK LOAN COPY**

This is a Library Circulating Copy  
which may be borrowed for two weeks.  
For a personal retention copy, call  
Tech. Info. Division, Ext. 6782



LBL-10526  
c.a.

## DISCLAIMER

This document was prepared as an account of work sponsored by the United States Government. While this document is believed to contain correct information, neither the United States Government nor any agency thereof, nor the Regents of the University of California, nor any of their employees, makes any warranty, express or implied, or assumes any legal responsibility for the accuracy, completeness, or usefulness of any information, apparatus, product, or process disclosed, or represents that its use would not infringe privately owned rights. Reference herein to any specific commercial product, process, or service by its trade name, trademark, manufacturer, or otherwise, does not necessarily constitute or imply its endorsement, recommendation, or favoring by the United States Government or any agency thereof, or the Regents of the University of California. The views and opinions of authors expressed herein do not necessarily state or reflect those of the United States Government or any agency thereof or the Regents of the University of California.

LBL-10526

CONTAMINATION OF GROUNDWATER BY ORGANIC POLLUTANTS  
LEACHED FROM IN-SITU SPENT SHALE

Gary L. Amy

Ph.D. Dissertation  
University of California,  
Berkeley

June 1978

Energy and Environment Division  
Lawrence Berkeley Laboratory  
University of California  
Berkeley, California 94720

This work was supported by the  
Division of Oil, Gas, and Shale Technology  
of the U.S. Department of Energy  
under Contract No. W-7405-ENG-48  
and the U.S. Department of the Interior  
under Contract No. 14-34-001-6220





CONTENTS

Abstract . . . . .	xiii
Chapter 1. Introduction . . . . .	1
Formation and Distribution of Oil Shale . . . . .	1
Chemistry of Oil Shale. . . . .	3
Pyrolysis of Oil Shale to Produce Shale Oil and Related Byproducts. . . . .	5
Retorting of Oil Shale. . . . .	7
In-Situ Retorting of Oil Shale. . . . .	7
Heating Alternatives for Retorting of Oil Shale . . . . .	9
Retorting Variables . . . . .	12
Groundwater Pollution Potential of In-Situ Spent Shale. . . . .	13
Chapter 2. Research Objectives. . . . .	17
Chapter 3. Literature Survey . . . . .	19
Denver Research Institute . . . . .	19
Colorado State University . . . . .	21
Texas Tech University . . . . .	22
Laramie Energy Technology Center. . . . .	27
Bureau of Mines . . . . .	28
University of Colorado. . . . .	28
Colorado School of Mines. . . . .	29
Chapter 4. Preparation of Spent Shale Samples and Procedure for Defining Characteristics . . . . .	30
Physical Characteristics. . . . .	30
Chemical Characteristics. . . . .	35
Retorting Characteristics . . . . .	35
Chapter 5. Laboratory Leaching Experiments. . . . .	37
Batch Experiments . . . . .	37
Experimental Variables Examined in Batch Experiments. . . . .	38
Continuous-Flow Column Experiments. . . . .	42
Experimental Variables Examined in the Continuous-Flow Column Experiments. . . . .	42
Summary of Experimental Variables Examined in the Batch and Continuous-Flow Column Leaching Experiments . . . . .	44
Chapter 6. Analytical Procedures for Defining Quality of Leachate. . . . .	45

Chapter 7. Experimental Results . . . . .	51
Characteristics of Spent Shale Samples. . . . .	51
Kinetic Batch Experiments . . . . .	55
Equilibrium Batch Experiments . . . . .	97
Continuous Flow Column Experiments. . . . .	99
Comparison of Results from Batch and Continuous-Flow Column Experiments. . . . .	105
Chapter 8. Data Analysis. . . . .	109
Kinetic Analysis of Batch Experiments . . . . .	109
Equilibrium Isotherms . . . . .	117
Kinetic Analysis of Continuous-Flow Column Experiments and Development of Framework for Packed-Column Mass Transfer Model . . . . .	138
Chapter 9. Assessment of the Environmental Transport and Fate of Leached Organic Contaminants . . . . .	167
Geohydrology of Lower Aquifer . . . . .	170
Hydraulics of a Typical In-Situ Retort. . . . .	171
Leaching within a Typical Retort. . . . .	172
Geohydrology of Upper Aquifer . . . . .	176
Discharge of Upper Aquifer into a Stream. . . . .	178
Chapter 10. Control Measures. . . . .	179
Source Control. . . . .	179
Site Location . . . . .	181
Treatment/Disposal. . . . .	182
Summary . . . . .	183
Chapter 11. Conclusions . . . . .	185
Conclusions Derived from Characterization of Spent Shale Samples . . . . .	185
Conclusions Derived from Kinetic Batch Experiments. . . . .	185
Conclusions Derived from Equilibrium Batch Experiments. . . . .	186
Conclusions Derived from Continuous-Flow Column Experiments . . . . .	187
Conclusions Derived from Data Analysis. . . . .	187
Conclusions Regarding Environmental Transport and Fate of Leached Organic Contaminants. . . . .	188
Conclusions Regarding Potential Control Measures. . . . .	189
General Conclusions . . . . .	

Chapter 12. Recommendations for Future Research . . . . .	190
Geohydraulics of Retort and Adjacent Aquifers . . . . .	190
Precise Definition of Equilibrium Isotherms and Estimation of Maximum Saturation Concentration of Organic Contaminants . . . . .	191
Kinetics of Leaching Phenomenon . . . . .	191
Analytical Characteristics of Organic Contaminants. . . . .	192
Environmental Transport of Organic Contaminants . . . . .	193
Public Health/Ecological Effects of Organic Contaminants. . .	194
More Detailed Assessment of Particular Types of Spent Shale . . . . .	194
References . . . . .	195
Appendix A. Sample Calculations for Kinetic Analysis of Continuous-Flow Column Experiments. . . . .	198

LIST OF FIGURES

Figure 1.	Areal extent of oil shale deposits in the Green River Formation . . . . .	2
Figure 2.	Vertical cross section of the Piceance Creek Basin. . .	4
Figure 3.	Pyrolytic decomposition of kerogen to shale oil and related by-products . . . . .	6
Figure 4.	Schematic of commercial in-situ oil shale facility. . .	8
Figure 5.	Possible alternative method of retort preparation and pyrolysis . . . . .	10
Figure 6.	Heating alternatives for pyrolysis of oil shale . . . .	11
Figure 7.	Establishment of communication between aquifers by in-situ retorting. . . . .	14
Figure 8.	Schematic of porosity determination . . . . .	32
Figure 9.	Laboratory permeameter. . . . .	34
Figure 10.	Schematic of equilibrium batch experiments. . . . .	39
Figure 11.	Schematic of continuous-flow column experiments . . . .	43
Figure 12.	Extraction fractionation technique. . . . .	47
Figure 13.	Distilled water batch experiments examining Type 1 spent shale at 20°C. . . . .	56
Figure 14.	Distilled water batch experiments examining Type 2 spent shale at 20°C. . . . .	57
Figure 15.	Distilled water batch experiments examining Type 3 spent shale at 20°C. . . . .	58
Figure 16.	Distilled water batch experiments examining Type 4 spent shale at 20°C. . . . .	59
Figure 17.	Summary of distilled water batch experiments conducted at a water temperature of 20°C. . . . .	60
Figure 18.	Distilled water batch experiments examining Type 1 spent shale at 80°C. . . . .	64
Figure 19.	Distilled water batch experiments examining Type 2 spent shale at 80°C. . . . .	65

Figure 20.	Distilled water batch experiments examining Type 3 spent shale at 80°C. . . . .	66
Figure 21.	Distilled water batch experiments examining Type 4 spent shale at 80°C. . . . .	67
Figure 22.	Summary of distilled water batch experiments conducted at a water temperature of 80°C. . . . .	68
Figure 23.	Groundwater batch experiments examining Type 1 spent shale at 20°C . . . . .	75
Figure 24.	Groundwater batch experiments examining Type 2 spent shale at 20°C . . . . .	76
Figure 25.	Groundwater batch experiments examining Type 3 spent shale at 20°C . . . . .	77
Figure 26.	Groundwater batch experiments examining Type 4 spent shale at 20°C . . . . .	78
Figure 27.	Groundwater batch experiments examining Type 1 spent shale at 80°C . . . . .	80
Figure 28.	Groundwater batch experiments examining Type 2 spent shale at 80°C . . . . .	81
Figure 29.	Groundwater batch experiments examining Type 3 spent shale at 80°C . . . . .	82
Figure 30.	Groundwater batch experiments examining Type 4 spent shale at 80°C . . . . .	83
Figure 31.	Continuous-flow column experiments examining Type 1 spent shale with distilled water . . . . .	101
Figure 32.	Continuous-flow column experiments examining Type 2 spent shale with distilled water. . . . .	102
Figure 33.	Continuous-flow column experiments examining Type 3 spent shale with distilled water. . . . .	103
Figure 34.	Continuous-flow column experiments examining Type 4 spent shale with distilled water. . . . .	104
Figure 35.	Hypothetical data derived from kinetic batch experiments . . . . .	110
Figure 36.	Comparison of experimental data and assumed reaction mechanism: Type 1 spent shale . . . . .	114

Figure 37.	Comparison of experimental data and assumed reaction mechanism: Type 2 spent shale . . . . .	115
Figure 38.	Comparison of experimental data and assumed reaction mechanism: Type 4 spent shale . . . . .	116
Figure 39.	Plot of linear form of Langmuir model . . . . .	119
Figure 40.	Plot of logarithmic form of Freundlich model. . . . .	121
Figure 41.	Linear form of Langmuir isotherm for Type 2 spent shale: distilled water. . . . .	122
Figure 42.	Linear form of Langmuir isotherm for Type 2 spent shale: groundwater. . . . .	123
Figure 43.	Linear form of Langmuir isotherm for Type 1 spent shale: distilled water . . . . .	124
Figure 44.	Linear form of Langmuir isotherm for Type 1 spent shale: groundwater . . . . .	125
Figure 45.	Logarithmic form of Freundlich isotherm for Type 2 spent shale: distilled water. . . . .	127
Figure 46.	Logarithmic form of Freundlich isotherm for Type 2 spent shale: groundwater. . . . .	128
Figure 47.	Logarithmic form of Freundlich isotherm for Type 1 spent shale: distilled water. . . . .	129
Figure 48.	Logarithmic form of Freundlich isotherm for Type 1 sent shale: groundwater . . . . .	130
Figure 49.	Plots of Langmuir and Freundlich equations for Type 1 spent shale examined with distilled water at 20°C . . . . .	133
Figure 50.	Plots of Langmuir and Freundlich equations for Type 2 spent shale examined with distilled water at 20°C. . . . .	134
Figure 51.	Estimated isotherm for Type 1 spent shale examined with distilled water at 20°C . . . . .	136
Figure 52.	Estimated isotherm for Type 2 spent shale examined with distilled water at 20°C. . . . .	137
Figure 53.	TOC concentration vs time: Type 1 spent shale. . . . .	144
Figure 54.	TOC concentration vs time: Type 2 spent shale. . . . .	145

Figure 55.	TOC concentration vs column length: Type 1 spent shale. . . . .	146
Figure 56.	TOC concentration vs column length: Type 2 spent shale. . . . .	147
Figure 57.	Approximated TOC concentration vs time curves for various column lengths: Type 1 spent shale . . . .	148
Figure 58.	Approximated TOC concentration vs time curves for various column lengths: Type 2 spent shale . . . .	149
Figure 59.	Geohydrologic cross section of the Piceance Creek Basin showing relationship of in-situ retorts to adjacent aquifers . . . . .	168
Figure 60.	Schematic describing environmental transport of leached contaminants. . . . .	169
Figure 61.	TOC concentration profiles within a retort as a function of time. . . . .	173
Figure 62.	TOC concentration as a function of time in the effluent from a retort. . . . .	173



LIST OF TABLES

Table 1.	Analysis of the organic fraction of oil shale derived from the Green River Formation. . . . .	5
Table 2.	Retorting variables employed to control the pyrolysis of oil shale. . . . .	12
Table 3.	Average water quality of the upper and lower aquifers in the Piceance Creek Basin . . . . .	15
Table 4.	Experimental results of percolation experiment conducted with TOSCO spent shale. . . . .	23
Table 5.	Material leached from spent shale samples . . . . .	24
Table 6.	Materials extracted from spent shale samples. . . . .	26
Table 7.	Mass of molybdenum, fluoride, and boron leached from TOSCO spent shale. . . . .	29
Table 8.	Experimental variables examined in leaching experiments . . . . .	44
Table 9.	Analyses selected for defining the quality of leachate. . . . .	50
Table 10.	Retorting characteristics of spent shale samples. . . . .	52
Table 11.	Physical and chemical characteristics of spent shale samples: composite particle size range . . . . .	53
Table 12.	Total organic carbon leached from various types of spent shale during batch experiments. . . . .	87
Table 13.	Estimated total dissolved solids (TDS) leached from various types of spent shale during batch experiments . . . . .	88
Table 14.	Acid, base, and neutral fractions of organic material in composite samples derived from batch experiments . . . . .	90
Table 15.	Comparison of extracted mass of organics with estimated mass of organics in leachate. . . . .	93
Table 16.	Organic nitrogen in composite samples derived from batch experiments . . . . .	95
Table 17.	Phenols in composite samples derived from batch experiments . . . . .	96

Table 18.	Equilibrium batch experiments: organic carbon concentration and mass of organic carbon leached per unit mass of spent shale. . . . .	98
Table 19.	Weight (W) and bulk density (D) of spent shale samples compacted into columns. . . . .	100
Table 20.	Total organic carbon leached from various types of spent shale: comparison of continuous-flow column experiments and batch experiments . . . . .	106
Table 21.	Estimated total dissolved solids (TDS) leached from various types of spent shale: comparison of continuous-flow column experiments and batch experiments . . . . .	108
Table 22.	Estimated values of $C_e$ and K for kinetic batch experiments: spent shale Types 1, 2, and 4 . . . . .	117
Table 23.	Constants for Freundlich and Langmuir models: spent shale Types 1 and 2 . . . . .	131
Table 24.	Estimates of parameters required for evaluation of rate constants for Type 1 spent shale at a column length of 7.5 cm . . . . .	150
Table 25.	Estimates of parameters required for evaluation of rate constants for Type 1 spent shale at a column length of 15 cm . . . . .	151
Table 26.	Estimates of parameters required for evaluation of rate constants for Type 1 spent shale at a column length of 22.6 cm. . . . .	152
Table 27.	Estimates of parameters required for evaluation of rate constants for Type 2 spent shale at a column length of 7.5 cm . . . . .	153
Table 28.	Estimates of parameters required for evaluation of rate constants for Type 2 spent shale at a column length of 15 cm . . . . .	154
Table 29.	Estimates of parameters required for evaluation of rate constants for Type 2 spent shale at a column length of 22.5 cm . . . . .	155
Table 30.	Estimates of $K_G$ (internal diffusion rate constant) for Type 1 spent shale. . . . .	158
Table 31.	Estimates of $K_E$ (external mass transfer rate constant) for Type 1 spent shale. . . . .	159

Table 32.	Estimates of $K_{BA}$ (external mass transfer rate constant) for Type 1 spent shale. . . . .	160
Table 33.	Estimates of $K_G$ (internal mass diffusion rate constant) for Type 2 spent shale. . . . .	161
Table 34.	Estimates of $K_E$ (external mass diffusion rate constant) for Type 2 spent shale. . . . .	162
Table 35.	Estimates of $K_{BA}$ (surface reaction rate constant) for Type 2 spent shale. . . . .	163
Table 36.	Masses of potentially leachable organic carbon. . . . .	174
Table 37.	Estimated saturation concentrations of organic carbon . .	175
Table 38.	Estimated minimum mass of organic carbon that can potentially be leached from a typical in-situ retort. . .	176
Table 39.	Pore volumes of water required to leach estimated minimum mass of potentially leachable organic carbon from a typical retort . . . . .	177
Table 40.	Relative technological and economic feasibility of control measures. . . . .	184

ABSTRACT

The potential for contamination of groundwater by organic pollutants leached from in-situ spent shale was studied in a series of laboratory leaching experiments. Both batch-mode and continuous-flow column experiments were conducted to study the leaching phenomenon. Experimental variables included retorting characteristics of spent shale, leaching time, initial quality of leach water, temperature of leach water, and particle size of spent shale.

Several unique samples of spent shale were examined during the leaching experiments, including spent shale samples produced during combustion retorting, inert gas retorting, and combustion retorting employing recycle gas. The solid-phase organic carbon content of spent shale samples ranged from 0.2 to 3.9 percent by weight.

Leachate derived from the batch-mode experiments was analyzed for organic carbon, organic nitrogen, phenols, and acid/base/neutral fractions. The highest levels of organic carbon were detected in leachate derived from spent shale produced during either inert gas retorting or combustion retorting using recycle gas. The highest levels of phenols were observed in leachate obtained from spent shale produced during inert gas retorting; significant levels of organic nitrogen were also detected in various leachate samples. The most predominant organic fraction measured in leachate samples was the neutral fraction associated with spent shale produced during inert gas retorting.

Batch-mode experimental results describing equilibrium conditions were analyzed according to the Freundlich and Langmuir isotherm models. Those models were found to be appropriate for describing equilibrium relationships between leachate and spent shale produced during inert gas retorting. To a somewhat lesser extent, these same models were found to be appropriate for modeling equilibrium relationships involving combustion-retorted spent shale.

A kinetic analysis of results derived from the continuous-flow column experiments was conducted in an attempt to identify a rate-controlling mass transfer mechanism. Internal diffusion appeared to be the most likely rate-limiting mechanism for leaching from combustion-retorted spent shale. In contrast, no single mass transfer mechanism appeared to control the leaching phenomenon for inert gas-retorted spent shale over the entire range of leaching times examined.

The results presented here suggest that groundwater resources in regions of potential in-situ development may be significantly degraded in quality as a consequence of leached organic contaminants. Overall, the leaching phenomenon represents a potentially chronic problem which may preclude beneficial uses of groundwater for decades.



## CHAPTER 1

### INTRODUCTION

Oil shale is a mineral material from which oil can be extracted. Vast reserves of oil shale exist throughout the United States, most of which are situated within the tri-state region of Colorado, Wyoming, and Utah. In recent times, considerable attention has been focused on the large-scale commercial recovery of oil from oil shale. The effective exploitation of oil shale as an energy resource is presently limited by both economic and environmental constraints. However, economic constraints are becoming increasingly less significant as prices of imported crude oil continue to rise and the technologies for oil shale development are refined. Thus, it is asserted that eventually environmental constraints will be the most significant factor controlling oil shale development.

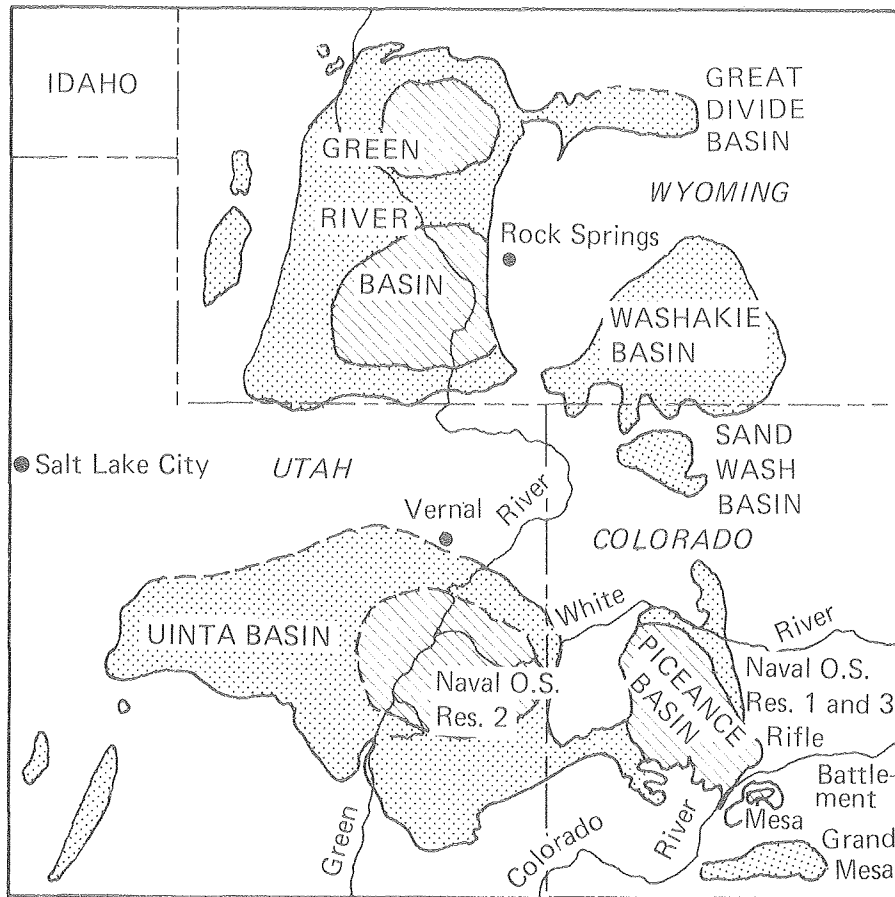
Among the various environmental concerns, the potential adverse effects of oil shale development on water resources are of particular significance. As a consequence of oil shale development, it is anticipated that the quality of both surface water and groundwater resources may be degraded.

#### Formation and Distribution of Oil Shale

Some of the richest deposits of oil shale in the world are in the tri-state region of Colorado, Wyoming, and Utah as part of the Green River geological formation. The areal extent of oil shale deposits in the Green River Formation are described in Figure 1 (Ref. 1). In reference to Figure 1, oil shale deposits containing 25 gallons of oil or more per ton of oil shale are considered to be economically exploitable in the near future. The richest deposits of oil shale associated within the Green River geological formation are in the Piceance Creek Basin. The location of the Piceance Creek Basin is also defined in Figure 1.

Deposits of oil shale were formed by sedimentary processes over long periods of time. Specifically, deposits were formed by the simultaneous sedimentation of mineral silt and algal remains upon the beds of ancient lakes. Those lakes subsequently disappeared due to climatic changes and upheaval of the surrounding terrain, thus leaving behind oil shale deposits (Ref. 2).

In geographical areas of rich oil shale deposits such as the Green River Formation, oil shale often occurs as a continuous, relatively impermeable layer situated between two groundwater aquifers. An example of this situation is the Piceance Creek Basin in Colorado where a rich layer of oil shale, known as the Mahogany Zone, persists throughout most of the basin. The Mahogany Zone, identified in the vertical



EXPLANATION



Area underlain by the Green River Formation in which the oil shale is unappraised or low grade.



Area underlain by oil shale more than 10 feet thick, which yields 25 gallons or more per ton of shale.

F XBL 792-525

Figure 1. Areal extent of oil shale deposits in the Green River Formation.

cross section of the Piceance Creek Basin shown in Figure 2, is located from 500 to 1,000 ft below the ground surface and averages 200 ft in thickness.

The Piceance Creek Basin is typical of areas of oil-rich shale deposits. In the Piceance Creek Basin, the Mahogany Zone is sandwiched between two groundwater aquifers. Normally, the lower aquifer is a confined aquifer of poor quality while the upper aquifer is an unconfined aquifer of good quality (Ref. 3).

#### Chemistry of Oil Shale

Oil shale is a sedimentary mineral in which organic material is contained within an inorganic matrix. The predominant components of the inorganic matrix are dolomite,  $\text{CaMg}(\text{CO}_3)_2$ , and calcite,  $\text{CaCO}_3$ .

There are three types of organic material found in oil shale: kerogen, bitumen, and aliphatic hydrocarbons. About 90 percent of the organic material is found in the form of kerogen, about 10 percent in the form of bitumen, and less than 1 percent in the form of aliphatic hydrocarbons (Ref. 4).

Kerogen is a high molecular weight, three-dimensional polymer which is composed primarily of heterocyclic components linked together by carbon chains acting as bridges. Individual monomer molecules are estimated to have a molecular weight of 3,000.

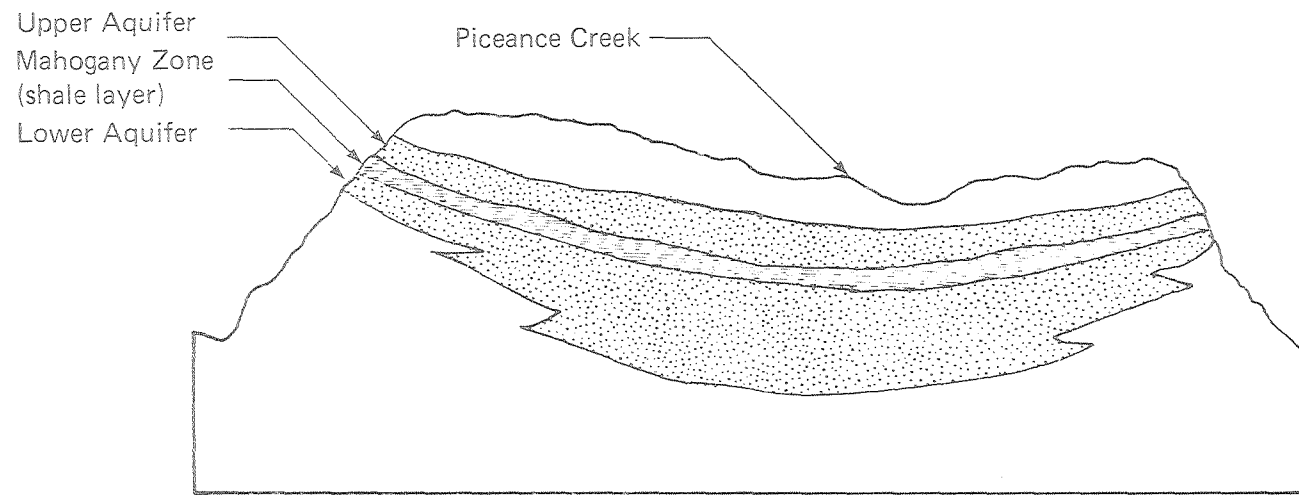
It is hypothesized that kerogen also contains various "entrapped" hydrocarbons and organic acids. Kerogen, one of the most common forms of organic carbon on earth, is insoluble in all common organic solvents and water (Ref. 5).

In contrast to kerogen, bitumen is a lower molecular weight "resin" composed primarily of condensed alicyclic hydrocarbons and polynuclear aromatic hydrocarbons. Individual molecules of bitumen often have side chains incorporating various organic functional groups.

Kerogen and bitumen are often differentiated by their solubility characteristics in organic solvents. Bitumen is soluble in certain organic solvents but is insoluble in water.

An elemental analysis of the organic fraction of oil shale is presented in Table 1. As revealed by Table 1, the major elements present in the organic fraction of oil shale are carbon and hydrogen, the "building blocks" of hydrocarbons. (It is interesting to note that the high nitrogen and sulfur content of oil shale may be a major concern in relation to air quality effects resulting from shale oil utilization.)





XBL 792-519

Figure 2. Vertical cross section of the Piceance Creek Basin.

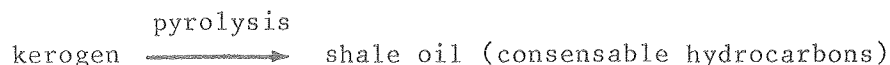
Table 1. Analysis of the organic fraction of oil shale derived from the Green River Formation.<sup>a</sup>

Element	Weight % of total organics
Carbon	76.5
Hydrogen	10.3
Nitrogen	2.5
Sulfur	1.2
Oxygen	9.5

(Source: Ref. 3) <sup>a</sup>This analysis is based on an oil shale sample with a Fischer assay (potential oil yield) of 26.7 gallons per ton.

#### Pyrolysis of Oil Shale to Produce Shale Oil and Related Byproducts

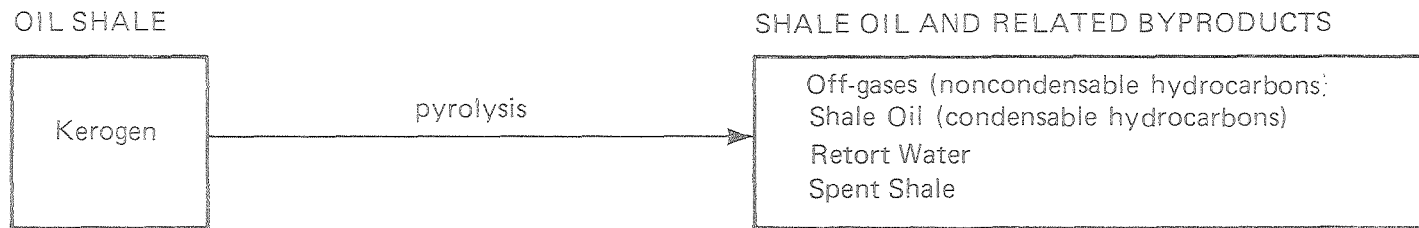
Oil can be produced from oil shale by pyrolysis (i.e., thermal decomposition) of kerogen. This thermal decomposition of kerogen occurs as follows:



The oil produced is in the form of condensable hydrocarbon vapors which are condensed and cooled to produce a semi-viscous liquid. Not all of the organic material originally associated with oil shale is converted to shale oil. During pyrolysis, various carbonaceous by-products are formed. The formation of by-products during pyrolysis is described in Figure 3.

The crude shale oil that is produced during pyrolysis is quite viscous with a high pour point. It contains many of the heavier hydrocarbons (i.e., distillation products in the higher temperature ranges) found in crude petroleum oil and normally must be upgraded during prerefinery operations prior to transporting it to a refinery. The objective of prerefinery operations is simply to lower the pour point in order to enhance transport of the produced oil.

Pyrolysis of kerogen produces some low-molecular-weight uncondensed hydrocarbons, such as methane and ethane, that are contained in the off-gas. In addition, off-gas contains various hydrocarbons and other organic compounds that are volatile and vaporized at high temperatures.



F XBL 792-520

Figure 3. Pyrolytic decomposition of kerogen to shale oil and related by-products.

Retort water, coproduced with shale oil during pyrolysis, contains approximately 2 percent organics by weight. Retort water is derived from (1) the liberation of free and bound water from the oil shale matrix, (2) the combustion of hydrocarbons, (3) the dehydration of various oxygen-containing compounds, and (4) the recombination of  $H^+$  and  $OH^-$  produced during pyrolysis. It is hypothesized that organic acids are a major organic component of retort water (Ref. 6).

One of the most important by-products of pyrolysis, from an environmental viewpoint, is spent shale. After pyrolysis, some organic material remains associated with the spent shale. Some of this residual organic material will likely reside within the pores of the spent shale matrix, partly as a coke-like substance, partly as oil that was not completely volatilized during pyrolysis, and partly as miscellaneous products of the pyrolytic process. In addition, some organic material will likely be associated with the exterior surface of the spent shale matrix. The amount and characteristics of organic material will largely be determined by conditions employed during pyrolysis, such as temperature and presence of oxygen. In some cases the resultant spent shale may contain up to 5 percent organic carbon residue (Ref. 5). Some of this organic residue may be soluble or sparingly soluble in water.

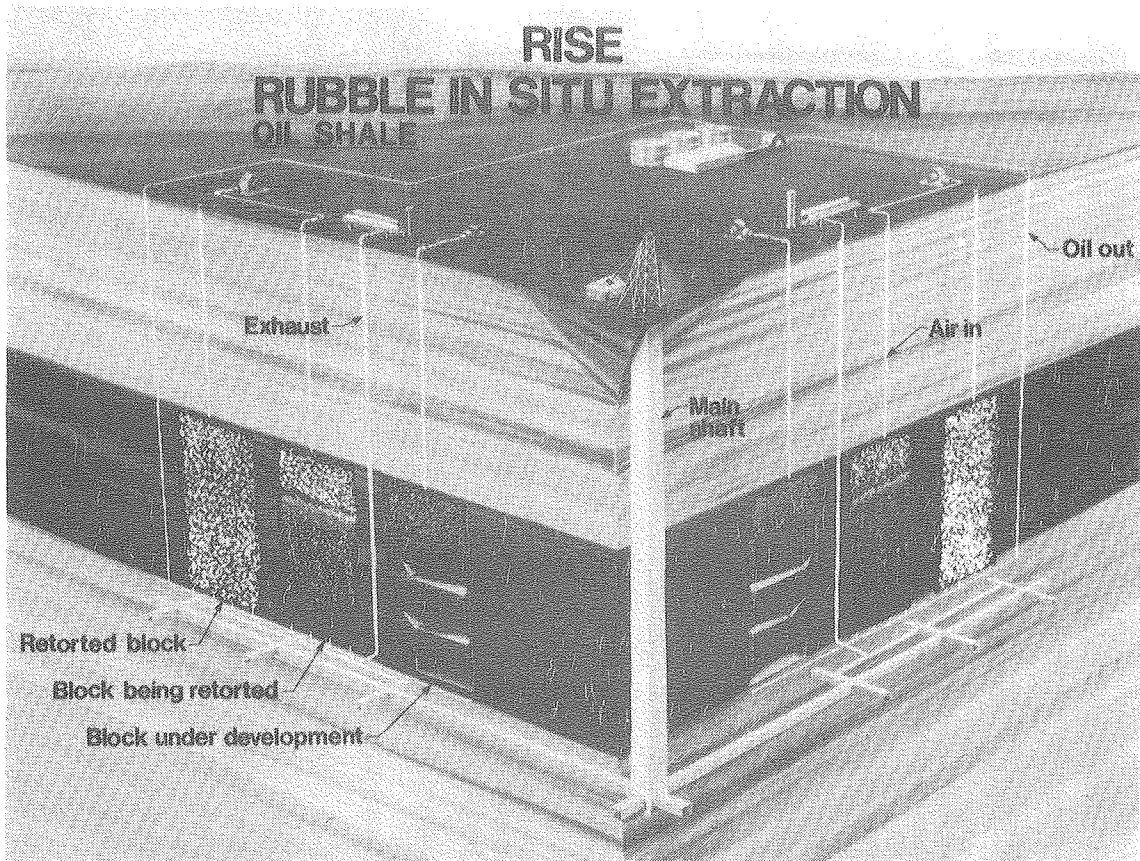
#### Retorting of Oil Shale

The process of converting kerogen to oil by pyrolysis is referred to as retorting and the reaction chamber in which the conversion occurs is called a retort. Oil shale may be retorted above ground or in-situ (i.e., in place below the ground surface). In-situ retorting is the subject of the subsequent discussion.

#### In-Situ Retorting of Oil Shale

In order to overcome the major disadvantages associated with above-ground retorting, recent emphasis has been placed on in-situ retorting; that is, retorting the shale in place below the ground surface. The production of oil from oil shale by the in-situ process involves several steps: (1) an in-situ retort is prepared by mining about 20 percent of a block of oil shale and then using underground explosives to rubblize the remaining oil shale; (2) the in-situ retort is heated by either external or internal means to provide heat for pyrolysis; and (3) the volatilized oil is condensed and collected in a sump below the retort and pumped to the surface. (As an alternative to collection of condensed oil in a sump below the ground, it may be possible to rapidly pump volatilized oil to the surface where it can be allowed to condense.)

The various steps involved in the in-situ oil shale recovery process are further described in the schematic of a proposed commercial-scale in-situ oil shale facility shown in Figure 4. Tentative plans suggest that a typical in-situ retort will be 50 meters by 50 meters and will extend downward to penetrate almost the entire thickness of the oil



CBB 790-14046

Figure 4. Schematic of commercial in-situ oil shale facility.

shale layer. It is likely that a large-scale commercial facility will develop a great number of these retorts each year.

The schematic shown in Figure 4 suggests that an in-situ retort will be developed in the following manner. The rectangular-shaped section of oil shale will be rubblized. Subsequently, the entire volume of oil shale within the retort will be pyrolyzed in a vertical direction. Pyrolysis will begin at the top of the retort and move in a downward direction, moving in response to the flow of input gas. Oil and gas produced during pyrolysis will be collected near the bottom of the retort.

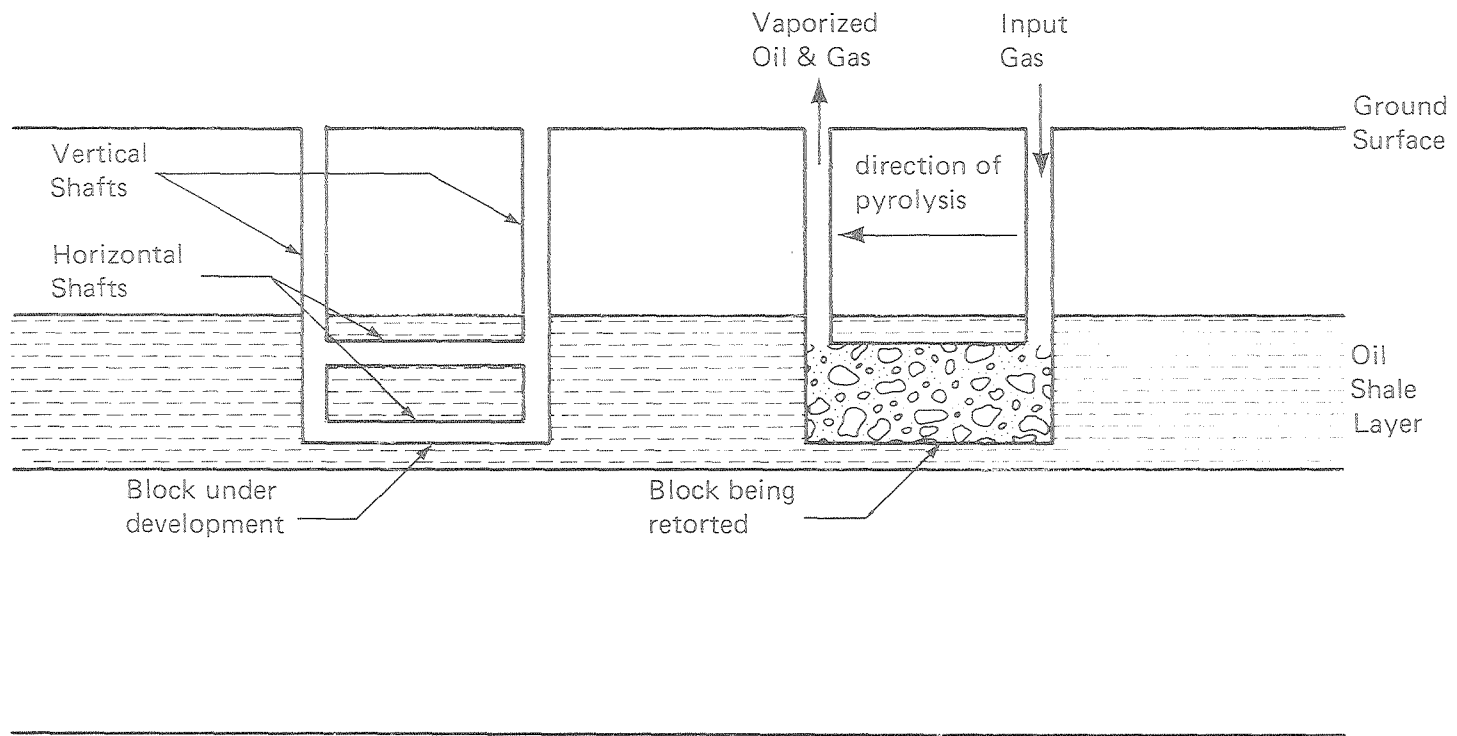
It is possible, of course, that other methods of retort preparation could be used. For example, one alternative method would involve the preparation of a retort that does not penetrate the entire thickness of the oil shale layer. It may be advantageous to pyrolyze such a retort in a horizontal direction; input gas would be supplied at one end of the retort and oil and gas collected at the other end. This alternative method of retort preparation and subsequent pyrolysis is schematically shown in Figure 5.

#### Heating Alternatives for Retorting of Oil Shale

As indicated previously, pyrolysis is defined as thermal decomposition in the absence of oxygen. This implies that pyrolysis of oil shale requires heat. Heat for the in-situ pyrolysis of oil shale can be supplied by either an external or internal heat source. These two alternative heat sources are schematically represented in Figure 6.

When an external heat source is employed, a hot inert gas (such as nitrogen) is pumped into a prepared in-situ retort. This leads to the formation of a distinct pyrolysis zone within the retort which moves in the direction of gas flow. As the pyrolysis zone moves through the retort, a zone of spent shale, containing significant residual organic material, is formed behind the pyrolysis zone. It should be recognized that, when this heating alternative is employed, reducing conditions exist throughout the retort.

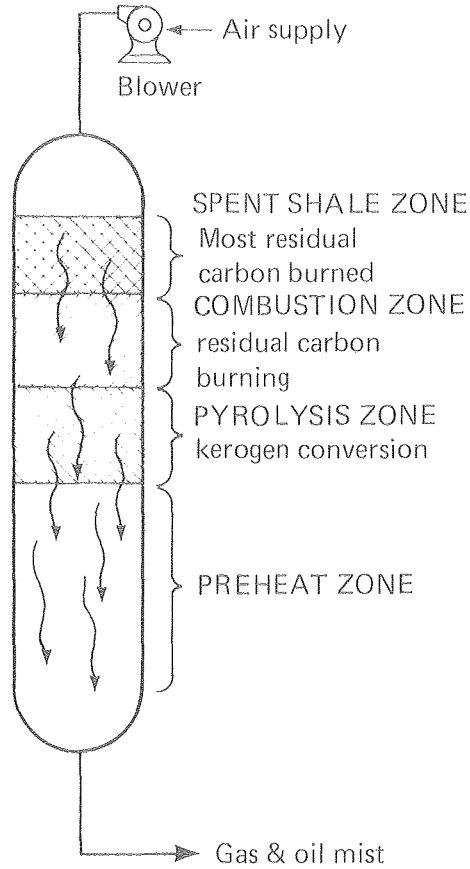
When an internal heat source is employed, heat for pyrolysis is supplied by combustion of some of the residual organic material remaining on the spent shale. Raw oil shale is initially ignited with an external heat source such as a propane burner and a continuous flow of air is supplied to the in-situ retort. This leads to the formation of both a pyrolysis zone and a combustion zone moving in the direction of gas flow. The pyrolysis zone moves in front of the combustion zone and leaves behind spent shale with significant amounts of residual organic material. The combustion zone forms behind the pyrolysis zone and burns some of the residual organic material on the spent shale in the presence of oxygen, thus providing heat for pyrolysis in the pyrolysis zone. Behind the combustion zone, a zone of spent shale is formed which contains a small amount of residual organic material (this small amount of residual organic material is



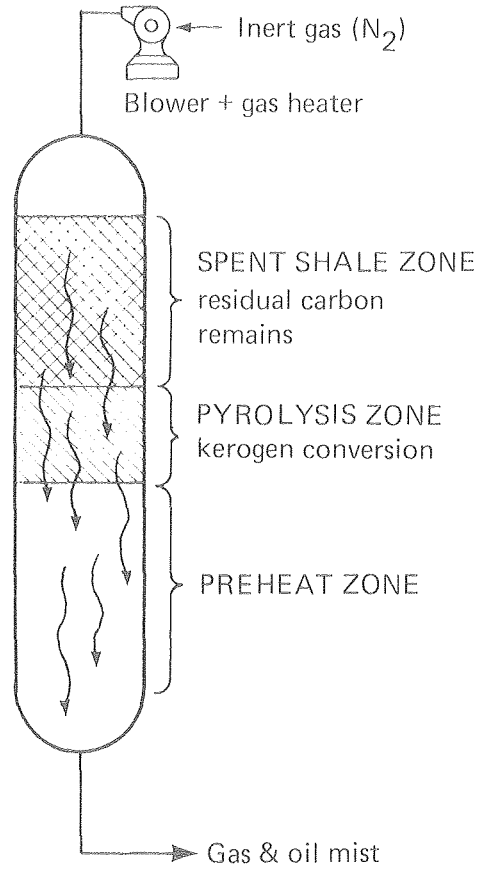
XBL 792-521

Figure 5. Possible alternative method of retort preparation and pyrolysis.

INTERNAL HEAT SOURCE  
(Combustion of residual carbon as spent shale)



EXTERNAL HEAT SOURCE  
(hot inert gas)



XBL 792-522

Figure 6. Heating alternatives for pyrolysis of oil shale.



due to incomplete combustion). Thus, when this heating alternative is employed, both oxidizing and reducing conditions simultaneously exist in different portions of the retort. However, since the combustion zone "follows" the pyrolysis zone, it is conventional practice to define the overall conditions within the retort as oxidizing. It should be recognized that the combustion of residual organic material associated with the spent shale is incomplete (i.e., the resultant spent shale will still contain some residual organic material after combustion).

### Retorting Variables

There are numerous operating conditions that can be varied to control the actual in-situ retorting (pyrolysis) of oil shale. A list of "retorting variables" is presented in Table 2. It is important to note that retorting variables will significantly affect the physical and chemical characteristics of the resultant in-situ spent shale. For example, spent shale produced during an inert gas run can be expected to contain significantly more residual organic material than spent shale produced during an ordinary combustion run, since some of the residual organic material is burned during a combustion run. Due to the fact that retorting variables significantly affect the characteristics of spent shale, it is apparent that retorting variables will largely determine the amount and composition of residual organic material remaining on the spent shale as well as the types of organic materials that may be leached or solubilized by groundwater coming into contact with in-situ spent shale.

Table 2. Retorting variables employed to control the pyrolysis of oil shale.

---

#### Gaseous environment

- Air
- Air + recycle gas
- Inert gas (N<sub>2</sub>)

#### Retorting temperature

- Effective pyrolysis occurs at 482°C (900°F)
- Carbonate decomposition begins at 621°C (1150°F)

#### Retorting rate

- Rate of movement of pyrolysis zone

#### Turbulence

- Turbulence within retort caused by flow of input gas

#### Heat Source

- Internal (combustion)
- External

---

With respect to the retorting variables described in Table 2, a few comments should be made regarding retorting temperature. Although Table 2 suggests that effective pyrolysis occurs at 482°C, it should be recognized that the temperature required to pyrolyze an organic molecule will vary according to the molecular weight and complexity of the molecule. For example, the temperature required to pyrolyze an aliphatic hydrocarbon containing 20 carbon atoms (i.e., C<sub>20</sub>) into two simpler components will be less than the temperature required to pyrolyze an aliphatic hydrocarbon containing six carbon atoms (i.e., C<sub>6</sub>) into two simpler components. This implies that the temperature required to convert kerogen into intermediate products of pyrolysis will be less than the temperature required to convert these intermediate products into both condensable and non-condensable hydrocarbons. Thus, the reported temperature at which effective pyrolysis occurs (i.e., 482°C) is essentially the minimum temperature required to convert complex molecules of kerogen into condensable and non-condensable hydrocarbons.

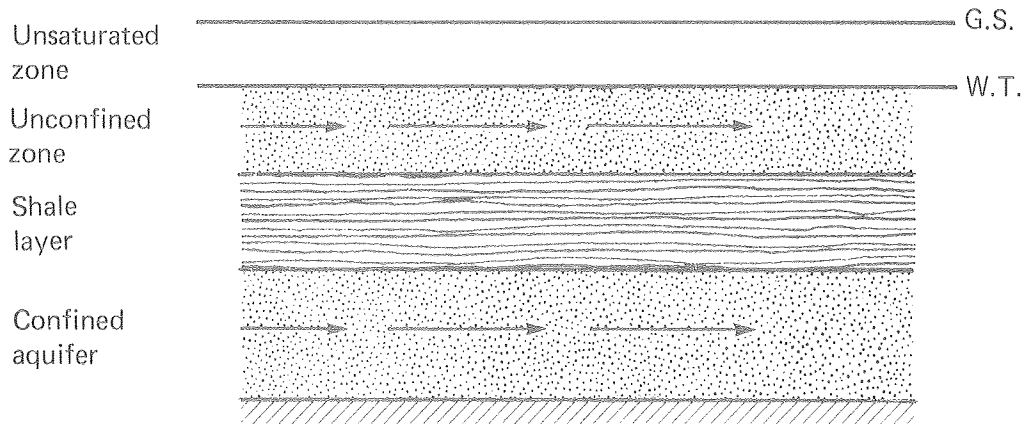
#### Groundwater Pollution Potential of In Situ Spent Shale

One of the major environmental hazards associated with in-situ oil shale development is that it creates a potential for establishing communication between the upper and lower aquifers surrounding a layer of oil shale. The shale layer and the aquifer configuration were previously described in Figure 2. Because the lower aquifer is usually a confined aquifer and the upper aquifer is usually an unconfined aquifer, the pressure difference between the lower and upper aquifer, in some cases, may be sufficient to produce flow through an abandoned retort in an upward direction, as depicted in Figure 7. Recall that the quality of the water in the lower aquifer is usually poor relative to that of the upper aquifer. The average water quality of each aquifer in the Piceance Creek Basin is described in Table 3. As revealed by Table 3, the total dissolved solids (TDS) of the lower aquifer is about an order of magnitude greater than that of the upper aquifer.

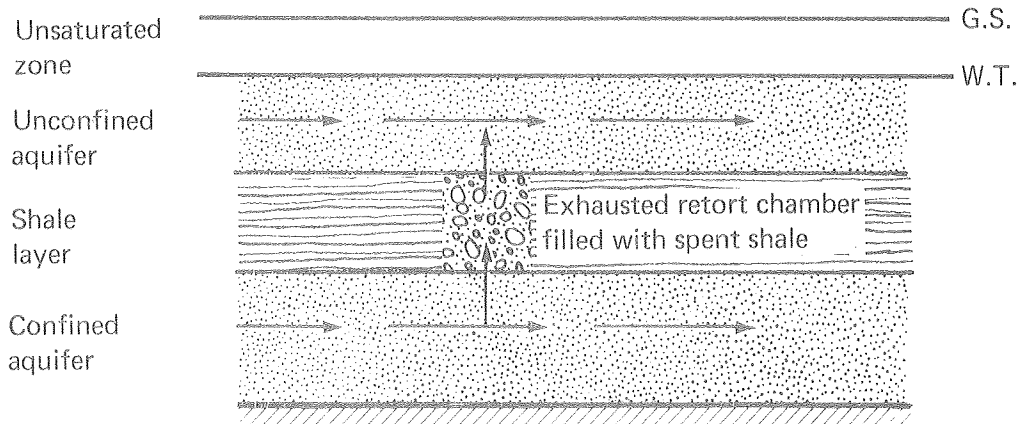
In the Piceance Creek Basin, groundwater from the upper aquifer is primarily used for agricultural purposes and, to a limited extent, for domestic water supplies for ranches located in various parts of the basin. The problems associated with creating aquifer communication by in-situ retorting are twofold:

1. Poor quality groundwater from the lower aquifer may flow into the upper aquifer
2. Various inorganic and organic contaminants may be leached from spent shale as groundwater migrates through an abandoned in-situ retort

The primary objective of this research is to assess the potential for groundwater pollution by organic contaminants leached from in-situ spent shale in either dissolved or colloidal form.



Layer of oil shale situated between an unconfined aquifer and a confined aquifer



Idealized flow of groundwater through an exhausted in-situ retort chamber

F XBL 792-517

Figure 7. Establishment of communication between aquifers by in-situ retorting.

Table 3. Average water quality of the upper and lower aquifers in the Piceance Creek Basin.

Chemical Constituent	Constituent concentration, mg/l	
	Upper Aquifer	Lower Aquifer
Potassium	1.5	11
Sodium	210	4000
Calcium	50	7.4
Magnesium	60	9.5
Bicarbonate	550	9100
Chloride	16	690
Sulfate	320	80
Fluoride	1.4	28
Dissolved solids	960	9400
Percent Variation <sup>a</sup>	1.3%	1.0%

(Source: Ref. 3)

<sup>a</sup>The percent variation was computed using the following formula:

$$\text{Percent variation} = \left[ \frac{(\sum \text{cations in } \frac{\text{meq}}{\text{l}}) - (\sum \text{anions in } \frac{\text{meq}}{\text{l}})}{(\sum \text{cations in } \frac{\text{meq}}{\text{l}}) + (\sum \text{anions in } \frac{\text{meq}}{\text{l}})} \right] \times 100$$

After migration through an abandoned retort and contact with spent shale, contaminated groundwater will enter the upper aquifer and mix with uncontaminated groundwater. In response to the hydraulic gradient, contaminated groundwater will then flow away from the retort and through the upper aquifer at an extremely slow rate. As contaminated groundwater flows through an aquifer, it undergoes natural treatment processes as a consequence of its contact with aquifer media. The concentration of various organic contaminants will decrease due to natural treatment phenomena, such as adsorption, ion exchange, and microbial degradation (Refs. 7, 8).

In addition to decreases in contaminant concentration resulting from natural treatment phenomena, the concentration of organic contaminants will also decrease as a consequence of diffusion/dispersion within the aquifer itself. Contaminated groundwater, after undergoing natural treatment and diffusion/dispersion, will eventually reach the surface by one of several pathways:

1. Pumping of groundwater from an aquifer
2. Discharge of groundwater at the surface as a spring
3. Discharge of groundwater into a stream, augmenting its surface flow with base flow.

## CHAPTER 2

### RESEARCH OBJECTIVES

As indicated by information presented in the previous section, there exists a significant potential for degradation of groundwater quality as a consequence of inorganic and organic contaminants leached from in-situ spent shale. Pyrolysis during retorting transforms oil shale from a relatively inert substance into spent shale, a relatively unstable substance containing various inorganic and organic components which are water soluble. It is anticipated that groundwater will be degraded in quality by various contaminants leached from spent shale as groundwater migrates through abandoned in-situ retorts. Although some research has been directed toward the leaching of inorganic contaminants (Ref. 9), little attention has thus far been directed toward organic contaminants that may be leached from in-situ spent shale.

The leaching of organic contaminants from in-situ spent shale is of concern because the pyrolytic process of recovering oil from oil shale may result in: (1) the production of certain organics that will persist in groundwater for extremely long periods of time and preclude various beneficial uses and (2) the production of potentially carcinogenic organic compounds (Ref. 5). It should be noted that this latter concern is based somewhat on speculation.

Based on the above concerns, the overall objective of this research is to assess the potential for groundwater pollution by organic contaminants leached from in-situ spent shale. Specifically, the following research objectives are proposed:

1. Identification of factors that influence the leaching of organic material from in-situ spent shale
2. Determination of the maximum amount of organic material that can be leached from in-situ spent shale under various conditions
3. Qualitative identification of various classes of organic compounds that may be present in leachate
4. Formulation of a mass transfer model to explain experimental results
5. Qualitative assessment of the environmental transport and fate of organic material present in leachate
6. Identification of possible control measures.

The strategy employed to accomplish most of the above objectives will be described in the following chapters. Basically, this strategy consisted of: (1) outlining a procedure for preparation and characterization of in-situ spent shale samples, (2) development of laboratory experiments to study the leaching phenomenon, (3) identification of parameters to define the resultant quality of leachate, and (4) selection of data analysis techniques to provide a mathematical framework for experimental data.

CHAPTER 3  
LITERATURE SURVEY

Several organizations and institutions have completed or are currently conducting research related to the leaching of organic and inorganic contaminants from both in-situ and surface-retorted spent shale. These organizations/institutions include:

Denver Research Institute (DRI)  
Colorado State University (CSU)  
Texas Tech University (TTU)  
Laramie Energy Technology Center (LETC)  
U.S. Bureau of Mines (USBM)  
University of Colorado (CU)  
Colorado School of Mines (CSM)

As previously indicated, the major objective of this research is to assess the leaching of organic material from in-situ spent shale. The completed and concurrent research by other organizations/institutions has focused largely on the leaching of inorganic contaminants from both in-situ and surface-retorted spent shale. However, certain aspects of research results described in the literature are relevant to this research study. Some of these results have been summarized and presented in this literature survey because they: (1) provide insight into the overall leaching phenomenon, (2) describe various experimental and laboratory methods that may be appropriate for studying the leaching of organic contaminants from in-situ shale, and (3) characterize the inorganic components of leachate that may significantly affect the types and amounts of organic contaminants leached from in-situ spent shale. The work accomplished by each of the organization/institutions noted above is summarized in the following sections.

Denver Research Institute

Schmidt-Collerus (Ref. 6) investigated the environmental impacts associated with the disposal of carbonaceous spent shale derived from surface-retorting oil shale operations. In the context of his research, Schmidt-Collerus defined "carbonaceous" spent shale as being spent shale containing a significant residual or organic material (i.e., 2 to 5 percent by weight) after oil recovery. He asserts that certain retorting processes produce spent shale with up to 5 percent organic carbon residue. The actual composition of the resultant spent shale will depend on the type of retorting process used and the conditions



of retorting. At high retorting temperatures, about 964°C (1800°F), in which residual carbon is combusted as a heat source, nearly complete decomposition of the carbonates (present as dolomite and calcite) to their oxides occurs and the resultant spent shale is almost free of organic carbon residue. In contrast, oil shale retorted at lower temperatures (900 to 1000°F) without combustion of residual carbon as a heat source causes very little mineral decomposition and the resultant spent shale may contain 2 to 5 percent residual organic carbon.

Carbonaceous organic matter in spent shale does not consist only of elementary amorphous carbon (C)<sub>x</sub> but also contains organic compounds. Certain of these organic compounds are soluble in organic solvents and in some cases water. As a consequence of the pyrolytic process employed during retorting, part of the organic matter associated with the spent shale may include polynuclear or polycyclic aromatic hydrocarbons (PAH) and aza-azarines (AA) in addition to other types of higher molecular weight organic compounds. It is important to note that some PAH's have proven carcinogenic or mutagenic effects. In addition to PAH compounds, spent shale will likely contain other polyaromatic and lower molecular weight organic compounds.

The major activities associated with Schmidt-Collerus' research were: (1) collection of samples of carbonaceous spent shale from various retorting processes and analysis of benzene extracts of spent shale for polycondensed organic matter (POM), in particular polynuclear aromatic hydrocarbons (PAH), and (2) collection of samples of soil, water, vegetation, and air from various pristine (undeveloped) areas of potential future oil shale development and analysis of benzene extracts from polycondensed organic matter (POM), in particular polynuclear aromatic hydrocarbons (PAH).

The results of Schmidt-Collerus' investigation are summarized below:

1. Carbonaceous spent shale, with up to 5 percent organic carbon, contains higher molecular weight and lower molecular weight organic compounds soluble in organic solvents. Schmidt-Collerus attempted to extract organic material from spent shale samples by using benzene as a solvent. He found that the benzene-soluble fraction ranged from 0.02 percent to 0.2 percent by weight of the total mass of spent shale, depending on the retorting conditions employed.
2. The benzene-soluble portion of spent shale contains polycondensed organic matter (POM) such as polynuclear aromatic hydrocarbons (PAH) and aza-azarines (AA). The PAH compounds contain (among other components) benzo(a)pyrene and other known carcinogenic compounds.
3. The amount of benzene-soluble material in carbonaceous spent shale is about one or two orders of magnitude higher than in soils from pristine areas.

4. The content of benzo(a)pyrene in benzene extracts of carbonaceous spent shale is about three orders of magnitude greater than in benzene extracts of soils from pristine areas. Schmidt-Collerus classified the amount of benzo(a)pyrene present in the benzene extract of carbonaceous spent shale as being "more than mildly carcinogenic."
5. Results indicate that groundwater leachate derived from carbonaceous spent shale may be three to four orders of magnitude higher in PAH content than groundwater from pristine areas. It is asserted that groundwater can suspend and transport POM/PAH compounds in colloidal form to some extent.
6. Polynuclear aromatic compounds can apparently be leached from carbonaceous spent shale by water to a considerable extent in the presence of water soluble inorganic salts. Schmidt-Collerus believes that solubilization of POM compounds in groundwater may be enhanced by the presence of certain inorganic salts.

Extrapolating the results of his research, Schmidt-Collerus asserts that in-situ retorting of oil shale may produce vast amounts of carbonaceous residues underground, creating a potential for interaction between in-situ spent shale and groundwater (this assertion served as an impetus for much of the research summarized herein).

#### Colorado State University

Margheim (Ref. 1) and Ward et al. (Refs. 10, 11) assessed the water pollution potential of spent shale derived from above-ground retorting operations. Spent shale from three pilot plant processes was examined: (1) from the U.S. Bureau of Mines (USBM) gas combustion retorting process; (2) from the Union Oil Company (UOC) retorting process; and (3) from The Oil Shale Company (TOSCO) retorting process. The investigation consisted of determining the physical properties of each type of spent shale and the chemical characteristics of leachate derived from several experiments.

Several types of laboratory experiments were run in order to assess the quality of leachate derived from spent shale. The first type of experiment was classified as a "blender experiment" and consisted of taking a 100 gram sample of spent shale which passed through a No. 40 sieve, mixing it with 1000 milliliters of distilled water in a blender, and blending for five minutes. The second type of experiment, classified as a "shaker experiment," consisted of taking a 100 gram sample of spent shale which passed through a No. 40 sieve, placing it in a one gallon container to which one liter of distilled water was added, and manually shaking the container for five minutes. The third type of laboratory experiment was conducted only with the TOSCO spent shale: a column percolation experiment employing a plastic column 120 centimeters in length and 10 centimeters in diameter and filled with 12,500 grams of TOSCO spent shale. During the column percolation experiment, a constant

head of two centimeters was maintained on top of the column. Leachate was first observed about 14 days after initiation of the column percolation experiment. After initial observation of leachate, volumes of leachate were collected at various time intervals for chemical analysis.

Table 4 describes the conductance and chemical composition of the first eight samples of leachate collected from the column. As revealed by Table 4, various ions were readily leached from the TOSCO spent shale during the column percolation experiments. As expected, the conductance and concentration of various ions decreased as a function of percolation time. This suggests that much of the inorganic material associated with the spent shale was readily leachable during initial time periods of leaching while, subsequently, increasingly smaller amounts of inorganic material were leached. During the column percolation experiment, several samples were analyzed for organic carbon. About 86 mg/l of organic carbon were detected in a sample taken from the column after 1320 milliliters of water had percolated through and about 55 mg/l was detected after 3150 milliliters of water had percolated through.

Table 5 describes the mass of various ions leached from the three types of spent shale examined during the aforementioned experiments. As shown in Table 5, the concentration of most ions was significantly greater for the UOC spent shale than for the USBM and TOSCO spent shales. This may be attributable to uniquely different retorting conditions associated with the UOC retorting process.

#### Texas Tech University

Parker (Ref. 9) has completed preliminary experiments assessing the leaching of soluble materials from oil shale retorted under simulated in-situ conditions. His approach consisted of:

1. Retorting oil shale samples under a range of simulated in-situ conditions
2. Leaching the resultant spent shale with either distilled water or groundwater
3. Analyzing the leachate for chemical composition
4. Interpreting data in a mathematical framework to allow extrapolation to field conditions.

Parker designed and fabricated a small laboratory-scale retort that simulates in-situ retorting conditions. Using this retort, he produced various types of spent shale by varying retorting temperature, retorting time, and gaseous environment.

Preliminary experiments were designed to assess: (1) the quantity of various inorganic materials leached during specified time periods and (2) the effect of retorting variables on the leaching of various components. This initial set of experiments examined 50 gram samples

Table 4. Experimental results of percolation experiment conducted with TOSCO spent shale.

Sample No.	Volume of leachate sample, cm <sup>3</sup>	Conductance of sample, $\mu$ mhos/cm at 25°C	Concentration of sample, mg/l				
			Na <sup>+</sup>	Ca <sup>++</sup>	Mg <sup>++</sup>	SO <sub>4</sub> <sup>=</sup>	Cl <sup>-</sup>
1	254	78,100	35,200	3,150	4,720	90,000	3,080
2	340	61,600	26,700	2,145	3,725	70,000	1,900
3	316	43,800	14,900	1,560	2,650	42,500	913
4	150	25,100	6,900	900	1,450	21,500	370
5	260	13,550	2,530	560	500	8,200	205
6	125	9,200	1,210	569	579	5,900	138
7	155	7,350	735	585	468	4,520	138
8	250	6,825	502	609	536	4,450	80

Table 5. Material leached from spent shale samples (mg/100g).

Type of spent shale	Parameter	Quantity of leachate, mg/100g			
		Shaker experiment	Blender experiment	Column experiment	Average
TOSCO	TDS	1,120	1,260	1,060	1,150
	Ca <sup>++</sup>	102	114	64	93
	Mg <sup>++</sup>	31	27	40	39
	Na <sup>+</sup>	206	165	258	210
	Cl <sup>-</sup>	5	8	18	10
	SO <sub>4</sub> <sup>=</sup>	775	728	675	726
USBM	TDS	970	1090	—	1030
	Ca <sup>++</sup>	—	42	—	42
	Mg <sup>++</sup>	—	3.5	—	3.5
	Na <sup>+</sup>	—	225	—	225
	Cl <sup>-</sup>	—	13	—	13
	SO <sub>4</sub> <sup>=</sup>	—	600	—	600
UOC	TDS	—	10,000	—	10,000
	Ca <sup>++</sup>	—	327	—	327
	Mg <sup>++</sup>	—	91	—	91
	Na <sup>+</sup>	—	2,100	—	2,100
	Cl <sup>-</sup>	—	33	—	33
	SO <sub>4</sub> <sup>=</sup>	—	6,230	—	6,230

of oil shale retorted in the presence of air and in the absence of air. Four retorting temperatures - 430°, 483°, 630°, and 780°C - and two retorting times - 15 and 30 hours - were employed. These retorting temperatures were selected because they span a range of temperatures from that at which kerogen begins to pyrolyze at a considerable rate to that at which considerable carbonate decomposition can be expected.

After retorting, the residual spent shale (less than the original 50 grams of raw shale) was transferred to a bottle and 200 milliliters of distilled water was added. The spent shale and water were mixed together for 15 hours. The samples were allowed to settle for 5 hours and then the supernatant was decanted and filtered. Subsequently, the chemical composition of the filtrate was analyzed.

The results of this initial set of experiments are presented in Table 6. Table 6 reveals that, at lower retorting temperatures (430° and 483°C), far less material was solubilized when the oil shale was retorted in the absence of air than when the oil shale was retorted in the presence of air. At higher retorting temperatures (630° and 780°C), comparable amounts of material were solubilized when the oil shale was retorted either in the presence or absence of air.

Generally, more material was solubilized at higher retorting temperatures. The large amount of material solubilized at high retorting temperatures is likely attributable to carbonate decomposition which occurs at high retorting temperatures. Carbonate decomposition results in large amounts of calcium and magnesium oxides which produce high pH leachates. Indeed, at high retorting temperatures (630° and 780°C), high pH leachates were obtained from spent shale samples retorted both in the presence and absence of air. It is interesting to note that the lowest TDS concentration was encountered in leachate derived from spent shale retorted in the absence of air at low retorting temperatures, and that the TDS concentration in leachate from spent shale retorted in the presence of oxygen was higher than that in leachate from spent shale retorted in the absence of oxygen. This is likely due to the fact that air provides an oxidizing atmosphere for reaction with certain easily oxidized metals in the shale matrix, thus liberating these metals as ions. Another possible explanation is the formation of soluble salts involving acidic organic anions and metal cations.

For spent shale retorted both in the presence and absence of air, large amounts of toxic metals such as Cr and Zn were not observed in the leachate. It is possible that certain heavy metals are present as insoluble salts. However, considerable amounts of soluble metals such as sodium, potassium, and calcium were dissolved in the leachate.

In a progress report describing his research, Parker provided an excellent discussion of the actual mechanics of the leaching process. This discussion is summarized below. Spent shale must first cool to below the boiling point of water to permit leaching. This may require as much as several years for spent shale residing within an in-situ retort. After spent shale has cooled sufficiently, liquid water will

Table 6. Materials extracted from spent shale samples.

Retorting temp, °C	Quantity of material extracted, mg/100g							
	TDS	Ca	Mg	Na	K	Cr	Pb	Zn
Retorting time, hr	(A/NA) <sup>a</sup>	(A/NA) <sup>a</sup>	(A/NA) <sup>a</sup>	(A/NA) <sup>a</sup>	(A/NA) <sup>a</sup>	(A/NA) <sup>a</sup>	(A/NA) <sup>a</sup>	(A/NA) <sup>a</sup>
430/15	405/ 108	97/14	8/0.88	35/21	2.4/0.76	0.05/--	--/ --	0.020/0.001
430/30	409/ 80	97/ 6	2.9/0.62	34/13	2.1/0.04	0.02/--	--/ --	0.016/0.002
483/15	512/ 100	150/ 9	0.2/0.093	22/12	2.7/0.86	0.12/--	--/ --	0.011/0.001
483/30	558/ 86	160/ 6	0.01/0.072	26/14	3.4/0.85	0.13/--	--/ --	0.012/0.002
630/15	615/ 878	150/80	0.01/0.038	11/10	5.2/1.3	0.12/--	--/0.014	0.016/0.020
630/30	895/ 927	210/78	0.002/0.035	12/ 9	7.6/1.2	0 /--	--/0.017	0.021/0.015
780/15	944/1110	75/89	0.001/0.04	64/43	16/2.9	0.56/0.004	--/ --	0.017/0.025
780/30	833/ 595	68/44	0.001/0.034	77/21	18/2.3	1.8/0.002	--/ --	0.008/0.006

<sup>a</sup>A = retorted in presence of air; NA = retorted in absence of air.

contact the spent shale and will be drawn into the shale matrix by capillary forces. The influx of water through the shale matrix will slowly displace most of the gases present in the matrix (although gases that are relatively soluble in water will dissolve to a certain degree).

After the pore space of the shale matrix has been filled with water by capillary forces, molecular diffusion will serve as the vehicle for transferring soluble material both to and from the spent shale matrix and the groundwater in which it is immersed.

When spent shale is sufficiently cool to permit water to exist as a liquid, various chemical reactions may occur between the water and spent shale. If the water is derived from condensing steam, only the ions available from the spent shale will participate in these reactions. However, if groundwater contacts the spent shale, ions supplied by the groundwater will also participate in these reactions. When groundwater is involved in the leaching process, groundwater may remove various ions from the spent shale while other ions may be removed from the groundwater by the spent shale. These reactions between ions originally present in groundwater and leached ions may be attributed to metathesis.

It should be noted that Parker's discussion of the actual mechanics of leaching did not include mention of refluxing as a significant factor. The phenomenon of refluxing involves the continuous process of vaporization and condensation of water within the retort. As groundwater initially enters a hot retort, steam will be formed and the resultant steam will advance through the retort. This steam will eventually condense when it encounters a cool spot in the retort. Subsequently, this same condensed water may again vaporize when it encounters another hot spot. This dynamic and continuous process of refluxing will create both turbulence and pressure changes within the retort. Generally, it is asserted that this advancing front of refluxing water will tend to enhance mass transfer during leaching.

According to Parker an important retorting variable that may influence potential chemical reactions is retorting temperature. At temperatures above 550°C, carbonates are decomposed to oxides of magnesium and calcium which, in the presence of water, are hydrated to form hydroxides which have a higher solubility product than the carbonates. Thus, carbonate decomposition completely changes the character of the original oil shale, creating soluble components in the spent shale which may react with components of groundwater.

#### Laramie Energy Technology Center

Jackson et al. (Ref. 12) conducted experiments to assess the quality of leachate from in-situ spent shale. He examined three size ranges of spent shale particles produced during combustion runs employing LETC's 10-ton simulated in-situ retort.



TDS concentrations as high as 762 mg/l, organic carbon concentrations as high as 38 mg/l, and pH values as high as 11.2 were measured during experimentation. Jackson maintains that the mass of material leached is often influenced by the volume of water used for leaching purposes. Bearing in mind that Jackson used 10 ml water per gram of spent shale, the results of his experiments indicate that, on the average, about 440 ml of TDS and 36 ml of organic carbon were leached per 100 g of spent shale.

#### Bureau of Mines

Culbertson et al. (Ref. 13) conducted some limited experiments to assess the inorganic quality of leachate produced from both spent shale and shale ash. Shale ash is defined as spent shale in which the residual carbon remaining after retorting is burned for the purpose of heat recovery. For all practical purposes, shale ash strongly resembles spent shale derived from high-temperature combustion runs in which virtually all carbon is combusted to provide heat for the pyrolytic extraction of oil from oil shale.

Culbertson's experiments demonstrated a significant potential for high concentrations of calcium, sodium, and potassium in leachate with concentrations as high as 1080, 950, and 310 mg/l respectively. Furthermore, his experiments indicated that as much as 540 mg of calcium, 480 mg of sodium, and 160 mg of potassium were leached per 100 g of shale ash, depending on the burning conditions employed, while about 160 ml of calcium and 200 ml of sodium were leached per 100 g of the spent shale examined. It is asserted that leachate derived from shale ash will resemble leachate derived from spent shale produced by high-temperature-combustion runs.

#### University of Colorado

Runnells et al. (Ref. 14) conducted two types of experiments to assess the leaching of soluble materials from TOSCO surface-retorted spent shale. These experiments consisted of: (1) slurry experiments in which deionized water and spent shale were contacted in a slurry apparatus for varying time periods and (2) column experiments in which deionized water was percolated through a column filled and compacted with spent shale. Partial results of the slurry experiments conducted over a 127 day period are presented in Table 7.

It is interesting to note the high concentrations of fluoride detected during the slurry experiments. High concentrations of fluoride in water can preclude its use as drinking water. The high concentrations of boron detected are of concern because boron is extremely toxic to certain plants. High concentrations of boron could preclude the use of groundwater leachate for agricultural purposes.

Table 7. Mass of molybdenum, fluoride, and boron leached from TOSCO spent shale.

Parameter	Mass leached over 127-day period, mg/kg of spent shale
Mo	8
F	80
B	12

Colorado School of Mines

Hines (Ref. 15) is currently conducting research related to the adsorption of inorganic and organic components from gaseous and liquid wastestreams onto spent shale. The impetus behind this research is to determine the potential for treating liquid and gaseous wastestreams derived from in-situ oil shale processing by passing these wastestreams through columns of spent shale (in a manner similar to activated carbon adsorption columns).

As a subsequent phase of his research, Hines intends to initiate spent shale leaching studies. He intends to conduct batch studies and packed-bed studies with spent shale produced at several retorting temperatures. The primary variables to be considered include: type of solvent, solvent flow rate, particle size, retorting temperature, shale grade, mineral composition, and bulk density of the shale.

Certain data recently generated by Hines are particularly relevant to the research presented here. Hines retorted samples of oil shale in a laboratory-scale retort over a range of retorting temperatures. The resultant spent shale, produced in an inert gas environment, was then employed in the adsorption studies. After retorting, Hines characterized the organic carbon content of the spent shale samples. As would be expected, he found that the organic carbon content (on a percent by weight basis) was inversely related to retorting temperature. Thus, the highest organic carbon content was detected in the spent shale sample produced at the lowest retorting temperature (Ref. 16).

## CHAPTER 4

### PREPARATION OF SPENT SHALE SAMPLES AND PROCEDURE FOR DEFINING CHARACTERISTICS

Spent shale samples employed in this research were derived from Lawrence Livermore Laboratory's (LLL) pilot-scale 125-kilogram simulated in-situ retort. The raw oil shale used by LLL was mined from the Anvil Points area in Colorado. The Fischer Assay (i.e., potential oil yield) of the raw oil shale was 24 gallons per ton, and it contained 10.8 percent organic carbon by weight (Ref. 17).

Bulk samples of spent shale supplied by LLL consisted of approximately 10 kilograms taken from randomly selected areas of the pilot-scale retort. After removal from the retort, the spent shale was subjected to a brief grinding operation at LLL in order to provide a homogeneous sample for analysis.

Bulk spent shale samples received at the University of California at Berkeley campus (UCB) were initially divided into a series of subsamples by a splitting technique and, subsequently, these samples were recombined in a random manner. The total recombined sample was considered to be homogeneous and generally representative of the spent shale originally produced in the pilot-scale retort. The potential loss of volatile matter during splitting/recombination was considered to be insignificant.

Each homogeneous sample of spent shale was sieved and divided into two particle size ranges: a small particle size range of 0.14 to 0.28 centimeters (0.055 to 0.110 inches) and a large particle size range of 0.28 to 0.64 centimeters (0.10 to 0.250 inches). From these two particle size ranges, a composite particle size range of 0.14 to 0.64 centimeters was developed. The selection of these particle size ranges was somewhat arbitrary. Generally, larger particles are more likely to be non-homogeneous and, thus a particle size of 0.64 centimeters was selected as a lower limit because smaller "dust-like" particles will represent only a minor portion of the spent shale produced under actual field conditions at a commercial-scale facility.

Each spent shale sample was characterized according to its physical, chemical, and retorting characteristics. These characteristics are important because they can influence the groundwater pollution potential of in-situ spent shale. The physical and chemical characteristics of each spent shale sample were determined after the samples were received by UCB. The retorting characteristics were defined by LLL at the time the samples were shipped to UCB.

#### Physical Characteristics

The physical characteristics of spent samples were defined by the following parameters:

- particle size range
- bulk density
- porosity
- solid density
- permeability.

Particle Size Range. In effect, the particle size range of particular spent shale samples was defined a priori by the sieve sizes employed during the sieving step of the sample preparation procedure. Prepared samples were characterized by the three aforementioned particle size ranges; a small particle size range of 0.14 to 0.28 centimeters, a large particle size range of 0.28 to 0.64 centimeters, and a composite particle size range encompassing the small and large particle size range (i.e., 0.14 to 0.64 centimeters).

Bulk Density. The following procedure was used in determining the bulk density of spent shale samples. An aliquot of spent shale of known weight was introduced into a graduated cylinder and compacted by tapping a rubber mallet on the side of the cylinder for a 60-second time period. Afterward, the volume of the spent shale sample was observed and recorded. The bulk density was thus determined by:

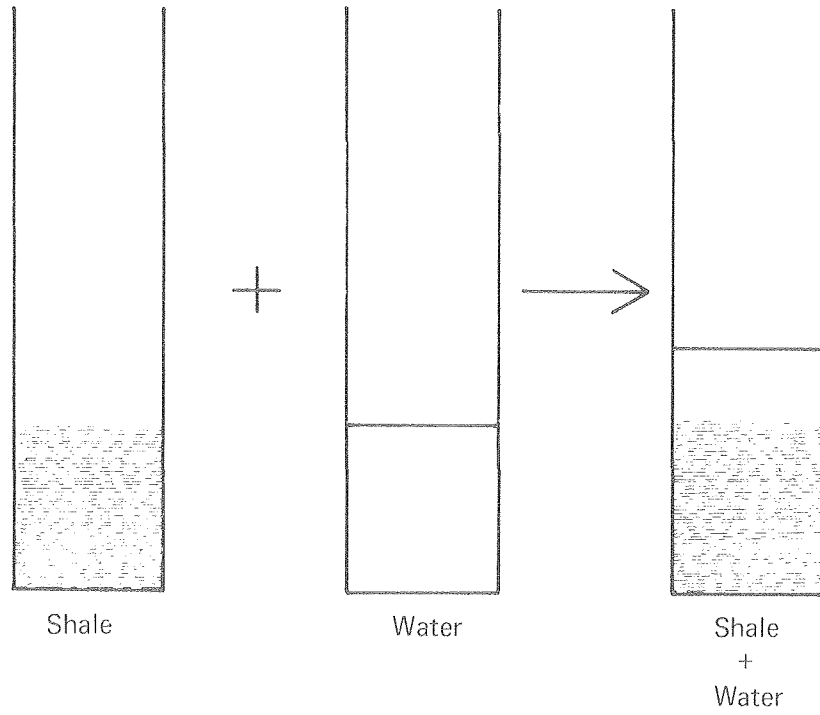
$$\text{Bulk Density} = \frac{\text{Weight of Spent Shale}}{\text{Volume of Spent Shale}}$$

Porosity. The porosity of spent shale samples was determined by the following procedure. In a manner similar to the determination of bulk density, an aliquot of spent shale was introduced into a graduated cylinder and compacted for 60 seconds after which the volume was observed and recorded. A known volume of distilled water (greater than the bulk volume of the compacted spent shale) was introduced into the cylinder; the cylinder was sealed off from the atmosphere; and the mixture of water and spent shale was allowed to sit for 24 hours. After 24 hours, the total volume was observed and recorded and the porosity was computed by:

$$\text{Porosity} = 1 - \frac{\text{Total Volume} - \text{Spent Shale Volume}}{\text{Spent Shale Volume}}$$

A schematic of the porosity determination is presented in Figure 8.

It should be recognized that this method of determining porosity does not differentiate between "macro-porosity" and "micro-porosity". Macro-porosity is due to the interstices between adjacent particles of shale while micro-porosity is due to the semi-porous infrastructure



XBL 792-523

Figure 8. Schematic of porosity determination.

of each individual shale particle. Based on what is known about the shape and structure of spent shale particles, it is roughly estimated that micro-porosity accounts for less than 10 to 20 percent of the total porosity.

Solid Density. If porosity and bulk density have previously been determined, there is no need for a direct determination of solid density. The solid density can be computed from the results of the porosity and bulk density determinations as follows:

$$\text{Solid Density} = \frac{\text{Bulk Density}}{(1 - \text{Porosity})}$$

The above procedure assumes that spent shale does not "swell" upon wetting. Based on both observation and a knowledge of the structural characteristics of spent shale, it is asserted that discernible "swelling" does not occur.

Permeability. The permeability of spent shale samples was determined by use of a laboratory permeameter, a schematic of which is shown in Figure 9. The determination of permeability consisted of filling and compacting a column with spent shale. The compaction procedure consisted of introducing incremental volumes of spent shale into the column and, after each increment, tapping the column with a rubber mallet for 60 seconds. The dimensions of the column were 12 inches in length by one inch in diameter. After the column was filled and compacted with spent shale, it was connected to the permeameter described in Figure 9. The permeameter was then operated at several flow rates and after steady-state conditions were attained, the incurred head loss at each flow rate was observed and recorded. Knowing the incurred head loss, the flow rate, and the length and diameter of the column, Darcy's Law was used to compute the permeability (Ref. 18). Darcy's Law is given by:

$$v = Ks$$

$$\text{and } K = \frac{v}{s}$$

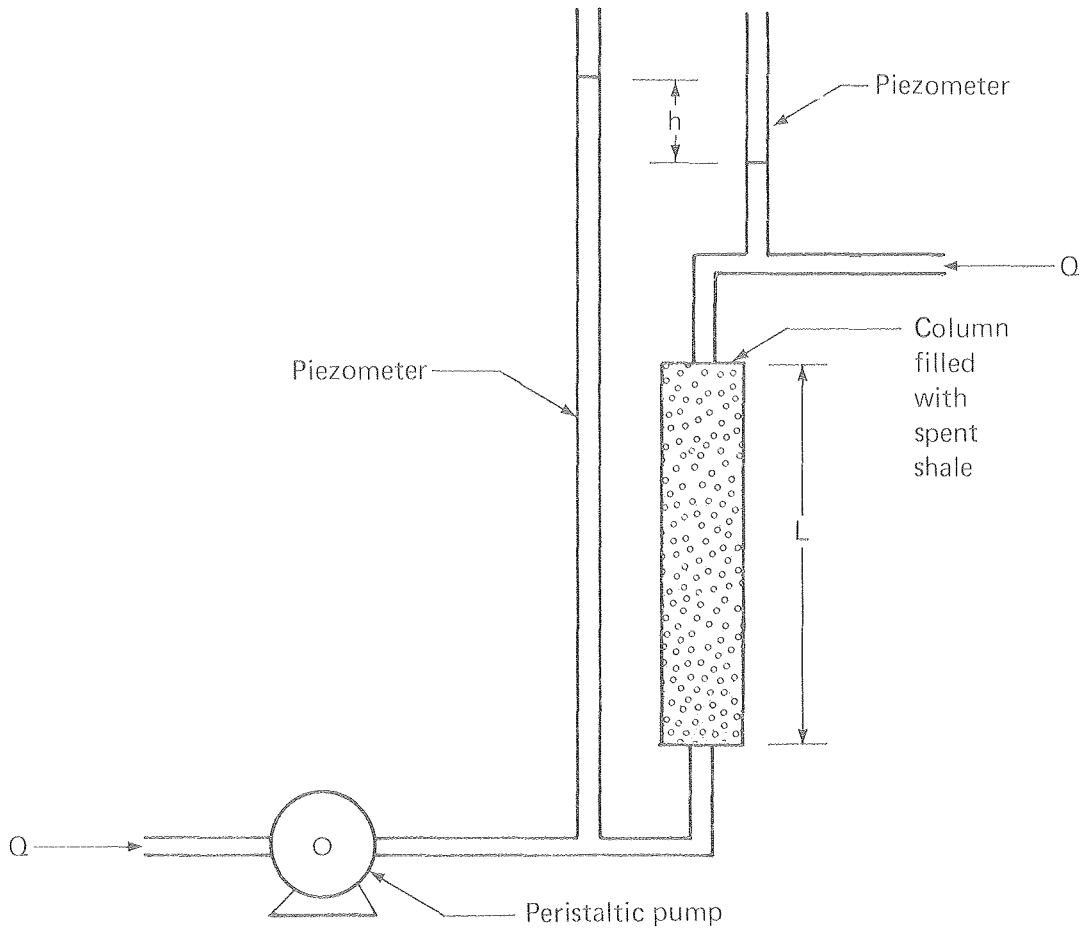
where K = coefficient of permeability (gallons per day/feet<sup>2</sup>)

v = approach velocity = Q/A (feet/day)

s = hydraulic gradient = h/L (feet/feet)

Q = flow rate (feet<sup>3</sup>/day)

A = cross-sectional area of column (feet<sup>2</sup>)



XBL 792-524

Figure 9. Laboratory permeameter.

$h$  = incurred head loss (feet)

$L$  = length of column (feet)

Employing Darcy's Law, several approximations of  $K$  (coefficient of permeability) were derived from the several corresponding values of incurred head loss and flow rate. The several approximations of  $K$  were then averaged to provide an overall estimate of permeability. Permeability is an important parameter because it describes the ability of water to flow through a particular type of porous material. Thus, the permeability of a spent shale sample will affect the time of contact between parcels of water and individual particles of spent shale which will in turn affect the leaching phenomenon.

#### Chemical Characteristics

An important characteristic of a spent shale sample is its organic carbon content on a percent by weight basis. A determination of the organic carbon content of a spent shale sample provides some indication of the potential mass of organic material that may be leached although it does not indicate the solubility of this organic material in water nor how this organic material is associated with the spent shale matrix.

Analysis for the organic carbon content of solid spent shale samples was accomplished with a Dietert Carbon Analyzer which is often used in determining the organic carbon content of sediments and sludge samples. The procedure involves the combustion of organic carbon to  $CO_2$  which is subsequently measured by the following technique. The amount of  $CO_2$  produced is measured by bringing a gaseous sample of known volume into contact with the hydroxide to form potassium carbonate. During this reaction,  $CO_2$  disappears from the gaseous phase and the potassium carbonate formed remains in the liquid phase. Therefore, the loss in volume of the gas is equal to the  $CO_2$  content.

#### Retorting Characteristics

Retorting characteristics represent the most important category of spent shale characteristics related to the leaching phenomenon. Previous studies have demonstrated that the conditions employed during the retorting of oil shale will greatly influence both the characteristics of the resultant spent shale and the quality of leachate derived from the spent shale. With respect to spent shale characteristics, the most important characteristics employed during retorting include:

- Gaseous Environment
- Retorting Temperature
- Retorting Rate



It should be noted that the retorting characteristics of spent shale samples are explicitly defined by the documented history of the retorting run. Specifically, Lawrence Livermore Laboratory provided a detailed retorting history of all spent shale samples given to the University of California.

Gaseous Environment. One of three general types of gaseous environment exists during oil shale retorting: (1) air, (2) air plus recycle gas, or (3) inert gas (such as nitrogen). The recycle gas will largely consist of both inert components as well as a variety of non-condensable hydrocarbons. The role of these gaseous environments in the retorting process is described in Chapter 1.

When the gaseous environment includes air (with or without recycle gas), combustion conditions exist during retorting and most residual organic material remaining on the shale after oil extraction is combusted to provide heat for pyrolysis. In contrast, combustion of residual organic material does not occur during an inert gas run in which combustion conditions do not exist. When recycle gas is employed, this provides an opportunity for certain volatile organic compounds to adsorb or condense onto particles of spent shale behind the flame front in the retort. Thus, it should be apparent that the gaseous environment employed during retorting can greatly affect the characteristics of spent shale and its susceptibility to leaching.

Retorting Temperature. The temperature employed during retorting can significantly affect the characteristics of the resultant spent shale. Retorting temperatures above 620°C (1150°F) result in carbonate decomposition which weakens the structure of the spent shale matrix and results in high TDS concentrations in leachate. When air is employed as a gaseous environment, higher retorting temperatures will lead to more complete combustion whereas, when an inert gas is employed as a gaseous environment, higher retorting temperatures will lead to the formation of different pyrolysis products than at lower temperatures.

Retorting Rate. Retorting rate is defined as the rate at which the zone of maximum temperature moves through a retort. A slower retorting rate, although perhaps less economical in shale oil production, will result in more complete pyrolysis and, when air is employed as a gaseous environment, in more complete combustion of residual organic material associated with the spent shale.

## CHAPTER 5

### LABORATORY LEACHING EXPERIMENTS

An effective assessment of the potential contamination of ground-water by organic material leached from in-situ spent shale requires the development of a series of laboratory-scale leaching experiments to generate required data. Two general categories of laboratory experiments were employed to assess the leaching of organic material from in-situ spent shale. These included:

- batch experiments
- continuous-flow column experiments

#### Batch Experiments

Two specific types of batch experiments were conducted:

- kinetic batch experiments
- equilibrium batch experiments

Kinetic Batch Experiments. The kinetic batch experiments (hereafter referred to simply as batch experiments) involved placing a small amount of spent shale (50 grams) into an individual flask and subsequently adding a fixed small volume of water (50 milliliters). After sealing the flask, it was allowed to quiescently sit for a designated time period, ranging from 0.5 to 30 days. At the end of the designated time period, all of the resultant leachate was decanted from the flask. (It should be noted that an individual flask was prepared in the above manner for each leaching time period investigated. This implies that a series of flasks containing spent shale and water were required to examine a range of leaching time periods for a particular type of spent shale under specified experimental conditions). The flasks employed during the batch experiments were 300 milliliter biochemical oxygen demand (BOD) and 300 milliliter Erlenmeyer flasks with ground glass tops. The BOD flasks were employed in experiments conducted at an ambient water temperature while the Erlenmeyer flasks were employed in experiments conducted at an elevated water temperature.

The leachate decanted from each flask was subsequently filtered through a Whatman GF/C fiberglass filter to remove suspended material. The filtrate, containing both dissolved and colloidal material, was then analyzed in order to define the quality of the leachate. (The conducted analyses are described in a following section.)

The major impetus behind the batch experiments was to identify factors that influence the leaching of organic material from in-situ spent shale. By employing a relatively simple system such as a batch

experiment, a number of experimental conditions can be varied in an attempt to define factors that influence the leaching phenomenon. Another obvious objective of the kinetic batch experiments was to assess the kinetics (i.e., changes in leachate quality as a function of time) of the leaching phenomenon.

Equilibrium Batch Experiments. The equilibrium batch experiments were generally similar in concept to the kinetic batch experiments. Employing the same type of flasks, a small amount of spent shale (50 grams) was placed into a flask and subsequently a variable amount of water was added (30 to 200 milliliters). After sealing the flask, it was allowed to sit quiescently for a period of 30 days. At the end of 30 days, the leachate was decanted, filtered, and analyzed for various parameters.

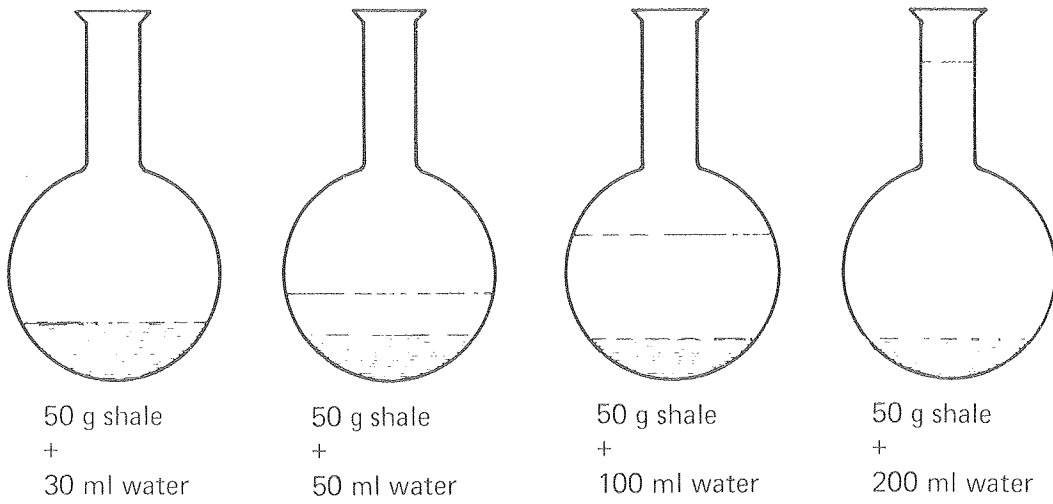
The major impetus behind the equilibrium batch experiments was to generate data enabling the development of equilibrium isotherms. It was assumed that 30 days were adequate for the establishment of equilibrium conditions. (This original assumption was verified by preliminary findings suggesting that 30 days appeared to be an adequate time period for the establishment of "pseudo-equilibrium" conditions).

A major limitation of the kinetic batch experiments described previously is that only one shale-to-water ratio was examined (i.e., 50 grams of shale to 50 milliliters of water). It is important to note that the shale to water ratio may significantly affect the quality of the resultant leachate. Intuitively, one would expect a different leachate quality if 50 grams of shale were mixed with 100 milliliters of water than if 50 grams of shale were mixed with 50 milliliters of water. Furthermore, the use of only one shale to water ratio does not provide any indication of whether saturated or unsaturated conditions exist with respect to various components of the leachate. However, by running a series of batch experiments which encompass a range of shale to water ratios, the equilibrium batch experiments (1) enable an assessment of the effect of shale-to-water ratio, (2) provide an indication of whether standard or unsaturated conditions exist, and (3) provide data for the development of equilibrium isotherms. A discussion of equilibrium isotherms is presented in a subsequent section related to data analysis.

A schematic describing the equilibrium batch experiments is presented in Figure 10. An important differentiation between the equilibrium batch experiments and the previously discussed kinetic batch experiments is that time is not a variable in the equilibrium batch experiments (30 days is considered adequate for the establishment of equilibrium conditions).

#### Experimental Variables Examined in the Batch Experiments

The experimental variables examined in the batch experiments included:



XBL 792-518

Figure 10. Schematic of equilibrium batch experiments.

- particle size range of spent shale
- retorting conditions associated with spent shale
- leaching time period
- water temperature
- water quality.

Examination of all the above variables in both types of batch experiments would (1) require an enormous amount of laboratory work and (2) generate a certain amount of redundant data. Consequently, a decision was made to examine only certain variables in each type of batch experiment. For example, if the effect of particle size was assessed in one type of batch experiment by examining both a small particle size range and a large particle size range, it seemed appropriate to examine only a composite particle size range in the other type of batch experiment.

Two general particle size ranges were examined during the kinetic experiments; a small particle size range of 0.14 to 0.28 centimeters and a large particle size range of 0.28 to 0.64 centimeters. The equilibrium batch experiments examined a composite particle size range of 0.14 to 0.64 centimeters.

Three general categories of retorting conditions were examined during the batch experiments, including (1) combustion runs, (2) combustion runs employing recycle gas, and (3) inert gas runs. The kinetic batch experiments examined all three categories of retorting conditions while the equilibrium batch experiments examined only combustion runs and inert gas runs. These three categories of retorting conditions encompass the range of retorting conditions that have thus far been studied by Lawrence Livermore Laboratory in their experimental retort.

The leaching time period examined during the kinetic batch experiments ranged from 0.5 to 30 days. This time period was selected to provide an indication of both short-term and long-term leaching phenomena. The maximum leaching time period, 30 days, was initially thought to be adequate for development of "pseudo-equilibrium" conditions. The leaching time period employed for the equilibrium batch experiments was a constant 30 days.

Two water temperatures were examined during the kinetic and equilibrium batch experiments, 20°C and 80°C. The lower of those two temperatures, 20°C, represents the ambient room temperature of the laboratory in which the experiments were conducted and is felt to be approximately representative of groundwater temperatures in the oil shale region. The higher temperature, 80°C, is felt to be approximately representative of water temperatures within an abandoned retort which has not cooled to ambient temperatures; water temperatures within a recently abandoned retort will likely approach 100°C.

Two general categories of water quality were examined during both the batch experiments: distilled water and synthetic groundwater.

The synthetic groundwater employed in the batch experiments was produced in a laboratory by mixing specified amounts of several reagent grade chemicals with distilled water. Specifically, the synthetic groundwater was prepared by mixing 6.0 grams of  $\text{NaHCO}_3$ , 2.0 grams of  $\text{NaCl}$ , 1.0 gram of  $\text{Na}_2\text{CO}_3$  and 1.0 gram of  $\text{Na}_2\text{SO}_4$  to a liter of distilled water. Thus, the only cation present in the synthetic groundwater was sodium while bicarbonate, carbonate, chloride, and sulfate were present as anions.

The rationale for employing the above mixture as synthetic groundwater is as follows. It was felt that synthetic groundwater should be generally indicative of poor quality groundwater from the lower aquifer of the Piceance Creek Basin and of poor quality groundwater throughout the oil shale region. The quality of groundwater from the lower aquifer of the Piceance Creek Basin was previously described in Table 3. Close scrutiny of Table 3 reveals that sodium, is by far, the most predominant cation while bicarbonate, chloride, and sulfate represent the major anions. Thus, laboratory groundwater was synthesized to roughly simulate the groundwater described in Table 3.

It should be recognized that the actual composition of synthetic groundwater will play a significant role in the leaching phenomenon. For example, a calcium-dominated groundwater would likely produce significantly different results than a sodium-dominated groundwater. Thus, many of the results presented in this thesis may be peculiar to the specific type of synthetic groundwater employed. Furthermore, it should be recognized that the inorganic quality of synthetic groundwater will change as a function of time during the leaching process. These changes in inorganic quality will result from (1) the leaching of inorganic material from spent shale, (2) ion exchange mechanisms involving the spent shale matrix, and (3) precipitation reactions.

The specific conductivity of the synthetic groundwater was 12,000 mhos/cm while its pH was 9.0. In contrast, the specific conductivity of the distilled water was only 19 mhos/cm while its pH was 7.8.

In addition to the above experimental conditions, the equilibrium batch experiments also examined various shale-to-water ratios including:

- 50 grams of shale and 30 milliliters of water
- 50 grams of shale and 50 milliliters of water
- 50 grams of shale and 100 milliliters of water
- 50 grams of shale and 200 milliliters of water

### Continuous-Flow Column Experiments

In the continuous-flow experiments, one-inch diameter columns of various lengths were each filled and compacted with a particular type of spent shale. The actual columns were fabricated from PVC piping. After compaction, a peristaltic pump was used to pump water through the packed column at a specified flow rate for a 96-hour time period. Time-averaged composite samples of leachate were collected in an enclosed container at designated time intervals. These composite samples were subsequently filtered through a Whatman GF/C fiberglass filter and analyzed for a series of quality characteristics that are described in the following chapter. A schematic of the continuous-flow column experiments is presented in Figure 11.

The major impetus behind the continuous-flow column experiments was an attempt to simulate the leaching phenomenon under actual field conditions. This concept is based on the premise that an actual in-situ retort will resemble a large column through which groundwater flows on a once-through basis.

It was initially anticipated that the major difference between the results of the column experiments and the results of the previously described batch experiments would be a more "rapid" leaching rate during the column experiments due to the continual replenishment of organic-laden leachate within the column by either distilled water or synthetic groundwater devoid of organic material. According to mass transfer theory, this would tend to enhance the leaching of organic material from spent shale.

#### Experimental Variables Examined in the Continuous-Flow Column Experiments

The experimental variables examined in the column experiments included: retorting conditions associated with spent shale, leaching time period, rate of flow, and column length. Experimental variables relating to retorting conditions were similar to those examined during the batch experiments; three general categories of retorting conditions were examined. However, only one water temperature, 20°C, one initial water quality, distilled water, and one particle size range, a composite particle size range of 0.14 to 0.64 centimeters, were examined during the column experiments.

The leaching time periods examined during the column experiments ranged from 0 to 96 hours. The overall 96-hour period was selected primarily as a matter of convenience; an experiment initiated on Monday morning could be terminated on Friday morning. It was felt that a much shorter time period (96 hours) than that employed during the batch experiments (30 days) would prove adequate due to the continual replenishment of leachate with distilled water which could tend to enhance the overall rate of leaching. Within the 96-hour time period, the actual time periods at which time-averaged composite samples were collected were selected in such a manner as to provide an indication

Two general categories of water quality were examined during both the batch experiments: distilled water and synthetic groundwater.

The synthetic groundwater employed in the batch experiments was produced in a laboratory by mixing specified amounts of several reagent grade chemicals with distilled water. Specifically, the synthetic groundwater was prepared by mixing 6.0 grams of  $\text{NaHCO}_3$ , 2.0 grams of  $\text{NaCl}$ , 1.0 gram of  $\text{Na}_2\text{CO}_3$  and 1.0 gram of  $\text{Na}_2\text{SO}_4$  to a liter of distilled water. Thus, the only cation present in the synthetic groundwater was sodium while bicarbonate, carbonate, chloride, and sulfate were present as anions.

The rationale for employing the above mixture as synthetic groundwater is as follows. It was felt that synthetic groundwater should be generally indicative of poor quality groundwater from the lower aquifer of the Piceance Creek Basin and of poor quality groundwater throughout the oil shale region. The quality of groundwater from the lower aquifer of the Piceance Creek Basin was previously described in Table 3. Close scrutiny of Table 3 reveals that sodium, is by far, the most predominant cation while bicarbonate, chloride, and sulfate represent the major anions. Thus, laboratory groundwater was synthesized to roughly simulate the groundwater described in Table 3.

It should be recognized that the actual composition of synthetic groundwater will play a significant role in the leaching phenomenon. For example, a calcium-dominated groundwater would likely produce significantly different results than a sodium-dominated groundwater. Thus, many of the results presented in this thesis may be peculiar to the specific type of synthetic groundwater employed. Furthermore, it should be recognized that the inorganic quality of synthetic groundwater will change as a function of time during the leaching process. These changes in inorganic quality will result from (1) the leaching of inorganic material from spent shale, (2) ion exchange mechanisms involving the spent shale matrix, and (3) precipitation reactions.

The specific conductivity of the synthetic groundwater was 12,000 mhos/cm while its pH was 9.0. In contrast, the specific conductivity of the distilled water was only 19 mhos/cm while its pH was 7.8.

In addition to the above experimental conditions, the equilibrium batch experiments also examined various shale-to-water ratios including:

- 50 grams of shale and 30 milliliters of water
- 50 grams of shale and 50 milliliters of water
- 50 grams of shale and 100 milliliters of water
- 50 grams of shale and 200 milliliters of water



### Continuous-Flow Column Experiments

In the continuous-flow experiments, one-inch diameter columns of various lengths were each filled and compacted with a particular type of spent shale. The actual columns were fabricated from PVC piping. After compaction, a peristaltic pump was used to pump water through the packed column at a specified flow rate for a 96-hour time period. Time-averaged composite samples of leachate were collected in an enclosed container at designated time intervals. These composite samples were subsequently filtered through a Whatman GF/C fiberglass filter and analyzed for a series of quality characteristics that are described in the following chapter. A schematic of the continuous-flow column experiments is presented in Figure 11.

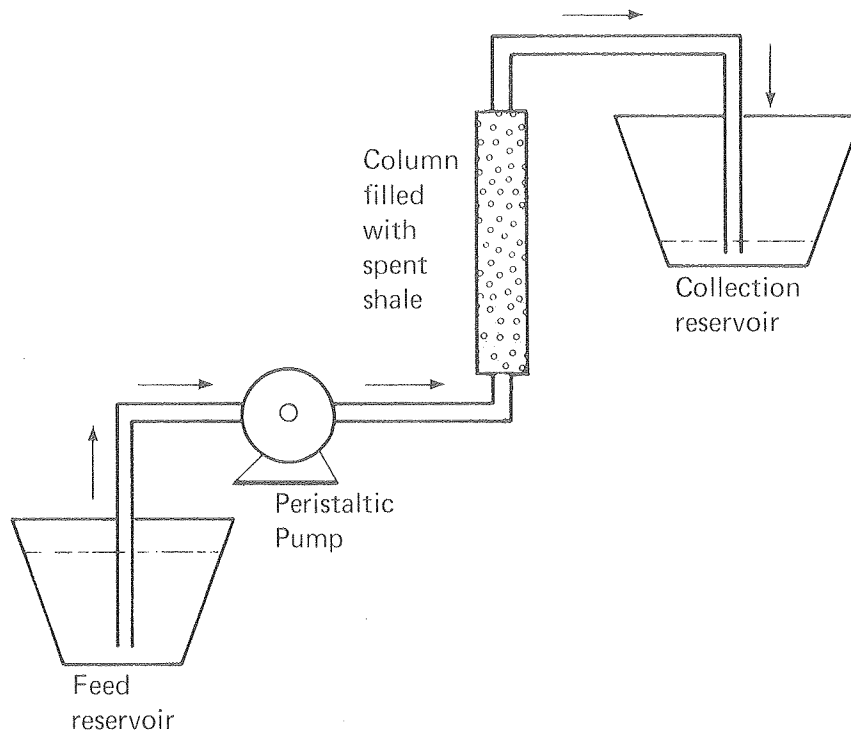
The major impetus behind the continuous-flow column experiments was an attempt to simulate the leaching phenomenon under actual field conditions. This concept is based on the premise that an actual in-situ retort will resemble a large column through which groundwater flows on a once-through basis.

It was initially anticipated that the major difference between the results of the column experiments and the results of the previously described batch experiments would be a more "rapid" leaching rate during the column experiments due to the continual replenishment of organic-laden leachate within the column by either distilled water or synthetic groundwater devoid of organic material. According to mass transfer theory, this would tend to enhance the leaching of organic material from spent shale.

### Experimental Variables Examined in the Continuous-Flow Column Experiments

The experimental variables examined in the column experiments included: retorting conditions associated with spent shale, leaching time period, rate of flow, and column length. Experimental variables relating to retorting conditions were similar to those examined during the batch experiments; three general categories of retorting conditions were examined. However, only one water temperature, 20°C, one initial water quality, distilled water, and one particle size range, a composite particle size range of 0.14 to 0.64 centimeters, were examined during the column experiments.

The leaching time periods examined during the column experiments ranged from 0 to 96 hours. The overall 96-hour period was selected primarily as a matter of convenience; an experiment initiated on Monday morning could be terminated on Friday morning. It was felt that a much shorter time period (96 hours) than that employed during the batch experiments (30 days) would prove adequate due to the continual replenishment of leachate with distilled water which could tend to enhance the overall rate of leaching. Within the 96-hour time period, the actual time periods at which time-averaged composite samples were collected were selected in such a manner as to provide an indication



XBL 792-531

Figure 11. Schematic of continuous-flow column experiments.

of both short-term and long-term leaching phenomena. The total leaching time period, 96 hours, was originally thought to be adequate for leaching most of the leachable organic material.

A water flow rate of 0.6 milliliters per minute was employed during the column experiments. The selection of this flow rate was based on the measured permeability of compacted columns (approximately 50 gallons per day per square foot) and the approximate head differential between the upper and lower aquifers in the Piceance Creek Basin (10 meters) in the vicinity of potential in-situ development (Ref. 3).

Two column lengths were examined during the continuous-flow column experiments: 12 inches and 6 inches. The major criteria for selection of column lengths included (1) cost of materials, (2) a column size appropriate for a laboratory environment, and (3) the limited amount of each spent shale sample available.

Summary of Experimental Variables Examined in the Batch and Continuous-Flow Column Leaching Experiments

A summary of experimental variables examined during the batch and continuous-flow column experiments is presented in Table 8. As revealed by Table 8, the kinetic batch experiments examined the greatest number of variables. This is consistent with the proposed rationale for the kinetic batch experiments--the identification of factors that influence the leaching of organic material from in-situ spent shale. The other types of experiments examined only particular variables of concern, based on the rationale behind the experiment.

Table 8. Experimental variables examined in leaching experiments.

Variable	Kinetic batch experiments	Equilibrium batch experiments	Column experiments
Particle size range	X		
Retorting conditions	X	X	X
Leaching time period	X		X
Water temperature	X	X	
Water quality	X	X	
Shale-to-water ratio		X	
Column length			X
Rate of flow			X

## CHAPTER 6

### ANALYTICAL PROCEDURES FOR DEFINING QUALITY OF LEACHATE

A series of analyses was conducted to define the quality of leachate samples derived from the previously described leaching experiments. Although most emphasis was placed on defining the organic quality of leachate, it was considered advantageous to analyze samples for certain inorganic parameters that would provide basic insight into the leaching phenomenon.

In the field of sanitary chemistry, the analysis and characterization of organic material present in samples of water and wastewater can be made on several levels of sophistication (Refs. 19-21):

1. A gross estimate of the organic material present in a water sample can be obtained by conducting composite or "lumper" analyses that provide a general indication of the overall levels of organic material present but do not distinguish between the various organic components. Typical composite or "lumper" analyses include Total Organic Carbon (TOC) and Chemical Oxygen Demand (COD).
2. A more refined estimate of the types and amounts of organic components present in a water sample can be obtained by testing for the presence of (a) particular functional groups or classes of organic compounds or (b) groups of organic compounds with similar properties based on their solubility in various solvents or their acid/base character.
3. The most precise estimate of the types and amounts of organic material present in a water sample can be obtained by testing for the presence of specific organic compounds. The tests employ various sophisticated instrumental methods such as chromatography, mass spectroscopy, etc., in conjunction with extraction and concentration techniques.

It is apparent that a detailed characterization of the organic composition of leachate could be derived if leachate samples are analyzed according to all three levels of sophistication described above. However, it is asserted that such a detailed characterization would be somewhat unreasonable because it would severely limit the total number of samples that could be analyzed and the number of experimental conditions that could be examined. Clearly, the two extremes available were (1) to produce only a few samples of leachate under select conditions and subsequently analyze them in great detail or (2) to produce many leachate samples under a wide range of conditions and analyze them in considerably less detail. The latter approach was selected because it is not presently clear which specific experimental conditions are important with respect to future oil shale development. Thus, the latter approach allows a wide range of many experimental conditions to be examined.

In light of the above remarks, it was proposed that only a partial analysis of organics be conducted with analyses being limited to the following:

- Total Organic Carbon (TOC)
- Acid/Base/Neutral Fractions of Organic Material
- Organic Nitrogen
- Phenols

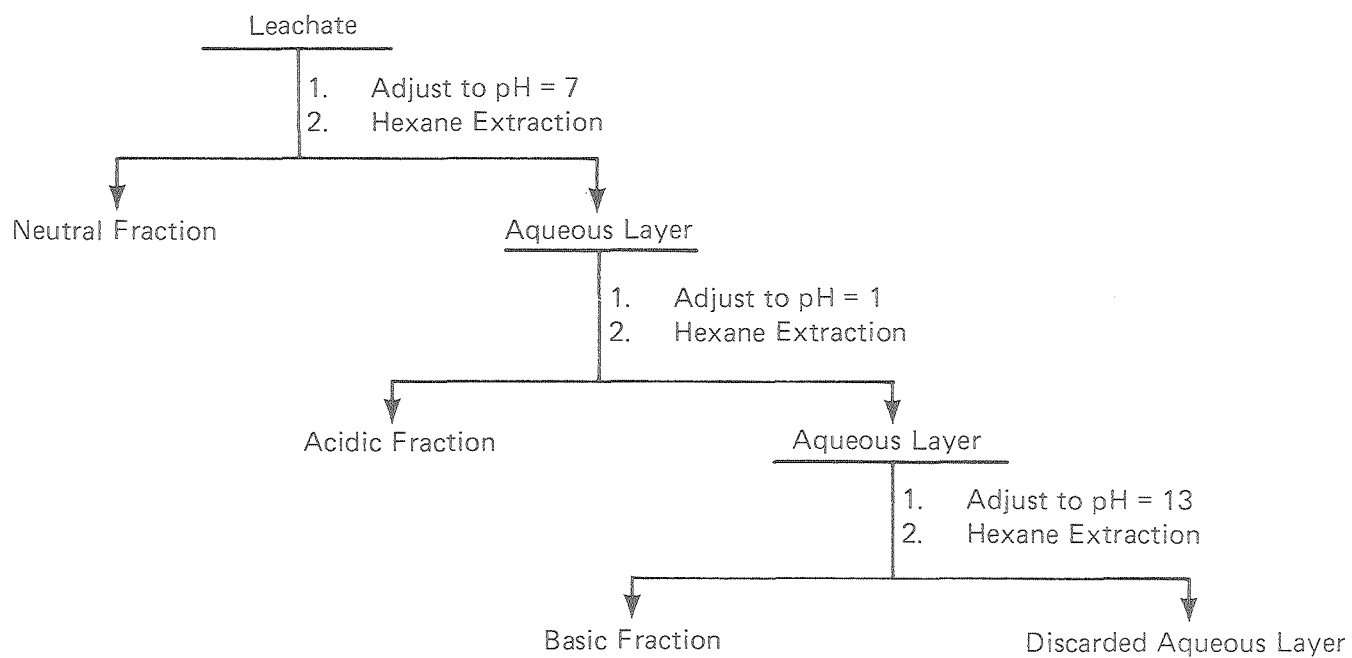
Analysis for TOC was accomplished by utilizing a Beckman total organic carbon analyzer. The basic principle behind the organic carbon analyzer involves the conversion of organically bound carbon atoms to CO<sub>2</sub> within an internal combustion chamber. The CO<sub>2</sub> produced is subsequently measured by an infrared analyzer. Analysis for TOC provides a general indication of the total amount of organic material present in leachate, since the carbon atom is the basic building block of all organic compounds.

The major limitation associated with assessing the organic quality of leachate by TOC measurements is that an estimate of organic carbon does not provide any indication of the types of organic compounds that may be present. In order to compensate for this limitation and to provide a more refined characterization, the organic material present in leachate samples was fractionated into acid, base, and neutral fractions. The determination of acid, base, and neutral fractions provides a general indication of the classes of organic compounds that may be present in leachate (Ref. 22).

Employing the extraction/fractionation technique presented in Figure 12, the organic material can be divided into three fractions based on the acid/base character of various organic compounds. The technique involves extraction of leachate samples with hexane at various pH values. The hexane is subsequently driven off using a rota-vacuum, leaving a residue that is desiccated and weighed. In this manner, the relative proportions of acid, base, and neutral fractions can be determined.

It is a common procedure in qualitative organic analysis to classify organic compounds according to their acid/base character. An acid is defined as a proton donor while a base is defined as a proton acceptor. Thus, some organic compounds behave as acids, some behave as bases, and some are neutral in character. Examples of organic compounds classified according to their acid/base character include (1) carboxylic acids, phenols, and mercaptans as acidic compounds, (2) amines, amino heterocyclics, and pyridines as basic compounds, and (3) hydrocarbons, aldehydes, and ketones as neutral compounds. Classification of organic compounds according to their acid/base character is particularly appropriate for water-soluble compounds.

EXTRACTION/FRACTIONATION TECHNIQUE: Acid, Base, and Neutral Fractions

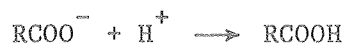


-47-

XBL 792-526

Figure 12. Extraction fractionation technique.

As indicated by the extraction/fractionation technique shown in Figure 12, the pH of the sample is first adjusted to 7 and neutral organic compounds are extracted from the water with hexane. The pH of the leachate is then adjusted to 1 and acidic organic compounds are extracted with hexane. At low pH (i.e., a pH of 1), acidic compounds exist in their un-ionized form as demonstrated below:



The un-ionized form of most organic acids is only sparingly soluble in water but is significantly soluble in a non-polar solvent such as hexane. Thus by lowering the pH to 1, the water-soluble radical  $\text{RCOO}^-$  is converted to the un-ionized  $\text{RCOOH}$  which is readily extractable with hexane. After acidic materials are extracted, the pH of the leachate is raised to 13 and basic organic compounds are extracted with hexane. At a high pH (i.e., a pH of 13), basic organic compounds exist in their un-ionized form as demonstrated below;



In a manner similar to organic acids, the un-ionized form of most organic bases is only sparingly soluble in water and thus is readily extracted by a non-polar solvent such as hexane. By raising the pH to 13, the water-soluble radical  $\text{RNH}_3^+$  is converted to the un-ionized  $\text{RNH}_2$  which is significantly more soluble in hexane. Thus, in summary, consecutive extractions at pH values of 7, 1, and 13 yield neutral, acidic, and basic fractions of organic material, respectively.

A major limitation associated with the above extraction/fractionation technique is that phenols behave as weak acids. As a consequence, one would expect the stronger phenols to be extracted in the acid fraction while the weaker phenols would be extracted in the neutral fraction. Thus, it should be recognized that one so-called "neutral" fraction may contain a significant amount of phenolic material. Furthermore, since higher molecular weight phenolics are not very soluble in hexane, appreciable amounts of phenolic material may not be extracted at all.

Analysis for organic nitrogen was accomplished by employing a "micro" Kjeldahl technique. The procedure is basically similar to the Kjeldahl Nitrogen Analysis described in Ref. 23 with certain modifications to allow detection of trace quantities. The technique basically involves an acid digestion step in which the amino nitrogen of many organic compounds is quantitatively converted to ammonium sulfate. Subsequently, the ammonia is distilled from an alkaline medium and absorbed in boric acid. The ammonia concentration is then determined by titration with a standard mineral acid. Thus, a measurement of the ammonia concentration before and after acid digestion provides an indication of the organic nitrogen present in the sample.

Analysis for phenols was accomplished by employing the procedure described in Ref. 23. Phenols are distilled at the more or less constant rate from the leachate sample, leaving behind the non-volatile components. The steam-distillable phenols are then reacted with 4-aminoantipyrine at a pH of 10 in the presence of potassium ferricyanide to form a colored antipyrine dye. This dye is extracted from aqueous solution with chloroform and absorbance is measured at 460 nm. The concentration of phenolic compounds is expressed as  $\mu\text{g/l}$  of phenol ( $\text{C}_6\text{H}_5\text{OH}$ ). It is asserted that this method has a sensitivity of about  $1 \mu\text{g/l}$ . However, a major limitation associated with this method of analysis for phenols is that higher molecular weight phenolics are not particularly volatile and thus would not be measured.

Phenols can exert a toxicity toward certain aquatic organisms and may preclude various beneficial uses of water, particularly the use of water as a domestic water supply; chlorination of such water may produce odoriferous and objectional-tasting chlorophenols. Furthermore, certain chlorophenols are suspected of being carcinogenic.

In addition to the previously defined organic analyses, specific conductivity and pH analyses were performed on leachate samples. Specific conductivity was measured with a Leeds and Northrup conductivity bridge. The basic principle behind a conductivity bridge involves measuring the ability of an aqueous solution to conduct an electrical current. Specific conductivity is a numerical expression of the ability of a water sample to carry a current and depends on (1) the total concentration of ionized substances dissolved in water, (2) the particular inorganic ionic species, and (3) the temperature at which the measurement is made. Conductivity is normally expressed in terms of  $\mu\text{mhos/cm}$ .

Analysis for conductivity is important since it can provide a general indication of the TDS concentration of a leachate sample. The concentration of TDS can significantly affect the solubility of certain organic compounds in leachate by either inhibiting or enhancing solubility. Since direct analysis for TDS is a laborious, time-consuming task, it is often advantageous to approximately estimate TDS concentrations from conductivity measurements. Estimates of TDS can be made by multiplying corresponding values of conductivity by an empirical factor ranging from 0.5 to 0.9 (Ref. 24). The pH level of leachate samples was measured with a Beckman digital pH meter. The pH of a leachate sample is an important parameter since the hydrogen ion concentration can affect the solubility of certain organic compounds, particularly acidic and basic organic compounds.

The total array of analyses selected for defining the quality of leachate is summarized in Table 9. It is asserted that this total array of selected analyses provides a general indication of (1) the total amount of organic material, (2) the possible classes of organic compounds that may be present, and (3) the effect of other characteristics of leachate (as estimated by conductivity and pH) on the solubility of organic components. Although these selected



Table 9. Analyses selected for defining the quality of leachate.

---

Organic analyses
Total organic carbon (TOC)
Acid/base/neutral fractions
Organic nitrogen
Phenols
Other Analyses
Specific Conductivity
pH

---

analyses do not precisely identify specific organic components of leachate, they enable an adequate assessment of factors and conditions that influence the leaching of organic material from spent shale. Furthermore, this limited array of analyses provides a framework for subsequent studies to focus on a detailed characterization of particular organic components.

At this point, it is important to note that measurements for TOC, conductivity, and pH were made on all individual leachate samples generated during the leachate experiments. However, due to (1) the relatively small mass of organic material present in individual samples and (2) the laborious and time-consuming effort involved in a complete analytical characterization of all individual samples, a decision was made to analyze composite samples for acid/base/neutral fractions, organic nitrogen, and phenols rather than analyzing individual samples. The procedure for developing composite samples basically involved combining all individual samples associated with a certain set of experimental conditions into a composite sample. For example, all individual samples of the small-scale batch experiments which examined the leaching of a particular sample of spent shale by distilled water at a temperature of 20°C were combined into a single composite sample.

## CHAPTER 7

### EXPERIMENTAL RESULTS

This section presents (1) the characteristics of spent shale samples employed in the leaching experiments and (2) the results of the leaching experiments. Accompanying the results of the leaching experiments is a discussion which identifies variables that affect the leaching of organic contaminants from in-situ spent shale. A subsequent section will employ various data-analysis techniques to (1) reduce the data presented in this section and (2) place the results of the leaching experiments into an analytical framework.

#### Characteristics of Spent Shale Samples

Retorting Characteristics. The retorting characteristics of spent shale samples employed in the leaching experiments are summarized in Table 10. As revealed by Table 10, the various types of spent shale represent a wide cross-section of the types of spent shale that may be produced under various retorting conditions.

The retorting variables defined in Table 10 include type of retorting run, input gas, maximum retorting temperature, and retorting rate. In addition, Table 10 presents an estimate of oil yield, defined in terms of percentage of Fischer Assay. The Fischer Assay is a laboratory technique for estimating the maximum potential oil yield of an oil shale sample. The laboratory technique involves a standard heating sequence in which a sample is heated up to 500°C and the resultant oil is collected and measured in terms of gallons per ton. Knowing the Fischer Assay of a sample, the oil yield achieved during a retorting run can be reported in terms of percentage of Fischer Assay.

Table 10 describes the retorting characteristics of four unique spent shale samples; hereafter referred to as Type 1, Type 2, Type 3, and Type 4. Each of these samples has unique characteristics as a consequence of the different set of retorting conditions associated with each sample. The information presented in Table 10 is of extreme importance to the research summarized in this thesis. The reader is warned that, beyond this point, considerable reference will be made to Table 10.

The Type 1 spent shale was produced during a combustion run in which the maximum temperature exceeded that required for carbonate decomposition. The Type 2 spent shale was produced during an inert gas run in which an extremely high oil yield (99 percent) was attained. The maximum temperature achieved was below that required for carbonate decomposition. The Type 3 spent shale was produced during a combustion run employing recycle gas. The air-to-recycle gas ratio was 1:1 and the maximum temperature was far above that required for carbonate decomposition. The Type 4 spent shale was produced during an

Table 10. Retorting characteristics of spent shale samples.

Retorting characteristic	Type 1 shale	Type 2 shale	Type 3 shale	Type 4 shale
Type of retorting run	Combustion	Inert gas	Combustion	Inert gas
Input gas	Air + N <sub>2</sub> (7.6% O <sub>2</sub> )	N <sub>2</sub>	Air + recycle gas (10.5% O <sub>2</sub> )	N <sub>2</sub>
Maximum retorting temperature, °C	750	510	935	460 to 530
Retorting rate, m/day	0.69	1.40	1.34	≅ 2
Oil yield, (% of Fischer Assay)	78	99	96	NR

(Source: Ref. 17).

"engineering test" inert gas run in which the maximum retorting temperature varied slightly throughout the length of the retort. It is hypothesized that the Type 4 spent shale may closely resemble spent shale produced under actual field conditions. This is because retorting conditions (particularly retorting temperature) are somewhat difficult to control under actual field operations (in contrast to laboratory pilot-scale operations). Thus, under actual field conditions, one would expect some variation in retorting conditions.

Physical and Chemical Characteristics. Each of the four spent shale samples was analyzed for a series of physical and chemical characteristics, as described in the section on preparation of spent shale samples. Each sample was divided into three particle size ranges: a small particle size range of 0.14 to 0.28 centimeters, a large particle size range of 0.28 to 0.64 centimeters, and a composite particle size range of 0.14 to 0.64 centimeters. Although the initial research dealt with both the small and large particle size range, most of the subsequent research focused on the composite particle size range.

The physical and chemical characteristics of the composite particle size range of spent shale samples are summarized in Table 11. As revealed by Table 11, the bulk and solid density of spent shale samples produced during inert gas runs was greater than samples produced during combustion runs. This is likely due to (1) carbonate decomposition which can dramatically alter the shale matrix and (2) the burning of residual organic material associated with the shale matrix during a combustion run. It is interesting to note that the permeabilities of the spent shale samples were generally similar with the exception of the Type 4 spent shale sample whose permeability was significantly higher.

Table 11. Physical and chemical characteristics of spent shale samples: composite particle size range.

Characteristic	Spent shale sample			
	Type 1	Type 2	Type 3	Type 4
<u>Physical characteristics</u>				
Min. particle size, cm	0.14	0.14	0.14	0.14
Max. particle size, cm	0.64	0.64	0.64	0.64
Bulk density, g/cm <sup>3</sup>	0.86	1.08	0.80	0.95
Solid density, g/cm <sup>3</sup>	2.0	2.2	2.0	2.1
Porosity, %	57	51	60	54
Permeability, gal/day/ft <sup>2</sup>	560	510	490	710
<u>Chemical characteristics</u>				
Organic carbon, % by wt.	0.2	1.8	2.1	3.9

Table 11 also reveals that spent shale samples produced during inert gas runs were characterized by lower porosities than spent shale produced during combustion runs. This is likely due to the burning of residual organic material inside the shale matrix during a combustion run, thereby creating additional "internal" porosity. Indeed, one would expect the "micro-porosity" (i.e., porosity due to the semiporous infrastructure of individual shale particles) to be greater for the combustion-retorted samples than for the inert gas-retorted samples.

An extremely important characteristic of spent shale samples is their solid-phase organic carbon content, as expressed on a percent-by-weight basis. It is interesting to note that the Type 1 spent shale contained substantially less organic carbon than all other samples. Prior to analysis, it was anticipated that the Type 1 spent shale would contain the least organic carbon since it was produced during a combustion run in which residual organic material associated with the shale matrix was combusted to provide heat for pyrolysis. Both the Type 2 and Type 4 spent shales contained a high content of organic carbon as anticipated since residual organic material remains associated with the shale matrix after an inert gas run. It is hypothesized that the Type 4 spent shale contained the highest organic carbon content since it was produced during an "engineering test" run in which retorting conditions were varied. It is likely that this lack of retorting control contributed to the high organic carbon content of the Type 4 spent shale.

The Type 3 spent shale is perhaps the most interesting with respect to organic carbon content. Since the Type 3 spent shale was produced during a combustion run, one would initially expect that little residual organic material would remain associated with the shale matrix. However, since recycle gas contains significant amounts of volatile organics (particularly hydrocarbons) (Ref. 25), it is hypothesized that the high organic carbon content may be due to (1) the adsorption of certain volatile organic compounds associated with the recycle gas onto the spent shale as input gas was supplied behind the flame front in the retort and (2) the condensation of condensable hydrocarbons onto the spent shale behind the flame front.

In addition to the "measured" characteristics described above, it is considered advantageous to make a few general comments on the "visual" characteristics of the spent shale samples. The Types 2 and 4 spent shales, both produced during an inert gas run, were black and appeared homogeneous. The Type 3 spent shale, produced during a combustion run employing recycle gas, was primarily yellowish-white in color with occasionally interspersed brownish particles. In contrast to the other types of spent shale, the Type 3 spent shale did not appear entirely homogeneous.

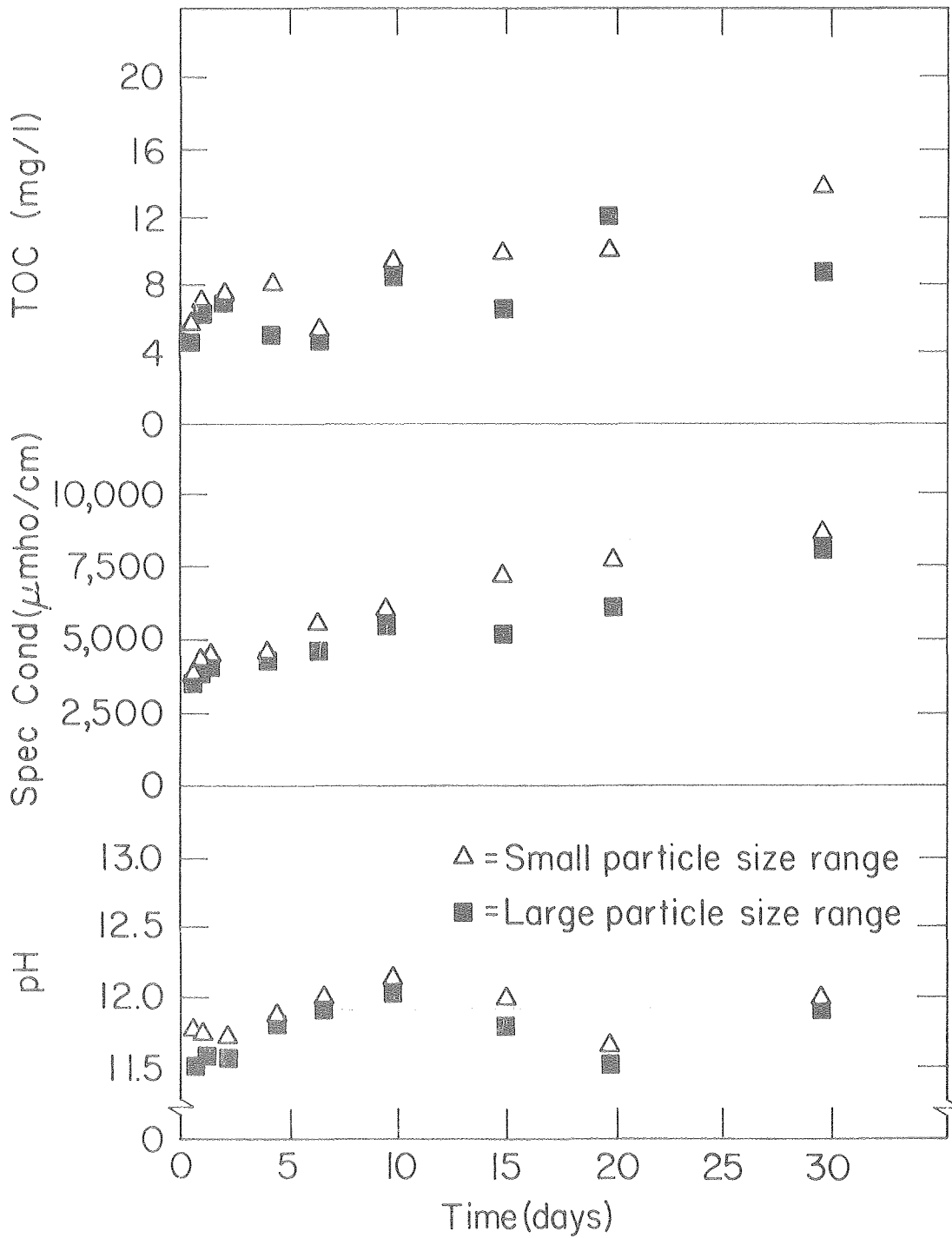
### Kinetic Batch Experiments

The kinetic batch experiments examined the leaching phenomenon over a leaching time period of 30 days. A 30-day time period was assumed to be adequate for the establishment of "pseudo-equilibrium" conditions. This original assumption, to a certain extent, was verified by results derived from the kinetic batch experiments.

Distilled Water Batch Experiments Conducted at a Water Temperature of 20°C. The results of the distilled water batch experiments conducted at a water temperature of 20°C are presented in Figures 13 through 16. These figures describe levels of organic carbon, conductivity, and pH at various leaching times for two particle size ranges; a small particle size range and a large particle size range. The organic carbon results presented in Figures 13 through 16 were subsequently summarized in Figure 17. The organic carbon values presented in Figure 17 were derived by averaging the organic carbon concentrations measured for small and large particle size ranges at each particular leaching time. Thus, the data in Figure 17 provide an estimate of the anticipated organic carbon levels in leachate derived from a composite particle size range encompassing both the small and large particle size range.

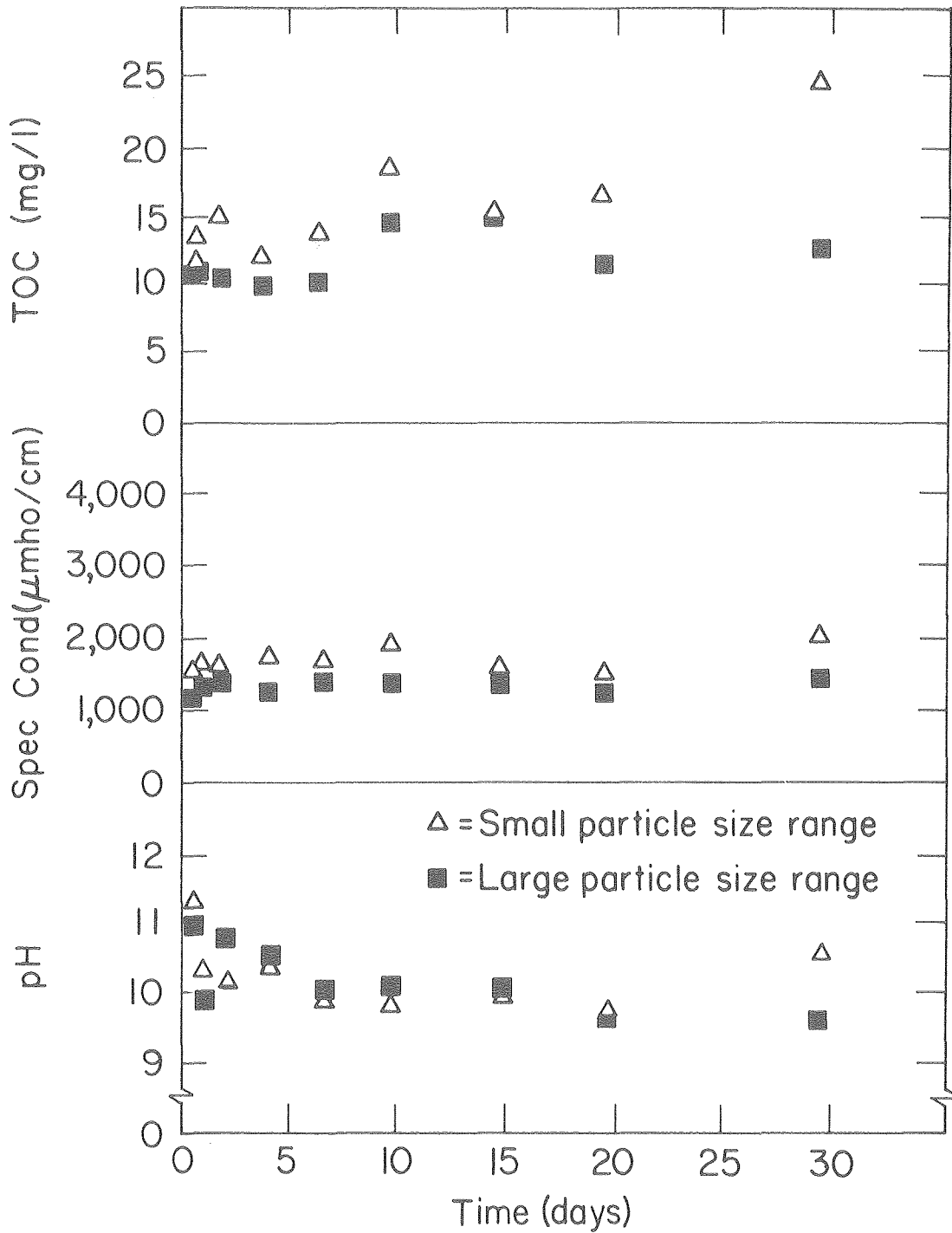
As revealed by Figure 17, leachate from the Type 3 spent shale contained the greatest concentration of organic carbon, whereas leachate from the Type 1 spent shale contained the least. The Type 1 spent shale was produced during a combustion run at a high retorting temperature in the presence of oxygen (without recycle gas) at a low retorting rate, thus enabling the combustion of most of the residual organic material remaining on the spent shale after pyrolysis.

The concentrations of organic carbon in leachate derived from Type 2 and Type 4 spent shale were intermediate to those derived from Type 3 and Type 1 spent shale. Type 2 and Type 4 spent shale were each produced during an inert gas run at a low retorting temperature in the absence of oxygen and thus no combustion of residual organic material occurred. Although the Type 3 spent shale was produced during a combustion run in the presence of oxygen at a high retorting temperature, its leachate contained the most organic carbon. It is hypothesized that this is likely due to the use of recycle gas as part of the input gas. Recycle gas contains various volatile or condensable organic compounds and thus it is hypothesized that certain volatile organic compounds associated with the recycle gas absorbed or condensed onto the Type 3 spent shale as input gas was supplied behind the flame front in the retort. Apparently, certain organics present in the recycle gas are volatile at high temperatures but condense at low temperatures. It is interesting to note that leachate derived from the Type 3 spent shale contained a greater concentration of organic carbon than leachate derived from either the Type 2 or Type 4 spent shale.



XBL 792-535

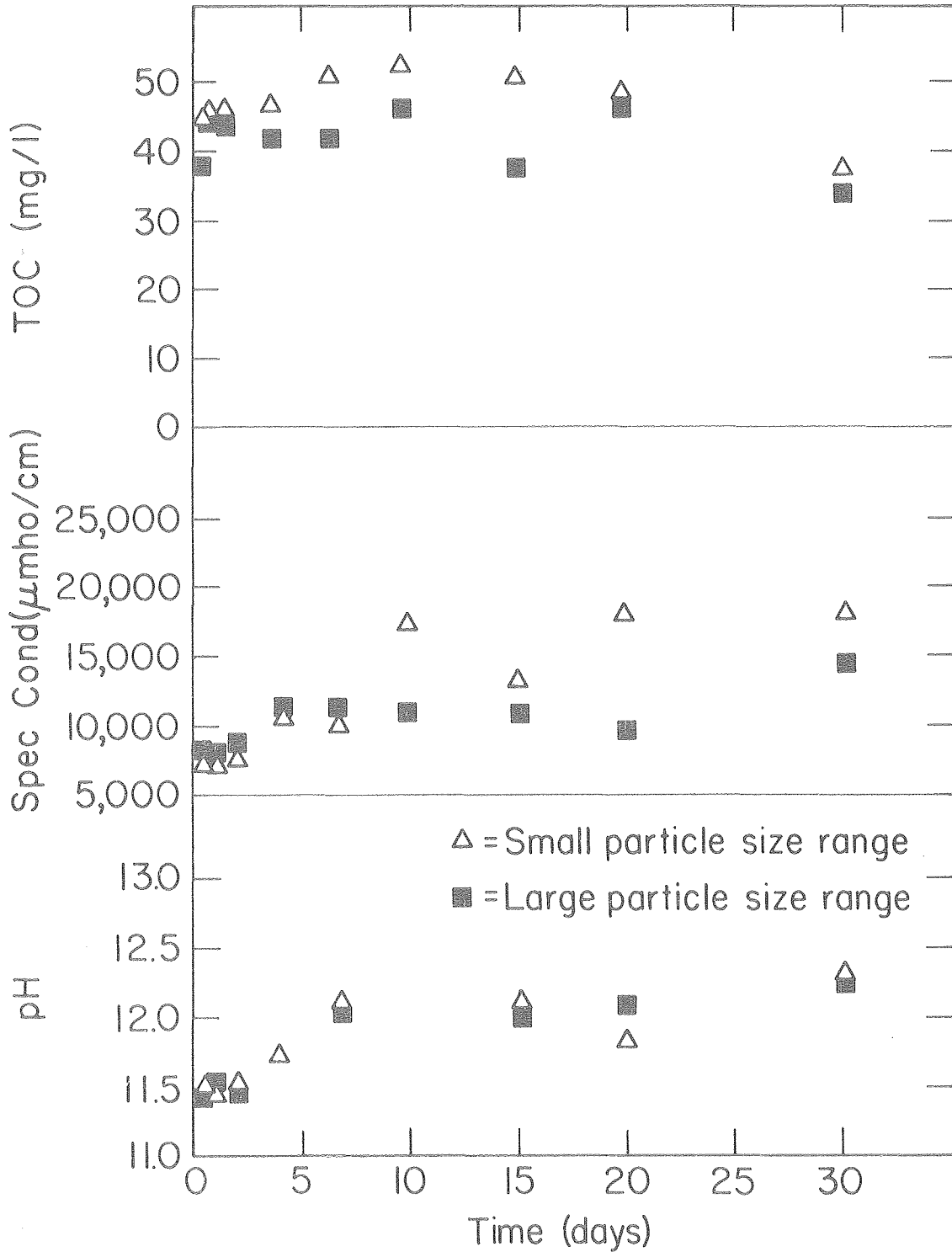
Figure 13. Distilled water batch experiments examining Type 1 spent shale at 20°C.



FXBL 792-544

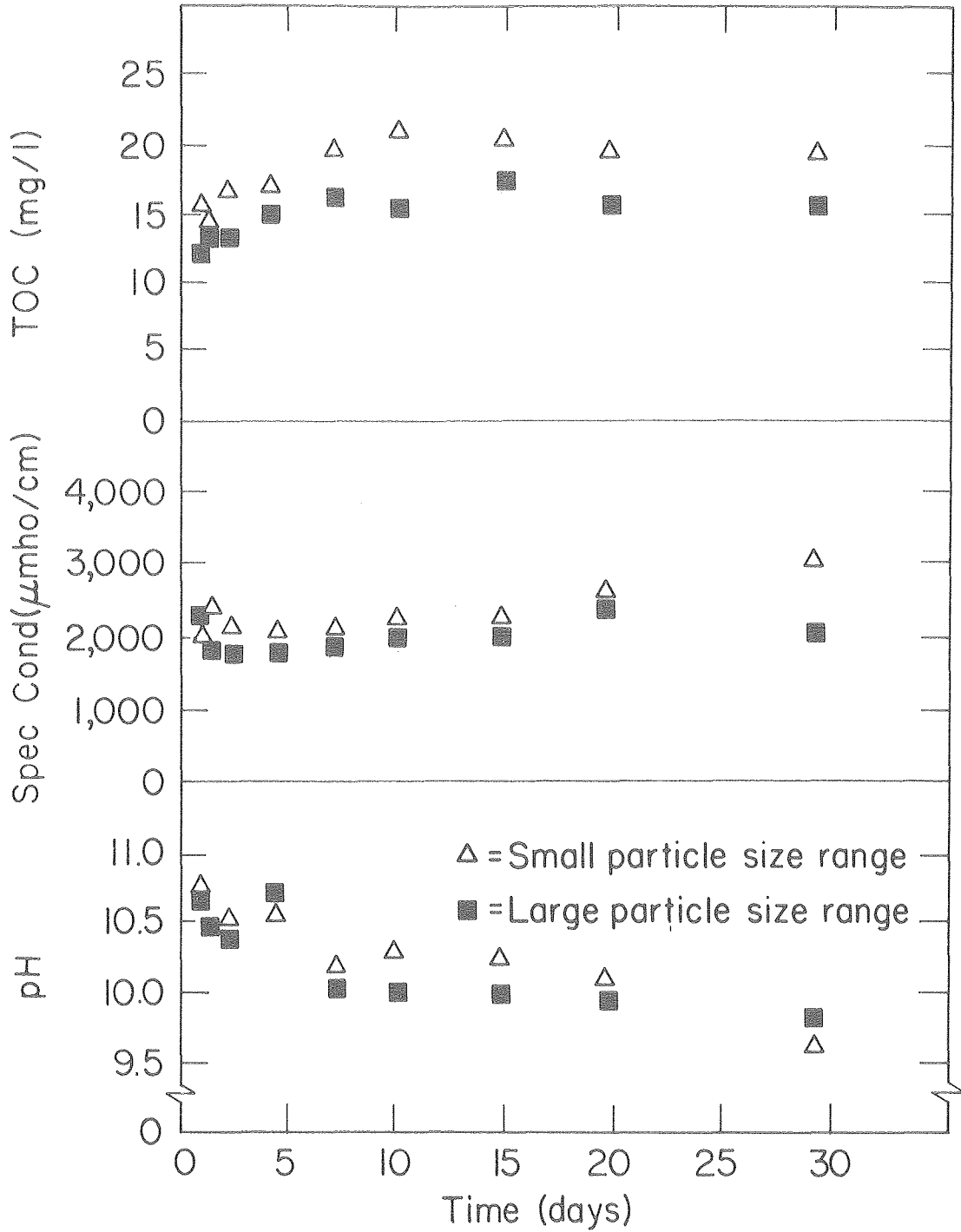
Figure 14. Distilled water batch experiments examining Type 2 spent shale at 20°C.





FXBL 792-564

Figure 15. Distilled water batch experiments examining Type 3 spent shale at 20°C.



XBL 792-527

Figure 16. Distilled water batch experiments examining Type 4 spent shale at 20°C.

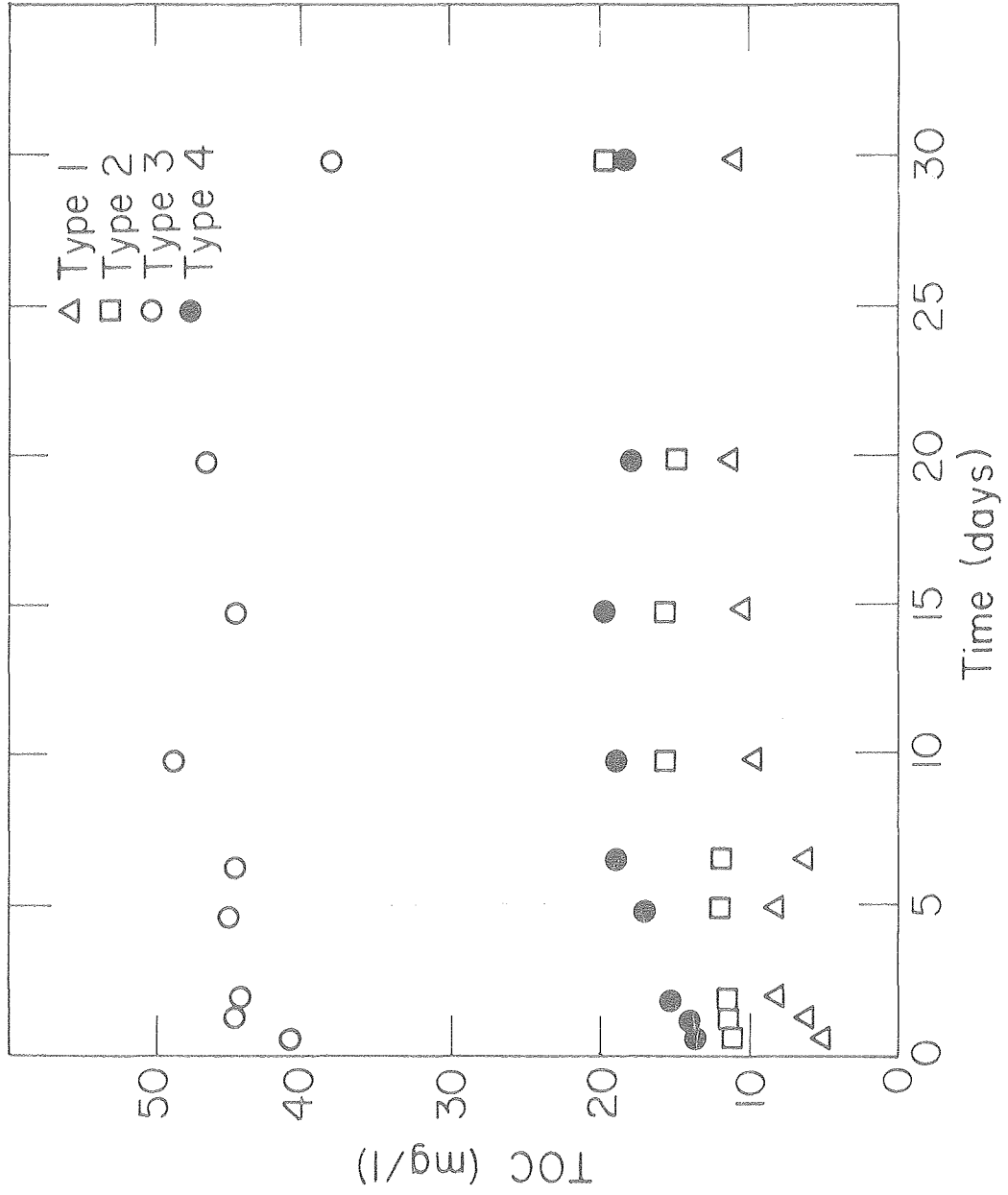


Figure 17. Summary of distilled water batch experiments conducted at a water temperature of 20°C. XBL 792 528

The size of spent shale particles significantly affects the amount of organic material leached, as revealed by Figures 13 through 16. In accordance with theory, leachate from particles in the smaller size range contained a greater concentration of organic carbon for all four types of spent shale investigated. This is due to the fact that, for the smaller particle size range, there is a greater surface area per given weight available for leaching. However, assuming equal initial solid-phase organic carbon content, it would be expected that larger size particles will leach over a longer period of time than smaller size particles. After an infinite leaching time period, one would expect leachate derived from the larger particles to be similar to leachate derived from smaller particles.

The amount of organic material leached from all five types of spent shale at a water temperature of 20°C generally appeared to increase as a function of leaching time, as revealed by Figures 13 through 16. However, scrutiny of these graphs indicates that there were occasional decreases in organic carbon concentration over certain ranges of leaching time. This is particularly apparent for the Type 3 spent shale (see Fig. 17) in which the organic carbon concentration generally increases up to day 10 and thereafter generally decreases from day 10 to day 30. It is also apparent for the Type 1 spent shale where there is a decrease from day 4 to day 7. Possible explanations of these occasional decreases in organic carbon concentrations over time include (1) the occurrence of precipitation reactions involving various soluble organic components of the leachate, (2) decreased solubility of various soluble organic compounds of the leachate as a consequence of inorganic material leached from spent shale (the leaching of inorganic material, as indicated by the conductivity measurements in Figures 13 through 16 was quite significant and possibly decreased the solubility of certain organic components present in the leachate), (3) microbial degradation of organics during leaching experiments, (4) re-adsorption of previously leached organics, (5) ion exchange mechanisms in which previously leached organic ions displace inorganic ions associated with the shale matrix, and (6) experimental error.

It is interesting to note that the greatest rate of leaching for all three types of spent shale occurred during the first day. Thereafter, the rate of leaching decreased significantly until "pseudo" equilibrium conditions were approached by the thirtieth day of leaching. It was originally assumed that a time period of 30 days was adequate for attainment of equilibrium conditions. Although actual equilibrium conditions were not attained, the results suggest that the "pseudo equilibrium" conditions existing after a 30-day period are representative of actual equilibrium conditions.

It is also interesting to note that significantly higher levels of conductivity (and thus TDS) were detected in leachate derived from spent shale produced during combustion runs (i.e., Type 1 and Type 3) than in leachate derived from spent shales produced during inert gas runs (i.e., Type 2 and Type 4). This is likely due to the fact that

the two combustion runs occurred at retorting temperatures above 650°C while the two inert gas runs occurred at retorting temperatures below 650°C. Furthermore, spent shale produced during a combustion run results in leachate of a higher inorganic content (and thus a higher conductivity) than leachate derived from spent shale produced in the absence of air; this is due to (1) water soluble products of carbonate decomposition and (2) the fact that air provides an oxidizing atmosphere for reaction with easily oxidized metals in the shale matrix, thus liberating these metals as ions (Ref. 9).

It was also noted that leachate derived from spent shale produced during a combustion run was characterized by a higher pH than leachate derived from spent shale produced during an inert gas run. This is due to the fact that carbonate decomposition results in large amounts of calcium and magnesium oxides which produce high pH leachates (Ref. 9).

It is also interesting to note the significant decrease in pH as a function of time for inert gas-retorted spent shales (i.e., Types 2 and 4). This decrease in pH may be due to the leaching of organics which behave as weak and strong acids (i.e., phenolics and carboxylic acids). Indeed, this behavior may be tentative proof of the presence of phenolics and carboxylic acids in leachate.

Finally, in order to further explain some of the results obtained, an analogy can be made between certain types of spent shale and activated carbon. Activated carbon is produced by oxidizing graphite (an oxidizing carbon environment must exist if activation is to occur). The resultant activated carbon is a porous matrix containing various functional groups, these functional groups being responsible for holding all types of organic material onto the matrix. In a like manner, oil shale can undergo an activation process if it is retorted in a combustion atmosphere (activation will not occur if retorting takes place in an inert gas atmosphere). Thus, combustion-retorted spent shale may, in certain respects, resemble activated carbon in its behavior and properties.

The general similarity between combustion-retorted spent shale and activated carbon suggests that more than simple desorption/leaching may have occurred in experiments which examined Type 1 and Type 3 spent shales. Based on the potential "activated" characteristics of these spent shale samples it is hypothesized that some re-adsorption of previously leached organics may have occurred. This hypothesis may in part explain the unusual results derived from Type 3 spent shale in which concentrations of organic carbon appeared to decrease near the end of the 30-day leaching period.

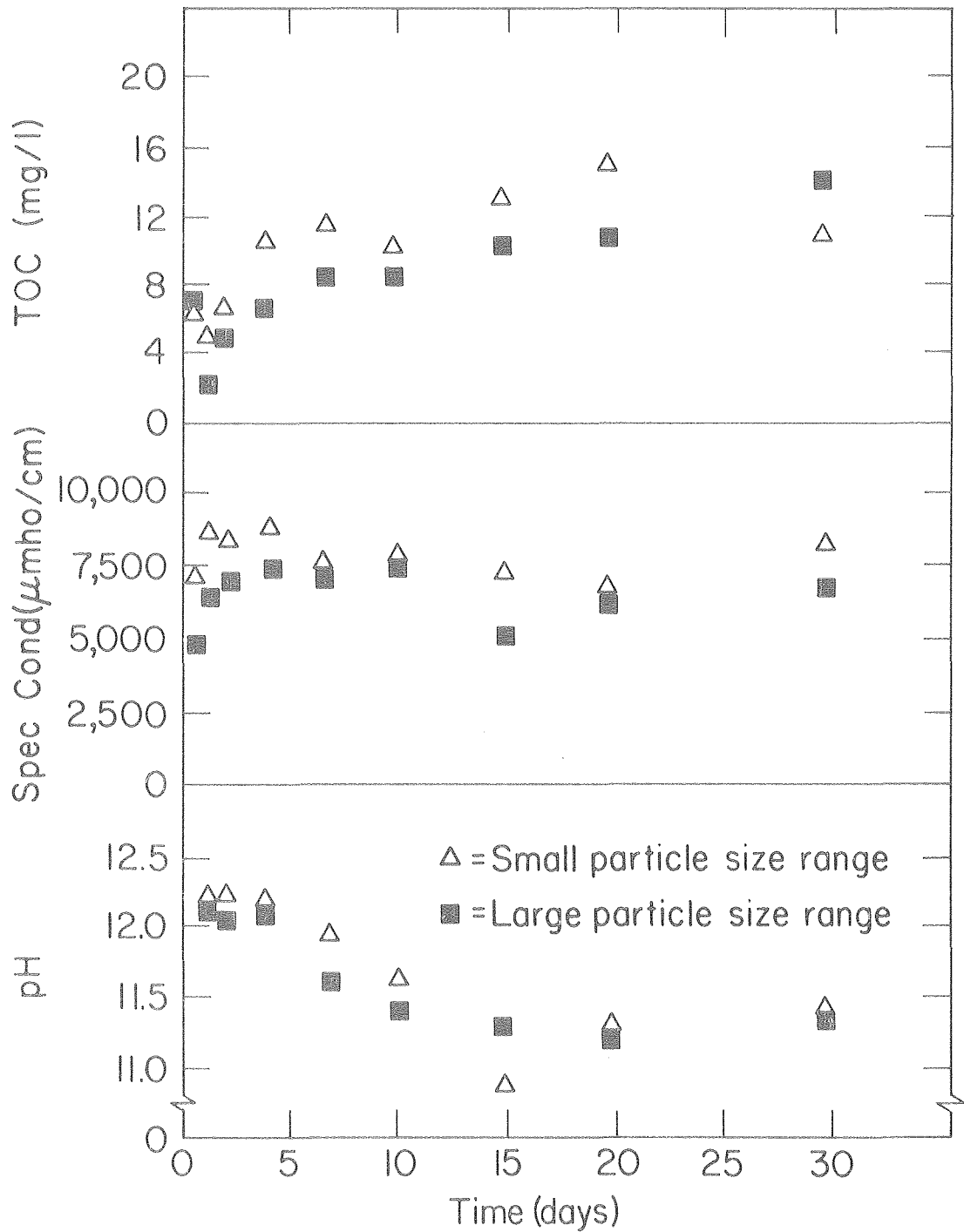
Distilled Water Batch Experiments Conducted At a Water Temperature of 80°C. The reason for conducting batch experiments at an elevated water temperature (i.e., 80°C) is as follows. Under actual conditions, an in-situ retort will be abandoned after the entire retort is pyrolyzed. After a retort is abandoned, a long time (perhaps as long as a year) may be required for the retort to cool to ambient temperatures. Prior to this, it is possible that groundwater may migrate into the retort

and be heated to an elevated temperature. Raising the temperature of groundwater in this manner may either enhance or inhibit the leaching of various contaminants. Groundwater, heated as it enters a retort, may (1) remain in a liquid phase where it is readily available for leaching or (2) be converted to steam in which case it must first condense before it can enter into the leaching process. Furthermore, it should be recognized that a refluxing zone (see the earlier "Literature Survey" section) may be formed in the retort in which water is continuously vaporizing and condensing over a period of time. These conditions may dramatically enhance the leaching process.

The results of the batch experiments conducted at a water temperature of 80°C are presented in Figures 18 through 21 and summarized in Figure 22. (The organic carbon levels presented in Figure 22 were derived by averaging the organic carbon concentrations measured for the small and large particle size ranges at each particular leaching time and thus are representative of organic carbon concentrations that would be anticipated for the composite particle size range.)

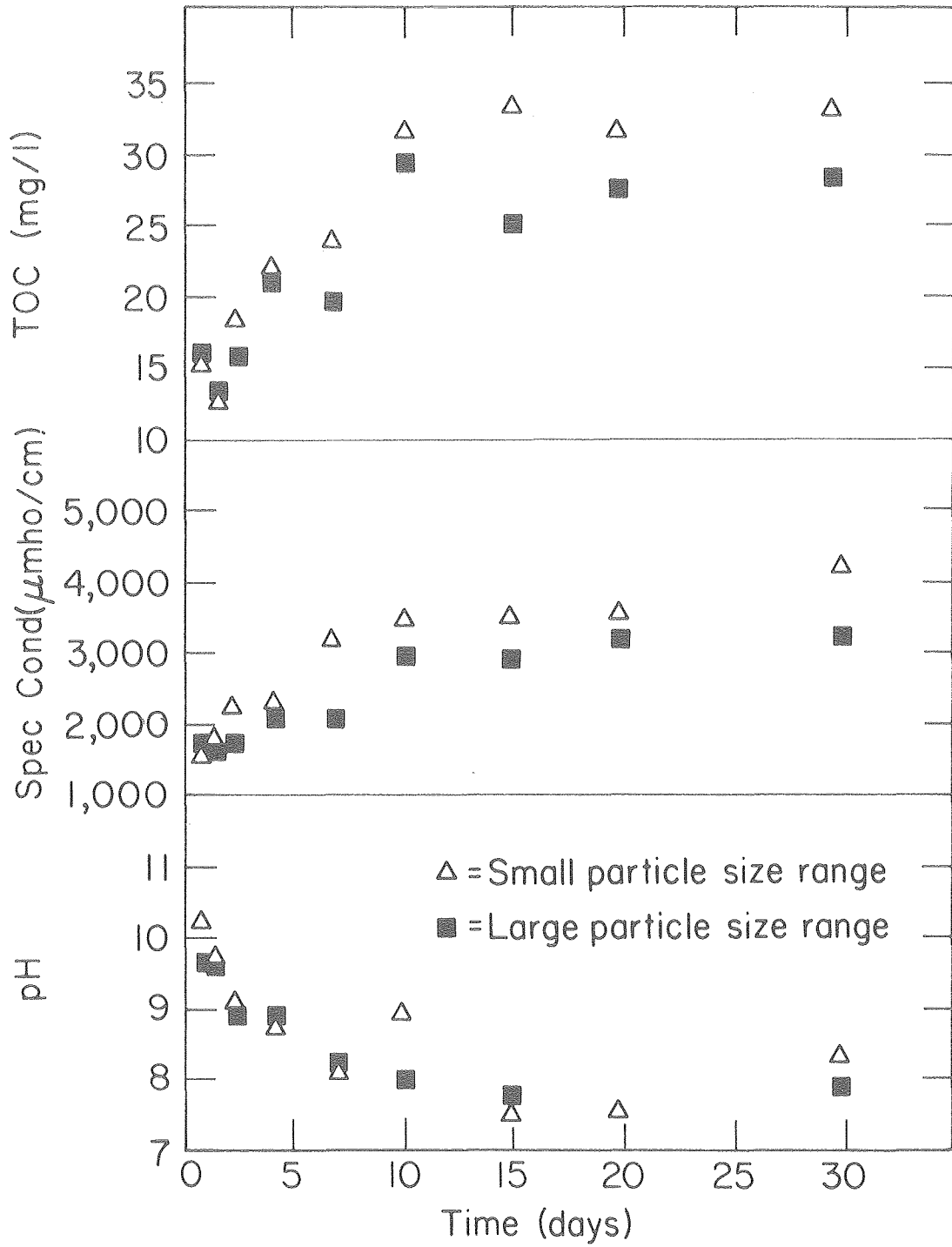
From Figure 22, it can be seen that leachate derived from Type 2, Type 3, and Type 4 spent shale at a water temperature of 80°C contained considerably greater concentrations of organic carbon than leachate derived from Type 1 spent shale. This is similar to observations made during the batch experiments conducted at a water temperature of 20°C in which the leachate from Type 1 spent shale contained considerably less organic carbon. This is due to the combustion of residual organic material during the retorting process.

A comparison of Figures 17 and 22 suggests that a higher water temperature significantly enhances the leaching of organic material from Type 2 and Type 4 spent shale, both of which were produced during inert gas runs. In contrast, a higher water temperature, over certain ranges of time, generally appears to inhibit the leaching of organic material from Type 3 spent shale. Thus, it appears that the organic components in leachate from Type 3 spent shale may be less soluble at higher water temperatures while the organic components in leachate from Type 2 and Type 4 shale may be more soluble at higher water temperatures. Possible explanations for the apparent high temperature inhibition of the leaching of organic material from Type 3 spent shale are (1) thermally catalyzed reactions involving leached organics, (2) possible volatilization of hydrocarbons or other organic compounds (originally present in the recycle gas) that may have adsorbed or condensed onto the spent shale during retorting, and (3) solubilization of certain inorganics during leaching that are more soluble at higher temperatures and which may subsequently react with and insolubilize certain organics. A comparison of Figures 17 and 22 suggests that water temperature had little overall effect on the leaching of organic material from Type 1 spent shale.



XBL 792-529

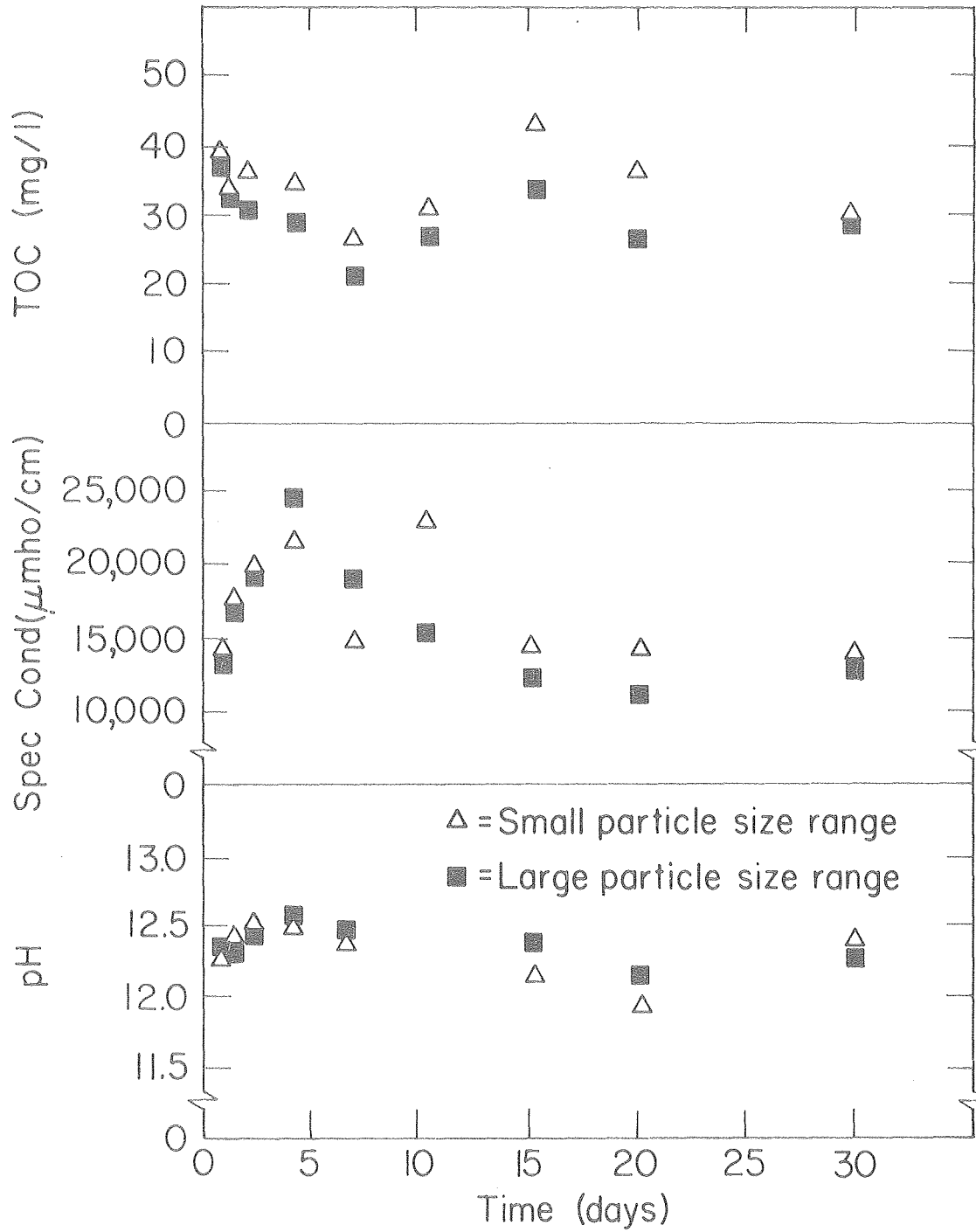
Figure 18. Distilled water batch experiments examining Type 1 spent shale at 80°C.



XBL 792-530

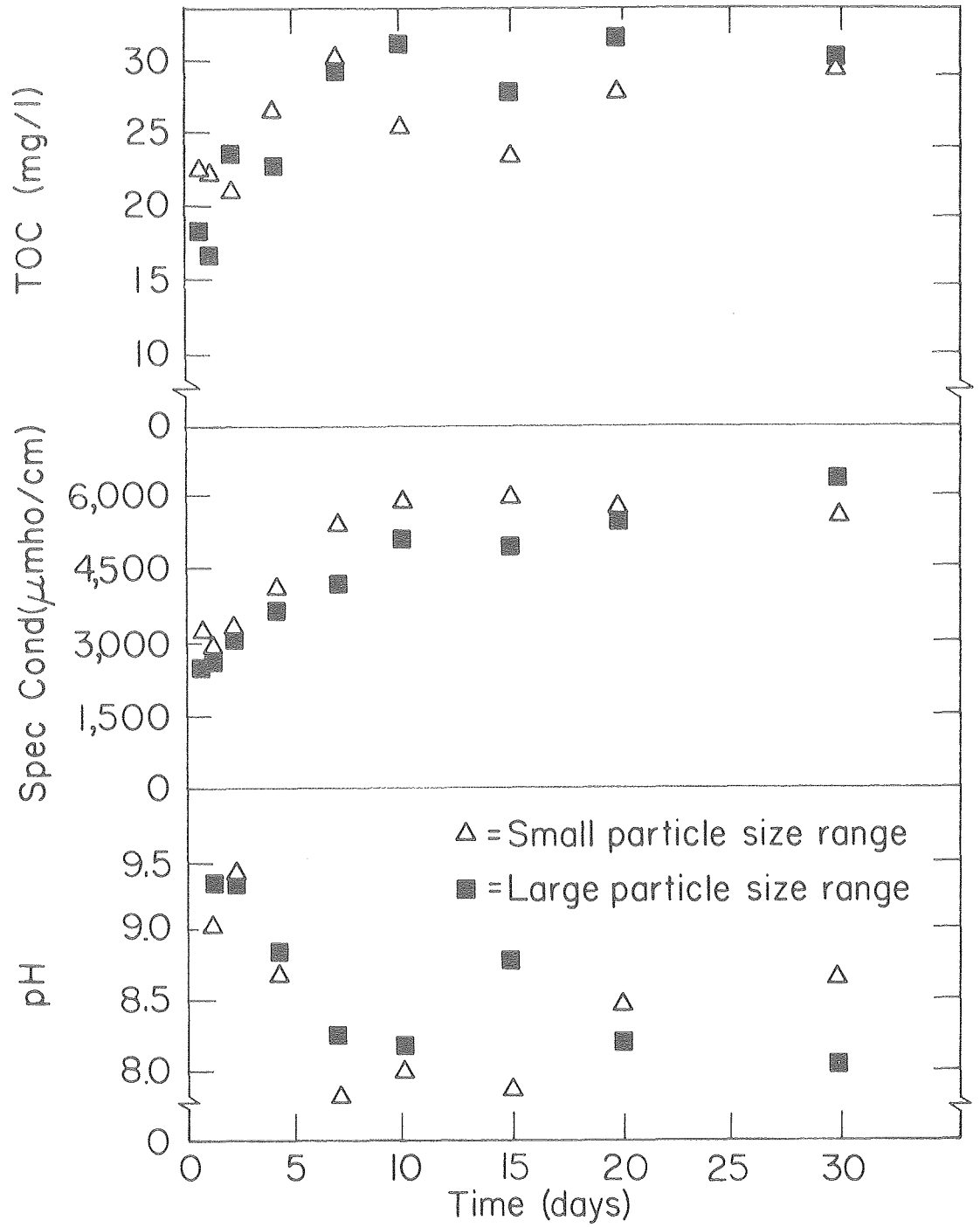
Figure 19. Distilled water batch experiments examining Type 2 spent shale at 80°C.





XBL 792-542

Figure 20. Distilled water batch experiments examining Type 3 spent shale at 80°C.



XBL 792-543

Figure 21. Distilled water batch experiments examining Type 4 spent shale at 80°C.

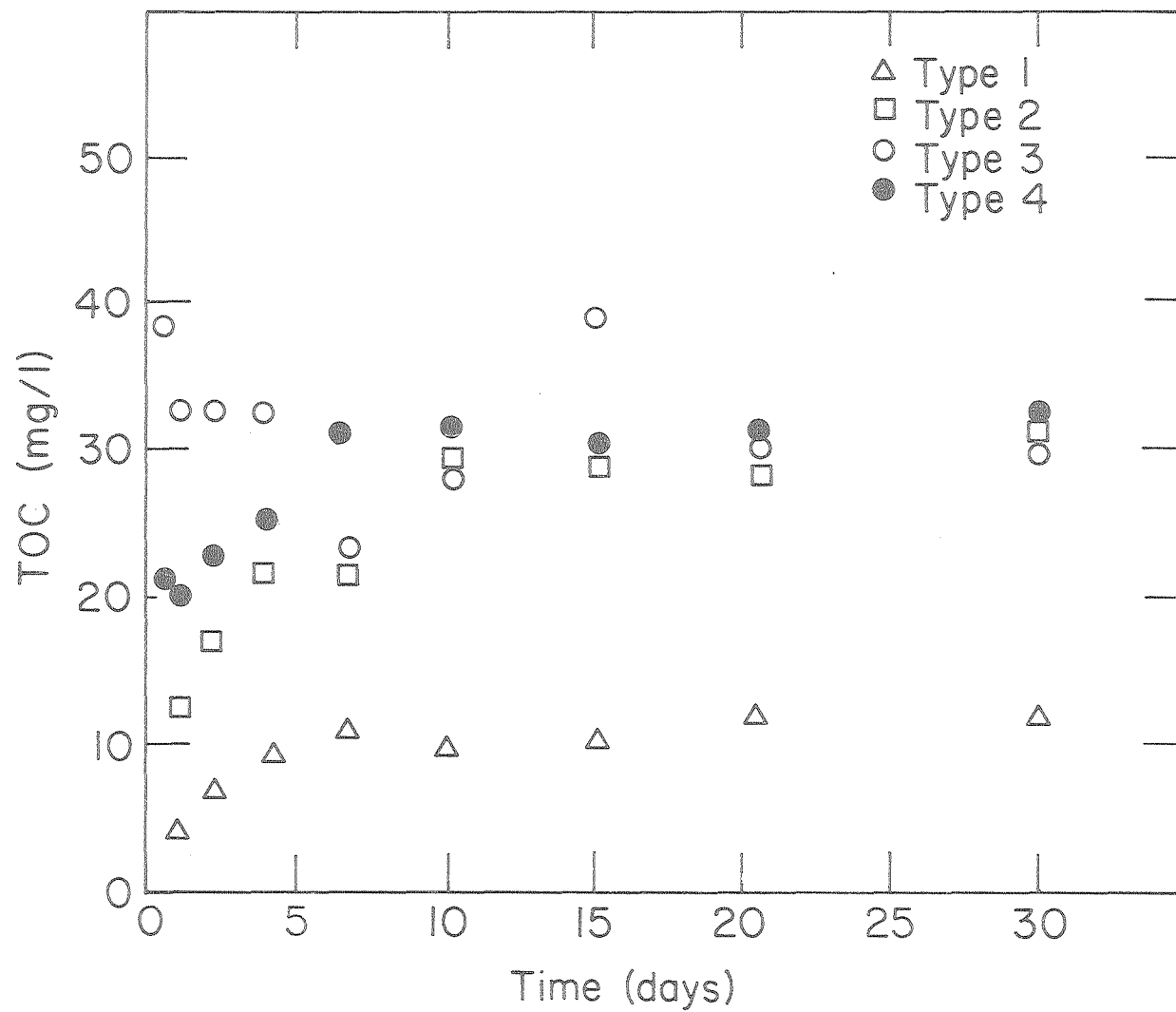


Figure 22. Summary of distilled water batch experiments conducted at a water temperature of 80°C. XBL 792-569

As a general statement, one would expect a higher temperature to enhance molecular diffusion and thus mass transfer during the leaching experiments since molecular diffusion is defined as the thermal agitation of molecules. Furthermore, higher temperatures decrease water viscosity and thus increase the rate at which water is drawn into the shale matrix by capillary action, thereby accelerating the leaching process. However, certain solubility equilibrium relationships and pH differences at higher temperatures may, in some cases, result in a lower organic carbon concentration than at a lower temperature.

The amount of organic material leached from the small particle size range at a water temperature of 80°C was greater than that from the large particle size range for four types of spent shale investigated, as revealed by Figures 18 through 21. The results correspond to the results of the batch experiments conducted at a water temperature of 20°C.

For Type 1, Type 2, and Type 4 spent shale, the concentration of organic carbon generally increased as a function of leaching time except for slight decreases occurring over certain ranges of leaching time. In contrast, the concentration of organic carbon in leachate from the Type 3 spent shale increased to a high level after one-half day of leaching and thereafter tended to decrease with time until the seventh day. After the seventh day, the concentration increased until the fifteenth day and thereafter decreased. This behavior may be due to precipitation reactions involving various organic components, decreased solubility of organic components resulting from inorganic materials leached from the spent shale, or microbial degradation of organics present in the leachate. Furthermore, a visual appraisal of the Type 3 spent shale indicated that it did not appear to be entirely homogeneous, as indicated previously. Possible non-homogeneity may have contributed to the somewhat perplexing results derived from the Type 3 spent shale.

For all four types of spent shale, the rate of leaching was greatest during the first day and thereafter decreased. "Pseudo equilibrium" conditions were roughly approached by the thirtieth day of leaching as was the case in the batch experiments conducted at a water temperature of 20°C.

The results suggest that the water soluble organics associated with the Type 3 spent shale attained equilibrium rapidly during the batch experiments whereas the leaching of water soluble organics from the other types of spent shale was more gradual. This may be due to the fact that (1) most of the organics associated with the Type 3 spent shale are situated near the exterior surface of individual spent shale particles where they are readily leachable or (2) organic materials leached after initial time periods are subsequently insolubilized by one of several mechanisms. In contrast, organics associated with the other types of spent shale are likely associated with both the exterior surface and the internal pores of individual spent shale particles. The leaching of organics situated within individual pores

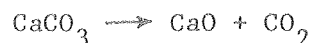
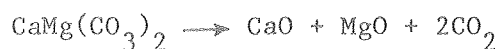
is a relatively slow process since these organics must diffuse a relatively greater distance than organics situated near the exterior surface of individual spent shale particles.

In a manner similar to the results of the low-temperature distilled water experiments, it was observed during the corresponding high temperature experiments that pH levels decreased as a function of time in leachate derived from inert gas-retorted spent shale. This suggests the possible leaching of weak organic acids and strong organic acids such as phenolics and carboxylic acids.

Discussion of Results Derived from Type 3 Spent Shale During Distilled Water Batch Experiments. At first glance, the most unusual data derived during the distilled water batch experiments were data derived from Type 3 spent shale. Results obtained using Type 3 spent shale differed significantly from other results. Concentrations of organic carbon for Type 3 spent shale tended to fluctuate in an oscillatory manner as a function of time, particularly at a higher water temperature. In contrast, TOC measurements for other types of spent shale generally increased with time until "pseudo-equilibrium" conditions were attained.

It is asserted that the most important factor responsible for the unusual results derived from Type 3 spent shale was a high retorting temperature. The Type 3 spent shale was produced at a retorting temperature of 935°C, substantially greater than that required for carbonate decomposition (620°C). In contrast, Type 1 spent shale was produced at a retorting temperature only moderately above that required for carbonate decomposition while Types 2 and 4 spent shales were produced at retorting temperatures less than that required for carbonate decomposition. Thus, the Type 3 spent shale, produced at a very high retorting temperature, underwent a considerable degree of carbonate decomposition, in contrast to other spent shale samples.

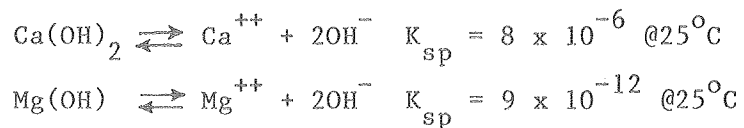
At retorting temperatures above 620°C, carbonate minerals such as dolomite,  $\text{CaMg}(\text{CO}_3)_2$ , and calcite,  $\text{CaCO}_3$ , decompose to form oxides of calcium and magnesium as follows:



After retorting, these oxides remain in association with the spent shale matrix where they are available for leaching. Eventually, when water comes into contact with spent shale, these oxides react with water to form hydroxides as follows:



The formation of the above hydroxides results in high pH leachates. These hydroxides can subsequently dissociate into bivalent cations and hydroxide ions to varying degrees, depending on the pH of the leachate.



The above dissociation liberates free  $\text{Ca}^{++}$  and  $\text{Mg}^{++}$  ions. Thus, as a consequence of carbonate decomposition, it should be apparent that bivalent cations will potentially be a more predominant component of Type 3 leachate than the other leachates, depending on pH.

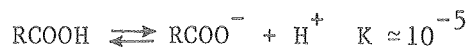
Furthermore, it is likely that both phenolics and carboxylic acids will be formed during certain stages of the pyrolysis of oil shale, regardless of the retorting conditions employed. The phenolics formed may range from simple phenol to polyphenolics while the carboxylic acids may range from short-chain to long-chain acids. After formation during the retorting process, these phenolics and carboxylic acids will either (1) undergo thermal decomposition, (2) be volatilized and subsequently removed from the retort as part of the oil and gas "mist," or (3) remain in association with the spent shale after pyrolysis. During low-temperature inert gas retorting, one would expect all of the above to occur to varying degrees, depending on retorting temperature. In contrast, during high-temperature combustion retorting without recycle gas, one would expect phenolics and carboxylic acids to be either thermally decomposed or volatilized and thus, the resultant spent shale would contain virtually no phenolics or carboxylic acids available for leaching. However, during combustion retorting employing recycle gas (as in the production of Type 3 spent shale), it is likely that some of the phenolics and carboxylic acids formed will be volatilized prior to thermal decomposition and thus, will become part of the recycle gas. Subsequently, some of these phenolics and carboxylic acids contained in the recycle gas will likely condense or adsorb onto spent shale particles as input gas is pumped into the retort behind the flame front. Thus, spent shale produced during combustion retorting employing recycle gas will likely contain phenolics and carboxylic acids available for leaching.

Both phenolics and carboxylic acids dissociate as follows:

Phenolics



Carboxylic Acids



Based on the above, it is apparent that high pH levels favor the formation of the ionized form of either the phenolic or the carboxylic acid. It should be recognized that the ionized form represents the water soluble form.

The ionized forms of phenolics and carboxylic acids can react with bivalent cations such as  $\text{Ca}^{++}$  to form phenolates and carboxylates as follows:



Phenolates and carboxylates formed with bivalent cations are sparingly soluble in water. Each phenolate and carboxylate is characterized by a solubility product and when that solubility product is exceeded, the appearance of more reactants will result in insolubilization/precipitation. Thus, leached organic material appearing in leachate as phenolics or carboxylic acids may subsequently be insolubilized if  $\text{Ca}^{++}$  and  $\text{Mg}^{++}$  ions are present in sufficient quantities and if the corresponding solubility product is exceeded.

It is important to note that pH plays an important role in the above process, affecting the solubility of bivalent cations as well as phenolics and carboxylic acids. Furthermore, it is important to note that water temperature can significantly affect the solubility of these materials.

It is asserted that the above phenomenon explains, to a certain degree, the unusual results derived from the Type 3 spent shale. Of the four types of spent shale examined, only the Type 3 spent shale provided the opportunity for significant amounts of both bivalent cations and phenolics/carboxylic acids to be leached and subsequently take part in the above reactions. Thus, the proposed phenomenon helps to explain the oscillatory fluctuations in organic carbon measurements as a function of time. These fluctuations are shown in Figures 15 and 20.

During both low-temperature and high-temperature distilled water experiments, leachate derived from Type 3 spent shale was characterized by high levels of conductivity and pH. These high levels of conductivity and pH (described in Figures 15 and 20) were likely related to carbonate decomposition and the formation of hydroxides of calcium and magnesium during the leaching process. At the initial high pH of these leachates (11.5 to 12.5), it would be expected that relatively few free  $\text{Ca}^{++}$  and  $\text{Mg}^{++}$  ions would exist in solution and that most calcium and magnesium would be in the form of  $\text{Ca}(\text{OH})_2$  and  $\text{Mg}(\text{OH})_2$ . However, as phenolics and carboxylic acids leach into a high pH solution, they will dissociate into their respective ionic forms. Subsequently, depending on solubility

products and pH, these ionic forms of phenolics and carboxylic acids may combine with available  $\text{Ca}^{++}$  and  $\text{Mg}^{++}$  ions, forming insoluble phenolates and carboxylates. In response to the disappearance of  $\text{Ca}^{++}$  and  $\text{Mg}^{++}$  ions in solution, both  $\text{Ca}(\text{OH})_2$  and  $\text{Mg}(\text{OH})_2$  will then dissociate to a certain degree, forming more  $\text{Ca}^{++}$  and  $\text{Mg}^{++}$  ions. Subsequently, these newly formed  $\text{Ca}^{++}$  and  $\text{Mg}^{++}$  ions may combine with ionic forms of phenolics and carboxylic acids as they appear in leachate. Thus, it is asserted that there is a series of inter-related reactions that may occur over the entire leaching time period.

It is important to note that this series of inter-related reactions is pH dependent. Furthermore, certain of these reactions may be controlled by kinetics to varying degrees. Thus, if a significant amount of phenolics and carboxylic acids are leached from Type 3 spent shale as anticipated, one would expect this series of inter-related reactions to possibly result in oscillatory fluctuations of organic carbon measurements as a function of time. These oscillations may be in part due to pH changes which affect certain of the above reactions.

Based on the above discussion, it is apparent that bivalent cations such as  $\text{Ca}^{++}$  and  $\text{Mg}^{++}$  may act as a "sink" for phenolics and carboxylic acids leached from Type 3 spent shale. Thus, for Type 3 spent shale, not all leached organics remain in soluble form throughout the leaching period. In contrast, results derived from other types of spent shale indicate that organic carbon generally increased as a function of time. This suggests that various organics were simply leached until their solubility was reached and thereafter remained in soluble form. It is expected that soluble forms of both phenolics and carboxylic acids would be present in leachate derived from inert gas-retorted spent shale.

Synthetic Groundwater Batch Experiments. The previously described batch experiments assessed the leaching of organic material with distilled water. The reason for using distilled water in these initial experiments was to study the leaching phenomenon under the least complicated conditions. However, it is felt that the results of these initial experiments may not be representative of what will occur under actual conditions since the quality characteristics of groundwater coming into contact with spent shale may significantly affect the types and amounts of organic materials leached. The quality characteristics of groundwater may either inhibit or enhance the leaching of organic material depending on various solubility relationships, the pH of the groundwater, and reactions/interactions between inorganic components of the groundwater and organic components of the leachate. Consequently, a decision was made to augment the results of the previous batch experiments by repeating certain selected experiments with "synthetic" groundwater. Although original plans called for use of actual groundwater, logistical problems made it more convenient to use synthetic groundwater produced in a laboratory with reagent grade chemicals. The quality of this synthetic groundwater was described in the section on laboratory leaching experiments. It should be recognized that experimental results derived from



this synthetic groundwater may differ dramatically from results derived from a groundwater of a different composition.

The ambient quality of groundwater coming into contact with in-situ spent shale may significantly affect the quality of leachate. Groundwater with a high TDS and alkalinity may influence the types and quantities of organic materials leached as a consequence of (1) high buffering capacity, (2) precipitation reactions involving components originally present in the groundwater and components leached from the spent shale, (3) counter-diffusion of ions originally present in the groundwater back into the shale matrix as a consequence of supersaturated conditions, (4) ion exchange reactions, (5) insolubilization reactions involving certain cations and certain organics leached from the spent shale, and (6) salting out effects.

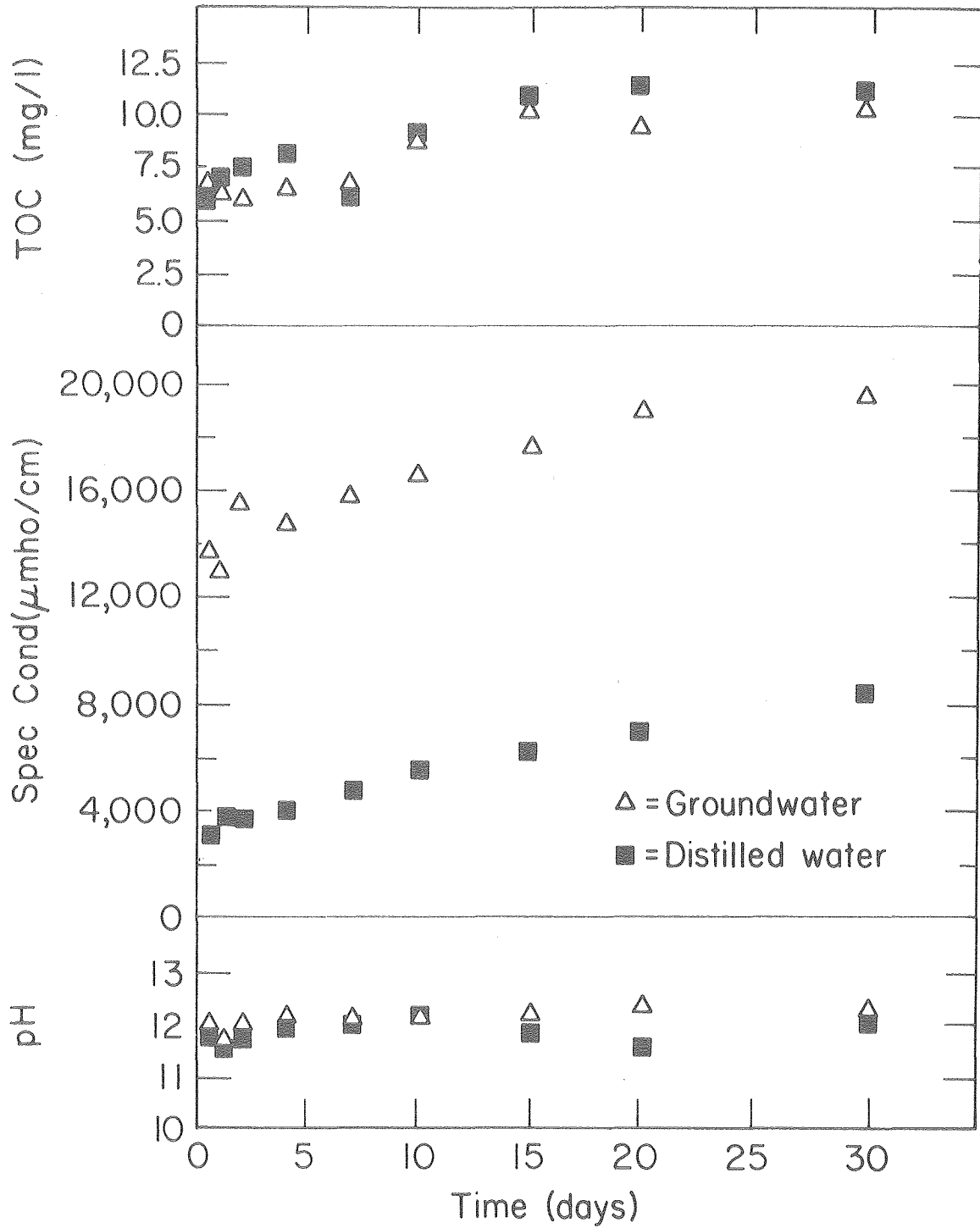
In contrast to the distilled water batch experiments, the synthetic groundwater batch experiments examined only the composite particle size range.

Synthetic Groundwater Batch Experiments Conducted at a Water Temperature of 20°C. The results of the synthetic groundwater batch experiments conducted at a water temperature of 20°C are presented in Figures 23 through 26. For purposes of comparison, the results of both the groundwater batch experiments and the distilled water batch experiments are presented in Figures 23 through 26. (The plotted data points for the distilled water batch experiments represent the average of the results for the small and large particle size ranges.)

Figure 23 reveals that, at 20°C, groundwater appeared to very slightly inhibit the leaching of organic material from the Type 1 spent shale for leaching time periods greater than 10 days. Conductivity levels as high as 19,000  $\mu\text{mhos/cm}$  were detected in leachate derived from Type 1 spent shale at 20°C. Since the conductivity of the synthetic groundwater was originally about 12,000  $\mu\text{mhos/cm}$ , it is apparent that considerable inorganic material associated with the spent shale matrix was leached during the 30-day leaching period.

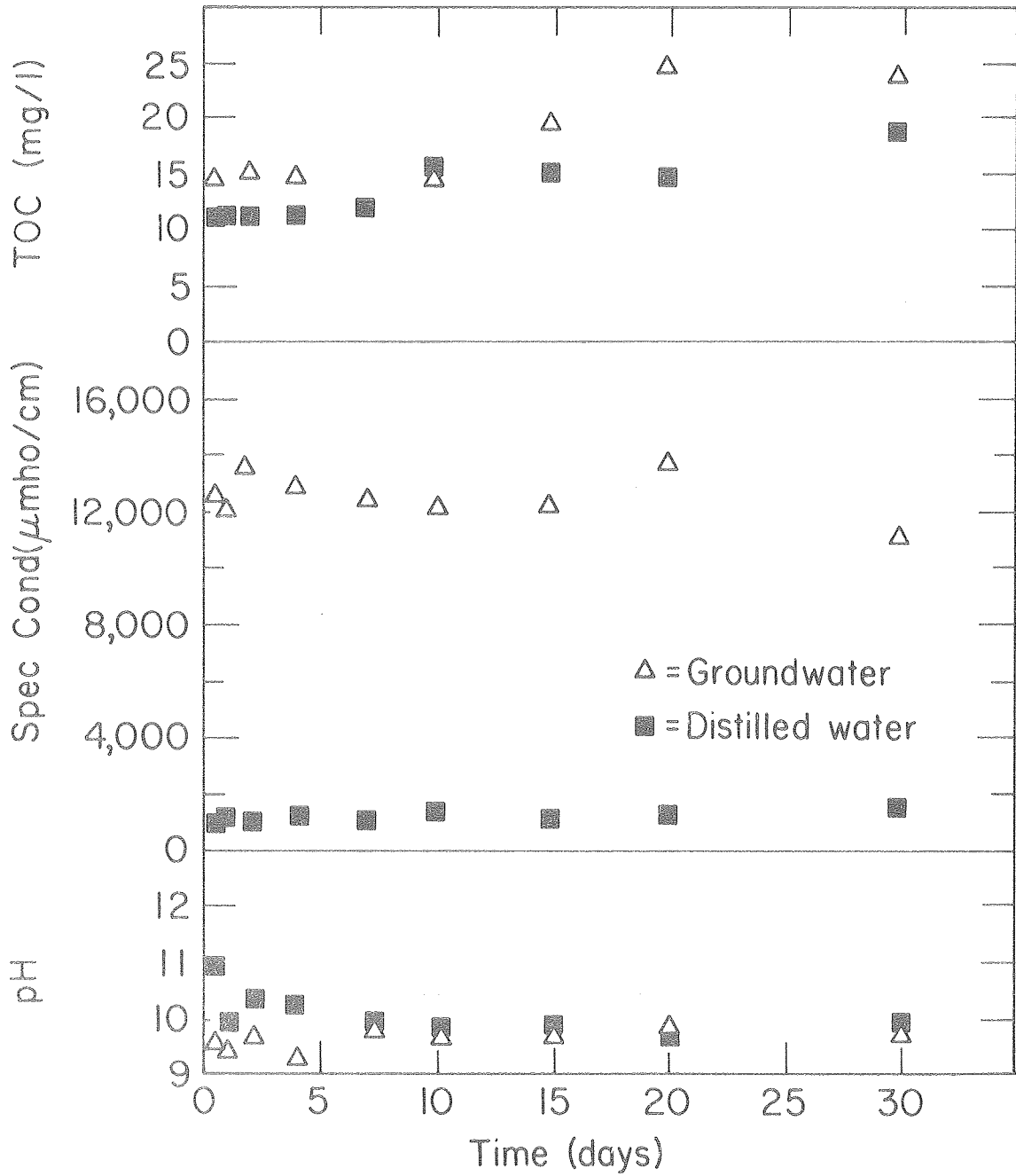
An examination of Figure 24 indicates that, at a temperature of 20°C, groundwater slightly enhances the leaching of organic material from Type 2 spent shale for most leaching time periods examined. After 30 days, approximately 5 mg/l more of organic carbon was leached from Type 2 spent shale during the groundwater experiments than during the distilled water experiments. Note that, during the groundwater experiments, the conductivity levels of the leachate derived from Type 2 spent shale were similar to the conductivity levels of the original groundwater, indicating that an insignificant portion of the soluble inorganics originally associated with the spent shale matrix were leached during the groundwater experiments.

Figure 25 reveals that, at 20°C, groundwater appeared to slightly inhibit the leaching of organic material from Type 3 spent shale for leaching time periods ranging up to 20 days. An examination of Figure



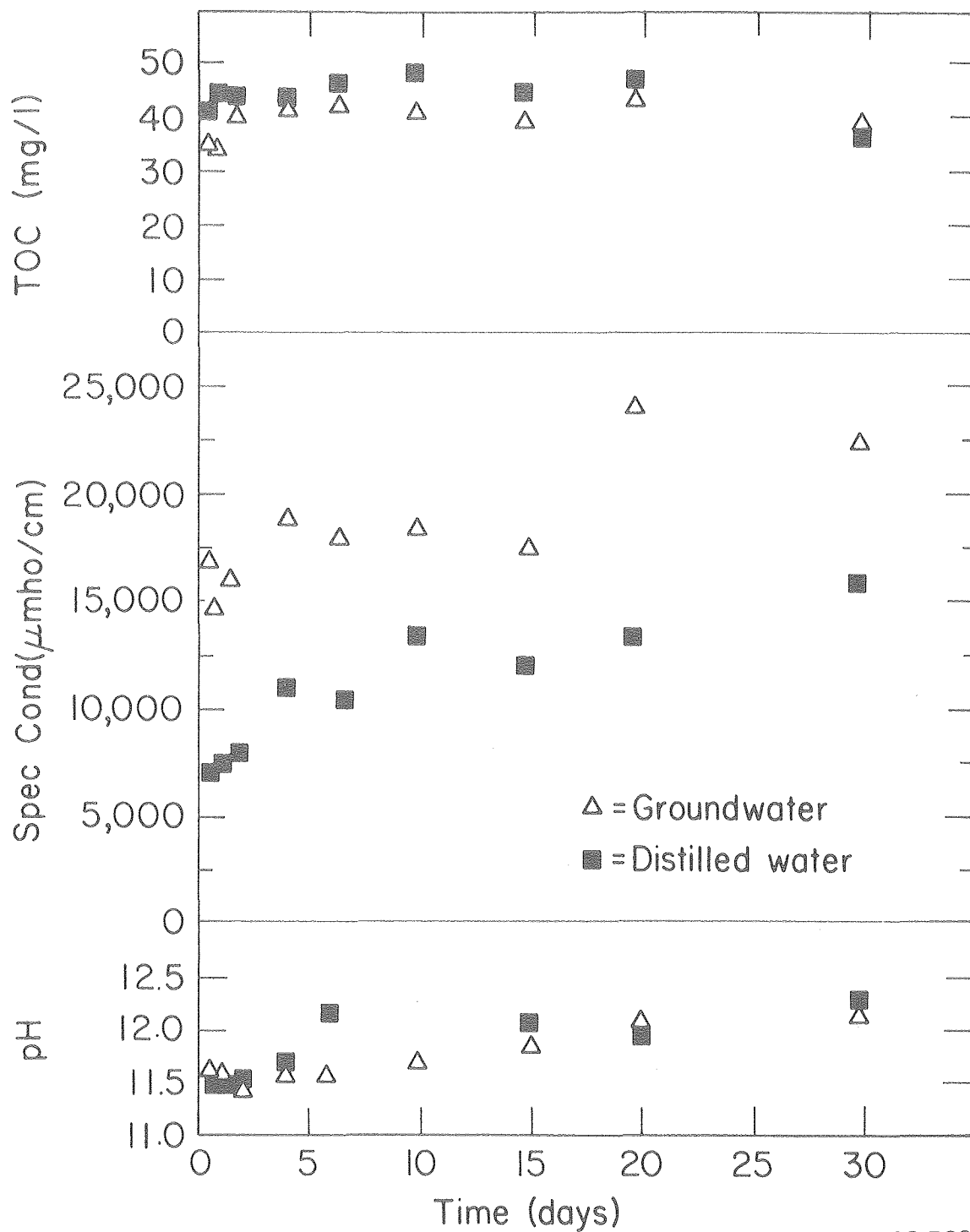
XBL 792-570

Figure 23. Groundwater batch experiments examining Type 1 spent shale at 20°C.



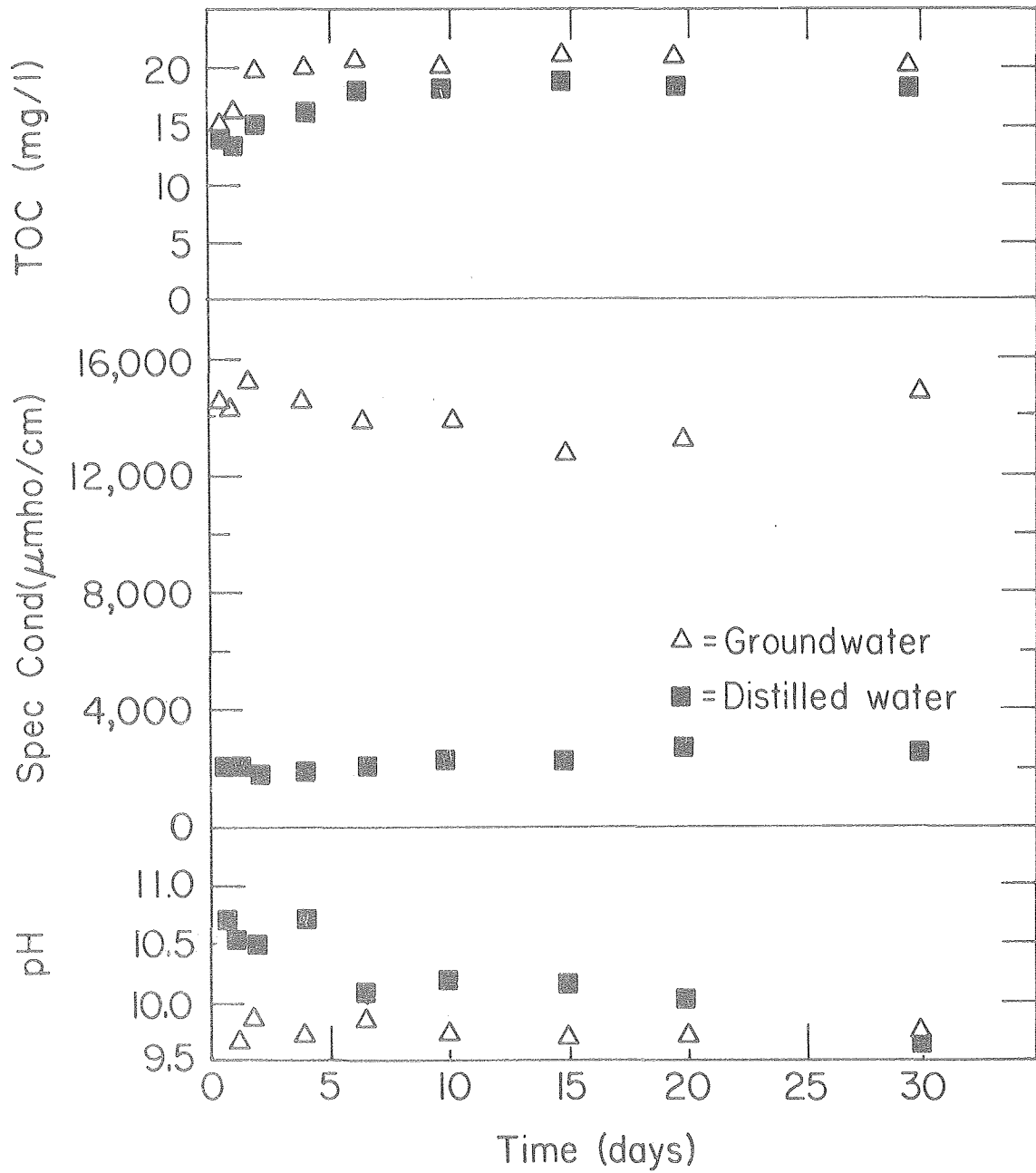
XBL 792-571

Figure 24. Groundwater batch experiments examining Type 2 spent shale at 20°C.



XBL 792-563

Figure 25. Groundwater batch experiments examining Type 3 spent shale at 20°C.



XBL 792-572

Figure 26. Groundwater batch experiments examining Type 4 spent shale at 20°C.

25 suggests that a significant amount of the organic carbon was readily leachable within the first day, regardless of whether ground-water or distilled water was employed. After the first day of leaching, organic carbon concentrations alternately increased and decreased over certain time periods within quite narrow limits, suggesting that reactions other than simple desorption were occurring. (Alternatively, these slight fluctuations in organic carbon concentrations over time may simply be due to experimental error.)

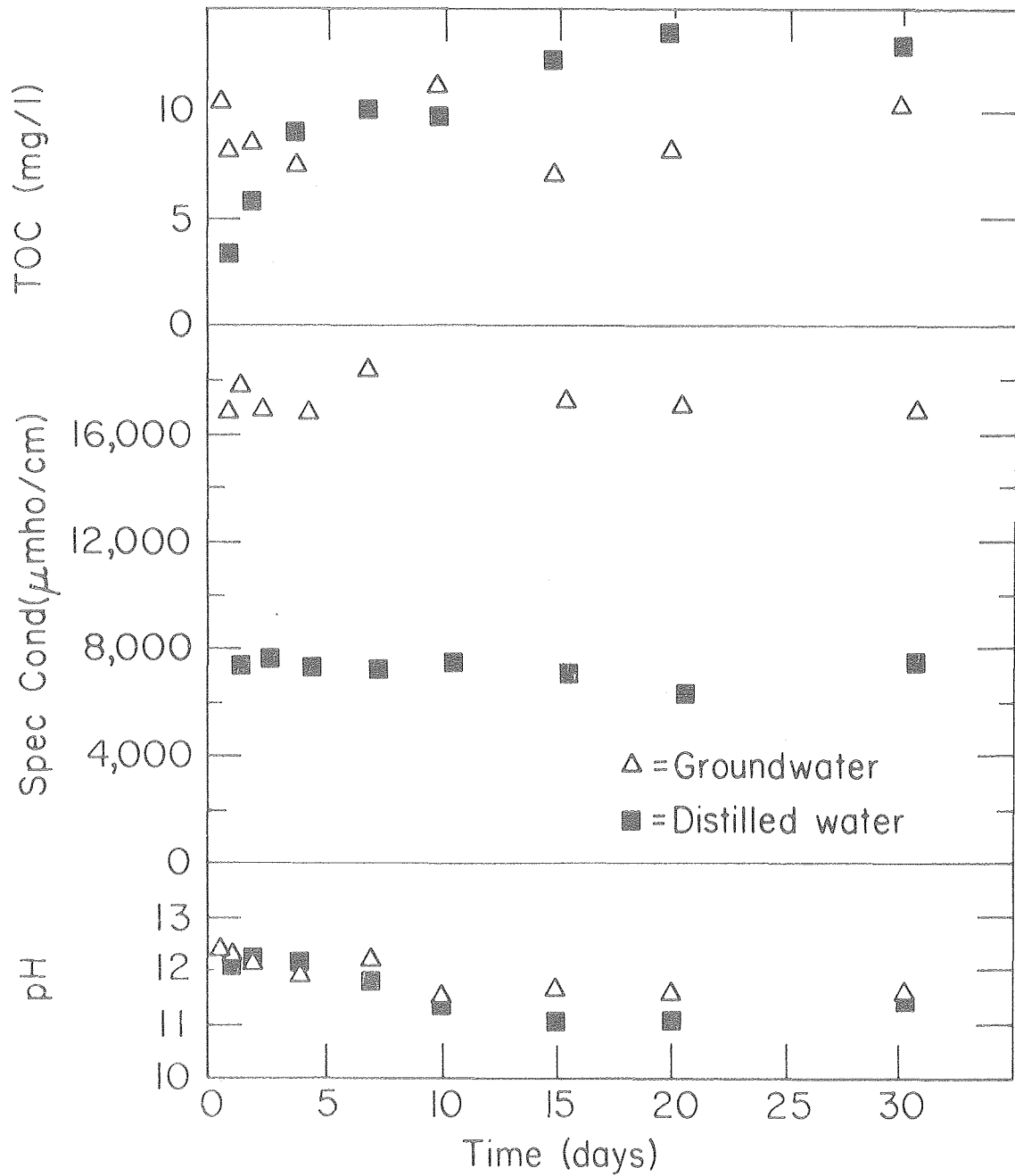
An examination of Figure 26 reveals that groundwater appeared to slightly enhance the leaching of organic material for the Type 4 spent shale.

In contrast to the distilled water batch experiments, it is interesting to note that pH levels did not greatly vary as a function of time during the synthetic groundwater experiments. This is likely due to the fact that certain anions present in the synthetic groundwater (i.e.,  $\text{HCO}_3^-$  and  $\text{CO}_3^{2-}$ ) served as a buffering system and thus resisted changes in pH during leaching.

Synthetic Groundwater Batch Experiments Conducted at a Water Temperature of 80°C. The results of the synthetic groundwater batch experiments conducted at a water temperature of 80°C are presented in Figures 27 through 30. As before, the results of both the groundwater batch experiments and the previous distilled water batch experiments are presented for purposes of comparison.

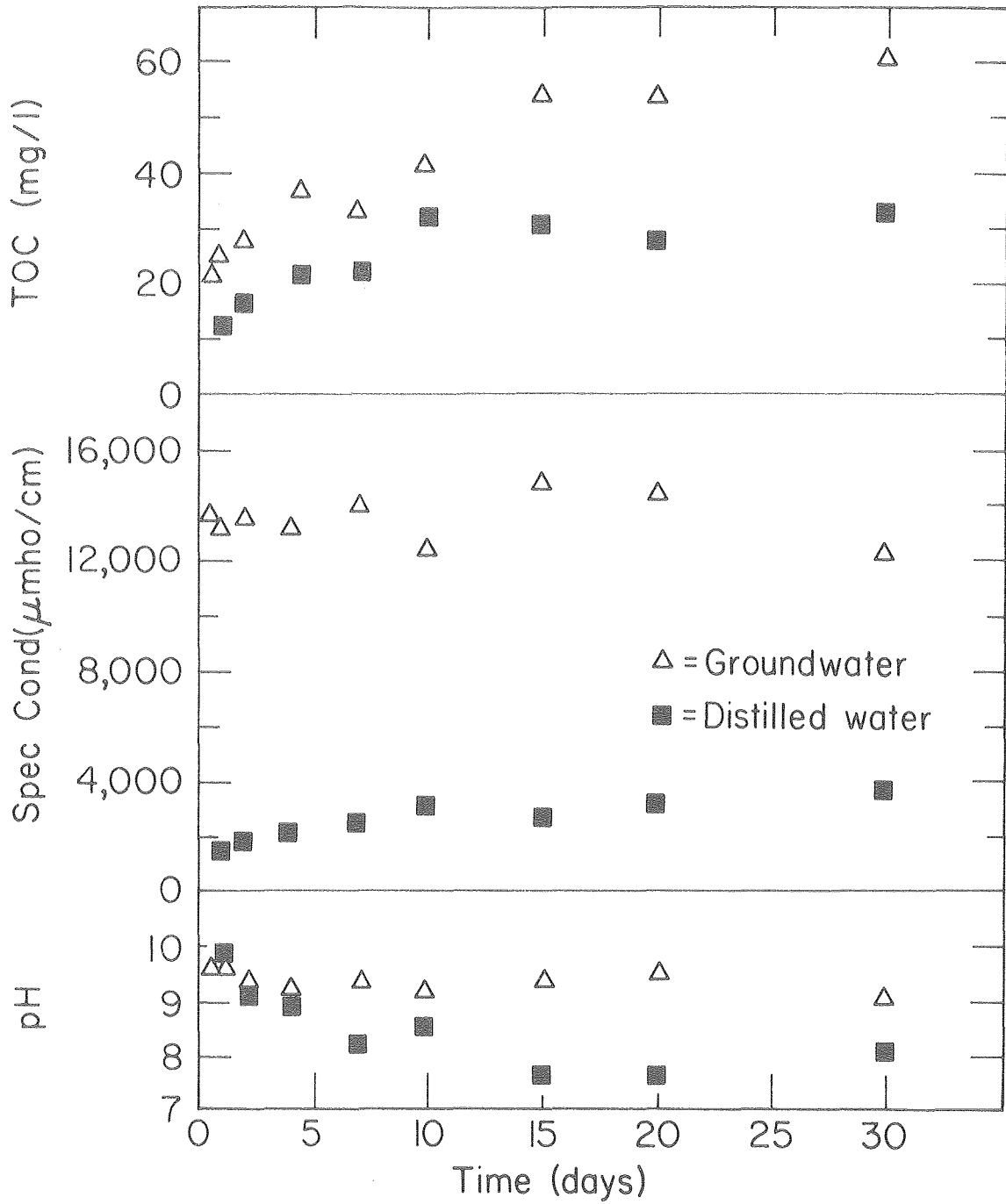
An examination of Figure 27 reveals that groundwater at 80°C inhibited the leaching of organic material from the Type 1 spent shale except for the initial 2 days and the tenth day of the leaching period. After 30 days, about 2.5 mg/l less organic carbon was leached by groundwater from the Type 1 spent shale than by distilled water. Conductivity levels for both the groundwater and distilled water batch experiments were fairly constant over all but the initial time periods investigated, indicating that a considerable amount of soluble inorganic material originally associated with the spent shale matrix was leached during initial periods of leaching by both groundwater and distilled water at 20°C.

The results presented in Figure 28 show that groundwater significantly enhances the leaching of organic material from the Type 2 spent shale at 80°C. After 30 days, approximately 25 mg/l more of organic carbon was leached by groundwater than by distilled water. During the groundwater experiments the highest TOC concentration - 58 mg/l - was detected after 30 days of leaching. This TOC concentration was the highest detected in any of the batch experiments. The significance of this high TOC concentration is that it is about one-half the TOC concentration of domestic sewage (the TOC concentration of typical domestic sewage is about 125 mg/l). Figure 28 also reveals that, during the entire leaching period of 30 days, conductivity levels remained at about 13,000  $\mu\text{mhos/cm}$ , indicating that soluble inorganics



XBL 792-561

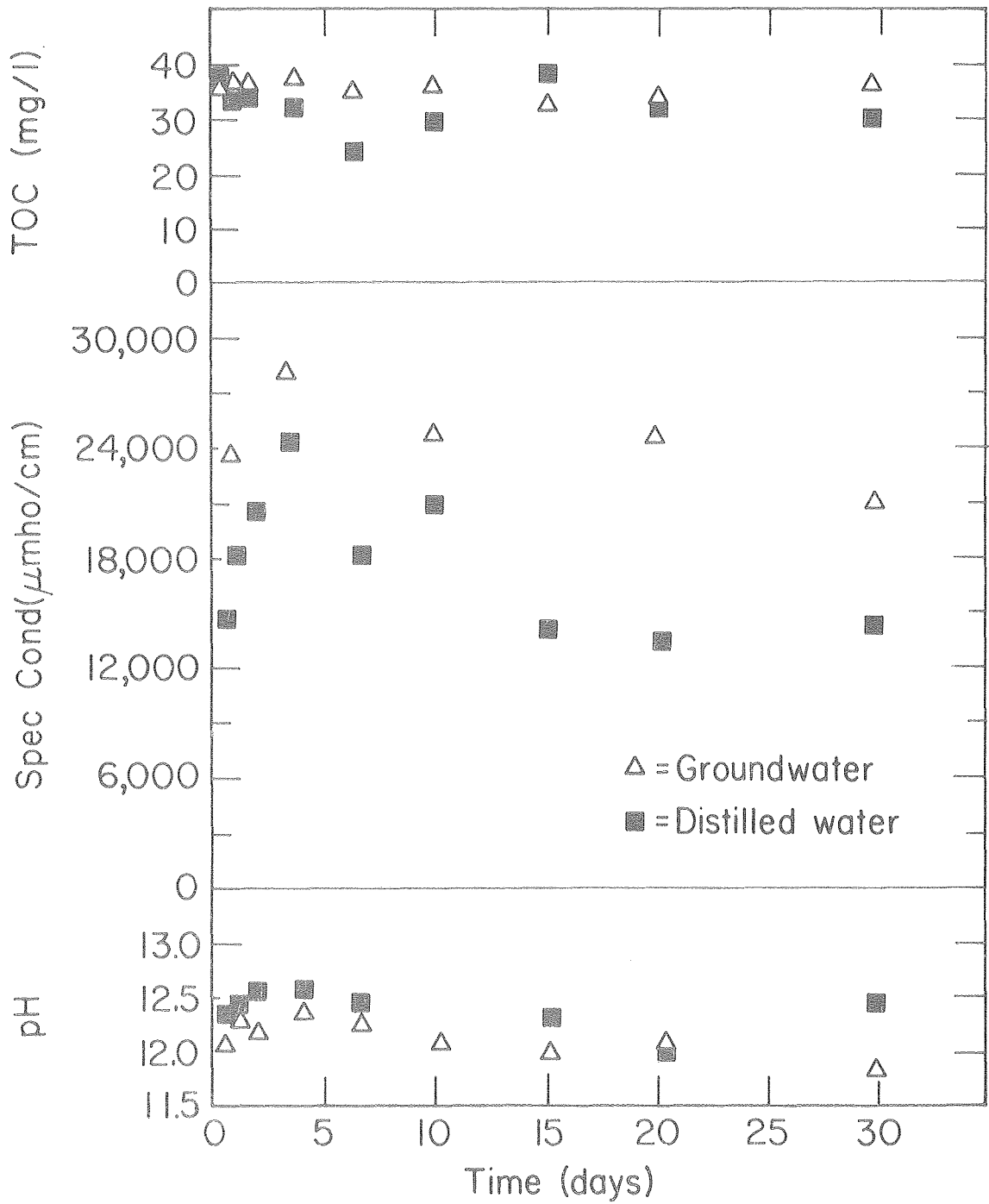
Figure 27. Groundwater batch experiments examining Type 1 spent shale at 80°C.



XBL 792-560

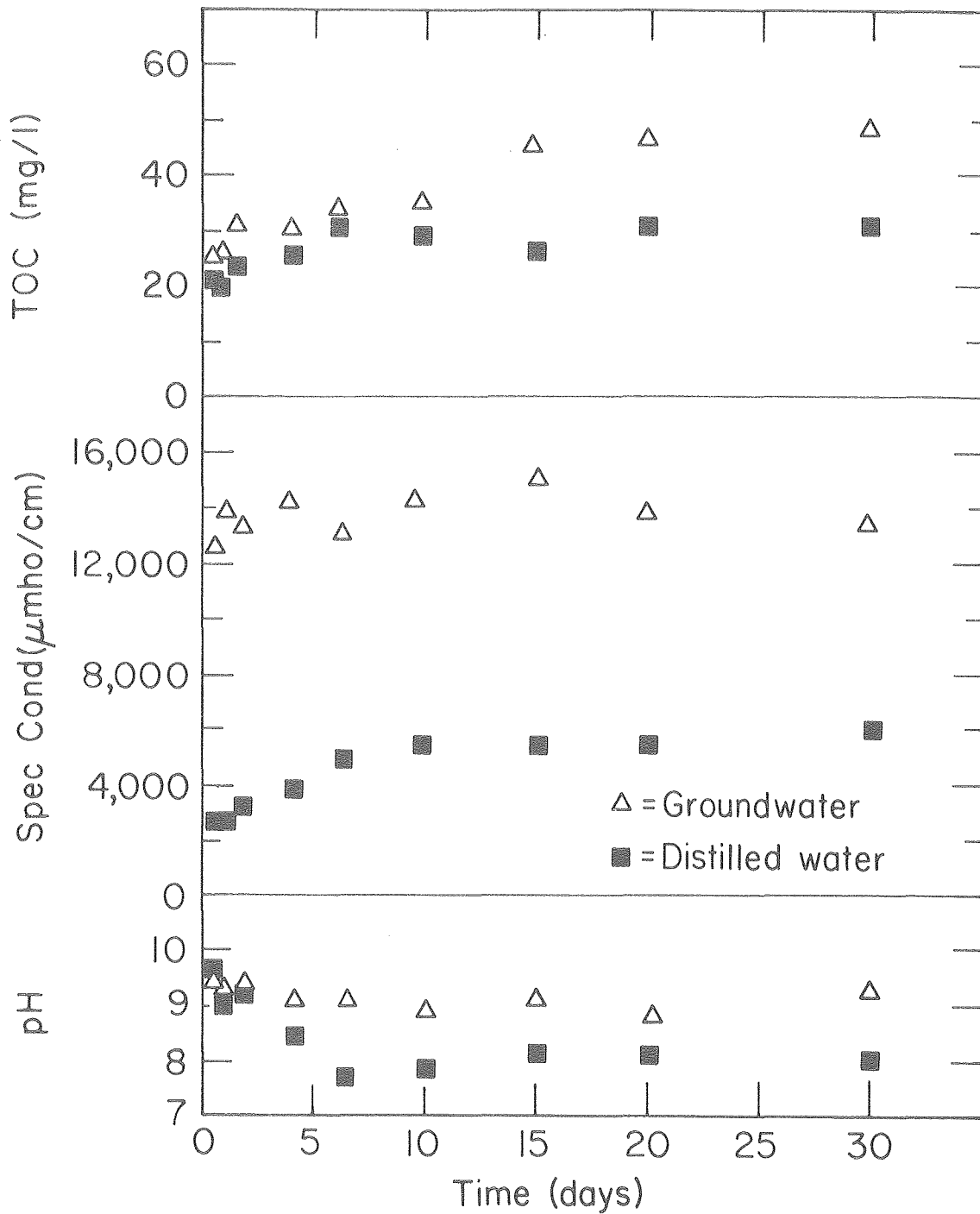
Figure 28. Groundwater batch experiments examining Type 2 spent shale at 80°C.





XBL 792-565

Figure 29. Groundwater batch experiments examining Type 3 spent shale at 80°C.



XBL 792-566

Figure 30. Groundwater batch experiments examining Type 4 spent shale at 80°C.

associated with the spent shale matrix were not readily leached by groundwater at 80°C.

Figure 29 reveals that, at a water temperature of 80°C, the quality characteristics of groundwater did not dramatically affect the leaching of organic material from Type 3 spent shale. In contrast, Figure 30 reveals that groundwater significantly enhanced the leaching of organic material from Type 4 spent shale at a water temperature of 80°C. These results derived from Type 4 spent shale are similar to the previous results derived from Type 2 spent shale. In both cases, groundwater at an elevated water temperature dramatically enhanced the leaching of organic material from spent shale produced during an inert gas run. It is hypothesized that this phenomenon is due to a synergistic effect, involving both the quality characteristics of groundwater and an elevated water temperature. Recall that during the distilled water batch experiments, an elevated water temperature only moderately enhanced the leaching of organic material from spent shales produced during inert gas retorting. Furthermore, at a low water temperature, the leaching of organic material from these types of spent shale was not significantly affected by the quality of the leach water (i.e., distilled water or groundwater). The dramatic enhancement of the leaching of organic material occurred when groundwater was employed at an elevated water temperature and thus, the observed phenomenon is likely attributable to the hypothesized synergistic effect, involving both water quality and water temperature. A possible explanation for this synergistic effect is related to (1) the greater solubility of phenolics and carboxylic acids at higher temperatures and (2) the presence of Na<sup>+</sup> ions in the synthetic groundwater. A combination of the above factors may lead to the formation of sodium phenolates and sodium carboxylates, both of which are very soluble salts. Furthermore, the high pH in leachate derived from synthetic groundwater compared to distilled water would produce a greater solubility of phenolics and carboxylic acids.

In summary, it is apparent that synthetic groundwater compared to distilled water enhances the leaching of organic material in some cases while, in other cases, it inhibits the leaching of organic material. The results of this limited set of groundwater batch experiments suggest that groundwater compared to distilled water slightly inhibits the leaching of organic material from spent shale produced during a combustion run such as the Type 1 spent shale. In contrast, it appears that groundwater enhances the leaching of organic material from spent shale produced during an inert gas run such as the Type 2 and Type 4 spent shales, this enhancement being very significant at elevated water temperatures.

These experiments indicate that the composition and pH of groundwater can significantly affect both the leaching phenomenon and the solubility of various organics in the leachate. These effects may be due to (1) solubility relationships, (2) equilibrium relationships, and/or (3) reactions and interactions between inorganic components of the leachate. One possible explanation of how groundwater may inhibit the leaching of organic material is that leached organic ions may subsequently combine with inorganic ions originally present in the groundwater and

form a precipitate. Another explanation is that an inorganic cation leached from the spent shale may react with and insolubilize certain leached organics. Another possible explanation is that an inorganic ion originally present in the groundwater may replace an organic ion originally present within the spent shale matrix as a consequence of an ion exchange mechanism, thus "liberating" the organic ion. It should be noted, however, that these are possible explanations only and are presented here for purposes of illustration; they may not describe the actual mechanisms responsible for the observed results.

In a manner similar to the low-temperature synthetic groundwater experiments, pH levels did not vary greatly as a function of time during the high-temperature synthetic groundwater experiments. This is likely due to the buffering effect of the synthetic groundwater which contained significant concentrations of  $\text{HCO}_3^-$  and  $\text{CO}_3^{=}$ .

Discussion of Results Derived from Type 3 Spent Shale During Synthetic Groundwater Batch Experiments. A previous section discussed results derived from Type 3 spent shale during distilled water batch experiments. In this previous discussion, it was asserted that phenolics and carboxylic acids leached from Type 3 spent shale may be subsequently insolubilized by combining with bivalent cations to form phenolates and carboxylates. The formation of phenolates and carboxylates involves a series of inter-related reactions, including both dissociation and insolubilization reaction. Certain of these reactions are influenced by pH and, in some cases, kinetics may play a key role.

During the synthetic groundwater experiments which examined Type 3 spent shale, concentrations of organic carbon dramatically increased during initial time periods of leaching and shortly thereafter, leveled off to a fairly constant value. The fluctuations in data observed during the corresponding distilled water experiments were much less observable in data derived from the synthetic groundwater experiments.

During the synthetic groundwater experiments, leachate derived from Type 3 spent shale was characterized by high levels of both conductivity and pH (pH values ranging from approximately 11.5 to 12.5). These high levels of conductivity and pH are described in Figures 25 and 29. It is asserted that high pH conditions in conjunction with the presence of bivalent cations enabled the formation of insoluble phenolates and carboxylates during the synthetic groundwater experiments (in a manner similar to the distilled water experiments). In contrast to the distilled water experiments, fluctuations in organic carbon measurements were much less discernible during the synthetic groundwater experiments. This was likely due to the fact that pH did not greatly vary over time as a consequence of the buffering capacity of the synthetic groundwater. It is likely that a fairly constant pH resulted in a relatively constant rate of phenolate and carboxylate formation as phenolics and carboxylic acids were leached.

As indicated previously, bivalent cations may serve as a "sink" for phenolics and carboxylic acids leached from Type 3 spent shale. Thus, phenolics and carboxylic acids leached from Type 3 spent shale may subsequently be insolubilized during the formation of phenolates and carboxylates. In contrast, for other types of spent shale, it is likely that various organics were leached until their solubility was reached and thereafter, leached organics remained in solution. Since it is anticipated that leachate derived from inert gas-retorted spent shale will contain both phenolics and carboxylic acids, one would expect that synthetic groundwater containing sodium ions may enhance the leaching of these materials due to the formation of sodium phenolates and sodium carboxylates, both of which are water-soluble salts. This enhancement related to inert gas-retorted spent shale may be particularly significant at higher water temperatures where the solubility of phenolics and carboxylic acids is greater.

Finally, it should be recognized that the results derived from the synthetic groundwater experiments may have been dramatically different if a synthetic groundwater containing high concentrations of  $\text{Ca}^{++}$  and  $\text{Mg}^{++}$  had been used. Instead, the actual synthetic groundwater contained only sodium as a cation. In contrast to  $\text{Ca}^{++}$  and  $\text{Mg}^{++}$ ,  $\text{Na}^+$  will not insolubilize phenolics or carboxylic acids.

Summary of Batch Experiments. The total organic and inorganic material leached during the batch experiments are summarized in Tables 12 and 13.

A summary of TOC levels after 30 days of leaching is presented in Table 12. In addition, Table 12 also describes the initial solid-phase organic carbon content of spent shale samples. As revealed by Table 12, relatively little of the organic material initially present in spent shale samples was leached. This may be due to (1) solubility limitations and/or (2) the fact that most of this solid-phase organic material may not be water-soluble. Furthermore, it is important to note from Table 12 that retorting conditions, water temperature, and initial water quality significantly affect the organic water pollution potential of in-situ spent shale.

Table 13 presents estimates of TDS levels after 30 days of leaching. These TDS estimates were derived by multiplying corresponding conductivity levels by an empirical factor of 0.6 (Ref. 24). It should be recognized that this method of estimating TDS provides, at best, a rough estimate. Although conductivity is an indicator of the total ions in solution, it can be significantly influenced by pH. Table 13 shows the dramatic effect of carbonate decomposition on the levels of TDS in leachate.

Table 12. Total organic carbon leached from various types of spent shale during batch experiments.

Experiment type	Total organic carbon (TOC) leached, mg/100g of spent shale			
	Type 1	Type 2	Type 3	Type 4
30-day distilled water batch, 20°C	1.1	1.9	3.5	1.7
30-day distilled water batch, 80°C	1.3	3.1	2.9	3.1
30-day groundwater batch, 20°C	1.0	2.3	3.8	2.0
30-day groundwater batch, 80°C	1.0	5.8	3.4	4.7
	Initial solid-phase organic carbon content of spent shale mg/100g of spent shale <sup>a</sup>			
	200	1800	2100	3900

<sup>a</sup>Originally presented in Table 11.

Table 13. Estimated total dissolved solids (TDS) leached from various types of spent shale during batch experiments.

Experiment type	Estimated total dissolved solids (TDS) leached, mg/100g of spent shale			
	Type 1	Type 2	Type 3	Type 4
30-day distilled water batch, 20°C	510	110	1,000	160
30-day distilled water batch, 80°C	470	230	850	360
30-day groundwater batch, 20°C	420	≈ 0	600	140
30-day groundwater batch, 80°C	250	≈ 0	520	70

<sup>a</sup>These estimates for TDS leached with groundwater were derived by taking into account the difference between the original TDS (as estimated from conductivity) of the synthetic groundwater and the final TDS (as estimated from conductivity) of the leachate after 30 days.

Fractionation of Composite Samples Derived from Batch Experiments and Various Fractions. As indicated previously, total organic carbon (TOC) provides a general indication of the total organic material present in leachate but provides no indication of the types of organic compounds that may be present. In order to provide a more refined characterization of organic material present in leachate, the organic material was fractionated into acid, base, and neutral fractions. Analysis for acid/base/neutral fractions of organic material provides a general indication of the classes of organic compounds that may be present in leachate, classified according to their acid/base character, include: (1) carboxylic acids and phenols as acidic compounds, (2) amines as basic compounds, and (3) hydrocarbons as neutral compounds.

During the previously described batch and column experiments, a myriad of samples was generated. Rather than analyze each sample for acid, base, and neutral fractions, a decision was made to analyze composite samples instead of individual samples. This was based on: (1) the relatively small mass of organic material present in individual samples and (2) the laborious and time-consuming effort involved in fractionating all of the individual samples generated.

Batch samples were composited according to the following procedure. All samples, regardless of particle size and leaching time, were first grouped according to spent shale type, water type, and water temperature. Each of these groups of samples was then mixed together to form a single composite sample. This procedure was generally considered to be valid since most of the leached organic material was leached during initial time periods and therefore, leaching time was not as important a variable as retorting conditions, water temperature, and water quality. This compositing scheme resulted in creation of eight distilled water composite samples (four types of spent shale, two water temperatures) and four groundwater composite samples (two types of spent shale, two water temperatures). It should be noted that only four groundwater composite samples were created for fractionation purposes; only individual samples derived from Types 1 and 2 spent shale were composited.

The results of the fractionation of composite samples derived from the batch experiments are presented in Table 14. While examining the results presented in Table 14, it is important to bear in mind that the order of extraction, described in Figure 12, will have some effect on the relative magnitude of the various extracted fractions. The defined order of extraction (i.e., acid fraction extracted before basic fraction) may lead to a more effective overall extraction of acidic material than basic material. Ideally, two series of extractions should have been employed: one extracting the acid fraction before the basic fraction and one extracting the basic fraction before the acid fraction. However, due to the laborious and time-consuming nature of organic extractions, a decision was made to employ only the order of extraction described in Figure 12. Unfortunately, this realization came as hindsight after completion of all extractions.

It is also important to note that the particular solvent selected for extraction purposes will influence the types of organics extracted and the relative proportion of acid, base, and neutral fractions. According to solvent extraction theory, a solvent is more effective in extraction (i.e., dissolving) substances that are of a similar physical and chemical character. Hexane, being a non-polar solvent of neutral character, will more effectively extract compounds of a similar character such as neutral hydrocarbons. Thus, water-soluble organic compounds of a polar or ionic character will preferentially remain dissolved in leachate rather than be extracted by the hexane. However, it should be noted that the ionic character and thus the solubility of acidic and basic compounds can be changed by varying the pH of the leachate during extraction.

As indicated previously, it is important to recognize that some phenolic material may be extracted as part of the neutral fraction while some of the more strongly acidic phenols may appear in the acidic fraction. Furthermore, it should be pointed out that polynuclear aromatic hydrocarbons (PAH), some of which are suspected carcinogens, would be extracted as part of the neutral fraction, if present in leachate.



Table 14. Acid, base, and neutral fractions of organic material in composite samples derived from batch experiment.

Batch experiment		Mass of organic material, mg/100g of spent shale			
		Type 1	Type 2	Type 3	Type 4
Distilled water, 20°C	Acid	0.68	0.37	0.36	0.88
	Base	0.46	0.51	0.29	0.54
	Neutral	0.86	0.88	0.28	1.05
	Total	2.00	1.76	0.93	2.47
Distilled water, 80°C	Acid	0.50	0.45	0.33	0.72
	Base	0.61	0.33	0.47	0.36
	Neutral	0.18	0.35	0.52	0.89
	Total	1.29	1.13	1.32	1.97
Groundwater, 20°C	Acid	0.42	0.92	---	---
	Base	0.37	0.44	---	---
	Neutral	0.66	1.60	---	---
	Total	1.45	2.96	---	---
Groundwater, 80°C	Acid	0.50	1.10	---	---
	Base	0.33	0.59	---	---
	Neutral	0.36	2.30	---	---
	Total	1.19	3.99	---	---

The results presented in Table 14 generally indicated that the greatest neutral fraction of organic material was detected in leachate derived from spent shales produced during inert gas runs (i.e., Type 2 and Type 4 spent shales). It is hypothesized that this neutral fraction may consist largely of unextracted hydrocarbons which are neutral in character and possibly some phenolics. According to this hypothesis, some hydrocarbons produced during the pyrolysis of kerogen may remain associated with the spent shale matrix as a consequence of capillary and adhesive forces. Subsequently, these hydrocarbons may be partially solubilized by water coming into contact with the spent shale. In contrast, one would not expect to find significant amounts of hydrocarbons - which are readily combustible - associated with spent shale produced during an ordinary combustion run (i.e., Type 1 spent shale). It should be noted that the acid fraction was the second most prevalent fraction in leachate derived from spent shales produced during inert gas runs. This acid fraction may consist of carboxylic acids and some phenolics produced as by-products during the pyrolysis of kerogen. (Phenolics, if extracted, may appear in both the neutral and acidic fractions to varying degrees.)

It is interesting to note the fractionation results of leachate derived from the Type 3 spent shale, produced during a combustion run employing recycle gas are lower than anticipated, based on data presented in Table 12. Recall that it was originally hypothesized that recycle gas supplied to the retort behind the flame front may lead to the adsorption or condensation of volatile hydrocarbons or other organics onto particles of spent shale. This hypothesis was advanced in order to explain the high concentrations of organic carbon detected in leachate derived from Type 3 spent shale. However, all of the fractions derived from the Type 3 spent shale leachate, including the neutral fraction, were lower than anticipated. This suggests that the original hypothesis may not be entirely valid or that volatile organics not readily extractable by hexane were adsorbed or condensed onto the spent shale from the recycle gas.

While leachate derived from the Type 1 spent shale had significantly lesser concentrations of organic carbon than leachate derived from Types 2, 3, and 4, the total amount of material extracted from the Type 1 leachate was fairly comparable to that extracted from the Type 4 leachate and greater than that extracted from the Type 2 and Type 3 leachates. Although the Type 1 leachate contained significantly less dissolved organic material (based on TOC measurements), it appears that the solvent employed (hexane) was more effective in extracting organic material from the Type 1 leachate than from Types 2, 3, and 4. Other possible explanations for this phenomenon include: (1) a greater proportion of the dissolved organics in the Type 1 leachate were nonpolar (and therefore, preferentially more soluble in hexane than in water) or (2) the formation of emulsions between hexane and water interfered with the extraction technique.

A comparison of the distilled water batch experiments conducted at a water temperature of 20°C with those conducted at a water temperature of 80°C reveals an interesting anomaly. It was determined during the distilled water batch experiments that water temperature seemed to enhance the leaching of organic material (as indicated by organic carbon measurements). As shown in Table 14, however, the total mass of organic material extracted from the high-temperature distilled water batch experiments was less than that extracted from the low-temperature experiments. This suggests that the types of organic materials leached during the high-temperature experiments were different (and less extractable by hexane) from the types of organic materials leached during the low-temperature experiments (which appeared to be more extractable by hexane).

In comparing the results of the distilled water and the groundwater batch experiments, it is seen that, in general, groundwater slightly affected the total amount of organic material leached and the relative amounts of the various fractions leached from the Type 1 spent shale. In contrast, groundwater greatly enhanced the overall leaching of organic material from the Type 2 spent shale, and in particular, the neutral fraction.

The data presented in Table 14 are not altogether conclusive. It appears that only three significant conclusions can be drawn from these data, the first being that there exists a variety of organic compounds in leachate derived from in-situ spent shale. Virtually all of the leachate samples had measurable amounts of acid, base, and neutral fractions, suggesting the possible presence of acidic compounds such as carboxylic acids and some phenols, basic compounds such as amines and pyridines, and neutral compounds such as hydrocarbons (recall that some phenols, if extracted, may appear in the neutral fraction). The second conclusion is that the neutral fraction (probably mostly hydrocarbons and possibly some phenols) is the most predominant fraction associated with leachate derived from spent shale produced during inert gas runs. The third conclusion that may be drawn is that the types of organic compounds leached at a water temperature of 20°C appeared to be different from the types of organic compounds leached at a water temperature of 80°C. Based on the result of Table 14, it is apparent that more sophisticated analytical work is required to accurately define the classes of organic compounds that are present in leachate.

The overall efficiency of the extraction technique in extracting organic material from the various leachates is described in Table 15. Table 15 presents tabulated values of (1) milligrams of TOC leached per 100 grams of spent shale, (2) estimated milligrams of organics leached per 100 grams of spent shale (estimated by dividing the

Table 15. Comparison of extracted mass of organics with estimated mass of organics in leachate.

Batch experiment	Type of spent shale	TOC leached, mg/100 g spent shale	Estimated organics leached, mg/100 g spent shale	Extracted organics leached, mg/100 g spent shale	Percent of organics extracted
Distilled water, 20°C	Type 1	1.1	1.4	2.0	100
	Type 2	1.9	2.5	1.8	72
	Type 3	3.5	4.6	0.9	20
	Type 4	1.7	2.2	2.5	100
Distilled water, 80°C	Type 1	1.3	1.7	1.3	76
	Type 2	3.1	4.1	1.1	27
	Type 3	2.9	3.8	1.3	34
	Type 4	3.1	4.1	2.0	49
Groundwater, 20°C	Type 1	1.0	1.3	1.5	100
	Type 2	2.3	3.0	3.0	100
Groundwater, 80°C	Type 1	1.0	1.3	1.2	92
	Type 2	5.8	7.6	4.0	53

milligrams of TOC by 0.765\*); (3) extracted milligrams of organics leached per 100 grams of spent shale; and (4) the percent of organics extracted. As revealed by Table 15, the extraction efficiencies ranged from 20 to 100 percent.

It is interesting to note that the overall extraction efficiencies were greatest for the Type 1 leachate. This is consistent with previous observations regarding the disproportionately high acid, base, and neutral fractions associated with the Type 1 leachate. In contrast, the extraction efficiencies for the Type 3 leachate were the lowest overall. This is consistent with the high organic carbon concentrations observed and the low acid, base, and neutral fractions detected from the Type 3 leachate. Theoretically, one would not anticipate an extraction efficiency of close to 100 percent due to the inability of the selected solvent to dissolve all organics present in leachate.

#### Organic Nitrogen in Composite Samples Derived from Batch Experiments.

The composite samples were analyzed for organic nitrogen in order to provide a general indication of the nitrogenous organic material present in leachate derived from various types of spent shale under various experimental conditions. The results of these analyses are presented in Table 16, which describes both concentration and mass leached per unit mass.

The results presented in Table 16 suggest that, employing distilled water, the highest concentration of organic nitrogen was detected in the Type 4 leachate, derived from spent shale produced during an inert gas run. During the distilled water batch experiments, the concentration of organic nitrogen in the Type 3 leachate was only slightly less than in the Type 4 leachate. The lowest concentration of organic nitrogen was detected in the Type 1 leachate, derived from spent shale produced during an ordinary combustion run. Employing distilled water, it appears that an elevated water temperature slightly enhanced the leaching of nitrogenous organic material from Types 3 and 4 spent shale while slightly inhibiting the leaching of organic nitrogen from the Type 1 spent shale.

Employing groundwater, the results presented in Table 17 indicate that leachate derived from spent shale produced during inert gas runs contained the highest concentration of nitrogenous organic material. Surprisingly, the Type 3 leachate contained the least. An elevated water temperature in some cases enhanced while in other cases it inhibited the leaching of organic nitrogen.

---

\*The rationale for the factor of 0.765 is as follows. The organic fraction of raw oil shale is comprised of 76.5 percent carbon. Correspondingly, water soluble organic material present in leachate is assumed to be 76.5 percent carbon. It is recognized that this is, at best, a rough estimate.

Table 16. Organic nitrogen in composite samples derived from batch experiments.

Batch experiment	Type 1 shale			Type 2 shale			Type 3 shale			Type 4 shale		
	Conc. <sup>a</sup>	Mass <sup>b</sup>	C/N <sup>c</sup>	Conc. <sup>a</sup>	Mass <sup>b</sup>	C/N <sup>c</sup>	Conc. <sup>a</sup>	Mass <sup>b</sup>	C/N <sup>c</sup>	Conc. <sup>a</sup>	Mass <sup>b</sup>	C/N <sup>c</sup>
Distilled water, 20°C	0.7	0.07	16	0.7	0.07	27	0.9	0.09	39	1.0	0.10	17
Distilled water, 80°C	0.4	0.04	33	0.7	0.07	44	1.3	0.13	22	1.4	0.14	22
Groundwater, 20°C	0.9	0.09	11	0.9	0.09	26	0.7	0.07	54	0.9	0.09	22
Groundwater, 80°C	0.7	0.07	14	0.9	0.09	64	0.6	0.06	57	1.2	0.12	39

<sup>a</sup>Concentration, mg/l.

<sup>b</sup>Mass leached per unit mass, mg/100g.

<sup>c</sup>Ratio of organic carbon to organic nitrogen.

Table 17. Phenols in composite samples derived from batch experiments.

Phenols in composite samples	Batch experiment	
	Distilled water, 20°C	Distilled water, 80°C
Type 1		
Conc. <sup>a</sup>	0.25	0.23
Mass <sup>b</sup>	0.025	0.023
Type 2		
Conc. <sup>a</sup>	0.43	0.30
Mass <sup>b</sup>	0.043	0.030
Type 3		
Conc. <sup>a</sup>	0.22	0.15
Mass <sup>b</sup>	0.022	0.015
Type 4		
Conc. <sup>a</sup>	0.41	0.35
Mass <sup>b</sup>	0.041	0.035

<sup>a</sup>Concentration, mg/l.

<sup>b</sup>Mass leached per unit mass, mg/100g.

It has been reported that the ratio of organic carbon to organic nitrogen in raw oil shale is approximately 35:1 (Ref. 4). Assuming that the organic carbon to organic nitrogen ratio in spent shale is also 35:1, it is possible to make a general assessment of the solubility of nitrogenous organic compounds associated with the spent shale matrix. The ratios of organic carbon to organic nitrogen in the various leachates are presented in Table 16. As revealed by Table 16, the C:N ratios in leachate ranged from 11:1 to 64:1. It is interesting to note that organic nitrogen was more predominant (based on C:N ratios) in the Type 1 leachate than in other leachates. In contrast, organic nitrogen appeared to be least predominant in the Type 3 leachate.

Phenols in Composite Samples Derived from Batch Experiments.

Certain of the composite samples analyzed for acid/base/neutral fractions and organic nitrogen were also analyzed for phenols. (Only composite samples generated with distilled water as leach water were examined.) Phenols represent a potentially significant pollutant in situations where oil and water come into contact. The results of analyses for phenols are presented in Table 17. The results of Table 17 suggest that, employing distilled water at a water temperature of 20°C, the

highest concentration of phenols was detected in leachate derived from spent shale produced in an inert gas environment while the lowest concentration of phenols was detected in leachate derived from spent shale produced under combustion conditions.

Employing distilled water at a temperature of 80°C, the highest concentration of phenols was again detected in leachate derived from spent shales produced during inert gas retorting. It is interesting to note that, at an elevated water temperature, the corresponding concentrations of phenols were less than at lower water temperatures.

During the batch experiments, concentrations of phenols as high as 0.43 mg/l were detected. At first glance, it appears that, on a mass basis, phenols represent a rather small percent of the overall total mass of organics leached from spent shale. However, it is important to note that polyphenolics (i.e., phenolics with more than one aromatic ring) may not be detectable using the particular method of analysis employed. Since the analytical method involved a distillation step, one would not expect all polyphenolics to be measured since higher molecular weight polyphenolics tend to be rather nondistillable. Consequently, the values presented in Table 17 are probably lower than the actual concentrations of phenolics.

#### Equilibrium Batch Experiments

The results of the equilibrium batch experiments are presented in Table 18. The major objective of the equilibrium batch experiments was to generate data required for developing equilibrium isotherms. The results presented in Table 18 will be used to develop equilibrium isotherms in a subsequent section on data analysis. As revealed by Table 18, the shale-to-water ratio significantly influenced the resultant concentration of organic carbon in leachate. As anticipated, the highest shale-to-water ratio (50 g + 30 ml) normally resulted in the highest concentration of organic carbon while the lowest shale-to-water ratio (50 g + 200 ml) normally resulted in the lowest concentration of organic carbon for each sample of spent shale examined.

It is interesting to note that, in some cases, organic carbon concentrations were approximately proportional to the corresponding shale-to-water ratios for particular experiments while, in other cases, organic carbon concentrations were not proportional to the corresponding shale-to-water ratios. In cases where organic carbon concentrations were proportional to shale-to-water ratio, saturation limitations did not yet exist and thus, doubling the shale-to-water ratio simply resulted in a doubling of the organic carbon concentration. In cases where organic carbon concentrations were not proportional to the corresponding shale-to-water ratios, saturation limitations existed at certain shale-to-water ratios.



Table 18. Equilibrium batch experiments: organic carbon concentration and mass of organic carbon leached per unit mass of spent shale.

Experiment	Shale-to-water ratio							
	Type 1				Type 2			
	$\frac{50 \text{ g}}{30 \text{ ml}}$	$\frac{50 \text{ g}}{50 \text{ ml}}$	$\frac{50 \text{ g}}{100 \text{ ml}}$	$\frac{50 \text{ g}}{200 \text{ ml}}$	$\frac{50 \text{ g}}{30 \text{ ml}}$	$\frac{50 \text{ g}}{50 \text{ ml}}$	$\frac{50 \text{ g}}{100 \text{ ml}}$	$\frac{50 \text{ g}}{200 \text{ ml}}$
Concentration of organic carbon, mg/l								
Distilled water, 20°C	18	11	5.0	3.9	25	19	11	5.4
Distilled water, 80°C	16	13	6.9	4.9	36	31	24	15
Groundwater, 20°C	19	10	6.9	3.6	25	23	10	6.7
Groundwater, 80°C	16	10	7.7	4.4	67	58	38	17
Mass of organic carbon leached per unit mass, mg/100g								
Distilled water, 20°C	1.1	1.1	1.0	1.6	1.5	1.9	2.2	2.2
Distilled water, 80°C	1.0	1.3	1.4	2.0	2.2	3.1	4.8	6.0
Groundwater, 20°C	1.1	1.0	1.4	1.4	1.5	2.3	2.0	2.7
Groundwater, 80°C	1.0	1.0	1.5	1.8	4.0	5.8	7.6	6.8

It is important to note a series of equilibrium batch experiments which delineates both shale to water ratios that results in saturated conditions and shale-to-water ratios that result in unsaturated conditions provides considerably more information than a series of batch experiments in which organic carbon concentrations are all proportional to the shale-to-water ratios and no delineation between saturated and unsaturated conditions is provided. Each of the equilibrium batch experiments could theoretically provide this information if high enough shale-to-water ratios were examined and ultimately, an estimate of the maximum saturation concentration could be derived for each spent shale examined under specified conditions. However, the highest shale-to-water ratio examined in the experiments (50 g + 30 ml) represents the highest "practical" shale-to-water ratio since employing 50 grams of spent shale and 30 milliliters of leach water results in a situation in which the volume of water barely submerges the entire volume of spent shale. Employing a higher shale-to-water ratio would result in the spent shale volume not being completely submerged in the water and therefore not all of the spent shale would be available for leaching.

#### Continuous-Flow Column Experiments

The primary purpose of these experiments was to assess the quality of leachate derived from once-through continuous-flow columns as a function of time. The major impetus behind the column experiments is an attempt to simulate the leaching phenomenon under actual field conditions. This is based on the premise that an actual in-situ retort will resemble a large column through which groundwater may flow on a once-through basis.

In these experiments, small-scale columns were filled with spent shale and compacted. Using a peristaltic pump, water was pumped through the columns at a constant flow rate for a period of 96 hours. Time-averaged composite samples of leachate were captured in an enclosed container at specified time intervals. These samples were subsequently filtered and analyzed for total organic carbon (TOC), conductivity, and pH.

The continuous-flow column experiments examined only the composite particle size range. The weight and bulk density of spent shale samples compacted into columns are presented in Table 19.

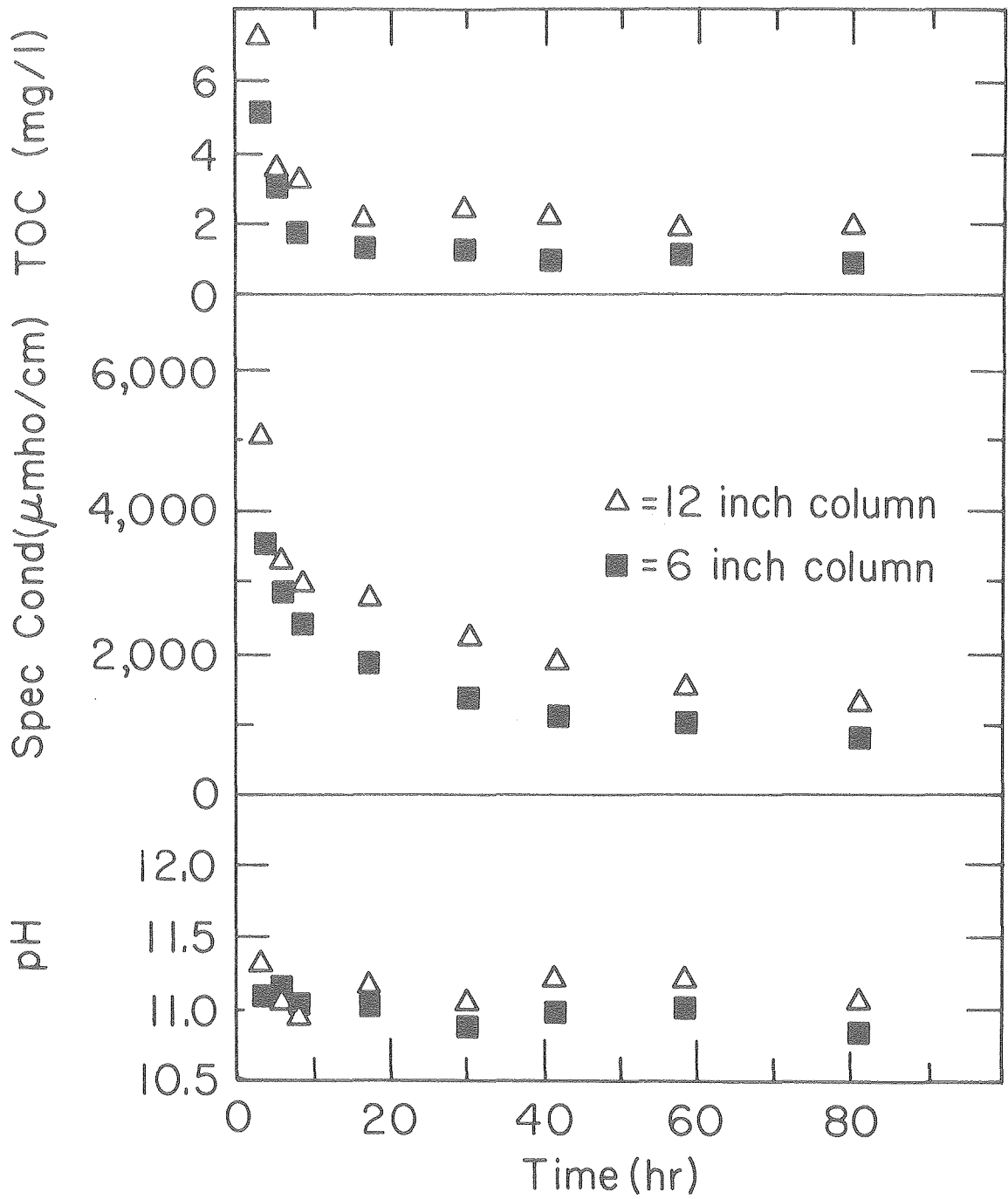
The flow rate selected for the continuous-flow column experiments was 0.6 milliliters per minute. The basis for selecting this flow rate was Darcy's Law used in conjunction with the experimental permeabilities presented in Table 11. By assuring a hydraulic gradient of 10 feet/100 feet (this is generally descriptive of the pressure difference between the upper and lower aquifers in the Piceance Creek Basin), it was estimated that the flow through a one-inch diameter column under these specified conditions would be about 0.6 milliliters per minute.

Table 19. Weight (W) and bulk density (D) of spent shale samples compacted into columns.

	Column length, in	
	12	6
Type 1		
W, g	206	102
D, g/cm <sup>3</sup>	1.40	1.39
Type 2		
W, g	210	106
D, g/cm <sup>3</sup>	1.43	1.44
Type 3		
W, g	168	84
D, g/cm <sup>3</sup>	1.14	1.14
Type 4		
W, g	186	93
D, g/cm <sup>3</sup>	1.26	1.26

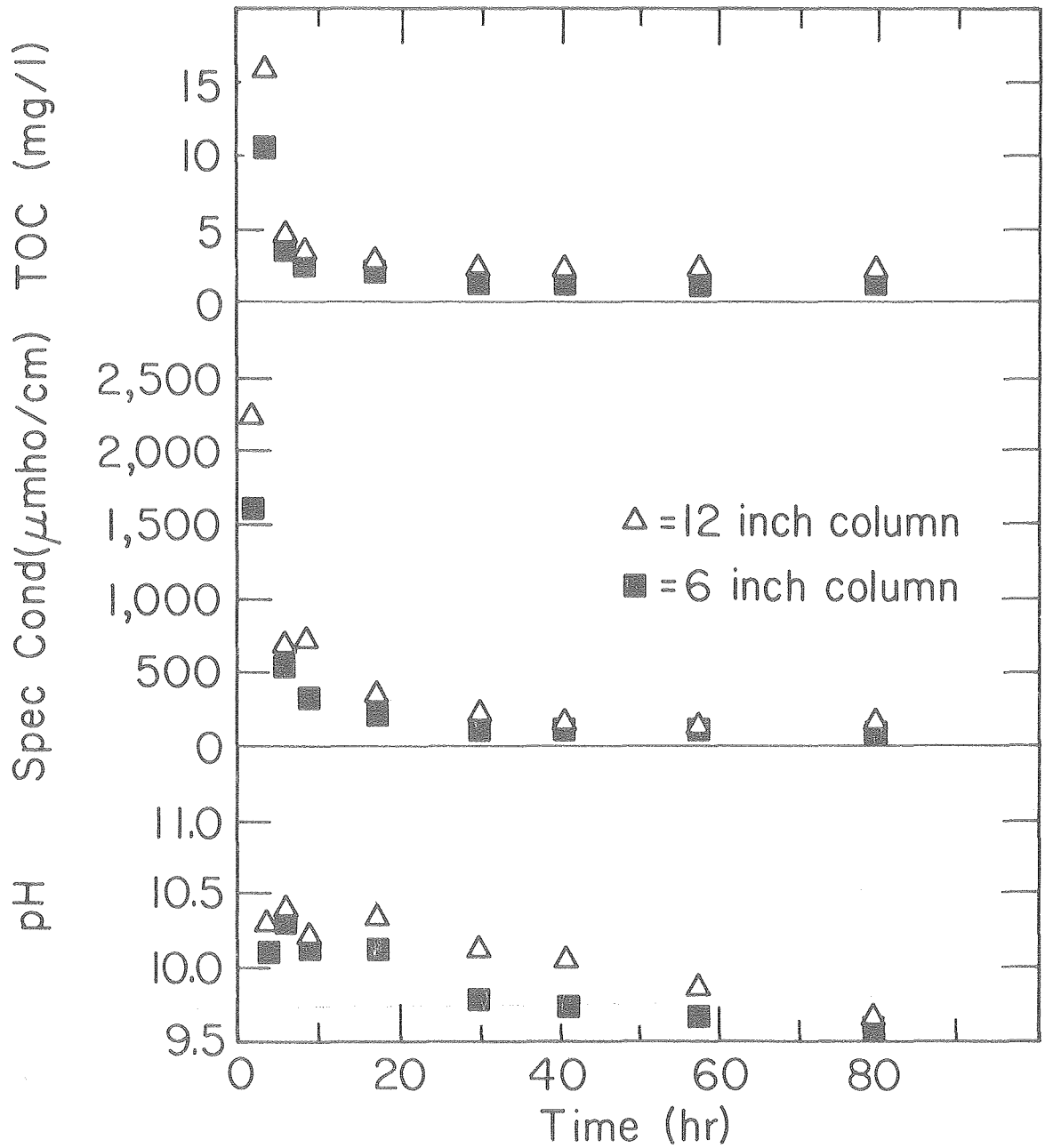
The results of the continuous-flow column experiments employing distilled water are presented in Figures 31 through 34. These results suggest that the rate at which organic material is leached is greatest during the initial periods of leaching. During subsequent time periods, the rate decreases. It is hypothesized that organic material leached during initial time periods is readily leachable due to (1) its proximity to the exterior surface of the spent shale where it is subject to eddy diffusion and (2) its weak association with the spent shale matrix due to weak physical forces. In contrast, it is hypothesized that organic material leached during subsequent time periods is not readily leachable due to (1) its proximity to the interior of the spent shale matrix where it must be slowly transported to the exterior by molecular diffusion or (2) its strong physical and/or chemical association with the spent shale matrix.

It is interesting to note the dramatic decrease in TOC concentration as a function of time for all four types of spent shale. This is particularly evident for the Type 3 spent shale in which the initial composite sample had a TOC concentration of approximately 60 mg/l while the TOC concentration of subsequent composite samples dramatically decreased. As discussed previously, the Type 3 spent shale was produced during a combustion run using recycle gas as part of the input gas. Recycle gas contains organic compounds that may



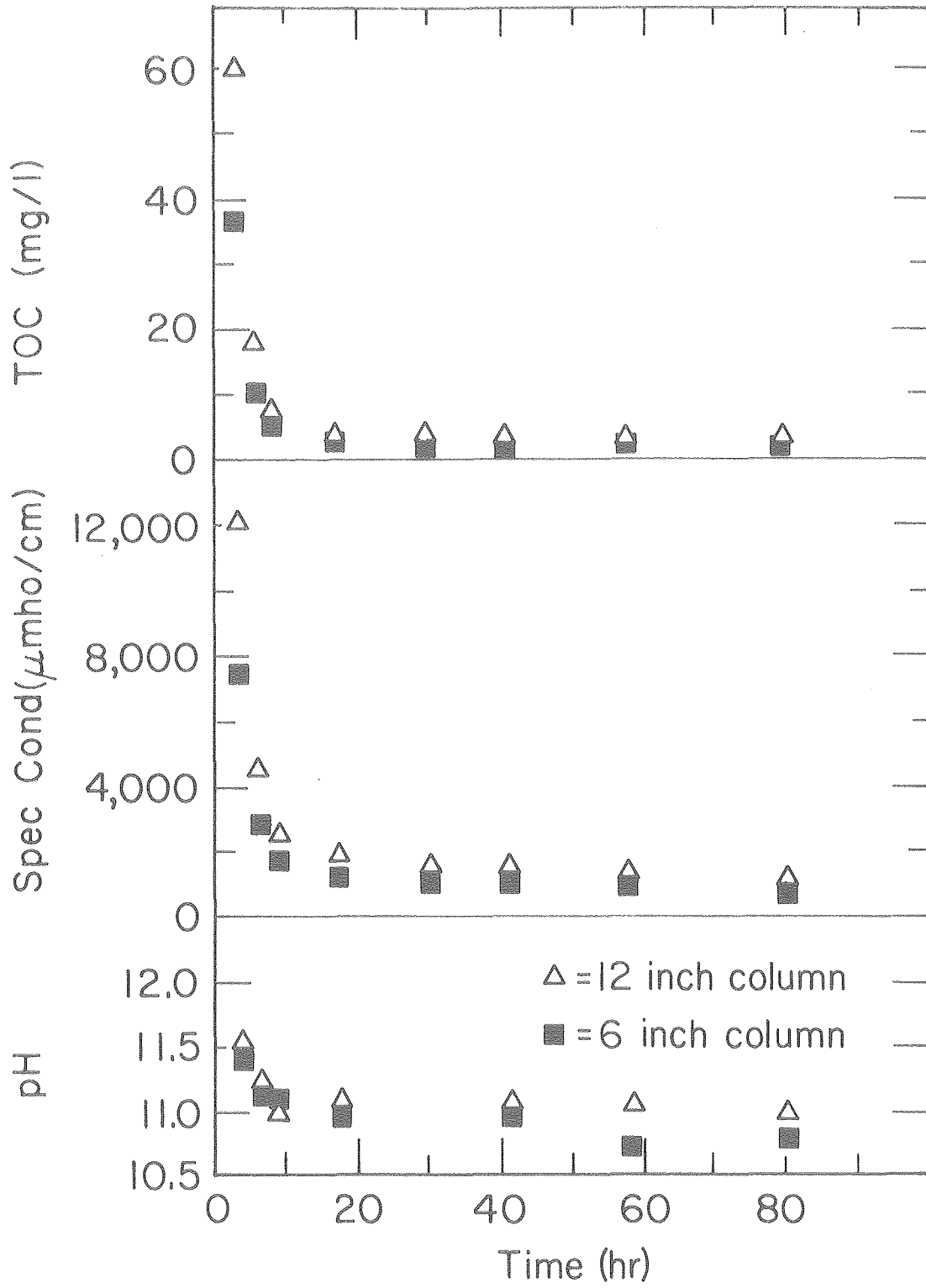
XBL 792-575

Figure 31. Continuous-flow column experiments examining Type 1 spent shale with distilled water.



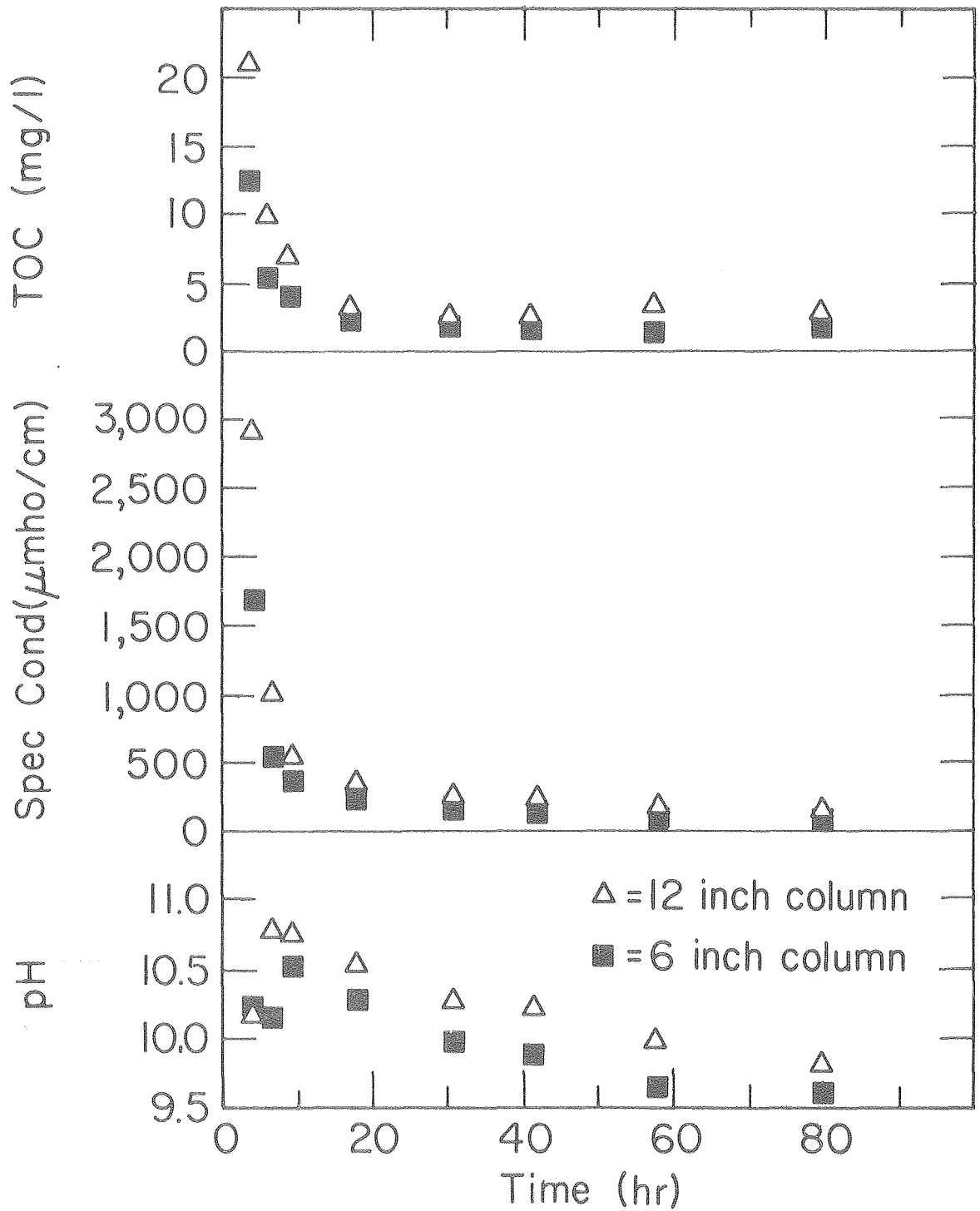
XBL 792-574

Figure 32. Continuous-flow column experiments examining Type 2 spent shale with distilled water.



XBL 792-573

Figure 33. Continuous-flow column experiments examining Type 3 spent shale with distilled water.



XBL 792-562

Figure 34. Continuous-flow column experiments examining Type 4 spent shale with distilled water.

adsorb or condense onto the spent shale behind the reaction front. Most of the adsorbed organic compounds were likely held by weak physical forces on the exterior of the spent shale where they were readily leachable by the initial flow of leach water.

As previously hypothesized, there are two mechanisms involved in the leaching process during the continuous-flow column experiments: (1) leaching from the exterior surface and macro-pores situated within the shale matrix and (2) leaching from internal micro-pores. A continuous flow of water can enhance the former but not the latter. Molecular diffusion is ultimately the limiting factor involved in mass transfer from internal micro-pores to the exterior. These hypotheses are particularly evident in the results derived from the Type 3 spent shale. The other types of spent shale also behave in a similar manner but to a lesser extent.

#### Comparison of Results from Batch and Continuous-Flow Column Experiments

Data describing the mass of organic material leached from the various types of spent shale per mass of spent shale during the continuous-flow column experiments and the batch experiments are presented in Table 20. As shown in Table 20, considerably more organic material (on a mass per unit mass basis) was leached during the continuous-flow column experiments than during the batch experiments. This is likely due to the continuous replacement of leachate with distilled water during the column experiments. According to mass transfer theory, this would tend to maximize the concentration gradient which represents the driving force for the leaching phenomenon. Furthermore, in the batch experiments, the only mass transfer mechanism is molecular diffusion, a slow process which may require an extremely long time for all leachable materials within the pores of the shale matrix to be leached and subsequently transported to the exterior of the shale matrix. However, in the continuous-flow experiments, an additional mass transfer mechanism, eddy diffusion, plays an important role and tends to enhance the kinetics of the leaching phenomenon.

The substantial difference between the mass of organic carbon leached during the batch experiments and the mass of organic carbon leached during the continuous-flow column experiments suggests that only a portion of the water soluble organics are leached during the batch experiments due to (1) solubility limitations and/or (2) the absence of eddy diffusion.

An examination of the data presented in Table 20 reveals that the mass of organic carbon leached per unit mass of spent shale was slightly greater for the short columns (6 inch) than for the long columns (12 inch). This is likely due to the fact that, prior to exiting from the column, the average concentration of leachate coming into contact with spent shale inside a short column was less than the average concentration of leachate coming into contact with spent shale inside a corresponding



Table 20. Total organic carbon leached from various types of spent shale: comparison of continuous-flow column experiments and batch experiments.

Experiment type	Water type	Total organic carbon (TOC) leached, mg/100g of spent shale			
		Type 1	Type 2	Type 3	Type 4
Cont.-flow column, 12 in	Distilled water	3.8	4.1	9.7	6.1
Cont.-flow column, 6 in	Distilled water	4.4	5.0	11.8	6.9
Batch, 20°C	Distilled water	1.1	1.9	3.5	1.7

long column. This is evidenced by the initial leachate concentrations detected during corresponding short column and long column experiments.

It is asserted that the effluent concentration of leachate from a short column, as estimated from Figures 31 through 34, is indicative of the leachate concentration at the midpoint of a long column at corresponding time periods. Consequently, it is likely that, during initial time periods, less organic carbon will be leached from the second-half of each column than from the first half (as suggested by a comparison of organic carbon concentrations at initial time periods during corresponding short- and long-column experiments). The rationale behind this assertion is that the average concentration of leachate in the second half of the column will be greater than in the first half and thus, the driving force (i.e., concentration gradient) for mass transfer will be less. This will not hold true for later time periods when more organic carbon will be leached from the second half since a greater portion of the water soluble organic carbon will have been leached from the first half of the column. Given enough time (i.e., a time period greater than the 96-hour time period examined), it is asserted that the mass of organic carbon leached per unit mass of spent shale will be equal for a particular type of spent shale examined in corresponding short- and long-column experiments.

Data describing the mass of leached inorganic material are presented in Table 21. These TDS estimates were derived by multiplying corresponding values of specific conductivity by 0.6; conductivity and TDS are related by an empirical factor ranging from 0.5 to 0.9 (Ref. 24). As indicated previously, this method of estimating TDS provides, at best, a rough estimate. Although conductivity is an indicator of the total ions in solution, it can be significantly affected by pH. Similar to the results presented in Table 20, the results in Table 21 reveal that (1) a greater mass of inorganic material was leached during the column experiments than during the batch experiments and (2) a greater mass of inorganics per unit mass of spent shale was leached from the short columns than from the corresponding long columns.

As indicated previously, the major impetus behind the column experiments is an attempt to simulate the leaching phenomenon under actual field conditions, based on the premise that an actual in-situ retort will resemble a large column through which groundwater may flow on a once-through basis. Since detectable levels of organic carbon were still present in leachate after 96 hours of leaching, the data presented in Table 20 for the column experiments are considered to be roughly representative of the minimum potential mass of leachable organic material under actual field conditions.

Table 21. Estimated total dissolved solids (TDS) leached from various types of spent shale: comparison of continuous-flow column experiments and batch experiments.

Experiment type	Water type	Total dissolved solids, (TDS) leached, mg/100g of spent shale			
		Type 1	Type 2	Type 3	Type 4
Cont.-flow Column, 12 in	Distilled water	2,000	230	2,100	300
Cont.-flow column, 6 in	Distilled water	2,700	360	2,800	440
Batch, 20°C	Distilled water	510	110	1,000	160

## CHAPTER 8

### DATA ANALYSIS

As indicated by the results presented in the previous section, a voluminous amount of data was generated during the leaching experiments. However, these data are only of academic interest unless they can be reduced and placed into an analytical framework. This section will identify and apply various data analysis techniques including (1) kinetic analysis of batch experiments, (2) development of equilibrium isotherms, and (3) kinetic analysis of continuous-flow column experiments and development of framework for packed-column mass transfer model.

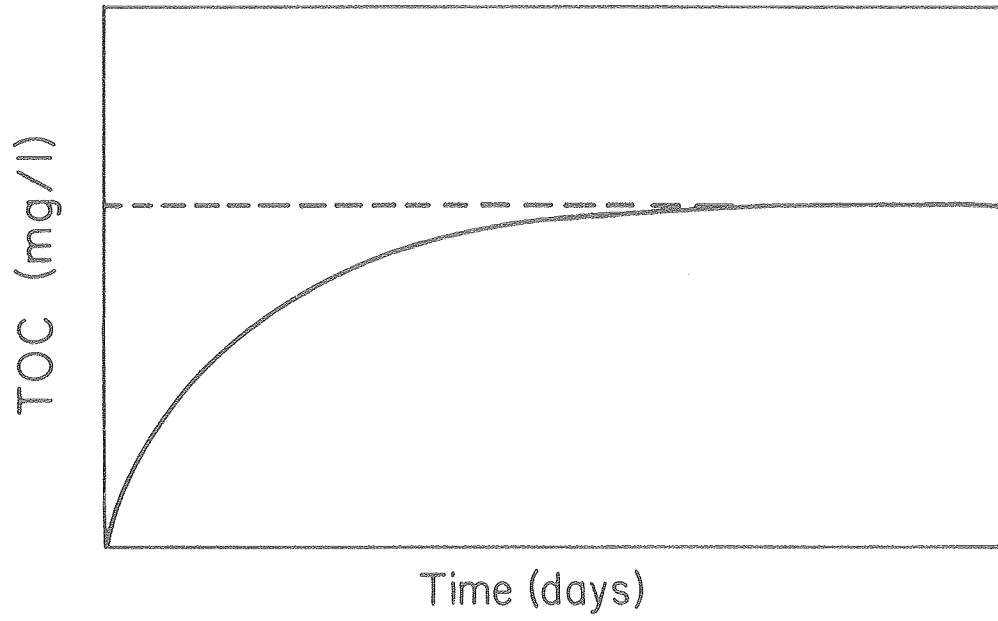
A presentation of the theory and rationale behind each data analysis technique will be followed by the application of each technique to the experimental results presented in the previous section.

#### Kinetic Analysis of Batch Experiments

Theory. The data derived from the kinetic batch experiments provide an indication of the kinetics of the leaching phenomenon. Most results derived from these experiments generally resembled the hypothetical data described in Figure 35. The hypothetical data presented in Figure 35 suggest that the TOC concentration rapidly increases during initial time periods while, during subsequent time periods, the concentration increases at a considerably slower rate until "pseudo-equilibrium" conditions are attained.

The results derived from Type 1 spent shale (produced during combustion retorting) and Types 2 and 4 spent shale (produced during inert gas retorting) generally resembled the hypothetical data described in Figure 35. In contrast, the data derived from Type 3 spent shale (produced during combustion retorting employing recycle gas) did not resemble the hypothetical data shown in Figure 35. In light of the unusual results derived from the Type 3 spent shale, the following kinetic analysis will not consider these results. (The results derived from the Type 3 spent shale suggest that the kinetics of leaching associated with this particular type of spent shale are considerably more complicated than those proposed in the following simplistic kinetic model.)

The theory and rationale behind the hypothetical data shown in Figure 35 are as follows (Ref. 26). It is assumed that the only occurring reaction is simple leaching/desorption of water soluble organic compounds. As revealed by Figure 35, the TOC concentration increases rapidly during initial time periods as readily soluble organic material goes into solution. This readily soluble material is likely associated with the exterior of the spent shale matrix or is situated within large pores inside the matrix. Thus, the rate of leaching is greatest during initial time periods. Subsequently, the rate of leaching decreases as progressively lesser amounts of organic material



XBL 792-546

Figure 35. Hypothetical data derived from kinetic batch experiments.

are leached and "pseudo-equilibrium" conditions are approached near the end of the leaching time period investigated (i.e., 30 days). The material leached during subsequent time periods is likely situated within small pores located deep inside the shale matrix and thus, must be transported to the exterior by molecular diffusion. The eventual establishment of "pseudo-equilibrium" conditions will likely be due to the influence of solubility limitations.

It is hypothesized that the only occurring reaction is simple leaching/desorption of water soluble organic compounds. This reaction can be represented by:



where  $C_* = C_e - C_t$  = the potential TOC concentration remaining to be leached at time t

$C_t$  = TOC concentration at time t

$C_e$  = equilibrium TOC concentration at  $t = \infty$   
(function of both the mass of organics available for leaching and solubility limitations).

The reaction rate of the above reaction is equal to the rate of disappearance of  $C_*$  and can be represented by:

$$-r_{C_*} = -\frac{dC_*}{dt} = KC_*^n$$

where  $r_{C_*}$  = rate of disappearance of  $C_*$

K = reaction rate constant

n = reaction order.

The above expression implies that the reaction rate (i.e., rate of disappearance of  $C_*$ ) is a function of (1) the potential TOC concentration remaining to be leached at time t, (2) the reaction order, and (3) the reaction rate constant.

The reaction order and the corresponding reaction rate constant of a particular reaction can be determined by an analysis of batch-mode kinetic data (Ref. 26). The procedure involves a trial-and-error analysis whereby (1) a reaction mechanism is hypothesized and (2) a reaction order is assumed. Subsequently, both the hypothesized reaction mechanism and the assumed reaction order are tested using batch-mode kinetic data. Unfortunately, this procedure is often laborious and time-consuming.

In order to simplify this kinetic analysis, it is assumed that the reaction mechanism is simply leaching/desorption of soluble compounds. Furthermore, it is assumed that first-order kinetics apply (i.e., the rate of reaction is assumed to be proportional only to  $C_*$ ). Although it is possible that the reaction kinetics are more complex than those assumed, it is felt that a more rigorous kinetic analysis is not warranted due to the fact that (1) only one TOC measurement was obtained during the initial half-day of leaching when the reaction rate was greatest and (2) very little is known about the types of organic compounds and "subreactions" participating in the overall leaching reaction.

Assuming first-order kinetics, the reaction order (n) is equal to one and the previous expression simplifies to:

$$-r_{C_*} = -\frac{dC_*}{dt} = KC_* \quad .$$

Rearranging the above expression into integral form yields:

$$-\int_{C_{*0}}^{C_*} \frac{dC_*}{C_*} = K \int_0^t dt \quad .$$

Integration yields:

$$-\ln \frac{C_*}{C_{*0}} = Kt \quad .$$

In the above expression, the term  $C_{*0}$  is equivalent to  $C_e$  and the term  $C_*$  is equivalent to  $(C_e - C_t)$ . Substituting these equivalent terms into the above expression yields:

$$-\ln \frac{C_e - C_t}{C_e} = Kt \quad .$$

By algebraic manipulation, the above expression can be converted to the following form:

$$C_t = C_e (1 - e^{-Kt}) \quad .$$

The above expression approximately simulates the hypothetical data described in Figure 35. It models the leaching phenomenon in a batch reactor if the only occurring reaction is simple leaching/desorption and if the kinetics are first order.

Finally, it is important to note that the above procedure can be used to develop an expression for testing a reaction for kinetics other than first order. For example, if it were advantageous to test a reaction for second-order kinetics, the reaction rate can be defined by:

$$-r_{C_*} = -\frac{dC_*}{dt} = KC_*^2$$

Rearranging and integrating the above expression would yield:

$$\frac{1}{C_*} - \frac{1}{C_{*0}} + Kt$$

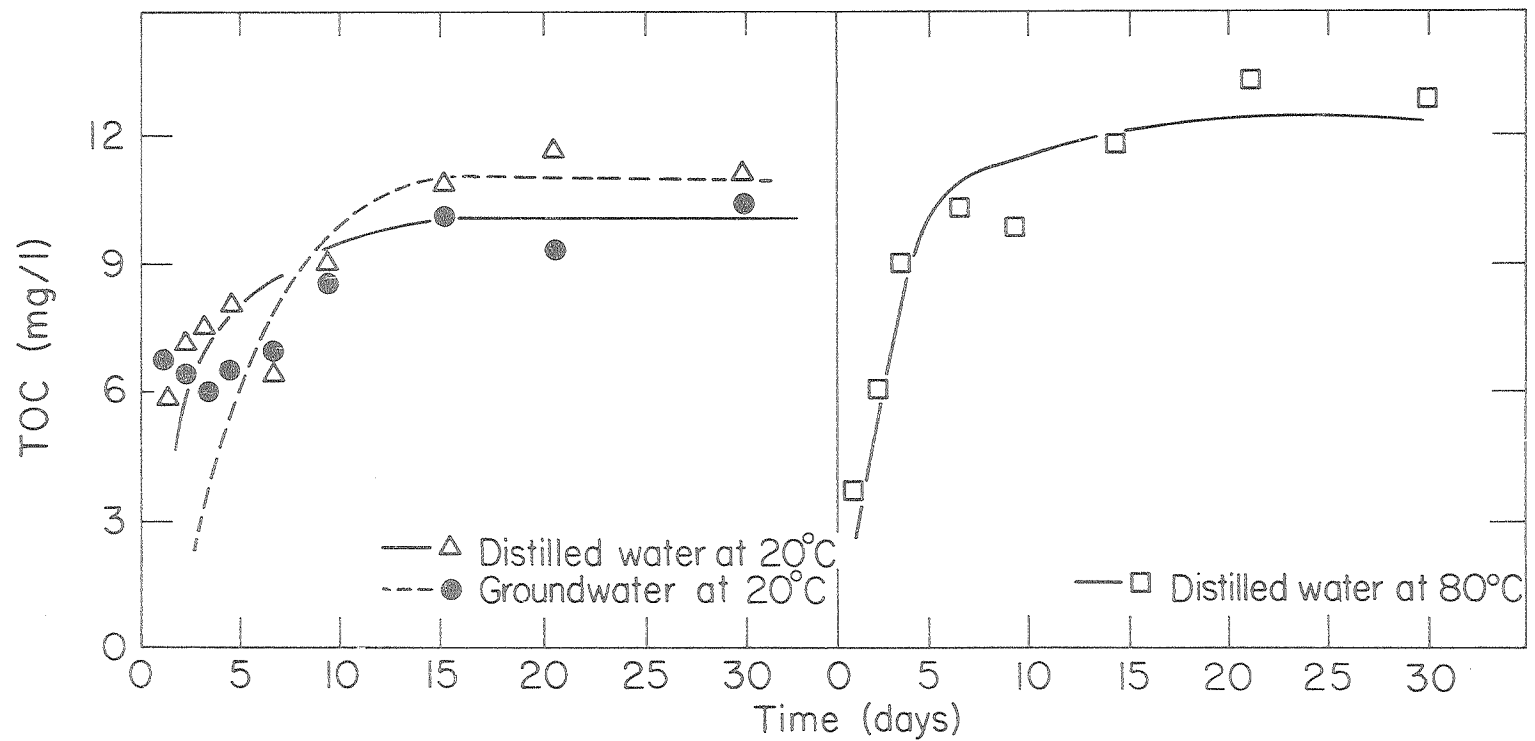
Application. It has been asserted that the results of the kinetic batch experiments, except those derived from the Type 3 spent shale, approximately resemble the hypothetical data portrayed in Figure 38. Assuming first-order kinetics, the hypothetical data portrayed in Figure 38 can be represented by the expression  $C_t = C_e (1 - e^{-Kt})$ .

A least squares analysis was employed to estimate values of  $C_e$  and  $K$ . These estimates are presented in Table 22. Using these values of  $C_e$  and  $K$ , the equation  $C_t = C_e (1 - e^{-Kt})$  was plotted next to actual data for each set of experimental data. These plots are presented in Figures 36 through 38.

An examination of Figures 36 through 38 suggests that the proposed reaction mechanism (i.e., simple leaching/desorption with first-order kinetics) roughly simulates the leaching phenomenon for Type 1, 2, and 4 spent shales. This simulation appears to be best for later time periods of leaching. During initial time periods, the simulation is not as good as during later time periods. This suggests that the assumption of first-order kinetics is not entirely valid for initial time periods of leaching. The poor simulation during initial time periods may be due, in part, to the fact that only one TOC measurement was taken during the initial one-half day when the rate of leaching was greatest. Thus, the initial portions of the curves shown in Figure 36 through 38 are not well-defined by data points.

Although this kinetic analysis was based on an assumption of first-order kinetics, an attempt was also made to test the data for second-order kinetics. However, a kinetic model assuming second-order kinetics was found to be completely inadequate for explaining experimental data. The results of this second-order kinetic analysis have not been





XBL 792-568

Figure 36. Comparison of experimental data and assumed reaction mechanism: Type 1 spent shale.

(Note: the experimental data derived from groundwater at 80°C were omitted because they obviously did not conform to the assumed reaction mechanism).

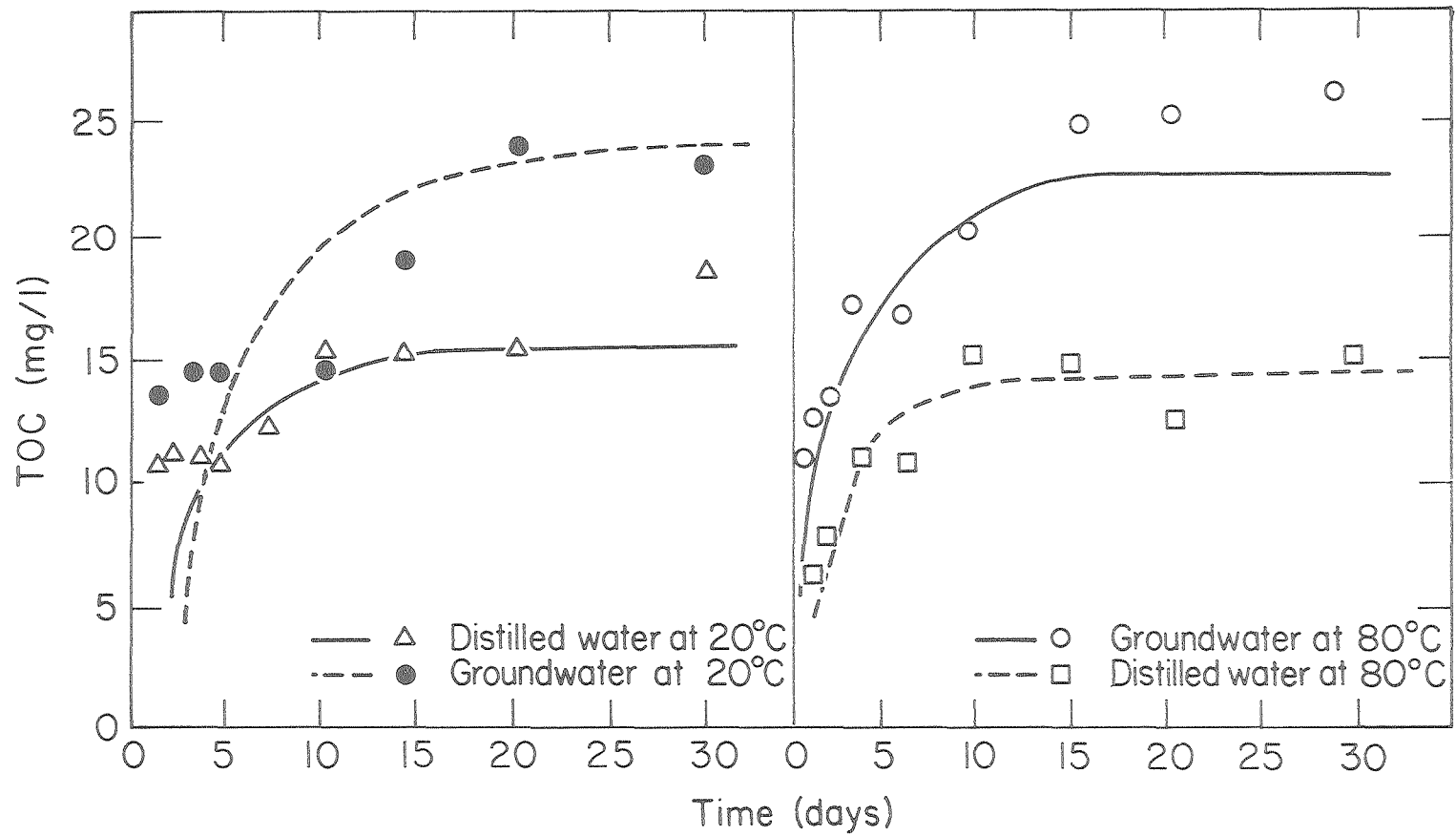
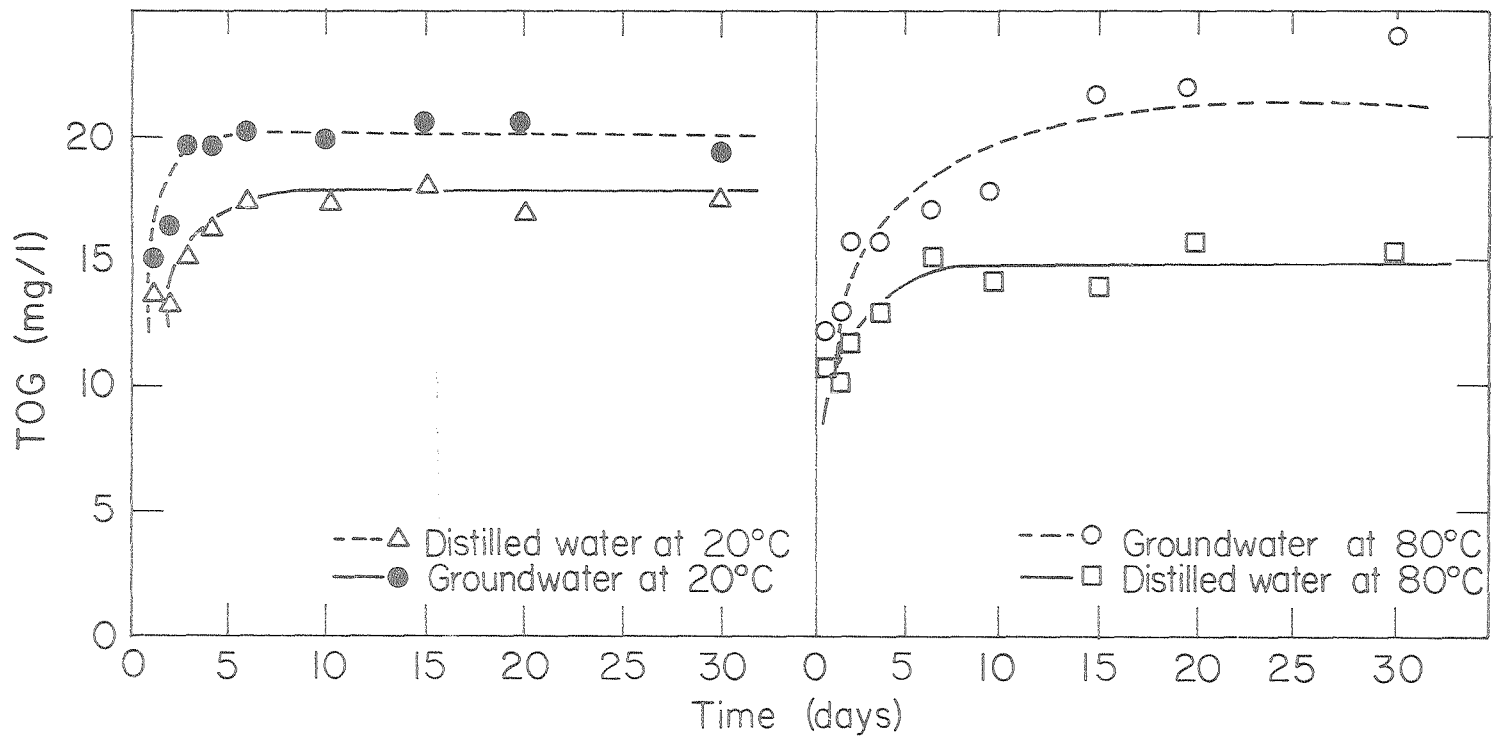


Figure 37. Comparison of experimental data and assumed reaction mechanism: Type 2 spent shale.

XBL 792-567



XBL 792-551

Figure 38. Comparison of experimental data and assumed reaction mechanism: Type 4 spent shale.

Table 22. Estimated values of  $C_e$  and K for kinetic batch experiments: spent shale Types 1, 2, and 4.

Experiment and spent shale type	$C_e$	K
Distilled water, 20°C		
Type 1	9.9	0.62
Type 2	14.6	0.81
Type 4	17.5	1.4
Distilled water, 80°C		
Type 1	11.7	0.33
Type 2	28	0.35
Type 4	29	0.87
Groundwater, 20°C		
Type 1	10.8	0.26
Type 2	23.5	0.21
Type 4	20	2.2
Groundwater, 80°C		
Type 1	--	--
Type 2	47	0.42
Type 4	41	0.63

included because they were considered to be of little value. If the reader wishes to conduct a second-order kinetic analysis, the required data have been presented.

The kinetic analysis of batch experiments conducted in this section represents a rather simplistic attempt at gaining a basic understanding of the leaching phenomenon in a batch reactor. In a following section, a much more rigorous kinetic analysis will be conducted, using the results of the continuous-flow column experiments.

#### Equilibrium Isotherms

Theory. Equilibrium isotherms are often employed in sanitary and chemical engineering to describe equilibrium conditions in unit operations such as adsorption (Ref. 27). In water treatment, a common application of equilibrium isotherms involves the removal of trace organics from a water supply by activated carbon adsorption (activated

carbon is a commonly employed adsorbent). With certain modifications equilibrium isotherms can be employed to describe equilibrium conditions in desorption/leaching studies.

An equilibrium adsorption isotherm is defined as a relationship between the mass of a solute adsorbed per unit mass of an adsorbent and the equilibrium concentration of the solute remaining in solution at a constant temperature (Ref. 28). A series of batch-mode experiments is normally employed to develop data which can be plotted in the form of an isotherm.

There are two general types of isotherm models commonly employed in sanitary and chemical engineering to describe the adsorption phenomenon. These include (1) the Langmuir model and (2) the Freundlich model. The Langmuir model is defined by:

$$q = \frac{abC}{1 + aC}$$

where  $q$  = mass of solute adsorbed per unit mass of adsorbent

$C$  = equilibrium concentration of solute

$a$  &  $b$  = constants.

In addition to the general form of the Langmuir model, there is a linear form expressed as:

$$\frac{1}{q} = \frac{1}{b} + \frac{1}{ab} \left[ \frac{1}{C} \right] .$$

In cases where data are appropriate, the above form of the Langmuir model yields an approximately linear plot when  $1/q$  is plotted against  $1/C$ . An example of a plot of the linear form of the Langmuir model is presented in Figure 39. From a linear approximation of data, as exemplified by Figure 39, the constants  $a$  and  $b$  can be evaluated.

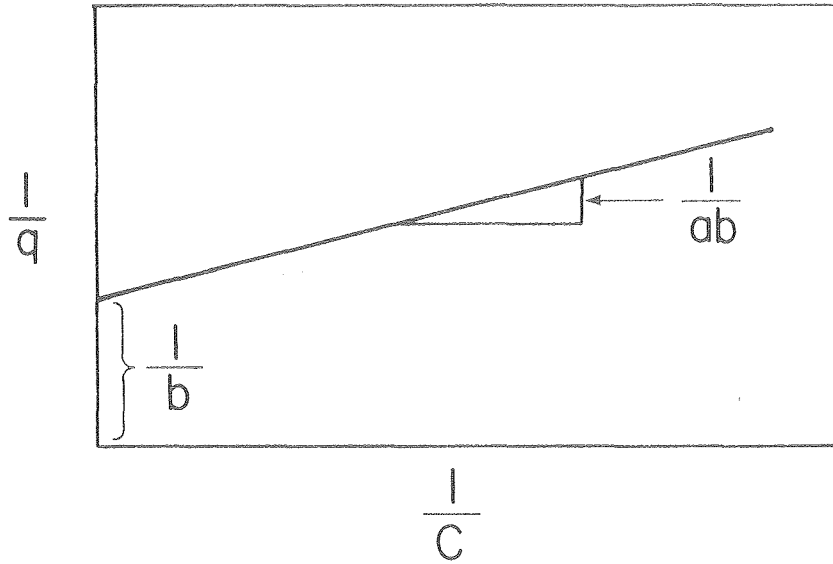
In contrast to the Langmuir model, the Freundlich model is defined by:

$$q = KC^{1/n}$$

where  $K$  and  $n$  = constants.

Transforming the above equation into logarithmic form yields:

$$\log q = \log K + 1/n \log C .$$



XBL 792-539

Figure 39. Plot of linear form of Langmuir model.

If data conform to the Freundlich model, a plot of experimental data according to the above equation will yield an approximate straight line, as described in Figure 40. From a straight line approximation of plotted data, the constants  $K$  and  $n$  can be evaluated.

In adsorption unit operations, the development of equilibrium isotherms, according to either the Langmuir or Freundlich model, enables one to predict the equilibrium concentration of a solute corresponding to a particular concentration of adsorbent. Using data derived from batch-mode experiments examining various adsorbent concentrations, the constants of either model can be evaluated. This allows the model to be used to predict the equilibrium concentration of a solute resulting from any mass of adsorbent placed in a specified volume of water.

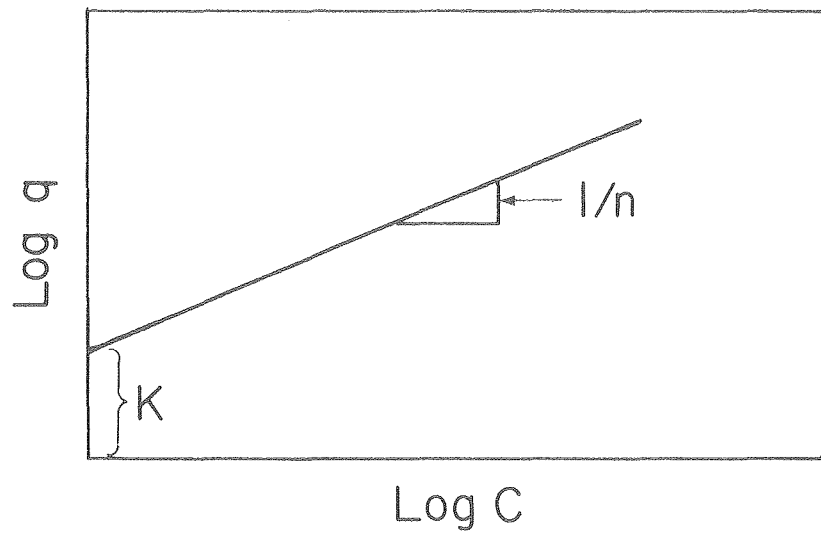
In the sanitary and chemical engineering literature, most existing information on equilibrium isotherms is based on the phenomenon of adsorption rather than the phenomenon of desorption/leaching (which is of particular concern in this study). Thus, the techniques for developing and interpreting adsorption isotherms must be slightly modified and adapted to the phenomenon of desorption/leaching.

In order to apply the above adsorption models to a desorption/leaching phenomenon, it is necessary to redefine the parameters  $C$  and  $q$ . The parameter  $C$  is defined as the equilibrium TOC concentration in leachate, expressed in terms of mg/l. The parameter  $q$  is defined as the mass of organic carbon remaining on the spent shale per unit mass of spent shale (expressed in terms of mg TOC/g spent shale). The parameter  $q$  can be estimated by subtracting the mass of organic carbon leached, as defined by measurements of  $C$  from the initial solid-phase organic carbon content of the spent shale samples, as defined in Table 11.

Application. The equilibrium batch experiments examined four shale-to-water ratios (i.e., 50 g/30 ml, 30 g/50 ml, 50 g/100 ml, and 50 g/200 ml) for each combination of spent shale type, leach water temperature, and leach water quality. Theoretically, this would provide four data points for the development of each isotherm. However, in two particular cases, a data point was obviously in error and thus, was not included in the following analysis.

Employing the previously described isotherm models in conjunction with the results of the equilibrium batch experiments, a series of equilibrium isotherms was developed to describe the leaching phenomenon for two types of spent shale: Type 1, produced during combustion retorting, and Type 2, produced during inert gas retorting.

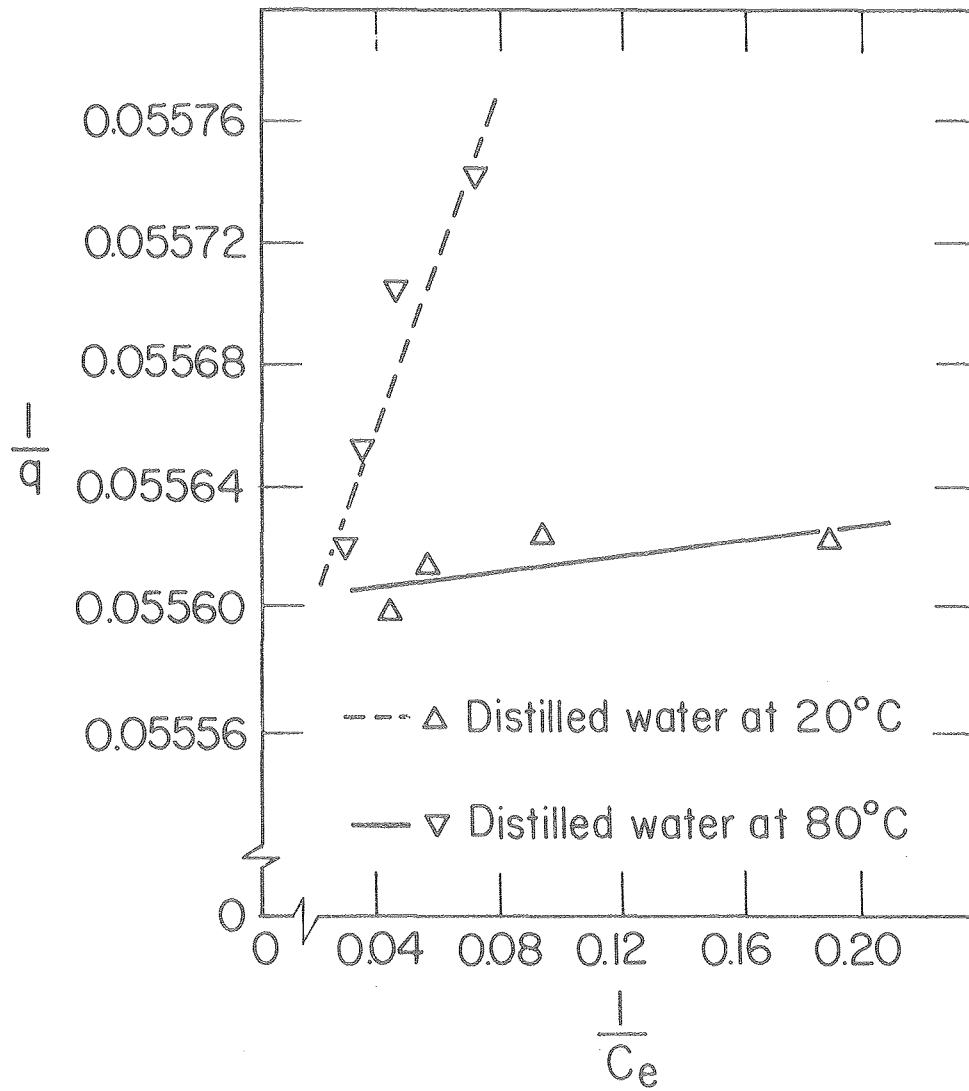
Plots of data according to the linear form of the Langmuir model are presented in Figures 41 through 44. Recall that, if data conform to the Langmuir model, then a plot of  $1/q$  versus  $1/C$  should be approximately linear. An examination of Figures 41 through 44 reveals that the Langmuir model appears to be fairly appropriate for modeling experimental data for the inert gas-retorted spent shale



XBL 792-540

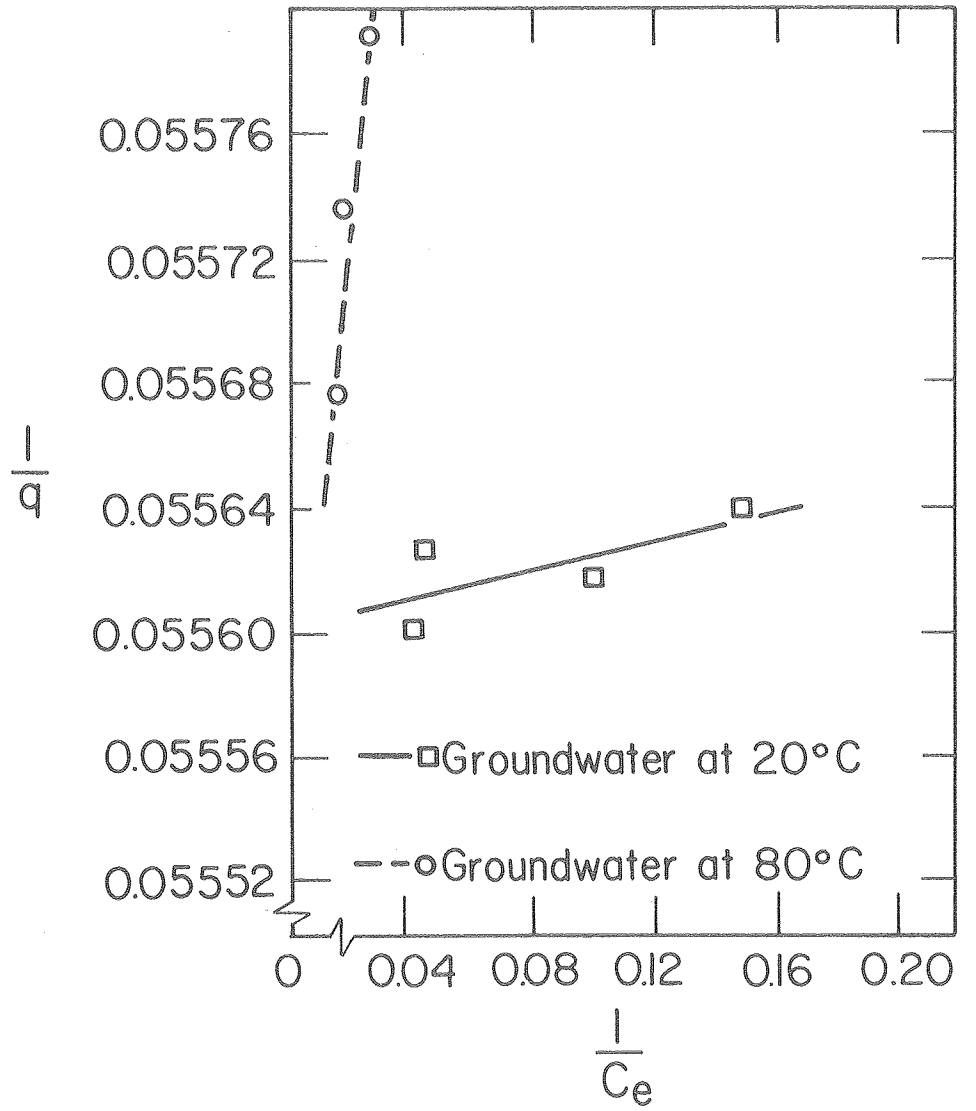
Figure 40. Plot of logarithmic form of Freundlich model.





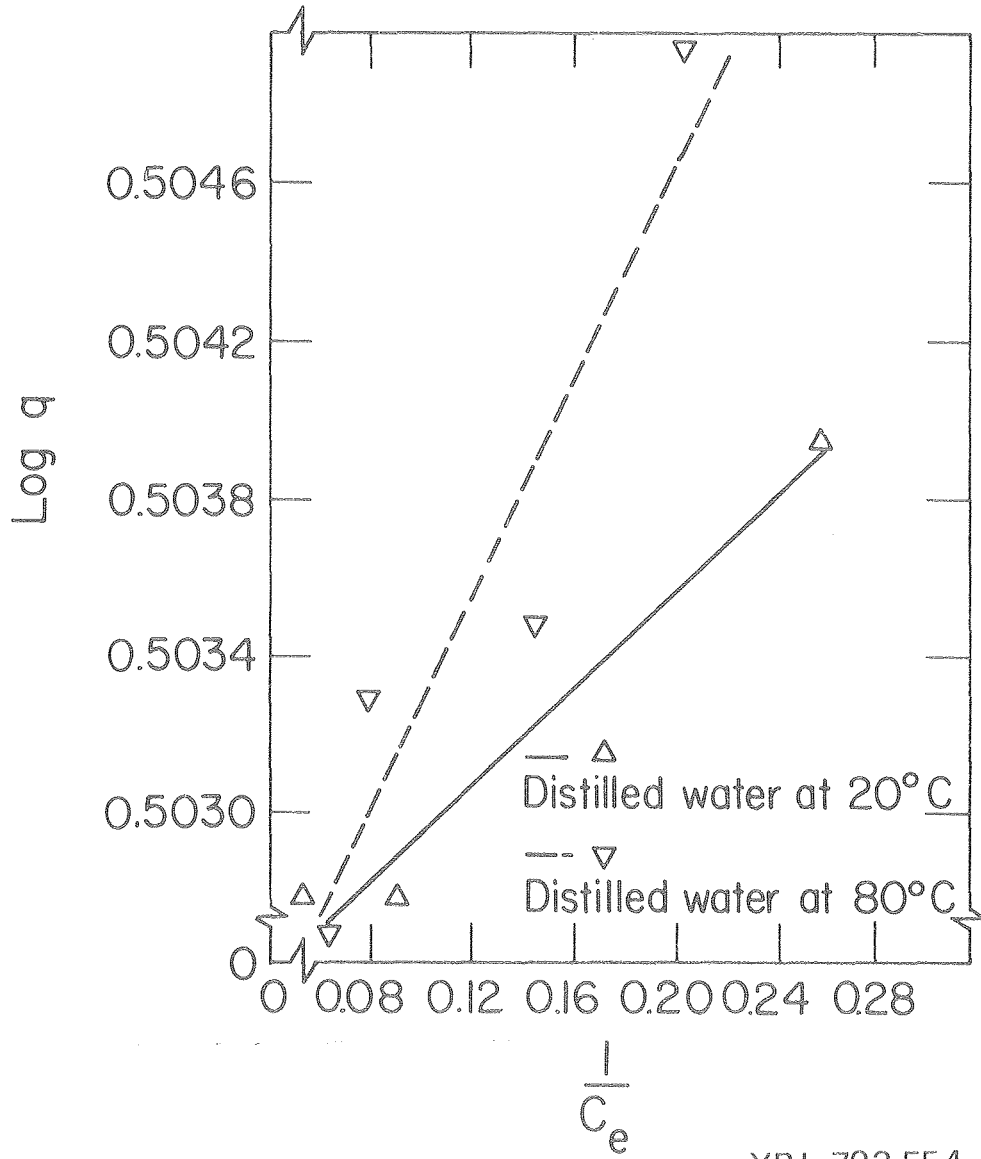
XBL 792-547

Figure 41. Linear form of Langmuir isotherm for Type 2 spent shale: distilled water.



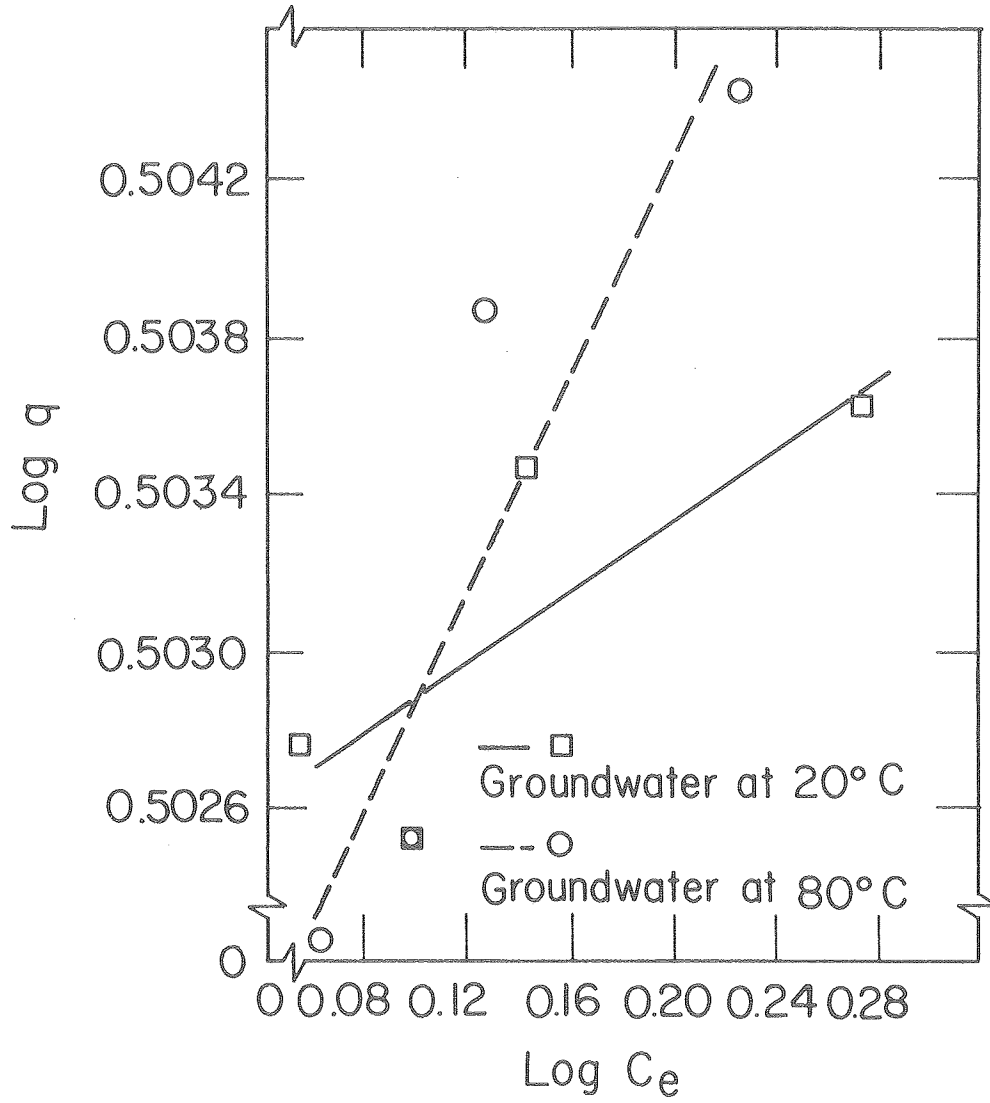
XBL 792-548

Figure 42. Linear form of Langmuir isotherm for Type 2 spent shale: groundwater.



XBL 792-554

Figure 43. Linear form of Langmuir isotherm for Type 1 spent shale: distilled water.



FXBL 792-555

Figure 44. Linear form of Langmuir isotherm for Type 1 spent shale: groundwater.

(Type 2) within the range of data (i.e., shale-to-water ratios) examined. In contrast, the Langmuir model appears to be slightly less appropriate for modeling experimental data derived from the combustion-retorted spent shale (Type 1) within the range of data examined.

Plots of data according to the logarithmic form of the Freundlich model are presented in Figures 45 through 48. Recall that, if data conform to the Freundlich model, then a plot of  $\log q$  versus  $\log C$  should approach linearity. Similar to the Langmuir model, the Freundlich model appears to be fairly appropriate for modeling experimental data derived from the Type 2 spent shale within the range of data examined, based on the linearity of  $\log q$  versus  $\log C$  plots.

Based on the above, both the Langmuir and Freundlich models approximately simulate the leaching phenomenon for spent shale produced during inert gas retorting for a particular range of shale-to-water ratios. These models appear to be slightly less appropriate for simulating the leaching of organic material from combustion-retorted spent shale. Although plots of  $1/q$  versus  $1/C$  and  $\log q$  versus  $\log C$  for the Type 1 spent shale appeared to roughly follow a linear trend, they were not as linear as corresponding plots for the Type 2 spent shale.

A least squares analysis was used to estimate constants for both the Langmuir and Freundlich models. Estimates of constants for each model are presented in Table 23. Employing these constants, either model can be used to predict the equilibrium TOC concentration resulting from a particular shale-to-water ratio. This can be accomplished by the Langmuir model:

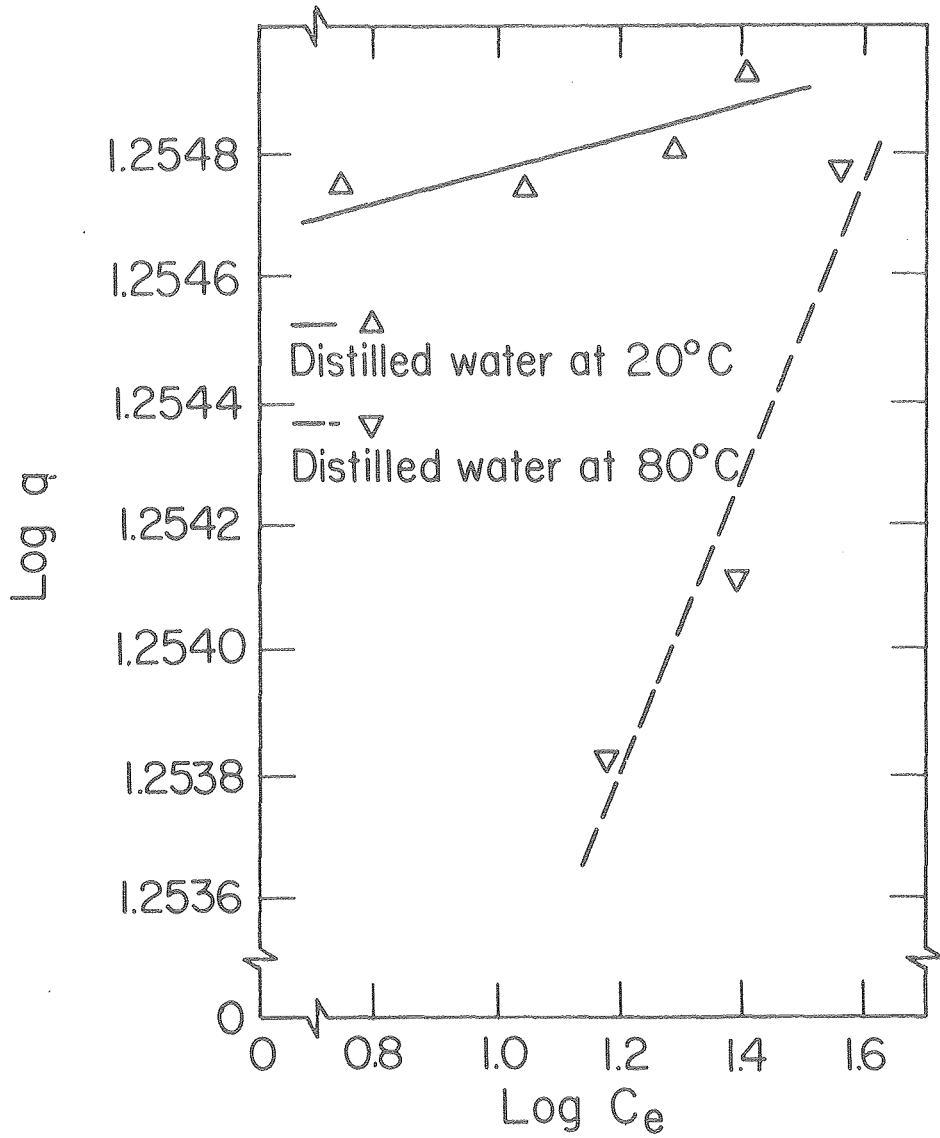
$$q = \frac{abC}{a + aC}$$

or the Freundlich model:

$$q = KC^{1/n}$$

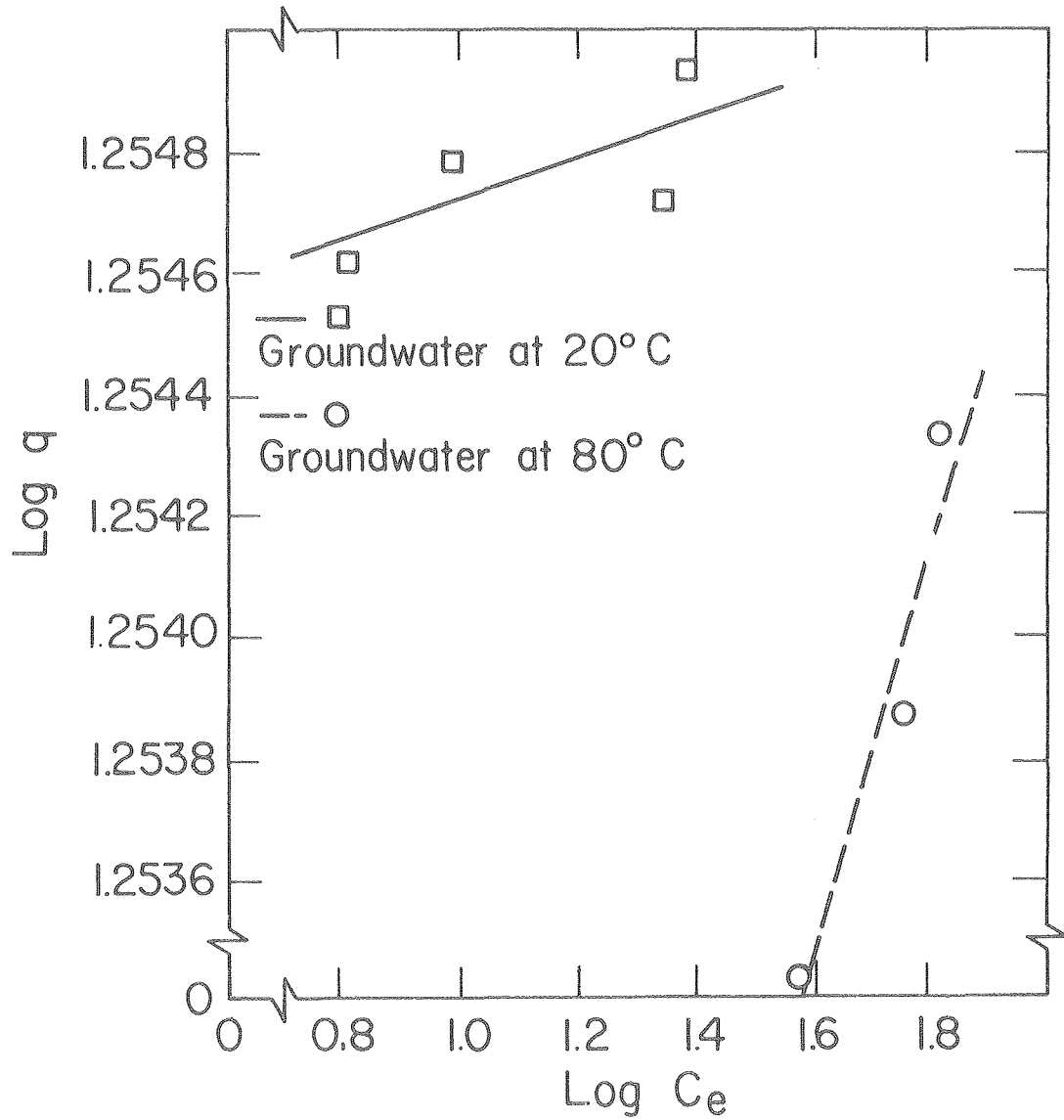
It is asserted that the isotherm models, as defined by the constants presented in Table 23, are fairly accurate in describing equilibrium relationships within a particular range of experimental data. This implies that interpolation within this range of data will provide a reasonable estimate of equilibrium relationships while extrapolation may not provide a reasonable estimate.

In retrospect, it may have been somewhat naive to expect a single isotherm model to accurately describe equilibrium relationships for a particular type of spent shale over the entire range of possible data. More realistically, one would expect a particular model to be most appropriate for a certain range of experimental data while another model may be more appropriate for another range of data.



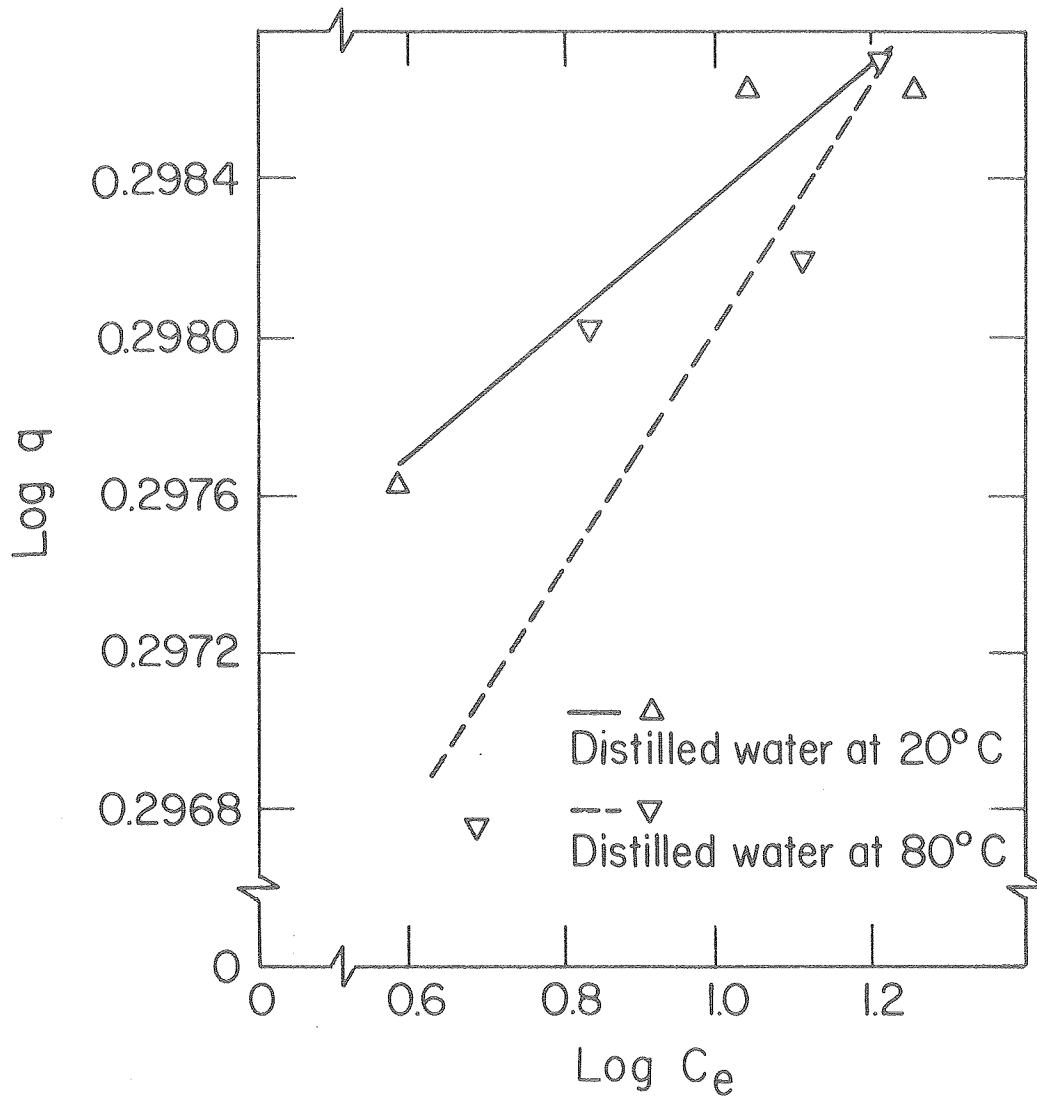
FXBL 792-550

Figure 45. Logarithmic form of Freundlich isotherm for Type 2 spent shale: distilled water.



FXBL 792-549

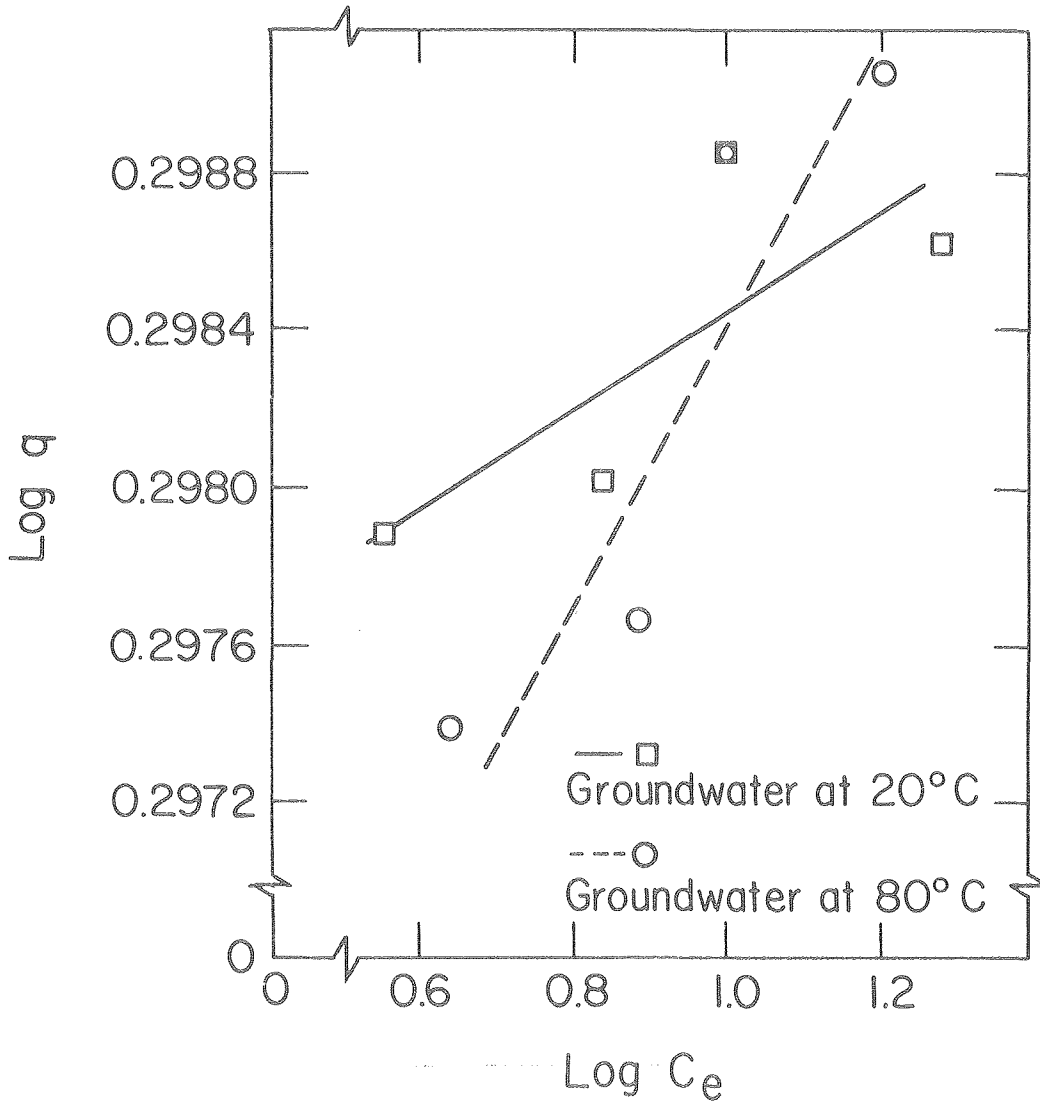
Figure 46. Logarithmic form of Freundlich isotherm for Type 2 spent shale: groundwater.



FXBL 792-553

Figure 47. Logarithmic form of Freundlich isotherm for Type 1 spent shale: distilled water.





FXBL 792-552

Figure 48. Logarithmic form of Freundlich isotherm for Type 1 sent shale: groundwater.

Table 23. Constants for Freundlich and Langmuir models: spent shale Types 1 and 2.

Experiment	Model constants, Type 1				Model constants, Type 2			
	Freundlich		Langmuir		Freundlich		Langmuir	
	K	n	a	b	K	n	a	b
Distilled water, 20°C	1.98032	615.433	81.1577	1.99075	17.9688	3850.47	433.849	17.9846
Distilled water, 80°C	1.97197	318.766	36.4383	1.99237	17.8187	408.520	19.1234	17.9995
Groundwater, 20°C	1.98256	816.308	111.354	1.99027	17.9638	3116.45	241.323	17.9852
Groundwater, 80°C	1.97152	274.904	36.5797	1.99405	17.7054	298.471	6.18471	17.9989

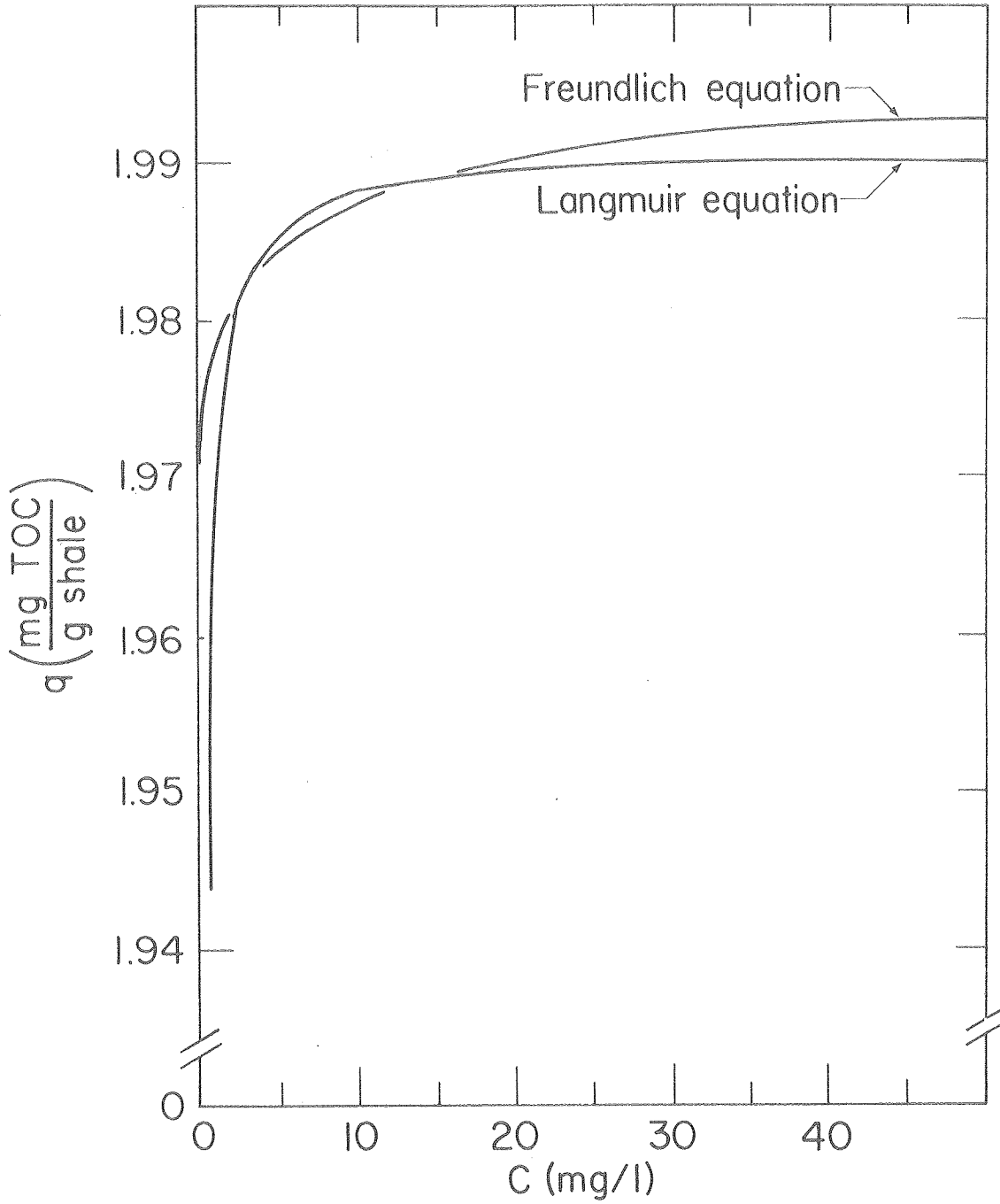
Recall that there are isotherm models other than the Langmuir and Freundlich models. Furthermore, it should be recognized that isotherm models are merely mathematical expressions to describe experimentally derived data.

Upon examination, there appears to be a problem associated with the Langmuir equations as defined by the constants presented in Table 23. If one substitutes a  $q$  value of 18.00 mg TOC/g spent shale into the mathematical expression for the Type 2 spent shale and then solves for  $C$ , the estimated value of  $C$  will be negative. The same situation will occur if a  $q$  value of 2.00 is substituted into the mathematical expression for Type 1 spent shale. The above values of  $q$ , 18.00 mg TOC/g spent shale for Type 2 and 2.00 mg TOC/g spent shale for Type 1, are important because they represent the theoretically maximum possible values of  $q$ , as estimated for the solid-phase organic carbon measurements originally presented in Table 11. Using the appropriate mathematical expressions for the Langmuir model, one would predict maximum  $q$  values of only 17.9846 mg/g for Type 2 and 1.99075 mg/g for Type 1. This suggests that, at high values of  $q$  and  $C$ , the Langmuir model may not present entirely realistic estimates of equilibrium relationships. This behavior of the Langmuir equation at high values of  $q$  and  $C$  may be due to the possibility that true equilibrium conditions were not established during certain equilibrium batch experiments used to generate data required for the development of equilibrium isotherms.

In contrast to the Langmuir model, the appropriate mathematical expressions based on the Freundlich model enable one to actually estimate a value of  $C$  corresponding to the theoretically maximum possible value of  $q$ , as defined previously. This is simply due to a mathematical peculiarity of the Freundlich equation whereby, as successively larger values of  $C$  are substituted into the equation, successively larger values of  $q$  can be calculated. This mathematical behavior of the Freundlich equation is due to the fact that it is based on a power function (i.e., the parameter  $C$  is raised to a constant power). The mathematical behavior of the Langmuir equation differs in that, at very high values of  $C$ , values of  $q$  eventually approach a constant value.

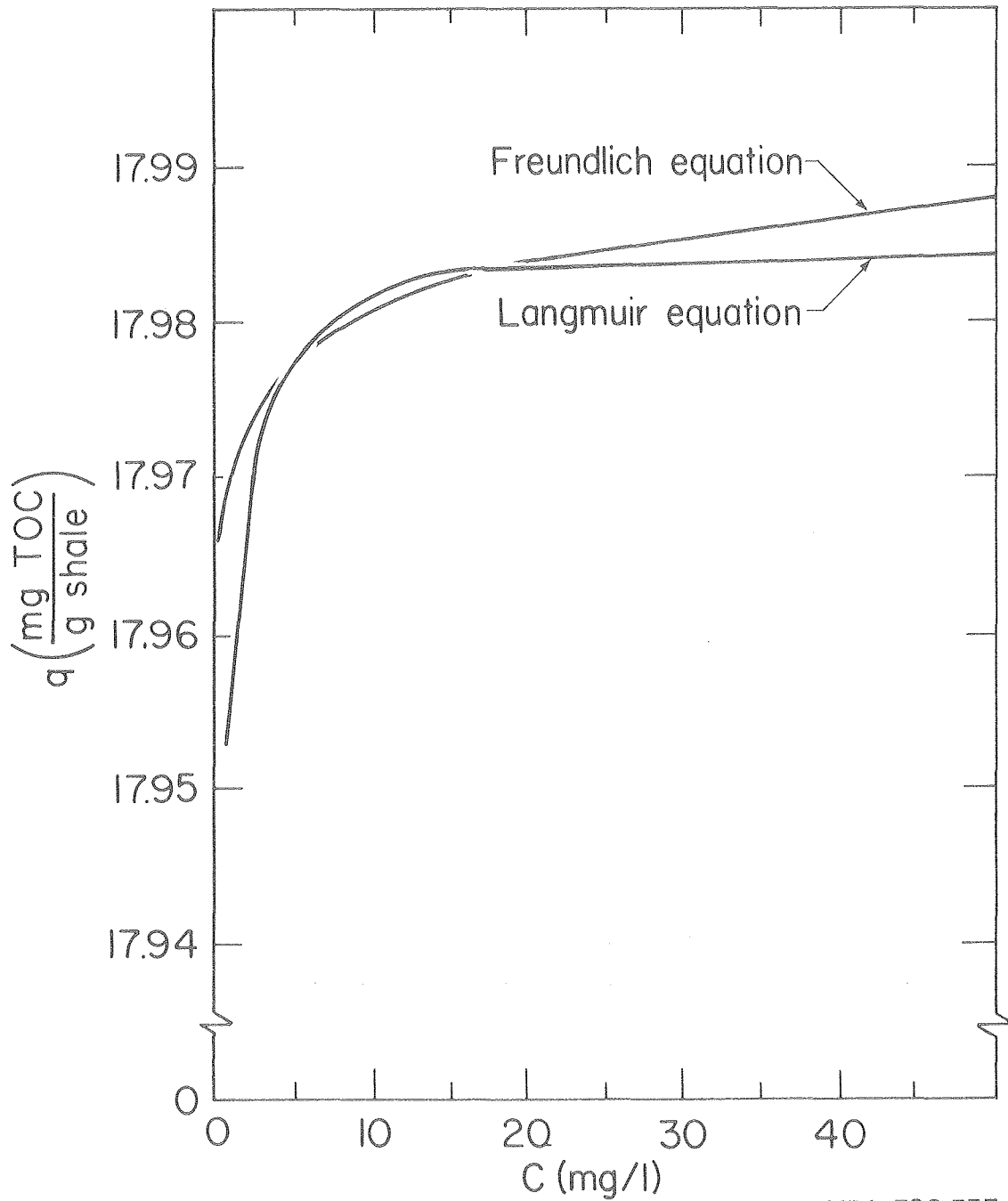
The differences between the Langmuir model and the Freundlich model can be portrayed by plotting corresponding mathematical expressions for each model using the constants presented in Table 23. Plots of both models are presented in Figures 49 and 50, representing plots of the isotherm for Type 1 spent shale examined with distilled water at 20°C and the isotherm for Type 2 spent shale examined with distilled water at 20°C, respectively.

An examination of Figures 49 and 50 reveals some interesting characteristics of each model. At higher values of  $q$  and  $C$ , the Langmuir model eventually levels off at a constant value of  $q$  below the theoretically maximum possible value of  $q$  whereas the Freundlich model yields continually increasing values of  $q$  as a function of  $C$ . At intermediate values of  $q$  and  $C$ , both models yield fairly similar



XBL 792-556

Figure 49. Plots of Langmuir and Freundlich equations for Type 1 spent shale examined with distilled water at 20°C.



XBL 792-557

Figure 50. Plots of Langmuir and Freundlich equations for Type 2 spent shale examined with distilled water at 20°C.

estimates of equilibrium relationships. At lower values of  $q$  and  $C$ , the Langmuir model generally behaves in a manner according to theoretical expectations. Use of the Langmuir model is normally preferred over the Freundlich model in situations where it behaves according to theoretical expectations (i.e., in this case, at lower values of  $q$  and  $C$ ).

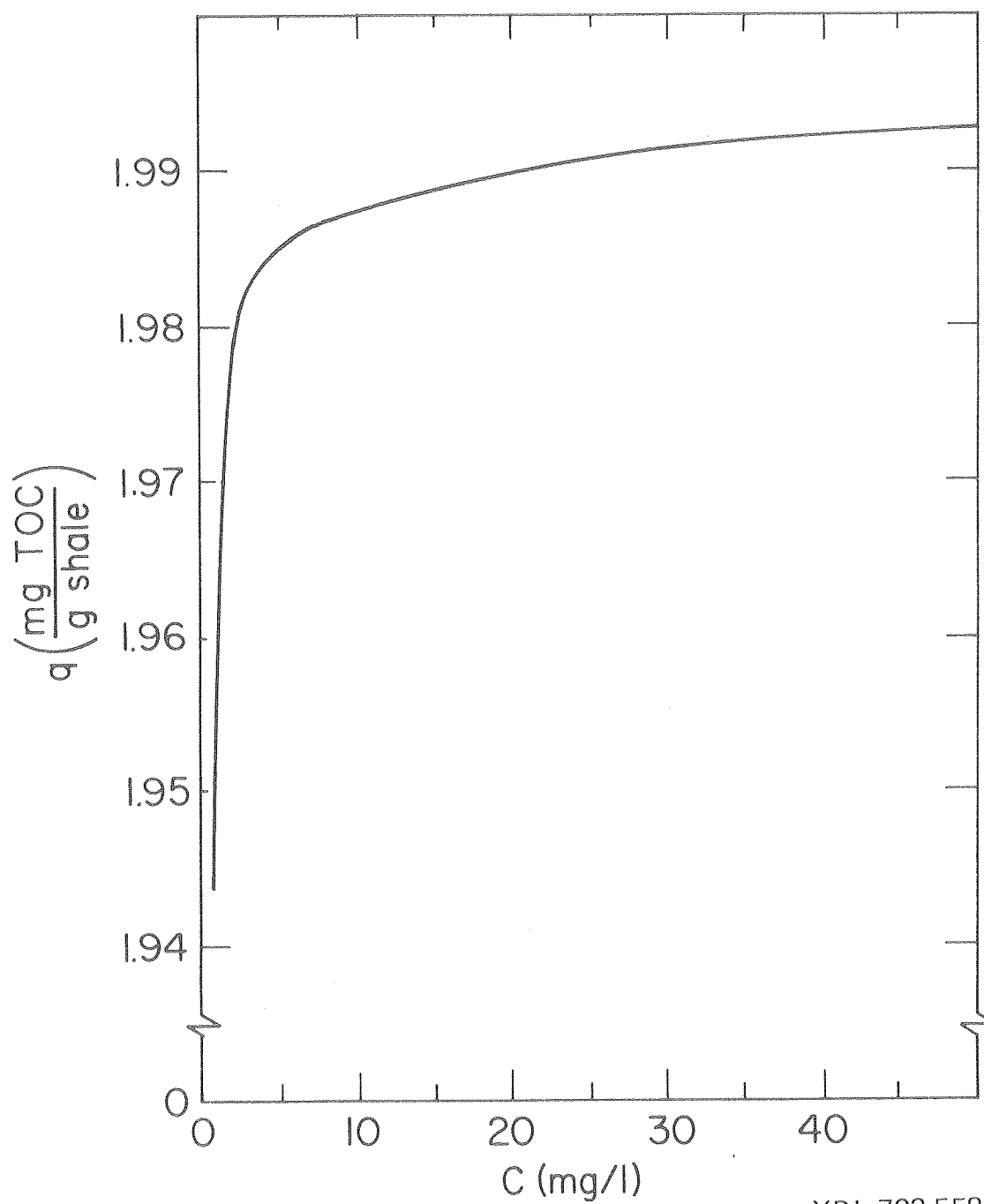
Based on the above observations, it would seem advantageous to use a combination of the two models in attempting to precisely define a complete isotherm for a particular type of spent shale examined under certain experimental conditions. In reference to Figures 49 and 50, the use of the Freundlich model would likely be more appropriate at higher values of  $q$  and  $C$ . Specifically, for the Type 1 spent shale described in Figure 49, the Freundlich model would likely be more appropriate at  $C$  values greater than 15 mg/l and corresponding  $q$  values greater than 1.9890 mg/g. In a similar manner, for the Type 2 spent shale described in Figure 50, the Freundlich model would likely be more appropriate at  $C$  values greater than 18 mg/l and corresponding  $q$  values greater than 17.9825 mg/g.

Furthermore, in reference to Figures 49 and 50, the use of the Langmuir model would likely be more appropriate at lower values of  $q$  and  $C$ . Specifically, for the Type 1 spent shale described in Figure 49, the Langmuir model would likely be more appropriate for values of  $C$  less than 4 mg/l and corresponding values of  $q$  less than 1.9850 mg/g. In a similar manner, for the Type 2 spent shale described in Figure 49, the Langmuir model would likely be more appropriate for  $C$  values less than 4.7 mg/l and corresponding  $q$  values less than 17.9760 mg/g.

For values of  $q$  and  $C$  intermediate to those previously described, a combination of the Freundlich and Langmuir models can be used to describe equilibrium relationships. This can be accomplished by graphically estimating a curve midway between the plots of the Langmuir and Freundlich equations over the intermediate range of values. Alternatively, this same task can be accomplished by taking the average of estimates derived from each model over the intermediate range of data.

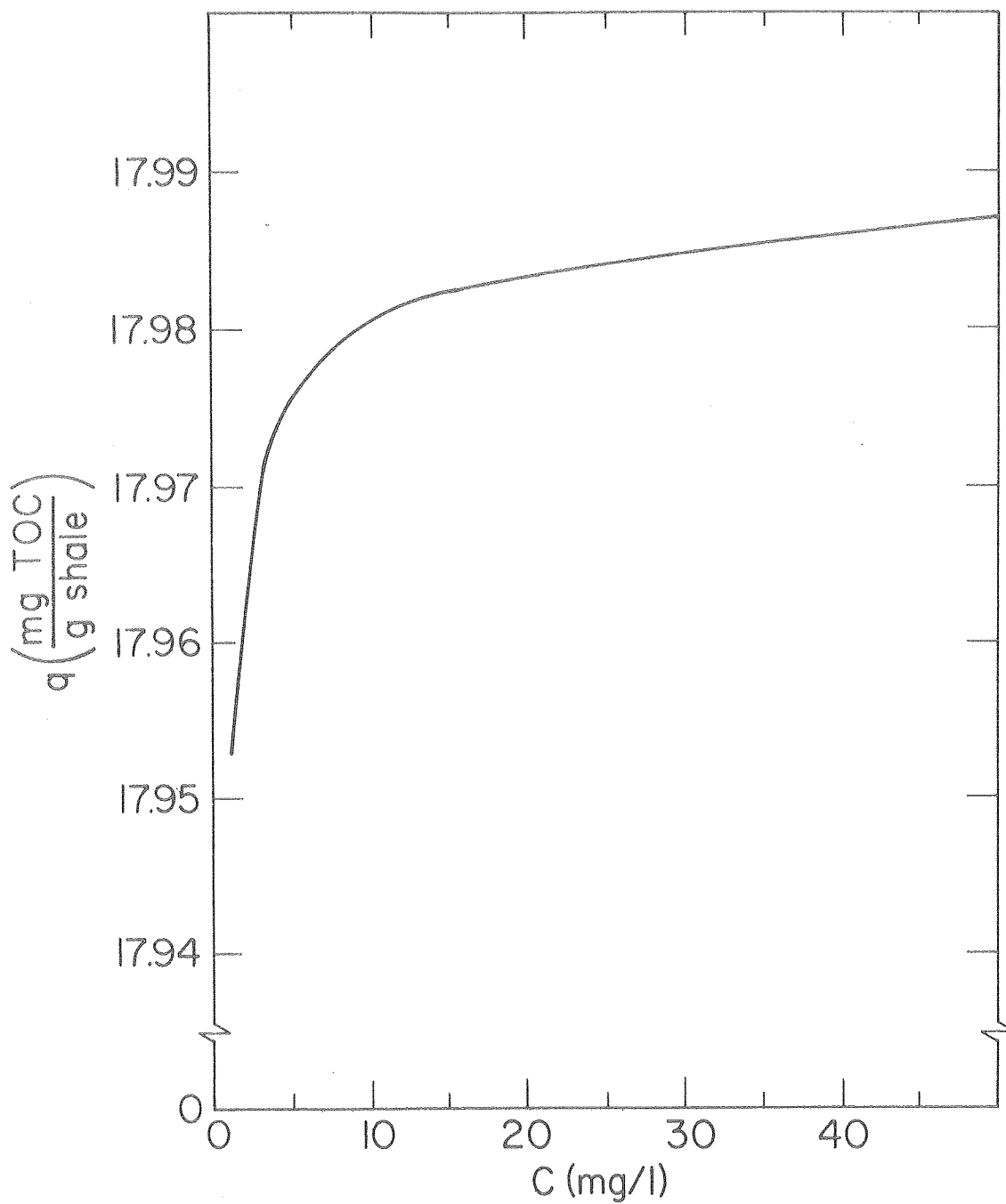
Therefore, it is asserted that complete isotherms are best described by (1) the Langmuir equation at lower values of  $q$  and  $C$ , (2) a combination of both the Langmuir and Freundlich equations at intermediate values of the  $q$  and  $C$ , and (3) the Freundlich equation at higher values of  $q$  and  $C$ . Based on the above, it was possible to derive an isotherm describing equilibrium relationships over a broad range of values for the following two cases: Type 1 spent shale examined with distilled water at 20°C and Type 2 spent shale examined with distilled water at 20°C. These isotherms are shown in Figures 51 and 52, respectively.

It should be recognized that complete isotherms for experimental conditions other than distilled water at 20°C could have been developed using the approach described above. The rationale for specifically



XBL 792-558

Figure 51. Estimated isotherm for Type 1 spent shale examined with distilled water at 20°C.



XBL 792-559

Figure 52. Estimated isotherm for Type 2 spent shale examined with distilled water at 20°C.



developing the two isotherms shown in Figures 51 and 52 is that these isotherms are used in an analysis presented in the following section.

Kinetic Analysis of Continuous-Flow Column Experiments and Development of Framework for Packed-Column Mass Transfer Model

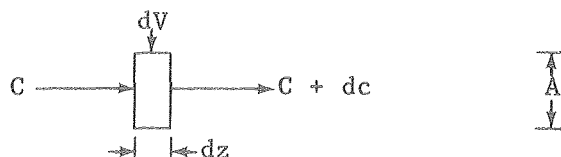
Theory. The leaching phenomenon involves the mass transfer of organic compounds from a solid phase (i.e., spent shale) to a liquid phase (i.e., leachate). The sequence of steps involved in the overall mass transfer process include (1) desorption of water-soluble organic compounds from an intraparticle surface, (2) diffusion of desorbed molecules through an intraparticle liquid surface film and into liquid contained within the pores and interstices of the shale matrix, (3) transport of desorbed molecules from internal pores to the exterior of the shale matrix, and (4) diffusion of molecules through a liquid surface film situated along the exterior of the shale matrix and into the bulk leachate (Ref. 29).

The overall rate of mass transfer during leaching is a function of one or more of the following mechanisms: (1) internal (intraparticle) diffusion, (2) surface reaction of the desorption process at liquid-solid interface, and (3) external mass transfer. Although two or more of these mechanisms may simultaneously limit the rate of mass transfer, only one of these mechanistic steps controls the overall rate in many cases (Ref. 30).

Ideally, it would be advantageous to develop a mass transfer model to simulate the leaching phenomenon in a packed column. Theoretically, a rigorous model would enable prediction of concentration as a function of both time and column length.

A mathematical model for desorption in a packed column requires (1) a mass balance on the component being transferred over a finite volume of the column, (2) a relationship for the equilibrium distribution of the component between liquid and solid phases (i.e., an equilibrium isotherm), and (3) an expression for the rate of desorption. The first of the above steps, a mass balance over a finite volume, will yield a partial differential equation which can theoretically be integrated if both the equilibrium isotherm and the rate of desorption are mathematically evaluated (Refs. 30-36).

Consider a differential volume of a packed column in which desorption occurs:



where  $C$  = input concentration (mg/l)

$C + dC$  = output concentration (mg/l)

$dV$  = volume of finite element ( $\text{cm}^3$ )

$dz$  = length of finite element (cm)

$A$  = cross-sectional area of column ( $\text{cm}^2$ ).

Conducting a mass balance over the finite volume, it follows that:

$$\text{Input} - \text{Output} = \text{Accumulation.}$$

The input to the finite volume is defined by:

$$\text{Input} = CFdt$$

where  $F$  = liquid flow rate (l/hr).

The output from the finite volume is defined by:

$$\text{Output} = (C + dC) Fdt.$$

The rate of accumulation (actually desorption) which occurs in the finite volume is:

$$\text{Accumulation} = \frac{\partial q}{\partial t} A \rho dz dt$$

where  $\frac{\partial q}{\partial t}$  = rate of desorption (mg/g-hr)

$\rho$  = bulk density of packed column ( $\text{g}/\text{cm}^3$ ).

Thus it follows that:

$$CFdt - (C + dC)Fdt = \frac{\partial q}{\partial t} A \rho dz dt$$

$$CFdt = \frac{\partial q}{\partial t} A \rho dz dt + (C + dC)Fdt$$

$$CFdt = \frac{\partial q}{\partial t} A \rho dz dt + CFdt + dCFdt \quad .$$

Rearranging:

$$- dC = \frac{A}{F} \frac{\partial q}{\partial t} \rho dz \quad .$$

Since C is a function of the variables z and t, the total differential is:

$$dC = \left( \frac{\partial C}{\partial z} \right)_t dz + \left( \frac{\partial C}{\partial t} \right)_z dt \quad .$$

From basic principles, it is also known that:

$$V = \frac{\partial z}{\partial t} \quad \text{and} \quad F = VA\alpha$$

where V = flow velocity through pores (cm/hr)

$\alpha$  = porosity of packed column.

Substituting the above expressions yields:

$$- \rho A \left( \frac{\partial q}{\partial t} \right)_z = F \left( \frac{\partial C}{\partial z} \right)_t + \alpha A \left( \frac{\partial C}{\partial t} \right)_z \quad .$$

The above expression, hereafter referred as the differential mass balance equation, can theoretically be integrated if the equilibrium isotherm and the rate of desorption can be mathematically evaluated. Unfortunately, this integration is extremely difficult and requires various simplifying assumptions, esoteric mathematical analysis, and a computer-assisted solution. Due to the complexity involved in integrating the above expression, this section will attempt only to assess the rate of desorption by employing several kinetic rate models. It is asserted that this assessment of the rate of desorption in conjunction with previously evaluated isotherms and the differential mass balance equation will roughly provide a framework for a packed column mass transfer model. It is hoped that future researchers will employ this framework to develop a rigorous mass transfer model to simulate the leaching phenomenon in a packed column.

The most important parameter in the differential mass balance equation is the term  $(\partial q/\partial t)_z$ , the rate of desorption. As indicated previously, a mathematical evaluation of this rate would provide part of the information required to theoretically integrate the differential mass balance equation.

It has been previously stated that the desorption phenomenon may encounter various resistances to mass transfer. These resistances to mass transfer may result in one of the following mechanisms being rate limiting: (1) external mass transfer, (2) surface reaction, and (3) internal mass transfer. A precise mathematical evaluation of  $(\partial q/\partial t)_z$  would take into account all of the above mechanisms. However, in order to simplify the mathematics involved, it is often advantageous to assume that one particular mechanism is rate controlling over (1) the entire time period investigated or (2) certain ranges of time within the entire time period.

Several rate models have been postulated in the literature to describe the rate of adsorption. These models can also be applied to the desorption phenomenon and are summarized below, classified according to the rate-controlling mechanism.

External Mass Transfer. If external mass transfer is the rate-controlling mechanism, the rate of desorption can be described by (Ref. 30):

$$\left(\frac{\partial q}{\partial t}\right)_z = K_E (C - C^*)$$

where  $(\partial q/\partial t)_z$  = rate of desorption  
(mg TOC/g shale-hr)

$K_E$  = external mass transfer coefficient  
(1/g-hr)

$C$  = actual measured TOC concentration in  
bulk leachate (mg/l)

$C^*$  = theoretical TOC concentration in equilibrium  
with actual solid-phase organic carbon on  
shale particles (mg/l), as estimated from  
isotherm equation.

In the external mass transfer model, the expression  $(C - C^*)$  represents the driving force for mass transfer/desorption and is defined as the difference between the actual TOC concentration and the theoretical TOC concentration (as estimated from the isotherm equation).

Internal Mass Transfer. If internal mass transfer is the rate-controlling mechanism, the following rate model, originally hypothesized by Glueckauf (Ref. 30), can be employed to describe the rate of desorption:

$$\left(\frac{\partial q}{\partial t}\right)_z = K_G(q^* - q)$$

where  $K_G$  = Glueckauf rate constant ( $\text{hr}^{-1}$ )

$q^*$  = theoretical solid-phase organic carbon on shale particles in equilibrium with actual measured TOC concentration in bulk leachate (mg TOC/g shale) as estimated from isotherm equation

$q$  = actual solid-phase organic carbon on shale particles (mg TOC/g shale).

In the Glueckauf model, the parameter  $(q^* - q)$  represents the driving force for mass transfer/desorption and is defined as the difference between the theoretical solid-phase organic carbon (as estimated from the isotherm equation) and the actual solid-phase organic carbon.

Surface Reaction. The following expression, known as the Bohart and Adams model, can be used to describe the rate of desorption when the rate-limiting mechanism is surface reaction (Ref. 31):

$$\left(\frac{q}{t}\right)_z = K_{BA}C(q_\infty - q)$$

where  $K_{BA}$  = Bohart and Adams rate constant (1/mg-hr)

$q_\infty$  = maximum potential solid-phase organic carbon on shale particles (mg TOC/g shale), as estimated from isotherm equation.

In the Bohart and Adams model, the parameter  $(q_\infty - q)$  represents the driving force for mass transfer/desorption and is defined as the difference between the maximum potential solid-phase organic carbon and the actual solid-phase organic carbon.

Application. The previous methodology can be applied to the results of the continuous-flow column experiments derived from Types 1 and 2 spent shale. Results derived from other types of spent shale cannot be considered since equilibrium isotherms were developed only for Types 1 and 2.

Equilibrium isotherms for Type 1 and Type 2 spent shales, as derived from distilled water at 20°C, were developed previously and presented in Figures 51 and 52. These isotherms define the theoretical relationship between the solid-phase organic carbon on shale particles

(q) in equilibrium with the TOC concentration in the bulk leachate (C). The isotherms presented in Figures 51 and 52 can be extrapolated by using (1) the appropriate Freundlich equation at higher values of q and C and (2) the appropriate Langmuir equation at lower values of q and C.

The results of the relevant continuous-flow column experiments are presented in Figures 53 and 54, representing plots of TOC concentration versus time. As shown in these figures, an attempt was made to draw a smooth "best fit" curve through the data. It should be noted that these plots differ slightly from the original plots shown in Figures 31 and 32 due to a slight adjustment of the time scale. In Figures 53 and 54, a time of zero corresponds to the instant when leach water began entering the column while, in Figures 31 and 32, a time of zero corresponds to the instant when effluent first appeared from the end of the column.

Plots of TOC concentration versus column length, as shown in Figures 55 and 56, were developed by extracting relevant information from the plots of TOC concentration versus time. These plots of TOC concentration versus column length represent "concentration profiles," describing the instantaneous concentration throughout the entire length of a 30 centimeter (12 inch) column at a designated time.

With respect to the kinetic analysis presented in this section a very serious limitation of the data presented in Figures 53 and 54 is that relationships between TOC concentration as a function of time are only described for two column lengths; 15 centimeters and 30 centimeters. However, it should be recognized that, by employing a "cross-plotting" technique in conjunction with the families of curves presented in Figures 55 and 56, TOC concentration versus time curves for column lengths can be approximated. Thus, using a "cross-plotting" technique, curves describing TOC concentration as a function of time for various column lengths were developed, as shown in Figures 57 and 58.

The various rate models that are employed in this analysis were summarized in the previous section along with descriptions of the various parameters required to test these models. The procedure for evaluating the rate models consists of first estimating all parameters in each rate model except the rate constant and then solving for the rate constant. For each model, the rate constant is then estimated at several different values of time and the resulting estimates compared to see if they approach a constant value.

The parameters required for an evaluation of the various rate models are present in Tables 24 through 26 for Type 1 spent shale and Tables 27 through 29 for Type 2 spent shale. As revealed by these tables, each parameter was estimated for three column lengths: 7.5, 15 and 22.5 centimeters; and for eight different values of time, ranging from 5 to 40 hours. Time values outside of this range were not considered because the TOC concentration versus time curves are not well-defined prior to 5 hours and after 40 hours.

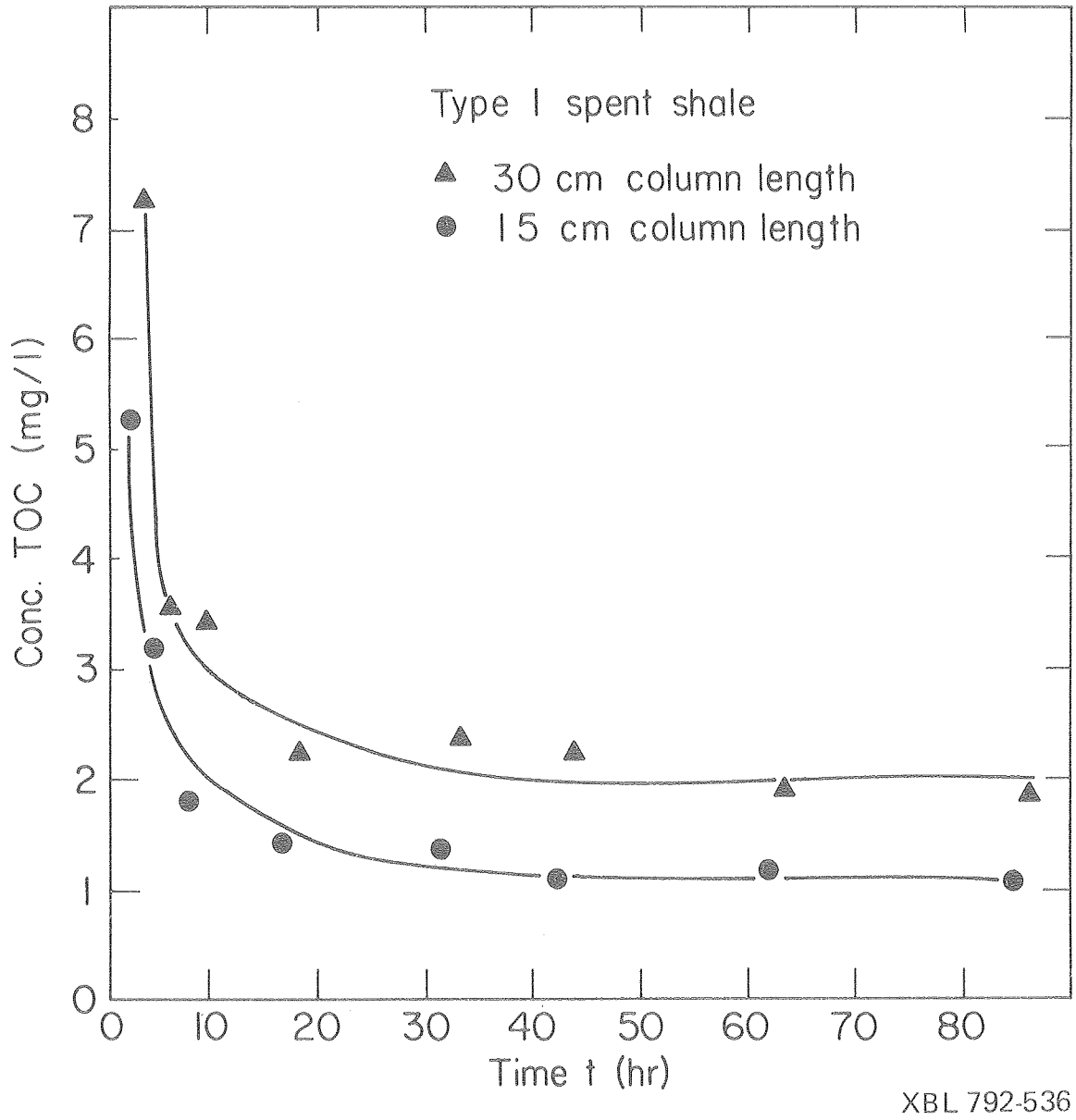


Figure 53. TOC concentration vs time: Type I spent shale.

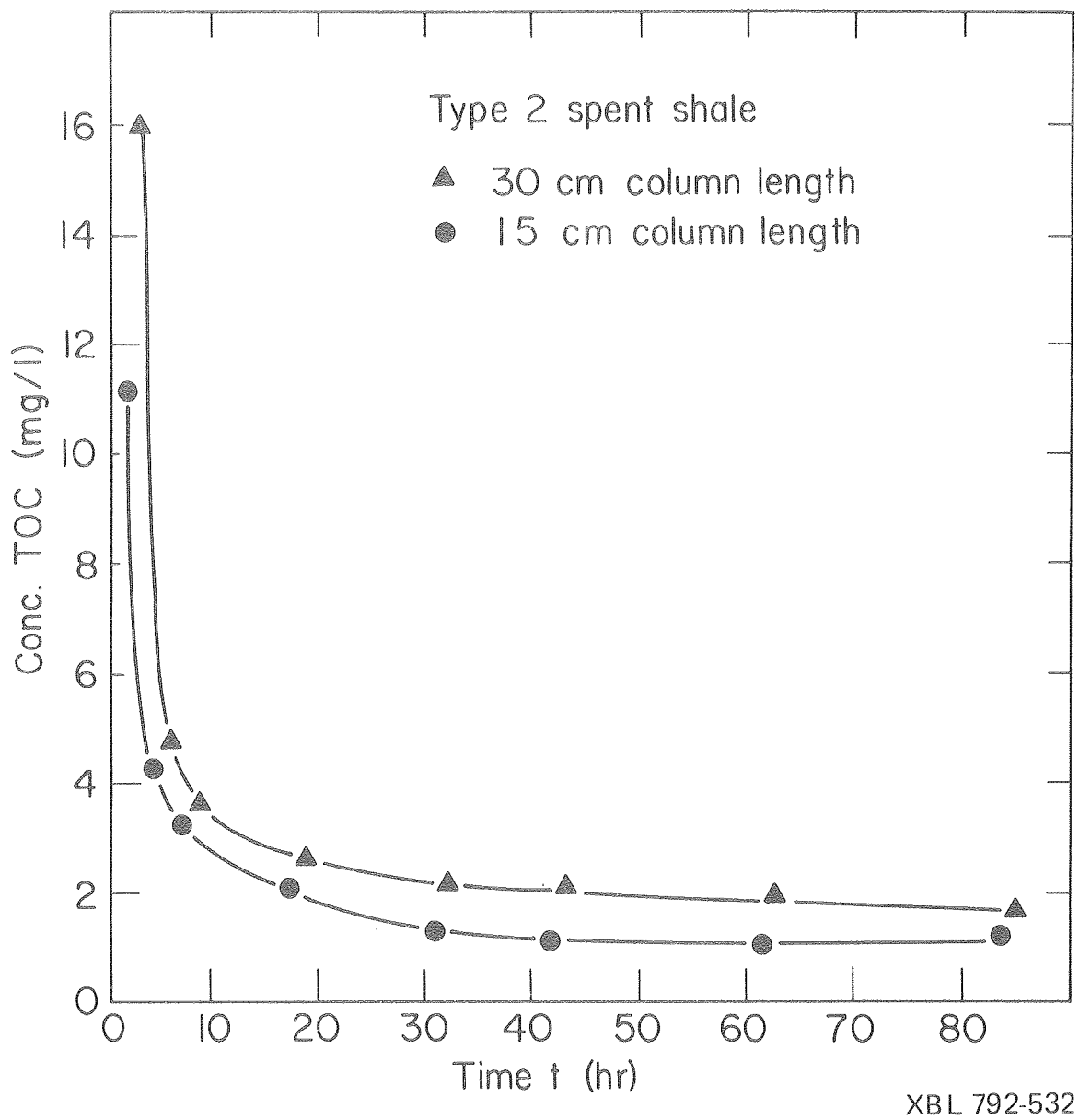


Figure 54. TOC concentration vs time: Type 2 spent shale.



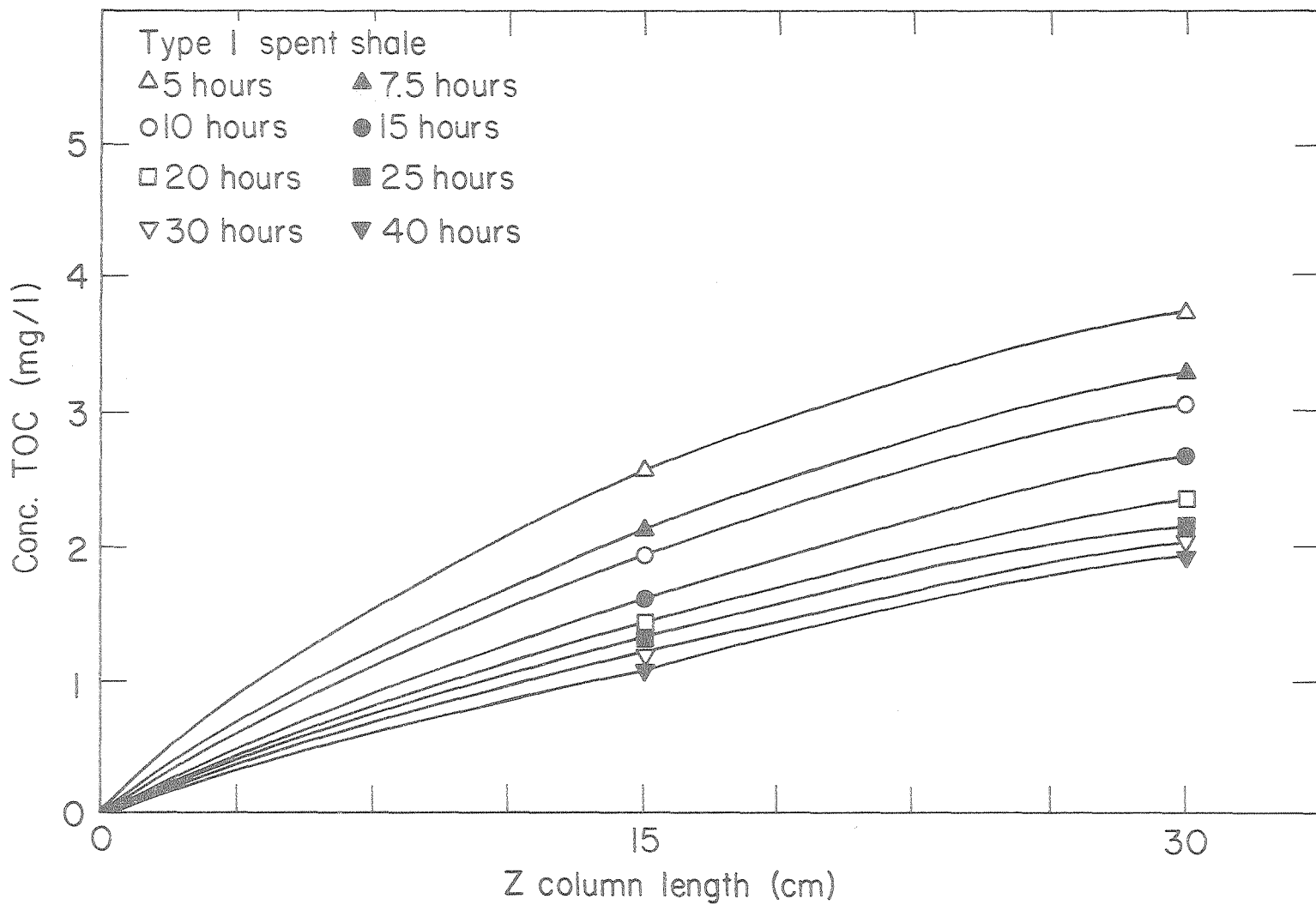


Figure 55. TOC concentration vs column length: Type 1 spent shale.

XBL 792-533

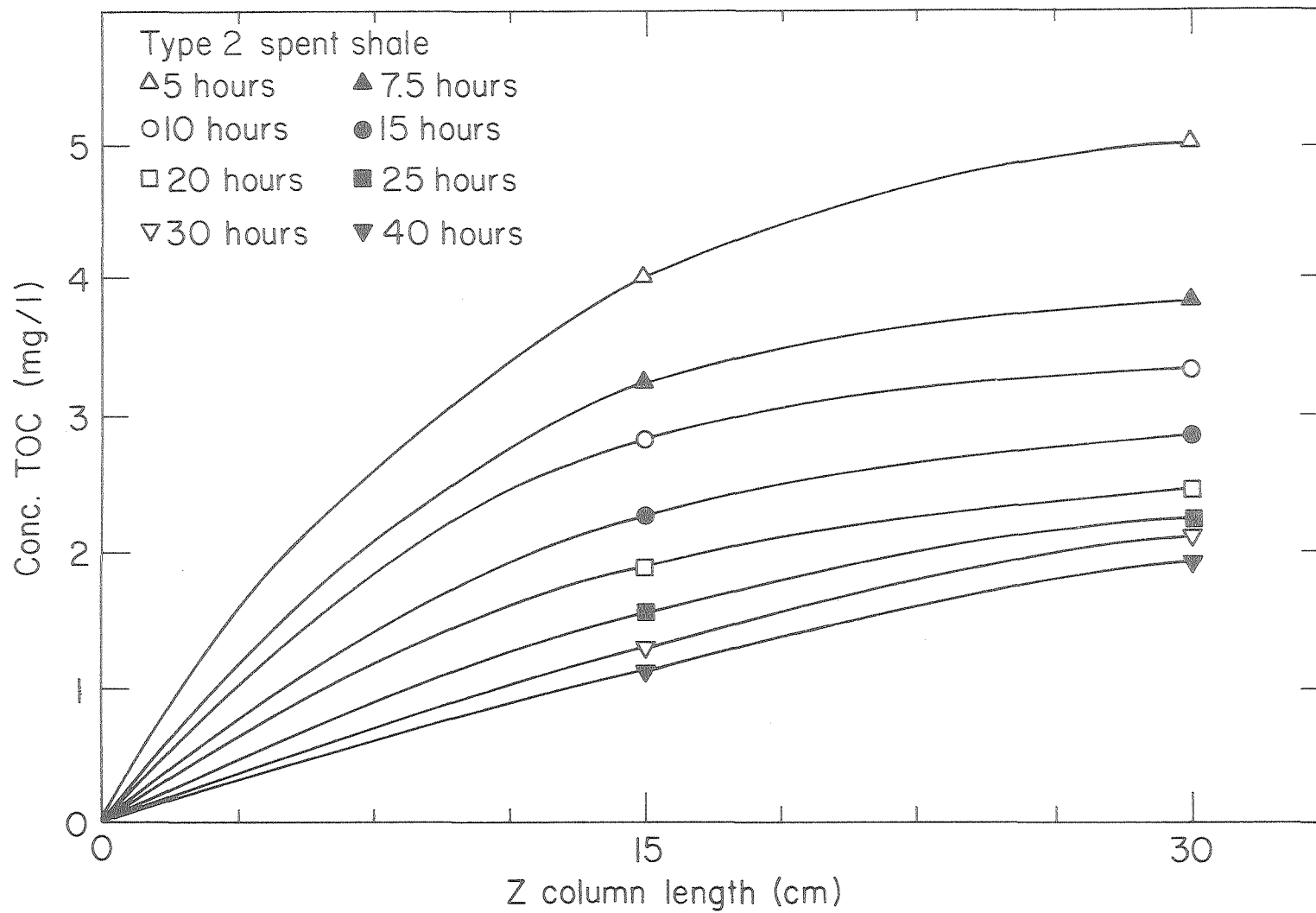
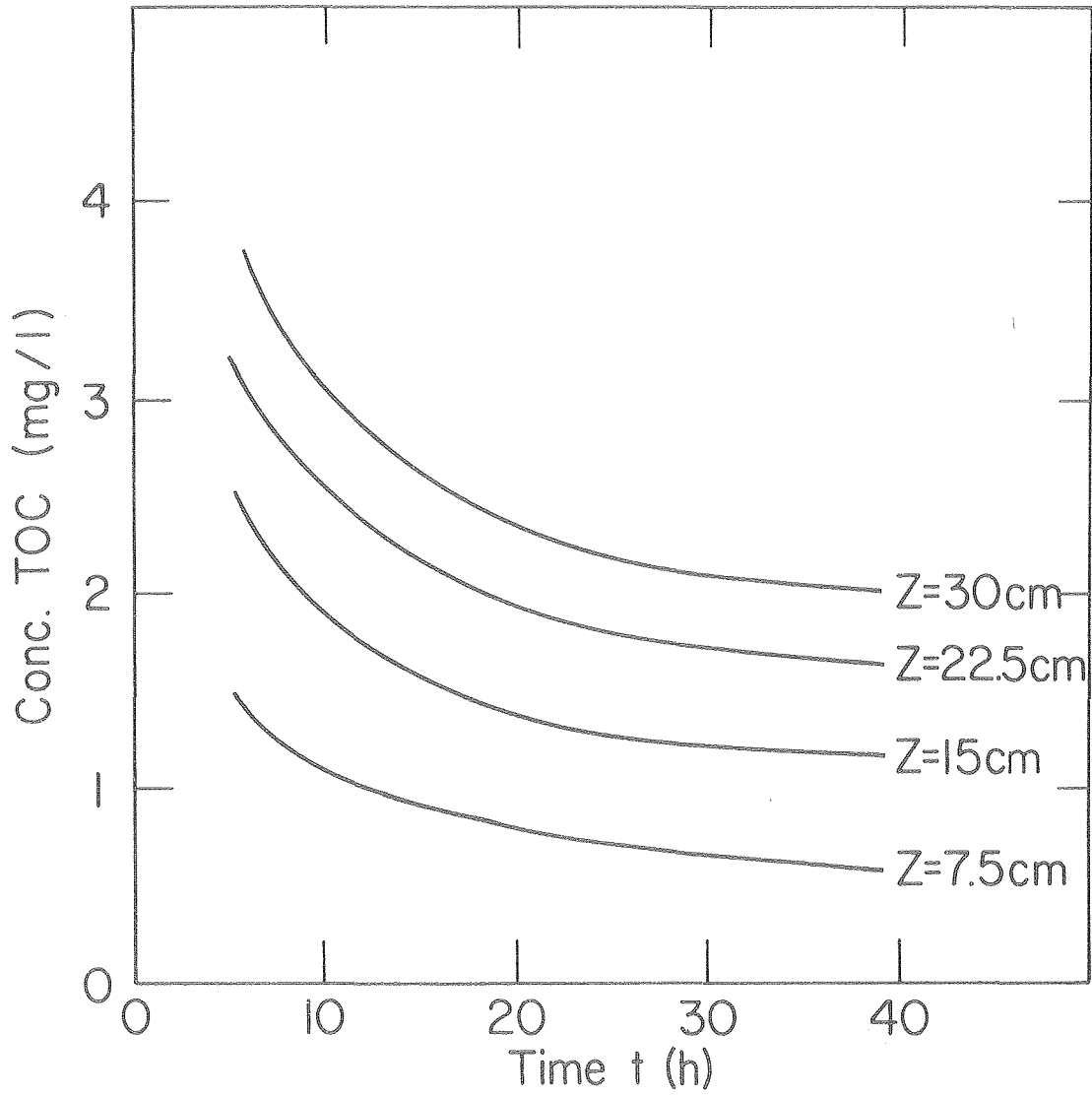


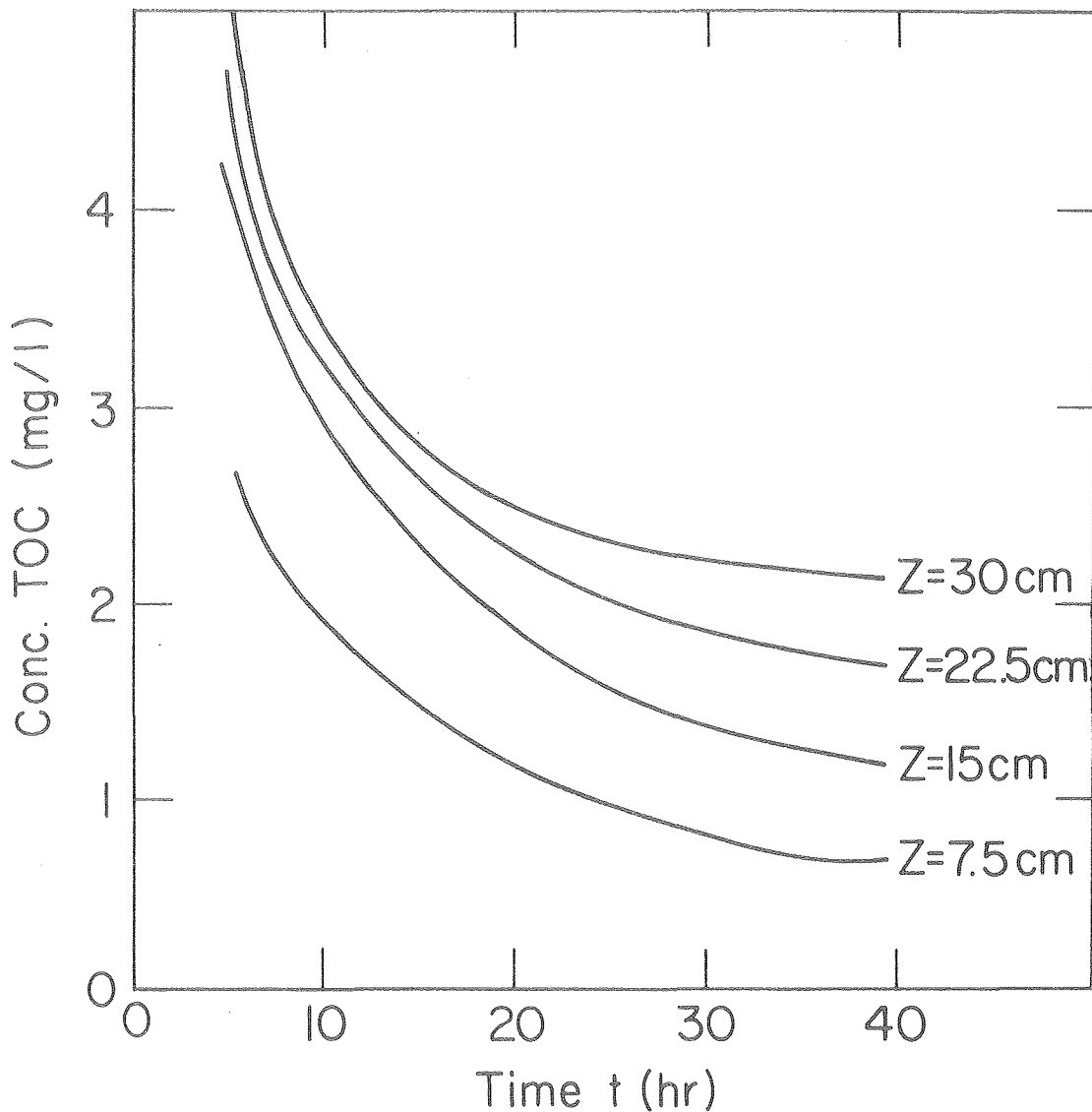
Figure 56. TOC concentration vs column length: Type 2 spent shale.

XBL 792-534



XBL 792-537

Figure 57. Approximated TOC concentration vs time curves for various column lengths: Type 1 spent shale.



XBL 792-538

Figure 58. Approximated TOC concentration vs time curves for various column lengths: Type 2 spent shale.

Table 24. Estimates of parameters required for evaluation of rate constants for Type 1 spent shale at a column length of 7.5 cm.

Parameter	Units	Parameter values estimated at various times							
		5 hr	7.5 hr	10 hr	15 hr	20 hr	25 hr	30 hr	40 hr
$\left(\frac{\partial C}{\partial t}\right)_z$	$\frac{\text{mg/l}}{\text{hr}}$	-0.150	-0.080	-0.040	-0.0233	-0.0188	-0.0133	-0.0125	-0.0100
$\left(\frac{\partial C}{\partial t}\right)_z$	$\frac{\text{mg/l}}{\text{cm}}$	0.149	0.136	0.128	0.109	0.096	0.0853	0.0800	0.0787
$\left(\frac{\partial q}{\partial t}\right)_z$	$\frac{\text{mg/g}}{\text{hr}}$	-0.001172	-0.001107	-0.001065	-0.000914	-0.000806	-0.000719	-0.000674	-0.000665
$q^*$	mg/g	1.974530	1.969826	1.967875	1.963863	1.960177	1.956314	1.952561	1.947128
$q_\infty$	mg/g	2.00	2.00	2.00	2.00	2.00	2.00	2.00	2.00
$\Delta q$	mg/g	0.005855	0.002849	0.002715	0.004948	0.004300	0.003813	0.003483	0.006695
$\Sigma \Delta q$	mg/g	0.005855	0.008704	0.011419	0.016367	0.020667	0.024480	0.27963	0.034658
$q$	mg/g	1.994145	1.991296	1.988581	1.9836333	1.979333	1.975520	1.972037	1.965342
$C$	mg/l	1.50	1.16	1.06	0.09	0.79	0.70	0.63	0.55
$C^*$	mg/l	72.4	30.0	12.3	3.43	2.14	1.60	1.30	0.95

Table 25. Estimates of parameters required for evaluation of rate constants for Type 1 spent shale at a column length of 15 cm.

Parameter	Units	Parameter values estimated at various times							
		5 hr	7.5 hr	10 hr	15 hr	20 hr	25 hr	30 hr	40 hr
$\left(\frac{\partial C}{\partial t}\right)_z$	$\frac{\text{mg/l}}{\text{hr}}$	-0.140	-0.114	-0.095	-0.055	-0.035	-0.020	-0.0075	-0.0030
$\left(\frac{\partial C}{\partial z}\right)_t$	$\frac{\text{mg/l}}{\text{cm}}$	0.116	0.107	0.0973	0.0827	0.0773	0.0760	0.0740	0.0720
$\left(\frac{\partial q}{\partial t}\right)_z$	$\frac{\text{mg/g}}{\text{hr}}$	-0.000897	-0.000837	-0.000767	-0.000669	-0.000636	-0.000635	-0.000626	-0.000612
q*	mg/g	1.980986	1.978913	1.977649	1.974948	1.972611	1.971318	1.970177	1.968294
q <sub>∞</sub>	mg/g	2.00	2.00	2.00	2.00	2.00	2.00	2.00	2.00
Δq	mg/g	0.004485	0.002168	0.002005	0.003590	0.003259	0.003175	0.003150	0.006190
ΣΔq	mg/g	0.004485	0.006653	0.008658	0.012248	0.015507	0.018682	0.021832	0.028022
q	mg/g	1.995515	1.993347	1.991342	1.987752	1.984493	1.981318	1.978168	1.971978
C	mg/l	2.50	2.06	1.86	1.54	1.34	1.25	1.18	1.08
C*	mg/l	110	56.6	30.0	9.00	3.91	2.59	1.94	1.29

Table 26. Estimates of parameters required for evaluation of rate constants for Type 1 spent shale at a column length of 22.5 cm.

Parameter	Units	Parameter values estimated at various times							
		5 hr	7.5 hr	10 hr	15 hr	20 hr	25 hr	30 hr	40 hr
$\left(\frac{\partial C}{\partial t}\right)_z$	$\frac{\text{mg/l}}{\text{hr}}$	-0.170	-0.115	-0.0975	-0.0600	-0.0375	-0.0250	-0.0150	-0.0083
$\left(\frac{\partial C}{\partial t}\right)_z$	$\frac{\text{mg/l}}{\text{cm}}$	0.085	0.080	0.075	0.072	0.0693	0.0587	0.0560	0.0560
$\left(\frac{\partial q}{\partial t}\right)_z$	$\frac{\text{mg/g}}{\text{cm}}$	-0.000612	-0.000606	-0.000575	-0.000574	-0.000566	-0.000484	-0.000468	-0.00472
q*	mg/g	1.983231	1.981902	1.981139	1.979458	1.978250	1.977456	1.976425	1.975723
q	mg/g	2.00	2.00	2.00	2.00	2.00	2.00	2.00	2.00
q <sub>∞</sub>	mg/g	0.003060	0.001523	0.001475	0.002870	0.002850	0.002625	0.002380	0.004700
Δq	mg/g	0.003060	0.004583	0.006058	0.008928	0.011778	0.014403	0.016783	0.021483
ΣΔq	mg/g	1.996940	1.995417	1.993942	1.991072	1.988222	1.985597	1.983217	1.978517
C	mg/l	3.25	2.76	2.54	2.16	1.95	1.83	1.70	1.62
C*	mg/l	171	107	68.0	28.0	10.6	5.10	3.24	1.99

Table 27. Estimates of parameters required for evaluation of rate constants for Type 2 spent shale at a column length of 7.5 cm.

Parameter	Units	Parameter values estimated at various times							
		5 hr	7.5 hr	10 hr	15 hr	20 hr	25 hr	30 hr	40 hr
$\left(\frac{\partial C}{\partial t}\right)_z$	$\frac{\text{mg/l}}{\text{hr}}$	-0.220	-0.140	-0.100	-0.0667	-0.0500	-0.0450	-0.0238	-0.0125
$\left(\frac{\partial C}{\partial z}\right)_t$	$\frac{\text{mg/l}}{\text{cm}}$	0.230	0.206	0.186	0.153	0.123	0.105	0.0867	0.0767
$\left(\frac{\partial q}{\partial t}\right)_z$	$\frac{\text{mg/g}}{\text{hr}}$	-0.001457	-0.001332	-0.001215	-0.001007	-0.000811	-0.000691	-0.000577	-0.000514
$q^*$	mg/g	17.968970	17.965067	17.962340	17.955454	17.950405	17.939654	17.928755	17.917987
$q_\infty$	mg/g	18.00	18.00	18.00	18.00	18.00	18.00	18.00	18.00
$\Delta q$	mg/g	0.007285	0.003485	0.003182	0.005555	0.004545	0.003755	0.003170	0.005450
$\Sigma \Delta q$	mg/g	0.007285	0.010770	0.013952	0.019507	0.024052	0.027807	0.030977	0.036427
$q$	mg/g	17.992715	17.989230	17.386048	17.980493	17.975948	17.972193	17.969023	17.963537
$C$	mg/l	2.65	2.12	1.86	1.42	1.21	0.92	0.74	0.62
$C^*$	mg/l	168	79.5	40.2	10.8	4.79	3.34	2.66	1.97



Table 28. Estimates of parameters required for evaluation of rate constants for Type 2 spent shale at a column length of 15 cm.

Parameter	Units	Parameter values estimated at various times							
		5 hr	7.5 hr	10 hr	15 hr	20 hr	25 hr	30 hr	40 hr
$\left(\frac{\partial C}{\partial t}\right)_z$	$\frac{\text{mg/l}}{\text{hr}}$	-0.400	-0.200	-0.145	-0.100	-0.075	-0.0533	-0.0325	-0.0175
$\left(\frac{\partial C}{\partial z}\right)_t$	$\frac{\text{mg/l}}{\text{cm}}$	0.128	0.0967	0.0783	0.0758	0.0700	0.0683	0.0683	0.0633
$\left(\frac{\partial q}{\partial t}\right)_z$	$\frac{\text{mg/g}}{\text{hr}}$	-0.000680	-0.000562	-0.000463	-0.000467	-0.000440	-0.000439	-0.000448	-0.000422
$q^*$	mg/g	17.974242	17.971655	17.969807	17.965777	17.962220	17.955737	17.946993	17.947331
$q_\infty$	mg/g	18.00	18.00	18.00	18.00	18.00	18.00	18.00	18.00
$\Delta q$	mg/g	0.003400	0.001553	0.001283	0.002325	0.002265	0.002200	0.002220	0.004350
$\Sigma \Delta q$	mg/g	0.003400	0.004953	0.006236	0.008561	0.010826	0.013026	0.015246	0.019596
$q$	mg/g	17.996600	17.995047	17.993764	17.991439	17.989174	17.986974	17.984754	17.980404
$C$	mg/l	4.00	3.20	2.80	2.20	1.85	1.52	1.10	1.11
$C^*$	mg/l	385	276	210	128	78.5	49.0	30.5	10.7

Table 29. Estimates of parameters required for evaluation of rate constants for Type 2 spent shale at a column length of 22.5 cm.

Parameter	Units	Parameter values estimated at various times							
		5 hr	7.5 hr	10 hr	15 hr	20 hr	25 hr	30 hr	40 hr
$\left(\frac{\partial C}{\partial t}\right)_z$	$\frac{\text{mg/l}}{\text{hr}}$	-0.333	-0.200	-0.130	-0.090	-0.060	-0.0367	-0.0287	-0.0100
$\left(\frac{\partial C}{\partial z}\right)_t$	$\frac{\text{mg/l}}{\text{cm}}$	0.0733	0.0400	0.0333	0.0417	0.0383	0.0500	0.0583	0.0600
$\left(\frac{\partial q}{\partial t}\right)_z$	$\frac{\text{mg/g}}{\text{hr}}$	-0.000341	-0.000177	-0.000163	-0.000241	-0.000232	-0.000322	-0.000382	-0.000403
$q^*$	mg	17.975784	17.973218	17.971775	17.969029	17.966112	17.957895	17.954170	17.947990
$q_\infty$	mg	18.00	18.00	18.00	18.00	18.00	18.00	18.00	18.00
$\Delta q$	mg	0.001705	0.000648	0.000425	0.001010	0.001185	0.001385	0.001760	0.003030
$\Sigma \Delta q$	mg	0.001705	0.002353	0.002778	0.003788	0.004973	0.006358	0.008118	0.012048
$q$	mg	17.998295	17.997647	17.997222	17.996212	17.995027	17.993642	17.991882	17.987952
$C$	mg/l	4.7	3.64	3.23	2.66	2.24	1.55	1.36	1.13
$C^*$	mg/l	553	481	440	354	275	204	104	60.5

Techniques for estimating each of the various parameters presented in Tables 24 through 29 are discussed below.

The parameter  $(\partial C/\partial t)_z$  was estimated from the slope of the TOC concentration versus time curves presented in Figures 57 and 58. Due to the shape of these curves, the parameter  $(\partial C/\partial t)_z$  was always negative. In a like manner, the parameter  $(\partial C/\partial z)_t$  was estimated from the slope of the TOC concentration versus column length curves presented in Figures 55 and 56. In reference to the aforementioned methods of estimating both  $(\partial C/\partial t)_z$  and  $(\partial C/\partial z)_t$ , it should be recognized that estimating the slope of a curve can be a rather subjective endeavor. The normal procedure is to draw a line tangent to the curve at a particular point of concern. In an attempt to overcome this subjectivity, slopes were estimated by assuming that a short segment of a particular curve encompassing the point of concern was approximately linear.

The parameter  $(\partial q/\partial t)_z$  was estimated from the differential mass balance equation. Values of  $(\partial q/\partial t)_z$  were computed by substituting in previously derived estimates of  $(\partial C/\partial t)_z$  and  $(\partial C/\partial z)_t$  into the differential mass balance equation along with values of A, F,  $\alpha$ , and  $\rho$ . It should be recognized that estimates of  $(\partial q/\partial t)_z$  are extremely important because this parameter represents the rate of desorption and is the principal parameter in the various rate equations.

The parameter  $q_\infty$  was estimated from the solid-phase organic carbon measurements originally presented in Table 11. These estimates, 2.00  $\mu\text{g}$  TOC/g spent shale for Type 1 and 18.00 mg TOC/g spent shale for Type 2, represent the theoretically maximum potential solid-phase organic carbon on shale particles.

The parameter  $\Delta q$  was estimated for each interval of leaching time by multiplying the average value of  $(\partial q/\partial t)_z$  during a particular interval by the time duration of the interval. Thus, as an example the value of  $\Delta q$  given for a leaching time of 15 hours was estimated by first averaging the value of  $(\partial q/\partial t)_z$  at 15 hours and the value of  $(\partial q/\partial t)_z$  at the preceding leaching time of 10 hours. This average value of  $(\partial q/\partial t)_z$  over the period of 10 to 15 hours was then multiplied by a leaching time interval of 5 hours (i.e., the duration of the interval between 10 and 15 hours), yielding an estimate of  $\Delta q$ . As an exception to the above procedure, the value of  $\Delta q$  for the interval of 0 to 5 hours was estimated by simply multiplying  $(\partial q/\partial t)_z$  at 5 hours times the interval duration of five hours (this is because a value of  $(\partial q/\partial t)_z$  was not obtained for a leaching time of 0 hours). The parameter  $\Delta q$  represents the mass of organic carbon leached during a specified interval of leaching time.

The parameter  $\Sigma \Delta q$  was estimated by summing values of  $\Delta q$  for all leaching time intervals up to and including the interval of concern. Thus, as an example, the value of  $\Sigma \Delta q$  given for a leaching time period of 15 hours includes (1) the value of  $\Delta q$  from 0 to 5 hours, (2) the value of  $\Delta q$  from 5 to 7.5 hours, (3) the value of  $\Delta q$  from 7.5 to 10

hours, and (4) the value of  $\Delta q$  from 10 to 15 hours. The parameter  $\Delta q$  represents the mass of organic carbon leached after a specified leaching time.

The parameter  $q$  was estimated by subtracting the quantity  $\Sigma \Delta q$  from the corresponding value of  $q_{\infty}$ . The parameter  $q$  represents an estimate of the actual solid-phase organic carbon remaining on spent shale particles after a specified leaching time.

The parameter  $q^*$  was estimated from the isotherms presented in Figures 51 and 52 by using the actual measured TOC concentration. This parameter represents an estimate of the theoretical solid-phase organic carbon on shale particles (i.e., the solid-phase organic carbon theoretically expected to be in equilibrium with the actual measured TOC concentration in the bulk leachate).

The parameter  $C$ , the actual TOC concentration in the bulk leachate, was directly measured during the column experiments.

The parameter  $C^*$  was estimated from the isotherms presented in Figures 51 and 52 by using the estimated values of  $q$  (recall that  $q$  is the actual solid-phase organic carbon on the shale particles). The parameter  $C^*$  represents an estimate of the theoretical TOC concentration (i.e., the TOC concentration theoretically expected to be in equilibrium with the actual solid-phase organic carbon).

The various rate models were tested by employing the estimated parameters presented in Tables 24 through 29. Sample calculations involved in estimating the rate constant for each model are presented in Appendix A. Estimates of rate constants for each model are presented in Tables 30-35.

An examination of Tables 30 through 32 suggests that, for Type 1 spent shale, the most likely rate-controlling mechanism is internal diffusion. The rate model which assumes that internal diffusion is rate-limiting, the Glueckauf model, yielded fairly constant values for  $K_G$  for all three column lengths during time periods ranging up to and including 30 hours. During this time period, values of  $K_G$  estimated for all three column lengths ranged from 0.0374 to 0.0783  $\text{hour}^{-1}$ . However, with the exception of a few individual pieces of data, values of  $K_G$  approximately ranged from 0.0400 to 0.0600  $\text{hour}^{-1}$ . After 30 hours, the value of  $K_G$  dramatically increased for two of the column lengths, suggesting that either (1) internal mass transfer was no longer limiting, (2) two or more mechanisms simultaneously controlled the rate of desorption after 30 hours, or (3) inaccurate experimental data were obtained. It is strongly suspected that the latter explanation is most likely, thus implying that internal diffusion is the sole rate-controlling step for Type 1 spent shale.

Table 30. Estimates of  $K_G$  (internal diffusion rate constant) for Type 1 spent shale.

$K_G$ , l/hr, estimated at various times	Column length, cm			
	7.5	15	22.5	Average
5 hr	0.0598	0.0617	0.0446	0.0554
7.5 hr	0.0516	0.0580	0.0448	0.0515
10 hr	0.0514	0.0560	0.0449	0.0508
15 hr	0.0462	0.0522	0.0494	0.0493
20 hr	0.0420	0.0535	0.0485	0.0480
25 hr	0.0374	0.0635	0.0524	0.0511
30 hr	0.0346	0.0783	0.0689	0.0606
40 hr	0.0365	0.1661	0.1689	0.1238
$K_G$ average	0.0449	0.0737	0.0653	0.0613

Table 31. Estimates of  $K_E$  (external mass transfer rate constant) for Type 1 spent shale.

$K_E$ , l/g-hr, estimated at various times	Column length, cm			
	7.5	15	22.5	Average
5 hr	0.0000165	0.0000083	0.0000036	0.0000095
7.5 hr	0.0000384	0.0000153	0.0000058	0.0000198
10 hr	0.0000948	0.0000272	0.0000088	0.0000436
15 hr	0.0003613	0.0000897	0.0000222	0.0001577
20 hr	0.0005970	0.0002480	0.0000654	0.0003035
25 hr	0.0007989	0.0004740	0.0001480	0.0004736
30 hr	0.0010060	0.0008237	0.0003040	0.0007112
40 hr	0.0016630	0.0029140	0.0012800	0.0019520
$K_E$ Average	0.0005719	0.0005750	0.0002297	0.0004588

Table 32. Estimates of  $K_{BA}$  (surface reaction rate constant) for Type 1 spent shale.

$K_{BA}$ , 1/mg-hr, estimated at various times	Column length, cm			
	7.5	15	22.5	Average
5 hr	-0.133	-0.080	-0.0615	-0.0915
7.5 hr	-0.110	-0.061	-0.0479	-0.0730
10 hr	-0.088	-0.0476	-0.0374	-0.0577
15 hr	-0.062	-0.0355	-0.0297	-0.0424
20 hr	-0.049	-0.036	-0.0246	-0.0424
25 hr	-0.042	-0.038	-0.035	-0.0696
30 hr	-0.038	-0.0243	-0.0184	-0.0263
40 hr	-0.035	-0.0202	-0.0136	-0.0229
$K_{BA}$ average	-0.0696	-0.0408	-0.0312	-0.0472

Table 33. Estimates of  $K_G$  (internal diffusion rate constant) for Type 2 spent shale.

$K_G$ , l/hr, estimated at various times	Column length, cm			
	7.5	15	22.5	Average
5 hr	0.0613	0.0304	0.0151	0.0356
7.5 hr	0.0551	0.0240	0.0072	0.0288
10 hr	0.0512	0.0193	0.0064	0.0256
15 hr	0.0402	0.0182	0.0087	0.0224
20 hr	0.0317	0.0163	0.0080	0.0187
25 hr	0.0212	0.0140	0.0090	0.0147
30 hr	0.0143	0.0119	0.0101	0.0121
40 hr	0.0113	0.0128	0.0101	0.0114
$K_G$ average	0.0358	0.0184	0.0093	0.0212



Table 34. Estimates of  $K_E$  (external mass transfer rate constant) for Type 2 spent shale.

$K_E$ , 1/g-hr, estimated at various times	Column length, cm			
	7.5	15	22.5	Average
5 hr	0.0000088	0.0000018	0.0000006	0.0000037
7.5 hr	0.0000172	0.0000021	0.0000004	0.0000066
10 hr	0.0000317	0.0000022	0.0000004	0.0000114
15 hr	0.0001074	0.0000037	0.0000007	0.0000373
20 hr	0.0002265	0.0000057	0.0000009	0.0000777
25 hr	0.0002855	0.0000092	0.0000016	0.0000988
30 hr	0.0003005	0.0000152	0.0000028	0.0001062
40 hr	0.0003807	0.0000440	0.0000068	0.0001438
$K_E$ average	0.00001698	0.0000105	0.0000018	0.0000607

Table 35. Estimates of  $K_{BA}$  (surface reaction rate constant) for Type 2 spent shale.

$K_{BA}$ , l/mg-hr, estimated at various times	Column length, cm			
	7.5	15	22.5	Average
5 hr	-0.0755	-0.0500	-0.0426	-0.0560
7.5 hr	-0.0583	-0.0352	-0.0207	-0.0381
10 hr	-0.0468	-0.0265	-0.0182	-0.0305
15 hr	-0.0364	-0.0248	-0.0239	-0.0284
20 hr	-0.0279	-0.0220	-0.0208	-0.0236
25 hr	-0.0270	-0.0222	-0.0327	-0.0273
30 hr	-0.0252	-0.0267	-0.0346	-0.0288
40 hr	-0.0228	-0.0194	-0.0296	-0.0239
$K_{BA}$ average	-0.0400	-0.0284	-0.0279	-0.0321

The values of  $K_E$  presented in Table 31 indicate that, at no time, did external mass transfer control the rate of desorption from Type 1 spent shale. Furthermore, Table 32 reveals that values of  $K_{BA}$  varied significantly except for later time periods. During later time periods, the trend in data indicates that values of  $K_{BA}$  were approaching a constant near the end of the time period investigated. This suggests that (1) surface reaction may have become the rate-controlling mechanism after 30 hours or (2) both internal diffusion and surface reaction simultaneously may have controlled the rate of desorption at later time periods. However, the trends in data are not strong enough to substantiate either of the above claims.

Overall, it is hypothesized that internal mass transfer is the rate-controlling mechanism for Type 1 spent shale. This is likely due to the high internal porosity of the Type 1 spent shale. As previously reported in Table 11, its total porosity was 57 percent and its internal porosity was probably a significant portion of the total porosity. As a consequence of its high internal porosity, desorbed material must diffuse through a "maze" of internal pores and interstices prior to appearing in the bulk leachate.

An examination of Tables 33 through 35 reveals that, for Type 2 spent shale, none of the proposed rate models appropriately describes the rate of desorption over the entire range of time considered.

The data presented in Table 33 indicate that internal mass transfer may have become rate-limiting during subsequent time periods. This assertion is strongly supported by data derived from column lengths of 15 and 22.5 centimeters. If one were to ignore data derived from a column length of 7.5 centimeters, it would appear that internal mass transfer was rate-controlling after approximately 10 hours of leaching. During the period of 10 to 40 hours, values of  $K_G$  ranged from 0.0064 to 0.0193  $\text{hour}^{-1}$  for column lengths of 15 and 22.5 centimeters. For all three column lengths, values of  $K_G$  became relatively constant at leaching times of greater than 25 hours.

At first glance, the values of  $K_E$  presented in Table 34 suggest that external mass transfer was not a rate-controlling mechanism at any time. However, close scrutiny of the data suggests that external mass transfer may have been initially rate controlling, particularly during the first 5 hours. For all three column lengths, values of  $K_E$  were initially low while subsequent values generally increased as a function of time. Furthermore, for column lengths of 15 and 22.5 centimeters, values of  $K_E$  remained fairly constant during the first 10 hours prior to increasing. The above trends in data suggest that external mass transfer may have possibly played a rate-limiting role during the first 5 hours of leaching. (This assertion is based on an extrapolation of observed data trends during initial time periods).

An examination of Table 35 indicates that values of  $K_{BA}$ , the rate constant for the surface reaction model, were relatively constant during the later time periods of leaching. After 10 hours of leaching, values of  $K_{BA}$  ranged from -0.0194 to -0.0364 l/mg-hr. These data suggest that surface reaction may have served as a rate-limiting step during subsequent time periods.

Overall, for time periods greater than 10 hours, it is hypothesized that desorption from Type 2 spent shale was controlled by (1) internal diffusion, (2) surface reaction, or (3) a combination of internal diffusion and surface reaction acting simultaneously. If internal diffusion played a rate-limiting role, this would likely be due to its significant degree of internal porosity. (The total porosity of the Type 2 spent shale, as previously reported in Table 11, was 51 percent.) Although the internal porosity of the Type 2 spent shale is thought to be significantly less than that of the Type 1 spent shale, the Type 2 spent shale is nevertheless porous enough to account for internal diffusion being rate controlling. Conversely, if surface reaction played a rate-limiting role, this would likely be due to the character of the physical/chemical forces holding organic molecules onto the surfaces (both within the infrastructure and along the exterior) of the spent shale matrix.

For the first 5 hours, the data suggest the possibility of external mass transfer playing some type of rate-limiting role. If external mass transfer was indeed the rate-controlling step during the first 5 hours, this is likely due to the high concentration of TOC in the bulk leachate during the initial few hours of leaching, serving as an external resistance to mass transfer. The rationale behind this explanation is that some of the organic material associated with the Type 2 spent shale, perhaps associated with the exterior surface, appears to be readily leachable during the initial few hours of leaching. Upon entering the bulk leachate, this readily leachable material results in high initial TOC concentrations, serving as an external resistance to mass transfer until this high TOC leachate exits from the column.

In summary, it was originally assumed that this analysis of rate models would precisely identify a single rate-controlling mechanism for both types of spent shale over the entire range of time considered. However, these expectations did not completely evolve for the following possible reasons: (1) different mechanisms were rate-controlling over different ranges of time, (2) two or more mechanisms were simultaneously rate-controlling at particular times, or (3) the quantity and quality of data were inadequate to conduct a rigorous kinetic analysis.

One of the original objectives of this data analysis section was to develop the framework for a packed column mass transfer model. Recall that a mathematical evaluation of the rate of desorption and the equilibrium isotherm would theoretically enable the differential mass balance equation to be integrated. It is suggested that future research (1) conduct additional packed column studies to provide more

basic data, (2) conduct a more rigorous analysis of the rate of desorption, (3) conduct more rigorous equilibrium studies to precisely define equilibrium isotherms, and (4) attempt a computer-assisted integration of the differential mass balance equation.

Suggestions for future research relative to further kinetic analysis and the development of a packed column mass transfer model are discussed in more detail in a subsequent section entitled "Recommendations for Future Research."

CHAPTER 9

ASSESSMENT OF THE ENVIRONMENTAL TRANSPORT  
AND FATE OF LEACHED ORGANIC CONTAMINANTS

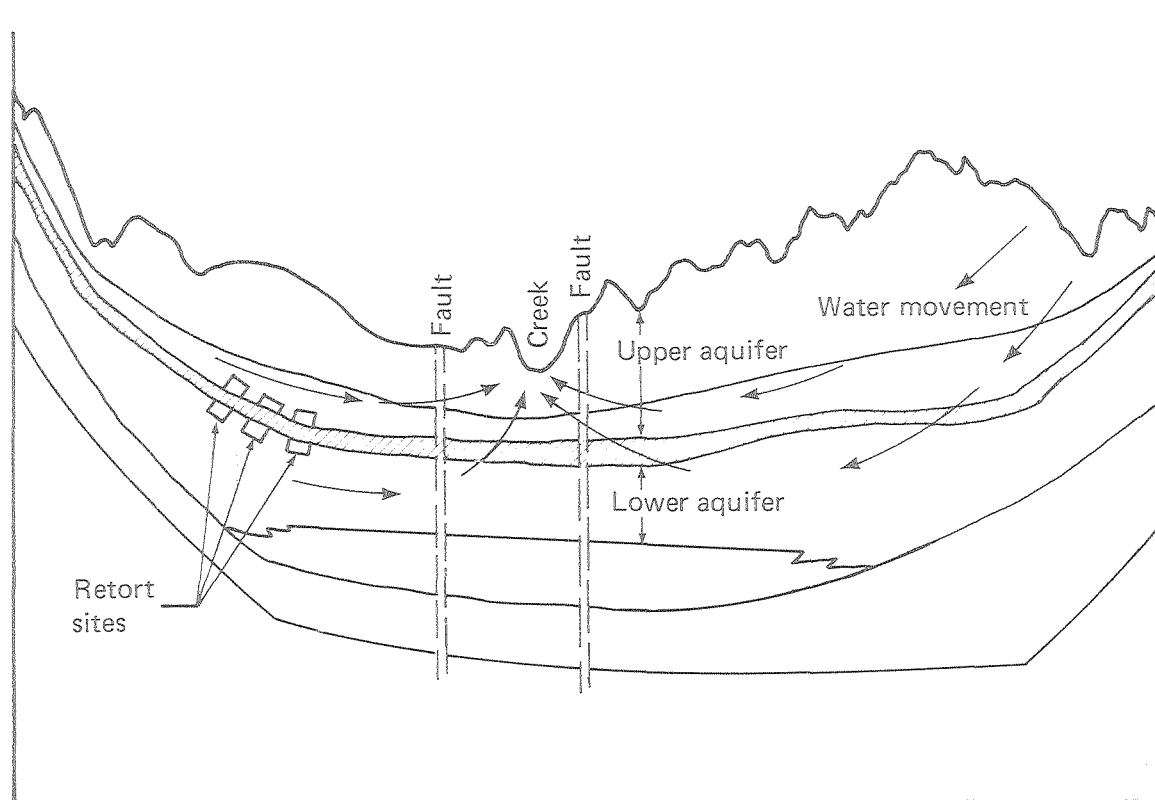
Based on the results presented in an earlier section, it is apparent that there exists a significant potential for contamination of groundwater by organic residuals leached from in-situ spent shale. The purpose of this chapter is to assess the environmental transport and fate of leached organic contaminants. This assessment will be somewhat qualitative since, in many areas, there is insufficient information to provide estimates for a quantitative assessment.

As previously disclosed in the introduction, rich deposits of oil shale often exist as impermeable strata situated between two groundwater aquifers. This is exemplified by the Piceance Creek Basin in which a continuous layer of oil shale (Mahogany Zone), ranging from 100 to 200 feet in thickness, traverses most of the basin. A schematic describing the stratigraphy of the Piceance Creek Basin is presented in Figure 59. This schematic shows the shale layer and adjacent aquifers in relation to several in-situ retorts.

Prior to and during retorting, adjacent aquifers will be continuously dewatered in order to prevent groundwater from interfering with the retorting process. Upon completion of retorting, dewatering operations will cease and groundwater will slowly migrate into abandoned retorts until steady-state flow conditions are eventually established. A likely pattern of groundwater flow through a retort was depicted in Figure 7. The flow pattern described in Figure 7 is highly idealized and assumes that (1) the shale layer is situated between two aquifers as in the Piceance Creek Basin, (2) the retort completely penetrates the shale layer and thus establishes communication between adjacent aquifers, and (3) the pressure difference between the upper and lower aquifers is sufficient to produce upward flow through the retort (as will occur in many parts of the Piceance Creek Basin).

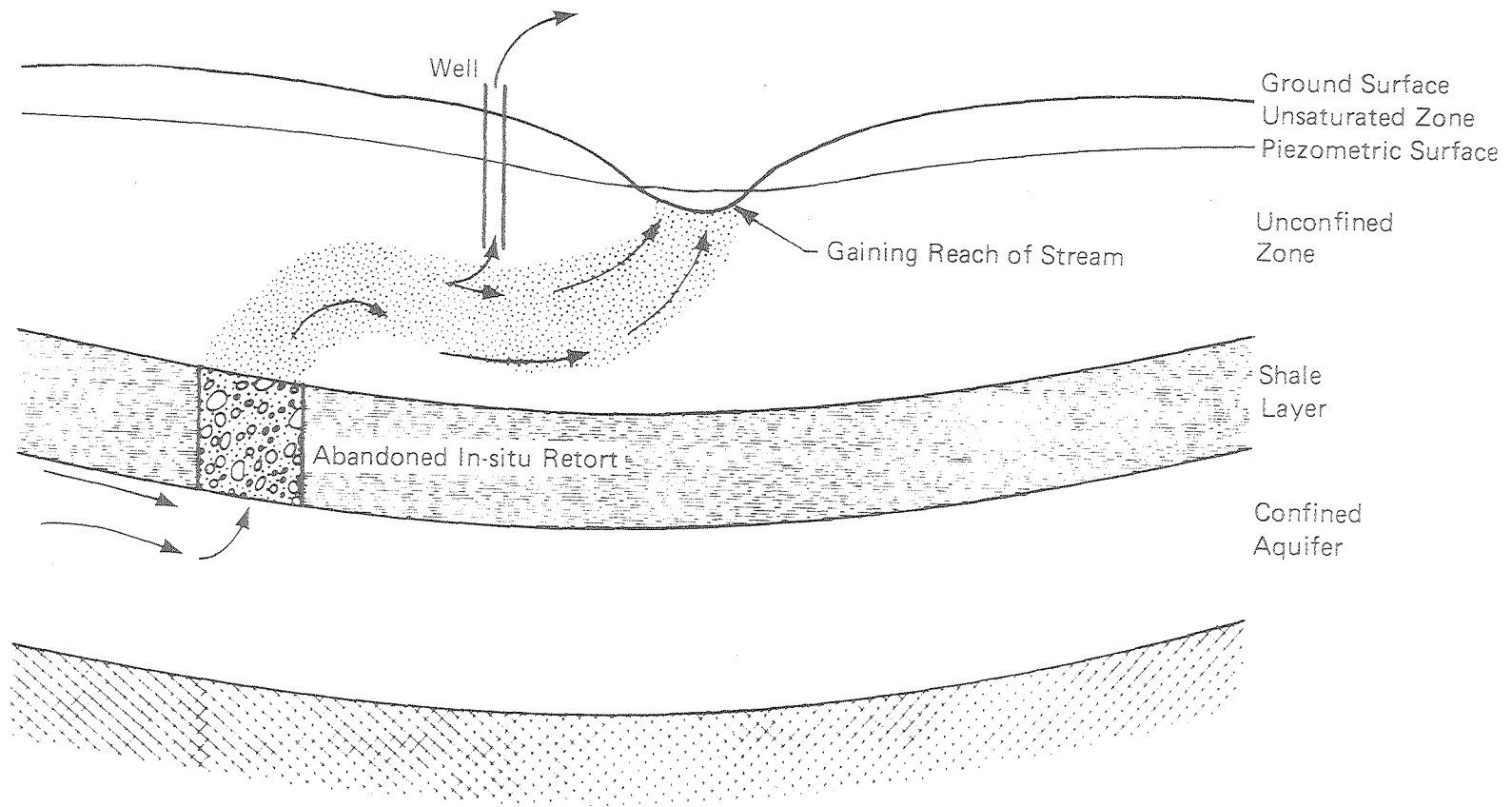
If groundwater flows according to the pattern depicted in Figure 7, a likely pathway for the environmental transport of leached contaminants is described in Figure 60. As portrayed in Figure 60, groundwater from the lower aquifer will migrate into an abandoned retort after dewatering operations have ceased and eventually, steady-state flow conditions will be established. Various organic contaminants will be leached from spent shale as groundwater flows upward through the retort. Subsequently, contaminated groundwater will enter the upper aquifer and, in response to the existing gradient, flow toward a point of discharge such as a well or the gaining reach of a stream.

As contaminated groundwater enters the upper aquifer, a certain degree of dilution will occur as it mixes with uncontaminated groundwater from the upper aquifer. As it flows through the upper aquifer, contaminated groundwater will be upgraded in quality as a consequence



XBL 792-545

Figure 59. Geohydrologic cross section of the Piceance Creek Basin showing relationship of in-situ retorts to adjacent aquifers.



XBL 792-576

Figure 60. Schematic describing environmental transport of leached contaminants.



of natural treatment phenomena such as adsorption, ion exchange, filtration, and microbial degradation. Furthermore, contaminant levels will decrease due to hydrologic dispersion within the upper aquifer. Eventually, contaminated groundwater may be pumped to the surface via a well or may discharge into the gaining reach of a stream, thereby contaminating streamflow.

In the following pages, an attempt will be made to assess both the leaching phenomenon and the environmental transport of leached contaminants without regard to the specific location of an actual development site. However, it should be recognized that the magnitude of potential water quality problems will be highly site-specific and will be influenced by local conditions such as (1) stratigraphy, (2) ambient groundwater quality, (3) ambient geohydrology, and (4) proximity of in-situ retorts to wells, streams, and springs. In order to provide some indication of the importance of site-specific conditions, certain parts of the following assessment will consider existing conditions in the general vicinity of the Piceance Creek Basin.

The following assessment will consider only a single retort and its potential impact on groundwater quality. Unfortunately, an assessment simultaneously considering a large number of retorts is considered to be beyond the scope of this study. This is primarily due to (1) the extremely complex geohydraulics involved, (2) the lack of information regarding the areal extent and spacing between a large number of retorts at a commercial-scale facility, and (3) the fact that the leaching phenomenon in one retort is not independent of the leaching phenomenon in nearby retorts.

It is assumed that a typical in-situ retort (1) will have approximate dimensions of 50 meters in length, 50 meters in width, and 60 meters in height and (2) will approximately penetrate the entire thickness of the shale layer, thus establishing communication between adjacent aquifers. Subsequent to retorting, it is assumed that this retort will contain roughly  $1.5 \times 10^8$  kg of spent shale (assuming the bulk density of spent shale is approximately 1.0 grams/cubic centimeter).

#### Geohydrology of Lower Aquifer

The geohydrology of an aquifer is primarily a function of its permeability, hydraulic gradient, and porosity. In particular, permeability is an important parameter which describes the "hydraulic conductivity" of an aquifer. The permeability of a good aquifer can range up to 500 gpd/ft<sup>2</sup> (representative of a sand and gravel aquifer) or more while the permeability of a poor aquifer can range down to 10 gpd/ft<sup>2</sup> (representative of a clay aquifer) or less (Ref. 3).

In areas of potential in-situ development, the permeability of the lower aquifer is important because the flow of groundwater through a retort may be limited by the permeability of the lower aquifer if it is extremely low in relation to the permeability of the retort.

For example, in the Piceance Creek Basin the permeability of the lower aquifer averages roughly 10 gpd/ft<sup>2</sup> (Ref. 3), indicative of a poor aquifer. This implies that groundwater flow through a retort situated in the Piceance Creek Basin may be controlled by this low permeability.

The flow of groundwater from the lower aquifer through a retort will also be greatly influenced by the head differential between the lower and upper aquifers. In many areas of potential development, the head of the lower aquifer is significantly greater than the head of the upper aquifer. For example, in the Piceance Creek Basin, the head differential averages about 10 feet and is sufficient, in most cases, to produce flow through a retort in an upward direction.

#### Hydraulics of a Typical In-Situ Retort

The flow of groundwater through a retort will be a function of (1) the permeability of the retort in relation to the permeabilities of adjacent aquifers and (2) the head differential between these aquifers. In many cases, flow will be in an upward direction.

The permeability of spent shale samples examined during the course of this research ranged from about 500 to 700 gpd/ft<sup>2</sup>. Temporarily ignoring the permeabilities of adjacent aquifers, the potential flow of groundwater through a retort filled with similar spent shale would be about 680,000 gallons per day (an estimate based on Darcy's Law, assuming the permeability of spent shale in the retort is 500 gpd/ft<sup>2</sup> and the head difference between the top and bottom of the retort is 10 feet). Although this represents a substantial flow, it is asserted that the permeabilities of the upper and/or lower aquifers will likely be substantially less than the permeability of the retort. A low permeability associated with either aquifer will likely control/limit flow through a retort. A low permeability associated with the lower aquifer will limit the flow of groundwater that can be discharged from the retort.

In the Piceance Creek Basin, the permeability of both the lower and upper aquifers averages about 10 gpd/ft<sup>2</sup>. These permeabilities are approximately 50 to 70 times less than the permeability of spent shale samples examined during the research summarized herein. Thus, the previous estimate of the potential flow through a retort, 680,000 gallons per day, would prove to be unrealistic for a retort situated in the Piceance Creek Basin. Instead, a much lower flow rate would be anticipated. Unfortunately, a more realistic estimate would be difficult without the use of a computer program which models groundwater movement. Presently, research is underway at the Lawrence Berkeley Laboratory in an attempt to model groundwater movement through a retort by a finite difference approach employing a computer (Ref. 37).

### Leaching Within a Typical Retort

Originally, it was intended that a model based on the results of the continuous-flow column experiments would be developed in order to provide an estimate of the quality of contaminated groundwater as a function of time as it exits from a retort. However, a decision was made not to develop such a model for the following reasons: (1) development of such a model would require a complex computer-oriented analysis, (2) the use of data derived from extremely small columns (12 or 6 inches in length by 1 inch in diameter) to simulate a very large retort (50 meters by 50 meters by 60 meters) represents an extreme extrapolation of data, (3) very little is known about the hydraulics of a retort in relation to adjacent aquifers (information required if a retort is to be modeled as a large column), and (4) the continuous-flow column experiments examined only distilled water at 20°C when, in fact, high-temperature groundwater will likely participate in the leaching phenomenon. As an alternative to this original approach, the following approach was developed as a means of roughly assessing the leaching phenomenon in a typical retort.

The leaching of organic material from an in-situ retort will likely represent a potentially chronic, long-term problem. As groundwater migrates into a retort, it will solubilize organic material until saturation conditions are attained. During the initial migration of groundwater, saturation conditions will be reached near the influent end of a retort whereas, during the subsequent inflow of groundwater, saturation conditions may not be attained until leachate nears the effluent end of a retort. Eventually, after a considerable time period of leaching, saturation conditions will not be established at any point within the retort. This phenomenon is schematically portrayed in Figure 61. Essentially, Figure 61 describes TOC concentration profiles within a retort as a function of time.

According to the above phenomenon, effluent exiting from the retort will likely be saturated with solubilized organics for a considerable time period. Thus, the concentration of dissolved organic material appearing in the effluent from a retort will remain relatively constant for a long period of time until eventually, levels begin to fall below saturation and slowly decrease. After a period of decrease, the concentration of dissolved organic material will become relatively constant at a fairly low level as a consequence of leaching being limited by internal diffusion through the porous infrastructure of the spent shale matrix. These low levels may persist for decades, representing a potentially chronic, long-term problem. The above phenomenon is schematically portrayed in Figure 62.

The above discussion provided a qualitative description of the leaching process as a function of both leaching time and position within the retort. The actual shapes of the curves presented in Figures 61 and 62 will be influenced by (1) dimensions of the retort, (2) characteristics of spent shale, (3) ambient groundwater quality, and (4) geohydrologic conditions.

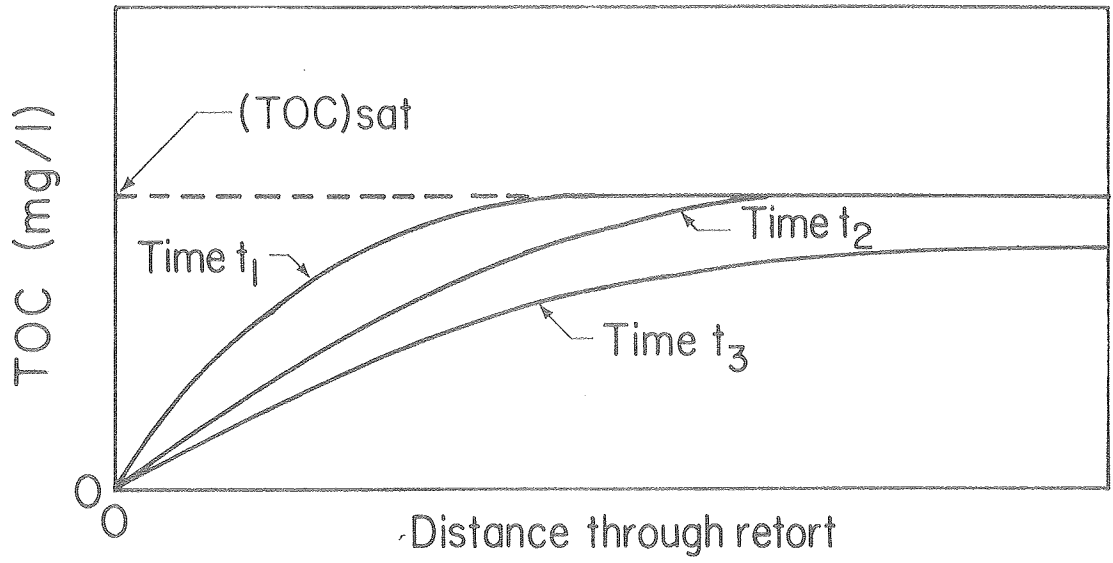
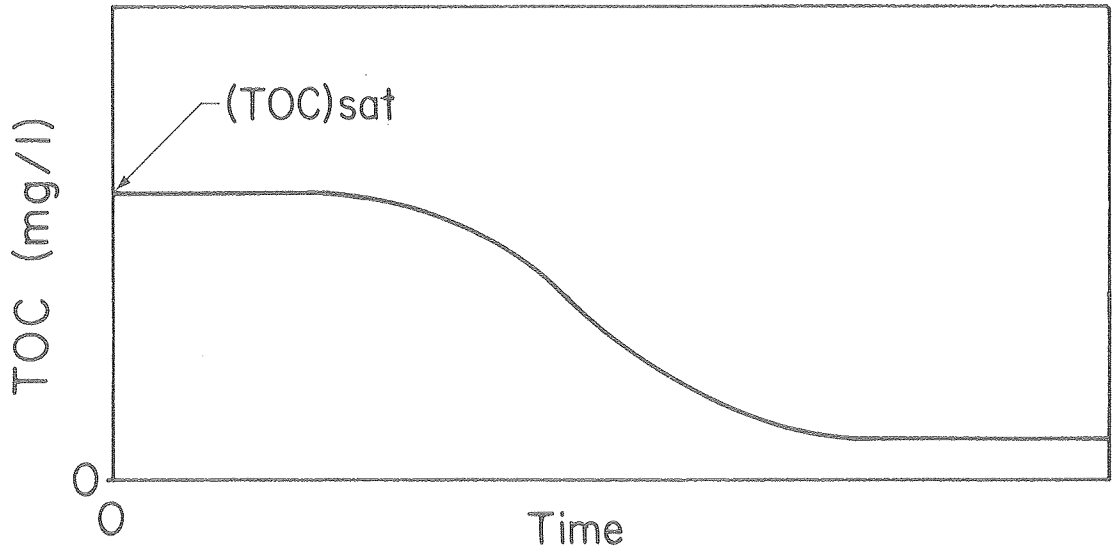


Figure 61. TOC concentration profiles within a retort as a function of time.



XBL 792-541

Figure 62. TOC concentration as a function of time in the effluent from a retort.

At this point, it would seem advantageous to estimate the mass of organic carbon that can potentially be leached from various types of spent shale. Estimates of the minimum mass of organic carbon that can potentially be leached from combustion-retorted (i.e., Type 1) and inert gas-retorted (i.e., Type 2) spent shales are presented in Table 36. These estimates were derived from data generated during both the (1) equilibrium batch experiments and (2) continuous-flow column experiments. Where there is a range of values appearing in Table 36, the lower value was derived from the results of equilibrium batch experiments while the higher value was derived from the results of continuous-flow column experiments. Where a single value appears in Table 36, this value was derived from the results of equilibrium batch experiments.

Table 36. Masses of potentially leachable organic carbon.

Type of leach water	Water temp, °C	Potentially leachable organic carbon, mg TOC/100g spent shale	
		Type 1 shale <sup>a</sup>	Type 2 Shale <sup>a</sup>
Distilled water	20	1.6 - 4.4	2.2 - 5.0
Distilled water	80	2.0	6.0
Groundwater	20	1.4	2.7
Groundwater	80	1.8	6.8

<sup>a</sup>Type 1 is a combustion-retorted spent shale; Type 2 is an inert-gas retorted spent shale.

Those data in Table 36 that were derived from equilibrium batch experiments correspond to a shale-to-water ratio of 50 grams/200 milliliters, the lowest shale-to-water ratio examined. The rationale for using these particular data is that solubility limitations will be the least significant for the lowest shale-to-water ratio. Thus, by employing a large volume of water (i.e., 200 milliliters), it was originally assumed that a significant portion of the water-soluble materials would be leached and that solubility limitations would not play a major role. Ideally, a volume of water greater than 200 milliliters should have been used to derive an estimate of the mass of organic material that can potentially be leached. However, the laboratory glassware used during the equilibrium batch experiments (i.e., 300 milliliter flasks) prevented a lower shale-to-water ratio

from being examined. However, it is asserted that experiments which examined the lowest shale-to-water ratio (i.e., 50 grams/200 milliliters) provide a rough estimate of the minimum mass of potentially leachable organic carbon.

Table 36 also contains a limited amount of data obtained from the continuous-flow column experiments. Unfortunately, column experiments only examined distilled water at 20°C. Although estimates derived from the column experiments are higher than estimates derived from corresponding equilibrium batch experiments, it is important to recognize that these estimates are, at best, indicative of the minimum potentially leachable mass. This is due to the fact that column experiments were run for a duration of only 96 hours and at the end of this period, a significant amount of organic material was still being leached.

Estimates of saturation concentrations of organic carbon in various types of leachates are presented in Table 37. The estimates shown in Table 37 are given in terms of a range, encompassing a lower and higher value.

Table 37. Estimated saturation concentrations of organic carbon.

Type of leach water	Water temp, °C	Concentration of organic carbon, mg/l TOC	
		Type 1 shale <sup>a</sup>	Type 2 shale <sup>a</sup>
Distilled water	20	18 - 440	25 - 790
Distilled water	80	16 - 90	36 - 63
Groundwater	20	19 - 1270	25 - 530
Groundwater	80	16 - 52	67 - 140

<sup>a</sup>Type 1 is a combustion-retorted spent shale; Type 2 is an inert-gas-retorted spent shale.

The lower values presented in Table 37 were derived from equilibrium batch experiments examining a shale-to-water ratio of 50 grams/30 milliliters, the highest shale-to-water ratio examined.

It is hypothesized that a significant portion of the water-soluble organic material will be leached during the initial few pore volumes of groundwater passing through a retort. Assuming a porosity of 50 percent, the pore volume of a typical retort is estimated to be about  $7.5 \times 10^7$  liters. Therefore, the approximate volume of groundwater required to leach the minimum mass of potentially leachable organic carbon from a typical in-situ retort (as estimated in Table 38) can be estimated by employing the estimates of TOC saturation concentrations presented in Table 37.

Table 38. Estimated minimum mass of organic carbon that can potentially be leached from a typical in-situ retort.

Type of leach water	Water temp, °C	Organic carbon, kg TOC	
		Type 1 shale <sup>a</sup>	Type 2 shale <sup>a</sup>
Distilled water	20	2,400 - 6,600	3,300 - 7,500
Distilled water	80	3,000	9,000
Groundwater	20	2,100	4,100
Groundwater	80	2,700	10,000

<sup>a</sup>Type 1 is a combustion-retorted spent shale; Type 2 is an inert-gas-retorted spent shale.

Table 39 presents estimates of the pore volumes required to solubilize the masses of organic carbon described in Table 38. These estimates were based on the lower values of estimated TOC saturation concentrations presented in Table 37. The estimated pore volumes shown in Table 39 provide a rough as well as a conservative indication of the volume of groundwater that may be degraded in quality by leached organic contaminants.

#### Geohydrology of Upper Aquifer

After contaminated groundwater from a retort reaches the upper aquifer, it will mix with groundwater from the upper aquifer which will serve to decrease contaminant levels as a consequence of dilution. Subsequently, this mixture, in response to the hydraulic gradient, will flow through the upper aquifer toward a point of discharge.

Table 39. Pore volumes of water required to leach estimated minimum mass of potentially leachable organic carbon from a typical retort.

Type of leach water	Water temp, °C	Pore volumes of water <sup>a</sup>	
		Type 1 shale <sup>b</sup>	Type 2 shale <sup>b</sup>
Distilled water	20	1.7 - 4.7	1.7 - 3.9
Distilled water	80	2.5	3.3
Groundwater	20	1.5	2.1
Groundwater	80	2.3	2.0

<sup>a</sup>One pore volume is equal to  $7.5 \times 10^7$  liters.

<sup>b</sup>Type 1 is a combustion-retorted spent shale; Type 2 is an inert-gas-retorted spent shale.

As indicated previously, the permeability of the upper aquifer may, in some cases, be substantially less than that of a retort. This will tend to inhibit the flow of groundwater through a retort. For example, in the Piceance Creek Basin, the permeability of the upper aquifer averages about 10 gpd/ft<sup>2</sup>, substantially less than the anticipated permeability of a retort.

The permeability of the upper aquifer is important because it will control (1) the period of time during which groundwater flows through aquifer media and is subjected to natural treatment processes and (2) the time required for contaminated groundwater to appear in a well or in a stream.

In order to illustrate the above concept, consider an in-situ retort developed 1000 feet up-gradient from a well. Assume that the upper aquifer has a permeability of 500 gpd/ft<sup>2</sup>, representative of a good sand and gravel aquifer (Ref. 38), a hydraulic gradient of 100 ft/mile (a steep gradient), and a porosity of 40 percent. Employing these assumptions and Darcy's Law, the velocity of groundwater flow is computed to be three feet/day. Thus, for this illustrative example, it would take almost one year for contaminated groundwater to reach the designated well. However, it should be noted that the above illustrative example is an extreme case. In most areas of potential development, wells and streams will likely be located more than 1000 feet from a retort and the upper aquifer will likely have a lower



permeability and hydraulic gradient. Thus, in some cases, contaminated groundwater may flow through the upper aquifer for literally decades or centuries before it discharges into a stream or is pumped from a well. As a more realistic illustrative example, consider a retort developed one mile up-gradient from the gaining reach of a stream. Assume that the upper aquifer has a permeability of 10 gpd/ft<sup>2</sup> (approximately representative of the upper aquifer in the Piceance Creek Basin), a hydraulic gradient of 50 ft/mile, and a porosity of 20 percent. Using these assumptions, the velocity of groundwater flow is estimated to be about 0.1 ft/day. Thus, approximately 150 years would be required for contaminated groundwater to reach the designated stream.

Based on the above, it is apparent that, in certain areas of potential development such as the Piceance Creek Basin, there will be highly localized degradation of groundwater quality. However, the magnitude of this quality degradation will decrease as one proceeds away from the development site. This is primarily due to the extremely slow flow velocity that is characteristic of groundwater in aquifers such as the upper aquifer in the Piceance Creek Basin.

#### Discharge of Upper Aquifer into a Stream

As indicated previously, contaminated groundwater may eventually discharge into the gaining reach of a stream, thereby indirectly contaminating streamflow. Many streams situated throughout the tri-state oil shale region receive a substantial influx of groundwater in comparison to direct surface runoff. For these particular streams, there exists a potential for contamination of streamflow by inflowing contaminated groundwater.

In the Piceance Creek Basin, the average annual flow of the Piceance Creek is 14,500 acre-feet per year, as measured by a gauging station at the mouth of the basin. About 80 percent of this flow is derived from groundwater inflow while the remainder is supplied by direct surface runoff. Thus, approximately 11,600 acre-feet of groundwater discharges into the Piceance Creek each year (Ref. 3).

## CHAPTER 10

### CONTROL MEASURES

Due to its proximity to groundwater, in-situ spent shale represents a significant source of groundwater quality degradation. This degradation of quality will occur as groundwater migrates through abandoned in-situ retorts, leaching various organic and inorganic contaminants from spent shale (Refs. 9,39,40).

The purpose of this section is to identify and describe measures that can be employed to control this source of groundwater contamination. Some of the control measures that will be subsequently suggested are considered to be reasonable engineering/planning solutions with a favorable cost/benefit ratio while others are considered to be less realistic solutions that are characterized by unfavorable economics. The discussion of the latter group of control measures is only of academic interest. Finally, a summary of the technological and economic feasibility of all suggested control measures will be presented.

There are three general categories of control measures that can be employed to control the contamination of groundwater by organic residuals leached from in-situ spent shale. These include:

- Source Control
- Site Location
- Treatment/Disposal

Control measures falling under the category of source control consist of various techniques for controlling the problem at its source and thus are considered to be "preventative" measures.

Control measures falling under the category of site location focus on the selection of a development site with various attributes that will tend to minimize the potential problem.

Control measures falling under the category of treatment/disposal consist of more conventional engineering solutions such as treatment and/or selection of environmentally optimum locations for disposal of contaminated groundwater.

#### Source Control

The following "source control" measures, to varying degrees, can be used to control the degradation of groundwater quality by leached organic contaminants.

Employ Environmentally Optimum Retorting Conditions. The retorting conditions employed to extract oil from shale greatly influence the characteristics of the resultant spent shale and its susceptibility to leaching. Greater amounts of dissolved organic materials will normally occur in leachate derived from spent shale produced during inert gas retorting or combustion retorting employing recycle gas. In contrast, lesser amounts of dissolved organic material will normally occur in leachate derived from spent shale produced during ordinary combustion retorting. Thus, if organic contaminants in groundwater are of most concern, ordinary combustion retorting can be employed to produce spent shale that will result in leachate with the lowest levels of organic contaminants. (However, it should be recognized that higher levels of dissolved inorganic materials will normally occur in leachate derived from spent shale produced during high-temperature combustion retorting in which the temperature required for carbonate decomposition is exceeded. If inorganic contaminants in groundwater are of most concern, inert gas retorting can be employed to produce spent shale that will result in leachate with the lowest levels of inorganic contaminants.)

Retort Only the Center Section of the Shale Layer. Rich deposits of oil shale often occur as continuous layers of up to 300 feet in thickness. An in-situ retort will likely penetrate the entire thickness of the shale layer, thus establishing communication between adjacent aquifers. This aquifer communication creates a significant potential for degradation of groundwater quality. However, this problem can be mitigated by developing in-situ retorts that do not penetrate the entire thickness of the shale layer but rather occupy only the center section of the shale layer, leaving a thin impermeable layer of unretorted oil shale above and below the developed retort. The development of a retort in this manner would tend to isolate in-situ spent shale from adjacent aquifers.

Seal Off Retort After Completion of Retorting. In order to prevent the migration of groundwater into abandoned retorts, each retort can be physically sealed off to isolate it from adjacent aquifers. This seal may consist of a concrete-like substance that is pumped into forms located near the upper and lower sections of a retort where it is allowed to solidify.

Continually Dewater Adjacent Aquifers on a Permanent Basis. During preparation of a retort and prior to commencement of retorting, adjacent aquifers must be dewatered to prevent groundwater from interfering with the retorting process. In order to prevent subsequent degradation of groundwater quality, it is possible to continually dewater adjacent aquifers to eliminate contact between groundwater and spent shale. Needless to say, this constitutes an expensive potential control measure.

Continually Dewater Adjacent Aquifers on a Temporary Basis. The impetus behind this control measure is to allow individual retorts to cool to ambient temperature prior to permitting groundwater to migrate into a retort. This is based on the premise that high temperatures can enhance the leaching of many organic contaminants. The time required for a retort to cool to ambient temperature may be several years.

Stabilize Spent Shale by Solvent Extraction. After completion of retorting, organic solvents (or water) can be continuously recirculated through a retort for a designated time period until most leachable materials have been extracted and become solubilized in the solvent. The particular solvent(s) used will depend on which contaminants are of most concern. For example, nonpolar solvents can be used to extract nonpolar organic contaminants. If solvent extraction is employed as a control measure, the use of organic solvents would be more effective than simply using water as a solvent due to solubility limitations associated with water. After solvent extraction, the resultant spent shale will be relatively stabilized with respect to specific organic contaminants. However, it should be noted that solvent extraction as a control measure creates a waste problem: disposal of the solvent after extraction. After extraction, the solvent must be pumped to the surface for recovery or disposal. Since it is likely that solvent recovery would be low, this particular control measure would probably be economically prohibitive.

#### Site Location

Several control measures, falling under the category of "site location," can be employed to control the degradation of groundwater by organic contaminants. These include:

Select a Site Remote from Important Surface Waters. Contaminated groundwater may potentially enter the gaining reach of a stream/river or discharge directly into a lake. The time required for contaminated groundwater to reach important surface waters will largely be determined by the proximity of in-situ retorts to these surface waters as well as the characteristics of the aquifer. The degradation of surface waters can be delayed for a long period of time if the development site is situated at considerable distance from important surface waters and aquifer characteristics ensure slow pollutant transport. However, it should be recognized that eventual surfacing of contaminated groundwater may have serious effects.

Select a Site with Optimum Aquifer Characteristics. It is possible to select a site where the characteristics of the aquifer will (1) ensure the slow transport of pollutants due to low permeability and (2) provide natural treatment of contaminated groundwater by processes such as adsorption, microbial degradation, etc. Optimum aquifer characteristics will delay the appearance of contaminated groundwater in wells or surface waters and will ensure that the quality of groundwater is significantly upgraded by the time it is pumped to the surface or discharges into a surface water.

Select a Site Remote from Wells and Good Quality Aquifers. In certain areas of potential development such as the Piceance Creek Basin, there are numerous wells which provide groundwater for domestic and irrigation uses. Furthermore, in these areas, the upper aquifer is often of good quality. The selection of development sites remote from wells and good quality aquifers will (1) enable existing users to continue using groundwater for various beneficial uses and (2) preserve existing good quality aquifers for future exploitation.

#### Treatment/Disposal

Various control measures, falling under the category of "treatment/disposal," can be employed to control the degradation of groundwater by organic contaminants. These include:

Pump Out and Treat Contaminated Groundwater. After groundwater flows through a retort, it can be pumped to the surface and subjected to various treatment processes in order to upgrade its quality. For example, organic contaminants can be removed by treatment processes such as adsorption. If adsorption is employed as a treatment process, nonpolar organic contaminants can be removed by adsorbents such as activated carbon while polar organic contaminants can be removed by adsorbents such as silica gel. Needless to say, this particular control measure would be rather expensive.

Pump Out Contaminated Groundwater and Re-inject at Up-gradient Location. Contaminated groundwater can be pumped to the surface and subsequently reinjected back into an aquifer at a location up-gradient to a retort. The impetus behind this control measure is to essentially recirculate contaminated groundwater through a retort for a designated period of time. This procedure represents a possible means of stabilizing spent shale (similar to the previously discussed technique of solvent extraction). As groundwater is continuously recirculated through a retort in this manner, increasingly greater amounts of contaminants are leached from spent shale until saturation conditions are approached. After the spent shale is relatively stabilized, the multi-recycled groundwater can be pumped to the surface for subsequent treatment/disposal.

Pump Out Contaminated Groundwater and Dispose of by Deep Well Injection. If geology and stratigraphy permit, contaminated groundwater can be pumped to the surface and transported to an appropriate location for disposal by deep well injection. An appropriate location would be a deep semi-isolated aquifer or a fractured geological formation situated below usable aquifers. It is apparent that this particular control measure would be rather site-specific and contingent upon suitable geology/stratigraphy in the general development area.

Pump Out Contaminated Groundwater and Dispose of by Land Application. Contaminated groundwater can be pumped to the surface and subsequently disposed of by land application in order to take advantage of natural treatment phenomena associated with the soil mantle. The feasibility of this disposal scheme depends on various factors including (1) depth

of unsaturated zone, (2) proximity of nearby streams and wells, (3) soil characteristics, and (4) vegetative cover. Natural treatment processes, occurring as contaminated groundwater percolates through the soil mantle, will upgrade the quality of groundwater; however, there may be some residual contaminants remaining after it has passed through the unsaturated zone and eventually reaches an aquifer. It should be recognized that, while this measure may prove effective in controlling organic contaminants, it will probably have little overall effect on inorganic contaminants.

Pump Out Contaminated Groundwater and Dispose of by Lined Evaporation Ponds. Much of the area suitable for in-situ development is semi-arid and thus is characterized by high evaporation rates. This suggests that a viable disposal scheme would be disposal into lined evaporation ponds. An impervious lining would prevent percolation of contaminated groundwater into aquifers situated below the pond. The major disadvantages of this particular control measure are the vast land requirements and the disposal of residue remaining after evaporation.

Pump Out Contaminated Groundwater and Use for On-Site Consumptive Uses. At a commercial-scale oil shale facility, there will be various water requirements by production activities such as shale oil upgrading, dust control, compaction and revegetation of surface-retorted spent shale disposal piles, etc. This suggests that contaminated groundwater can be pumped to the surface to meet certain water requirements. Associated with these various requirements, some water will be lost by consumptive uses (i.e., uses that actually consume water). An example of a consumptive use is the evapotranspiration that occurs during irrigation of revegetated disposal piles containing surface-retorted spent shale. These on-site consumptive uses essentially represent an environmentally sound disposal scheme for contaminated groundwater. Furthermore, use of contaminated groundwater to satisfy on-site water requirements will decrease requirements for primary sources of water.

### Summary

A number of control measures have been suggested to eliminate or minimize the potential degradation of groundwater quality by leached organic contaminants. Certain of these control measures are considered to be both economically and technologically feasible. In contrast, other suggested control measures are considered to be economically and/or technologically infeasible at the present time. Control measures which are not presently feasible have been discussed, in part, as a matter of academic interest, and, in part, as a means of stimulating the future development of new control measures.

A general assessment of the relative technological and economic feasibility of all proposed control measures is presented in Table 40. This assessment of relative feasibility is based on the professional opinion of both the author and various researchers in the general field of oil shale development.

Table 40. Relative technological and economical feasibility of control measures.

CONTROL MEASURE	Technologic feasibility <sup>a</sup>	Economic feasibility <sup>a</sup>
Source control		
Employ environmentally optimum retorting conditions	3	1
Retort only center section of shale layer	1	2
Seal off retort after completion of retorting	1	3
Continually dewater on a permanent basis	3	1
Continually dewater on a temporary basis	3	1
Stabilize spent shale by solvent extraction	1	1
Site location		
Select a site remote from surface waters	3	1
Select a site with optimum aquifer characteristics	3	1
Select a site remote from wells and good quality aquifers	3	2
Treatment disposal		
Pump out leachate and treat	1	1
Pump out leachate and reinject upgradient	3	2
Pump out leachate and dispose of by deep-well injection	3	2
Pump out leachate and dispose of by land application	3	2
Pump out leachate and dispose of by evaporation ponds	3	2
Pump out leachate and use for on-site uses	3	2

<sup>a</sup>Feasibility ratings: 3 = high feasibility, 1 = low feasibility.

## CHAPTER 11

### CONCLUSIONS

#### Conclusions Derived from Characterization of Spent Shale Samples

The solid-phase organic carbon content of spent shale samples examined during the leaching experiments ranged from 0.2 to 3.9 percent, by weight. This high organic carbon content is indicative of the water pollution potential of in-situ spent shale.

#### Conclusions Derived from Kinetic Batch Experiments

1. The levels of organic contaminants in leachate are influenced by various factors, including:

- retorting characteristics of spent shale
- temperature of leach water
- initial quality of leach water
- particle size range of spent shale
- leaching time period

2. The highest levels of organic carbon were observed in leachate derived from spent shale produced during inert gas retorting and during combustion retorting employing recycle gas. In contrast, the lowest levels were detected in leachate derived from spent shale produced during ordinary combustion retorting.

3. An elevated water temperature appeared to enhance the leaching of organic material from spent shale produced during inert gas retorting but, in contrast, appeared to have little overall effect on the leaching of combustion-retorted spent shale samples.

4. The initial quality of leach water did not appear to significantly affect the leaching phenomenon except when spent shale produced during inert gas retorting was leached with groundwater at a high temperature. In this particular case, it appeared that some kind of interaction, involving the quality characteristics of groundwater, a high temperature, and pH, dramatically enhanced the leaching of organic material.

5. The particle size range of spent shale samples influenced the leaching phenomenon according to theory. Slightly higher levels of organic carbon were observed in leachate derived from a smaller particle size range than in leachate derived from a larger particle size range over a leaching period of 30 days.



6. For most spent shale samples, the levels of organic carbon in leachate generally increased as a function of leaching time. Over a 30-day period, the greatest rate of leaching generally occurred during the first day. Thereafter, the rate of leaching generally decreased significantly until "pseudo-equilibrium" conditions were approached by the thirtieth day of leaching.

7. The most unusual results derived during the kinetic batch experiments were those related to spent shale produced during combustion retorting employing recycle gas. The organic carbon levels in leachate obtained from this type of spent shale tend to fluctuate in an oscillatory manner as a function of time. Organic carbon levels in other spent shale leachates increased as a function of leaching time. This behavior is most likely related to insolubilization reactions involving leached bivalent cations and leached phenolics and carboxylic acids, leading to the formation of insoluble phenolates and carboxylates.

8. During the batch experiments, significant levels of organic carbon, organic nitrogen, phenols, and acid/base/neutral fractions were observed in most samples of leachate.

9. The highest levels of phenols were observed in leachate obtained from spent shale samples produced during inert gas retorting. The highest concentration of phenols observed during the batch experiments was 430 g/l. Due to the inadequacy of the method of analysis employed, it is believed that estimated levels of phenols are conservative and that actual levels of phenols are significantly greater.

10. Significant levels of organic nitrogen were detected in various samples of leachate, ranging up to 1.4 mg/l. Generally, the highest levels were observed in leachate obtained from inert gas-retorted spent shale.

11. During the fractionation of organic material, the largest observed fraction was the neutral fraction extracted from leachate derived from spent shale produced during inert gas retorting. It is hypothesized that this neutral fraction may consist largely of unextracted hydrocarbons which are neutral in character or possibly weakly acidic phenols.

#### Conclusions Derived from Equilibrium Batch Experiments

The shale-to-water ratio examined in equilibrium batch experiments significantly influenced the resultant organic carbon concentration in leachate. As anticipated, higher concentrations of organic carbon were detected in leachate derived from higher shale-to-water ratios. Equilibrium batch experiments that examined a series of shale-to-water ratios provided an indication of the particular shale-to-water ratio at which solubility limitations began to play a role.

### Conclusions Derived from Continuous-Flow Column Experiments

1. The results of the continuous-flow column experiments, employing distilled water at 20°C, were generally similar to the results of the corresponding batch experiments. The highest levels of organic carbon were observed in leachate obtained from spent shale produced during combustion retorting employing recycle gas. In contrast, the lowest levels were detected in leachate obtained from spent shale during ordinary combustion retorting.

2. During the continuous-flow column experiments, levels of organic carbon were greatest during initial time periods of leaching and thereafter decreased. This implies that the rate of leaching was greatest during initial time periods.

3. It is hypothesized that organic material leached during initial time periods was readily leachable due to its proximity to the exterior surface of the spent shale matrix while material leached during subsequent time periods was not readily leachable due to its proximity to the interior of the spent shale matrix. The leaching of organic material during subsequent time periods is likely controlled by internal diffusion.

4. The mass of organic carbon leached per unit mass of spent shale was greater during the continuous-flow column experiments than during the corresponding batch experiments. This implies that solubility limitations played a key role during the batch experiments.

### Conclusions Derived from Data Analysis

1. A kinetic analysis of results derived from the kinetic batch experiments revealed that the leaching phenomenon in a batch reactor can be roughly approximated as a first-order desorption reaction for both combustion-retorted and inert gas-retorted spent shale. In contrast, the kinetics associated with spent shale produced during combustion retorting employing recycle gas could not be simulated by simple first-order kinetics. This implies that, during the leaching of spent shale produced during combustion retorting employing recycle gas, additional reactions were possibly occurring such as re-adsorption of leached organics or insolubilization/precipitation of leached organics.

2. Both the Freundlich and Langmuir isotherm models appeared to be appropriate for modeling equilibrium relationships associated with inert gas-retorted spent shale over a certain range of experimental data. To a somewhat lesser extent, these same models were fairly appropriate for modeling equilibrium relationships for combustion-retorted spent shale. Within the range of experimental data, these models can be used to predict, with a fair degree of accuracy, the equilibrium concentration of organic carbon resulting from a particular shale-to-water ratio. However, it must be emphasized that extrapolation of these models beyond the range of experimental data will provide a less accurate estimate of equilibrium relationships. Based on the recognition that isotherm

models are merely mathematical expressions to describe experimentally derived data, it is asserted that a single isotherm model will not precisely describe equilibrium relationships for a particular type of spent shale over the entire range of possible data.

3. A kinetic analysis of results derived from the continuous-flow column experiments revealed that, for combustion-retorted spent shale, internal diffusion appeared to be the rate-limiting mass transfer mechanism. This is attributed to the high internal porosity of combustion retorted spent shale. As a consequence of its high internal porosity, desorbed organics must diffuse through internal pores and interstices prior to appearing in the bulk leachate. For inert gas-retorted spent shale, a similar kinetic analysis suggested that external mass transfer may possibly have been rate-controlling during initial time periods of leaching while, during subsequent time periods, either (1) internal diffusion, (2) surface reaction, or (3) a combination of both internal diffusion and surface reaction became rate-limiting. The possible influence of external mass transfer during initial time periods is related to the likelihood that some of the organic material associated with inert gas-retorted spent shale is situated along the exterior of spent shale particles where it is readily available for leaching during the initial few hours. Upon entering the bulk leachate, this readily leachable material results in high initial TOC concentrations, serving as an external resistance to mass transfer until this high TOC leachate exits from the column.

#### Conclusions Regarding Environmental Transport and Fate of Leached Organic Contaminants

The environmental transport and fate of leached organic contaminants will be strongly affected by (1) stratigraphy, (2) geohydrology, (3) ambient groundwater quality and (4) proximity of in-situ retorts to streams, wells, and springs. The actual flow of groundwater through a retort will be extremely slow as a consequence of the relatively low permeability of adjacent aquifers. As a parcel of water flows through a retort, organics will be solubilized until saturation conditions are reached. The initial leachate effluent from an in-situ retort will most likely be saturated with organics. Saturation levels of organics in leachate effluent will likely persist for a significant period of time. Subsequently, when levels fall below saturation, low concentrations of organics will appear in leachate effluent for extremely long periods of time. This is due to the fact that mass transfer will ultimately be controlled by internal diffusion. These lower levels of organics may persist for years and represent a very significant chronic pollution problem. Although some leached organics will be removed by natural treatment processes associated with an aquifer, it is important to note that (1) certain organic contaminants will not be affected by these natural treatment processes and (2) eventually the "treatment capacity" of an aquifer may be exhausted.

### Conclusions Regarding Potential Control Measures

A variety of control measures have been advocated to mitigate potential problems associated with in-situ spent shale leachate. Unfortunately, most of these control measures are characterized by unfavorable economic and/or technological feasibility. It is asserted that one of the most economically and technologically reasonable control measures presently available involves the continual dewatering of aquifers adjacent to an abandoned in-situ retort until the retort has cooled to ambient temperature. The impetus behind this control measure is that high temperatures in an abandoned retort will, in certain cases, greatly enhance the leaching process as a consequence of refluxing and different solubilities.

### General Conclusions

The exploitation of oil shale resources by in-situ processes may adversely affect the quality of both groundwater and surface water resources within the tri-state region of Colorado, Wyoming, and Utah. There is significant potential for the leaching of organic contaminants from in-situ spent shale by groundwater on a massive scale. Leached organic material may include contaminants with potential public health ramifications or ecological effects. Degradation of groundwater quality by leached organic contaminants will be a chronic and irreversible problem that may persist for decades or even centuries. The eventual appearance of contaminated groundwater at the surface will further compound the problem by degrading the quality of surface water resources. It is the inescapable conclusion of the author of this report that commercial-scale in-situ development of oil shale resources should not be permitted until the completion of additional research related to the assessment and control of in-situ spent shale leachate.

## CHAPTER 12

### RECOMMENDATIONS FOR FUTURE RESEARCH

The research summarized herein provides a general indication of the potential for contamination of groundwater by organic residuals leached from in-situ spent shale. However, during the course of this research, it became apparent that certain information required for an accurate assessment of the problem does not presently exist. It is strongly recommended that commercial-scale in-situ development not be permitted until there are adequate data and information for use in the decision-making process. Therefore, in order to generate this required information, it is suggested that future research focus on the following areas:

geohydraulics of retort and adjacent aquifers

precise definition of equilibrium isotherms and estimation of maximum saturation concentrations of organic contaminants

kinetics of leaching phenomenon

environmental transport of organic contaminants

public health/ecological effects of leached organic contaminants

more detailed assessment of particular types of spent shale

#### Geohydraulics of Retort and Adjacent Aquifers

It is recommended that the geohydraulics of one or more retorts in relation to adjacent aquifers be defined by employing one of several existing computer programs which model groundwater movement. A groundwater flow model can be used to estimate flow through a retort, thereby providing insight into the kinetics of leaching and the time required for all water soluble organic compounds to be leached from spent shale. Another application of a groundwater flow model would be to define flow conditions in the upper aquifer and thus, provide additional insight into the environmental transport of leached contaminants.

There is presently a research effort at the Lawrence Berkeley Laboratory involving an attempt to modify and adapt an existing groundwater flow model for application to the problem of in-situ development (Ref. 37). This research effort involves the development of a comprehensive model that will account for groundwater flow conditions from the period of initial dewatering, to subsequent migration of groundwater into a retort, to subsequent flow of contaminated groundwater through an aquifer. The ultimate objective of this research is to incorporate a chemical transport model into the overall groundwater flow model for use in leaching studies.

Precise Definition of Equilibrium Isotherms and Estimation of Maximum Saturation Concentration of Organic Contaminants

An attempt was made during the research described in this study to define equilibrium isotherms and describe equilibrium relationships between spent shale and leachate. Although this attempt provided valid data, it is recognized that a more rigorous attempt at defining equilibrium isotherms could have been made. More specifically, since the research presented here only assessed four shale-to-water ratios for each type of spent shale examined under specified experimental conditions, it is recommended that future research assess a much larger number of shale-to-water ratios. Furthermore, since this research only assessed equilibrium conditions after 30 days in a quiescent environment, it is recommended that future research conduct equilibrium studies in an agitated environment (i.e., shaker studies) for a time period longer than 30 days. Finally, since this research assessed the equilibrium leaching of organics from discrete "particles" of spent shale, it is recommended that future research employ "pulverized" samples of spent shale to ensure that only solubility limitations will limit the amount of organic material solubilized.

Using the general approach described above, a considerable amount of equilibrium data can be obtained. These data can then be modeled by one of the models employed in this study (i.e., the Langmuir or Freundlich models) or another model such as the BET isotherm model (Ref. 27).

Kinetics of Leaching Phenomenon

It is recommended that additional research can be conducted on the kinetics of the leaching phenomenon. This future research should be an extension of research already summarized here and should focus on the kinetics of leaching during continuous-flow column experiments. Future kinetic analysis should consider composite parameters such as total organic carbon (TOC) as well as groups or classes of organic compounds of particular concern such as phenols or carboxylic acids.

Future research should employ large-scale columns, in contrast to the small-scale columns used during this research. These large-scale columns should be a minimum of six inches in diameter (to minimize flow boundary effects) and approximately 10 to 20 feet in length. There should be a series of sampling ports situated along the column at one to two foot intervals. These sampling ports should be constructed in such a manner as to enable the periodic withdrawal of samples with a syringe. The overall column system should include a variable speed pump, enabling leach water to be pumped through the column at different flow rates.

The above system can be used to assess leaching kinetics for a wide range of experimental variables such as:

- column length
- flow rate
- initial quality of leach water
- characteristics of spent shale samples

Using the above system, it is recommended that future research assess the leaching phenomenon over extremely long periods of time. One of the inadequacies of the continuous-flow column experiments conducted during this research was the relatively short leaching time period studied (i.e., 96 hours). Employing this relatively short time period, it was observed that a significant concentration (i.e., up to 2 mg/l) was still being leached after 96 hours. This suggests that leaching may actually persist for an extremely long period of time, thus representing a potentially chronic groundwater pollution problem. In order to study the long-term aspects of the leaching problem, it is recommended that a considerably longer time period than 96 hours be employed during future continuous-flow column experiments.

The proper utilization of the experimental apparatus described above will enable the development of a series of (1) concentration versus time curves and (2) concentration versus column length curves (i.e., concentration profiles). These curves will enable an accurate assessment of leaching kinetics, including identification of rate-controlling mass transfer mechanisms. Finally, the data and information derived during this kinetic analysis can be used to formulate a mass transfer model describing the leaching process in a column packed with spent shale.

#### Analytical Characterization of Organic Contaminants

The analytical parameters employed in this research--total organic carbon (TOC), acid/base/neutral fractions, organic nitrogen, and phenols--provide a general indication of the types of organic contaminants that may be present in leachate. However, it is apparent that the identification of specific organic compounds would enable a more accurate assessment of (1) the public health and ecological implications of leached organic contaminants and (2) the environmental transport and fate of these contaminants.

Presently, one of the most widely advocated instrumental techniques for identifying organic compounds present in water or wastewater is a Gas Chromatograph/Mass Spectrometer (GC/MS) system (Ref. 41). However, it should be recognized that, when GC is employed as part of an identification system, only those compounds that are volatile enough to pass through a MS can be measured and possibly identified. Furthermore, compounds that can be identified by GC are usually further restricted

to those that can be extracted from water by a nonpolar solvent such as hexane or chloroform, or compounds that can be increased in solubility by forming derivatives.

The following general approach, although somewhat esoteric, has been advocated as a procedure to fully characterize aqueous organic compounds (Ref. 42). First, nonpolar compounds can be extracted from water by use of an appropriate nonpolar organic solvent. Next, the extracted nonpolar organic material can be concentrated by evaporating the organic solvent. Finally, polar organic material can be recovered and concentrated by evaporating the water remaining after the initial solvent extraction.

Concentrates of nonpolar and polar organic material (and/or derivatives thereof) can then be injected into both a Gas Chromatograph (GC) and a High-Pressure Liquid Chromatograph (HPLC), each coupled to a Mass Spectrometer (MS) which records spectra of all separated compounds. A computer system can then be used to identify unknown compounds by matching their spectra with those of known compounds in a computer library. The GC/MS system enables identification of both nonpolar and polar volatile compounds while the HPLC/MS system enables identification of both nonpolar and polar nonvolatile compounds.

Needless to say, the above approach represents an extremely expensive procedure requiring experienced analytical chemists. However, a detailed characterization of organic material in leachate, in which specific organic compounds are identified, will require a sophisticated analytical system similar to the one proposed.

If a sophisticated GC/MS system is not available, less sophisticated techniques such as ultraviolet spectroscopy or thin layer chromatography can be employed. In addition, more basic "wet-chemistry" types of laboratory analyses can be employed for characterization of leached organics. These more basic types of analyses may include (1) "color-forming" tests which qualitatively indicate the presence or absence of particular groups or classes of organic compounds, (2) fractionation of organic material into acid/base/neutral fractions using solvents other than hexane, and (3) extraction of a weakly acidic fraction of organics to provide a general indication of the potential presence of phenols. Finally, it would be advantageous to test for the presence of certain organics with potential public health effects such as Polynuclear Aromatic Hydrocarbons (PAH).

#### Environmental Transport of Organic Contaminants

It is recommended that the environmental transport of leached organic contaminants be evaluated in a laboratory environment. This evaluation can be accomplished by conducting experiments employing large-scale columns filled and compacted with actual aquifer media taken from an area of potential in-situ development. (These large-scale columns should be similar to those described in the previous section regarding future recommended research for kinetic analysis



of continuous-flow column experiments.) After compaction, water containing leached contaminants can be continuously pumped through these columns at a specified flow rate, as estimated from actual geohydrologic conditions. At various times, samples can be withdrawn from sampling ports situated along the entire length of the column and analyzed for various parameters, including TOC. Overall, this general procedure enables an assessment of experimental variables such as column length, characteristics of aquifer media, flow rate, and initial quality of contaminated water.

Utilization of the above approach enables one to evaluate the assimilative capacity of an aquifer and to assess the effectiveness of certain natural treatment processes in removing contaminants from groundwater (Ref. 8).

#### Public Health/Ecological Effects of Organic Contaminants

It is suggested that future research be directed toward defining the carcinogenesis/mutagenesis of organic contaminants. These particular public health aspects are of concern where there exists a potential for domestic use of local groundwater in the vicinity of in-situ development. Relatively uncomplicated tests such as the Ames Test can be used to assess potential carcinogenesis.

Research should also be conducted on the potential ecological effects of organic contaminants entering the gaining reach of a stream. The toxicity of these contaminants toward aquatic biota should be evaluated by bioassay techniques. Research is presently underway at the University of California to assess the toxicity of retort water toward stream biota (Ref. 43). This research is being conducted in a laboratory environment using artificial stream channels as a method of bioassay. This same approach could readily be adapted to an assessment of the potential toxicity of leached organic contaminants toward stream biota.

#### More Detailed Assessment of Particular Types of Spent Shales

Research results summarized here suggest that spent shale samples with the most significant potential for organic contamination of groundwater are those produced during either inert gas retorting or combustion retorting employing recycle gas. However, none of the research organizations presently involved in the development of in-situ technologies are advocating the use of combustion retorting employing recycle gas on a commercial scale. It appears that either inert gas retorting or ordinary combustion retorting will be the most viable technology in the near future. Therefore, it is recommended that future research focus specifically on spent shale produced during inert gas retorting until it becomes very apparent which in-situ technology will most likely be employed on a commercial scale.

REFERENCES

1. G. Margheim, "Water Pollution from Spent Oil Shale," Ph.D. Thesis, Colorado State University (1975).
2. D. R. Williamson, "Oil Shales, Part 3: The Nature and Origins of Kerogens," Colorado School of Mines Mineral Industry Bulletin (1964).
3. J. B. Weeks, G. H. Leavesley, F. A. Welder, and G. J. Sauluier, Jr., "Simulated Effects of Oil-Shale Development on the Hydrology of Piceance Basin," USGS Prof. Paper 908 (1974).
4. T. A. Sladek, "Recent Trends in Oil Shale; Parts 1, 2, and 3," Colorado School of Mines Mineral Industry Bulletin (1974-75).
5. T. F. Yen, Progress Report on Retort Water Project Quarterly Progress Report for quarter ending February 29, 1976, Laramie Energy Research Center (1976).
6. J. Schmidt-Collerus, "The Disposal and Environmental Effects of Carbonaceous Solid Wastes from Commercial Oil Shale Operations," Denver Research Institute (1974).
7. P. H. McGauhey, Engineering Management of Water Quality (1968).
8. H. E. Legrand, "Environmental Framework of Groundwater Contamination," in Water Quality in a Stressed Environment, Ed. Wayne Pettyjohn (1972).
9. H. W. Parker, Simulated Groundwater Leaching of In-Situ Retorted or Burned Oil Shale, Texas Tech University (1976).
10. J. C. Ward, G. A. Margheim, and G. O. G. Löf, "Water Pollution Potential of Spent Shale Residues from Above-ground Retorting," American Chemical Society, Div. of Fuel or Chemistry, Preprints, 15, No. 1, 13 (1971).
11. Water Pollution Potential of Spent Oil Shale Residues, U.S. Environmental Protection Agency Report 14030 EDB 12/71 (1971).
12. L. P. Jackson et al., "Characteristics and Possible Roles of Various Waters Significant to In Situ Oil Shale Processing," Quarterly of Colorado School of Mines Oil, 70, No. 4, 105 (1975).
13. W. C. Culbertson, T. D. Nevens, and R. D. Hollingshead, "Disposal of Oil Shale Ash," in Proceedings of Colorado School of Mines Oil Shale Symposium (1969).
14. D. Runnells et al., Trace Elements in Oil Shale; Release, Transport, and Fate of Some Potential Pollutants, University of Colorado, (1977).

15. A. L. Hines, The Role of Spent Shale in Oil Shale Processing and the Management of Environmental Residuals, Proposal submitted to U. S. Energy Research and Development Administration (1976).
16. A. L. Hines, Proceedings of the Second Pacific Area Chemical Engineering Congress (1977).
17. W. Sandholtz, Personal Communication (1977).
18. R. Collins, Flow of Fluids through Porous Media (1961).
19. W. Liethe, The Analysis of Organic Pollutants in Water and Waste Water (1973).
20. L. Keith, Identification and Analysis of Organic Pollutants in Water, (1976).
21. University of Minnesota, Characterization of Aquatic Organics and Complexes, Proposal submitted to National Science Foundation (1977).
22. N. Cheronis, Identification of Organic Compounds (1963).
23. American Public Health Association, Standard Methods for the Examination of Water and Wastewater (1977).
24. P. McCarty, Chemistry for Sanitary Engineers (1971).
25. Engineering Science Inc., Air Quality Assessment of the Oil Shale Development Program in the Piceance Creek Basin (1974).
26. O. Levenspiel, Chemical Reaction Engineering (1972).
27. W. Weber, Physicochemical Processes for Water Quality Control (1972).
28. E. Schroder, Water and Wastewater Engineering Treatment (1977).
29. T. Sherwood et al., Mass Transfer (1975).
30. A. Rimpel et al., "Kinetics of Physical Adsorption of Propane from Helium on Fixed Beds of Activated Alumina," in American Institute of Chemical Engineers, Chemical Engineering Progress Symposium Series, No. 74 (1967).
31. J. Kostecki, The Kinetics of Physical Adsorption of Liquid Water from Benzene in Fixed Bed Adsorbent Columns, Ph.D. Thesis, Carnegie Institute of Technology (1964).
32. D. Camp, Physical Adsorption of Argon and Nitrogen on Fixed Beds, Ph.D. Thesis, Carnegie Institute of Technology (1963).

33. I. Klotz, "The Adsorption Wave," Chem. Rev. 239-241 (1946).
34. J. B. Rosen, "General Numerical Solution for Solid Diffusion in Fixed Beds," Industrial and Engineering Chemistry (August 1954).
35. J. B. Rosen, "Kinetics of a Fixed Bed System for Solid Diffusion into Spherical Particles," Journal of Chemical Physics (March 1952).
36. C. R. Antonson et al., "Nonlinear Equilibrium and Particle Shape Effects in Intraparticle Diffusion Controlled Adsorption," in American Institute of Chemical Engineers, Chemical Engineering Progress Symposium Series, No.96 (1969).
37. W. G. Hall, Hydraulic Calculations for a Modified In-Situ Retort, Lawrence Berkeley Laboratory Report LBL-10431 (1980).
38. D. Todd, Groundwater Hydrology (1959).
39. G. R. Amy and J. F. Thomas, "Factors that Influence the Leaching of Organic Material from In-Situ Spent Shale," in Proceedings of the Second Pacific Chemical Engineering Congress (1977).
40. G. L. Amy, J. F. Thomas, and A. L. Hines, "Leaching of Organic Residuals from Simulated In Situ Retorted Oil Shale," in Preprints of Division of Fuel Chemistry, American Chemical Society, 175th ACS Convention (1978).
41. K. H. Mancy, Instrumental Analysis in Water Pollution Control (1971).
42. W. Donaldson, "Trace Organics in Water," Environmental Science and Technology (April 1977).
43. P. Russell, The Effects of Oil Shale-Related Effluents On Some Benthic Freshwater Organisms, Ph.D. Thesis, University of California, 1980; Lawrence Berkeley Laboratory Report LBL-9818 (1980).

APPENDIX A

SAMPLE CALCULATIONS FOR KINETIC ANALYSIS OF CONTINUOUS-FLOW COLUMN :  
EXPERIMENTS

The following sample calculations describe the estimation of all parameters required for an evaluation of each rate constant described in the various rate models. These sample calculations will focus on data derived from the Type 1 spent shale leachate at a column length of 15 cm (i.e.,  $z = 15$  cm) and a leaching time of 15 hours (i.e.,  $t = 15$  hrs).

I. ESTIMATION OF PARAMETERS

A. Estimation of  $(\partial C/\partial t)_z$

This parameter was estimated from a linear approximation of the slope of the appropriate concentration versus time curve presented in Figure 35. At  $z = 15$  cm and  $t = 15$  hrs, a linear approximation of the curve was estimated to be:

$$\left(\frac{\partial C}{\partial t}\right)_z = \frac{\Delta C}{\Delta t} = \frac{C_2 - C_1}{t_2 - t_1}$$

$$\left(\frac{\partial C}{\partial t}\right)_z = \frac{1.725 \text{ mg/l} - 1.45 \text{ mg/l}}{17.5 \text{ hrs} - 12.5 \text{ hrs}}$$

$$\left(\frac{\partial C}{\partial t}\right)_z = -0.055 \frac{\text{mg/l}}{\text{hr}}$$

B. Estimation of  $(\partial C/\partial z)_t$

This parameter was estimated from a linear approximation of the slope of the appropriate Concentration versus Column Length curve presented in Figure 34a. At  $z = 15$  cm and  $t = 15$  hrs, a linear approximation of the slope of the curve was estimated to be:

$$\left(\frac{\partial C}{\partial z}\right)_t = \frac{\Delta C}{\Delta z} = \frac{C_2 - C_1}{z_2 - z_1}$$

$$\left(\frac{\partial C}{\partial z}\right)_t = \frac{1.70 \text{ mg/l} - 1.39 \text{ mg/l}}{16.875 \text{ cm} - 13.125 \text{ cm}}$$

$$\left(\frac{\partial C}{\partial z}\right)_t = 0.0827 \frac{\text{mg/l}}{\text{cm}}$$

C. Estimation of  $(\partial q/\partial t)_z$

This parameter was estimated by substituting computed values of  $(\partial C/\partial t)_z$  and  $(\partial C/\partial z)_t$  into the differential mass balance equation. The differential mass balance equation is defined by:

$$-\rho A \left( \frac{\partial q}{\partial t} \right)_z = F \left( \frac{\partial C}{\partial z} \right)_t + \alpha A \left( \frac{\partial C}{\partial t} \right)_z$$

Or, upon rearranging:

$$\left( \frac{\partial q}{\partial t} \right)_z = \frac{F \left( \frac{\partial C}{\partial z} \right)_t + \alpha A \left( \frac{\partial C}{\partial t} \right)_z}{-\rho A}$$

where

$$(\partial C/\partial z)_t = 0.0827 \text{ mg/l/cm}$$

$$(\partial C/\partial t)_z = -0.055 \text{ mg/l/hr}$$

$$F = 0.036 \text{ l/hr}$$

$$\alpha = 0.57$$

$$A = 4.91 \text{ cm}^2$$

$$\rho = 0.86 \text{ g/cm}^3$$

Substituting the above values into the partial differential equation yields:

$$\begin{aligned} \left( \frac{\partial q}{\partial t} \right)_z &= \frac{(0.036 \frac{1}{\text{hr}}) (0.0827 \frac{\text{mg}}{1\text{-cm}})}{- (0.86 \frac{\text{g}}{\text{cm}^3}) (4.91 \text{ cm}^3)} \\ &+ \frac{(0.57) (4.91 \text{ cm}^2) (-0.055 \frac{\text{mg}}{1\text{-hr}})}{- (0.86 \frac{\text{g}}{\text{cm}^3}) (4.91 \text{ cm}^2) (1000 \frac{\text{cm}}{1})} \end{aligned}$$

$$\left(\frac{\partial q}{\partial t}\right)_z = -0.000669 \frac{\text{mg/g}}{\text{hr}}$$

D. Estimation of  $q_\infty$

This parameter was estimated from the solid-phase organic carbon measurements originally presented in Table 12. From Table 12, the solid-phase organic carbon content of Type 1 spent shale is estimated to be 0.2 percent by weight. This implies that  $q_\infty$  for Type 1 spent shale is 2.00 mg TOC/g spent shale, representing the theoretically maximum potential solid-phase organic carbon on shale particles.

E. Estimation of  $\Delta q$

This parameter was estimated by multiplying the average value of  $(\partial q/\partial t)_z$  during a particular interval by the time duration of the interval. The value of  $(\partial q/\partial t)_z$  at  $t = 15$  hrs was estimated to be  $-0.000669$  mg/g/hr while the value of  $(\partial q/\partial t)_z$  at  $t = 10$  hrs was estimated to be  $-0.000767$  mg/g/hr. Thus, the average value of  $(\partial q/\partial t)_z$  during the interval from 10 to 15 hours can be estimated by:

$$\text{Average } \left(\frac{\partial q}{\partial t}\right)_z = \frac{\left(\frac{\partial q}{\partial t}\right)_z @ 10 \text{ hrs} + \left(\frac{\partial q}{\partial t}\right)_z @ 15 \text{ hrs}}{2}$$

$$\text{Average } \left(\frac{\partial q}{\partial t}\right)_z = \frac{(-0.000762 \frac{\text{mg/g}}{\text{hr}}) + (-0.000669 \frac{\text{mg/g}}{\text{hr}})}{2}$$

$$\text{Average } \left(\frac{\partial q}{\partial t}\right)_z = -0.000716 \frac{\text{mg/g}}{\text{hr}}$$

The value of  $\Delta q$  for the interval from 10 to 15 hours can then be computed by:

$$\Delta q = \text{Average } \left(\frac{\partial q}{\partial t}\right)_z \times \Delta t$$

$$\Delta q = 0.000716 \frac{\text{mg/g}}{\text{hr}} \quad 5 \text{ hours}$$

$$\Delta q = 0.003590 \frac{\text{mg}}{\text{g}}$$

F. Estimation of  $\Sigma\Delta q$

This parameter was estimated by summing all values of  $\Delta q$  for all leaching intervals up to and including the interval of concern. Thus, the value of  $\Sigma\Delta q$  for a leaching time period of 15 hours can be estimated by:

$$\Sigma\Delta q = (\Delta q)_{0-5\text{hrs}} + (\Delta q)_{5-7.5\text{hrs}} + (\Delta q)_{7.5-10\text{hrs}} + (\Delta q)_{10-15\text{hrs}}$$

$$\Sigma\Delta q = 0.004485 \frac{\text{mg}}{\text{g}} + 0.002168 \frac{\text{mg}}{\text{g}} + 0.002005 \frac{\text{mg}}{\text{g}} + 0.003590 \frac{\text{mg}}{\text{g}}$$

$$\Sigma\Delta q = 0.012248 \frac{\text{mg}}{\text{g}}$$

G. Estimation of  $q$

This parameter was estimated by subtracting the quantity  $\Sigma\Delta q$  from the corresponding value of  $q_{\infty}$ . At  $t = 15$  hours, the parameter  $q$  was estimated to be:

$$q = q_{\infty} - \Sigma\Delta q$$

$$q = 2.00 \frac{\text{mg}}{\text{g}} - 0.012248 \frac{\text{mg}}{\text{g}}$$

$$q = 1.987752 \frac{\text{mg}}{\text{g}}$$

H. Estimation of  $q^*$

This parameter was estimated from the isotherm presented in Figure 32 by using the value of actual measured TOC concentration. At  $t = 15$  hours, the actual measured TOC concentration was estimated to be 1.54 mg/l from Figure 35. From Figure 32, the corresponding value of  $q^*$  was estimated to be 1.974948 mg/g.

I. Estimation of  $C$

This parameter represents the actual measured TOC concentration in the bulk leachate. From Figure 35, the parameter  $C$  was estimated to be 1.54 mg/l at  $t = 15$  hours.



J. Estimation of C\*

This parameter was estimated from the isotherm presented in Figure 32 by employing the previously estimated value of q. At t = 15 hours, the actual value of q was 1.987752 mg/g. From Figure 32, the corresponding value of C\* was estimated to be 9.00 mg/l.

II. EVALUATION OF RATE CONSTANTS

The rate constant for each rate model was evaluated by employing the previous estimates of parameters for z = 15 cm and t = 15 hours.

A. External Mass Transfer

$$K_E = \frac{\left(\frac{\partial q}{\partial t}\right)_z}{C - C^*}$$

$$K_E = \frac{-0.000669 \frac{\text{mg/g}}{\text{hr}}}{1.54 \text{ mg/l} - 9.00 \text{ mg/l}}$$

$$K_E = 0.0000897 \frac{1}{\text{g-hr}}$$

B. Internal Mass Transfer

$$K_G = \frac{\left(\frac{\partial q}{\partial t}\right)_z}{q^* - q}$$

$$K_G = \frac{-0.000669 \frac{\text{mg/g}}{\text{hr}}}{1.974948 \frac{\text{mg}}{\text{g}} - 1.987752 \frac{\text{mg}}{\text{g}}}$$

$$K_G = 0.0522 \text{ hour}^{-1}$$

C. Surface Reaction

$$K_{BA} = \frac{\left(\frac{\partial q}{\partial \tau}\right)_z}{C(q_\infty - q)}$$

$$K_{BA} = \frac{-0.000669 \frac{\text{mg/g}}{\text{hr}}}{1.54 \frac{\text{mg}}{\text{l}} (2.00 \frac{\text{mg}}{\text{g}} - 1.987752 \frac{\text{mg}}{\text{g}})}$$

$$K_{BA} = -0.0355 \frac{1}{\text{mg-hr}}$$

